Characterisation of the myeloid compartment in ovarian cancer

Danielle O'Neill

A thesis submitted to the University of Birmingham for the degree of

DOCTOR OF MEDICINE

Institute of Cancer and Genomic Sciences

College of Medical and Dentist Sciences

University of Birmingham

May 2022

Abstract

This research was conducted to interrogate the myeloid compartment of the immune response within the tumour microenvironment of ovarian cancer and its metastatic sites. Despite the advances in the surgical approach of managing ovarian cancer, the prognosis remains dismal, highlighting the urgent need to develop immunotherapeutic agents to control disease progression and prevent relapse. Little is currently known about the myeloid compartment in ovarian cancer, and as such this thesis focuses upon these cells to fully phenotype and characterise the cells present in the primary site of ovarian cancer but also its secondary metastatic sites. This work demonstrated the presence of myeloid-derived suppressor cells (MDSC) in both benign and malignant neoplasms, a finding that has not been demonstrated previously. It was also shown that the ratio of granulocytic to monocytic MDSC was more predictive of underlying pathology, with high-grade serous ovarian cancer having a much greater ratio compared to healthy donors. Further functional characterisation of these MDSC was then performed in order to demonstrate their immunosuppressive function, where it was demonstrated that there were potential flaws within the laboratory technique of suppression assays. It was shown that MDSC have a great phagocytic capability, which led to phagocytosis of the Dynabeads thus affecting their ability to cause T cell proliferation and demonstrating an inaccurate immunosuppressive effect. Further suppression analyses demonstrated a lack of consistent immunosuppression and as such their phenotypic characterisation was sought through their gene expression using single cell RNA sequencing. The myeloid cells were identified through their unique genetic signatures and a cluster of MDSC-like cells were identified and were found to be in greatest number in the ovarian cancer specimens compared to the metastatic adenocarcinoma and normal samples. They were shown to have an upregulation in arginine and S100A8, both known to have a role in immunosuppression, which may suggest that these MDSC may serve a function in causing immunosuppression despite being unable to demonstrate this experimentally. This may suggest MDSC as a potential therapeutic target within ovarian cancer, however further functional work needs to be done in order to validate these findings.

Acknowledgments

Firstly, I would like to thank my supervisor Jason Yap for providing me with guidance, feedback and encouragement throughout this project to not only complete this work, but to develop my skills in critical appraisal of research, interpretation of results and problem-solving. These attributes are integral for both clinical and academic roles and his support in developing these skills have changed my approach to tackling new challenges.

To both Professor Moss and Professor Kehoe, I extend further gratitude for their patience and support throughout this project and for providing me with access to the expertise and tools required in order to complete this work.

I would like to express my thanks to my clinical supervisors Miss Soo Hoo and Mr Murphy, who have been eternally supportive of my clinical and research needs and have helped me obtain the vital samples required for the project. To this end, I would like to thank all the patients who consented to be part of this research and the surgical team at New Cross, Wolverhampton and City Hospital, Birmingham for allowing me access to patient samples without which I could not have performed my research.

I would also like to extend deep gratitude to:

Dr Hayden Pearce and Dr Wayne Croft for supervising me on a daily basis and helping me to overcome the many obstacles faced throughout this project. Without their support and guidance, this project would not have been possible. In addition, special thanks to Wayne for his contribution to the single cell RNA sequencing chapter, as his work on the data analysis formed the basis to the chapter and as such would not have been performed without his contribution.

Dr Guido Frumento for his support, expertise and patience in teaching me about laboratory technique and his contribution to my work on developing suppression assays.

Dr Rachel Pounds for her help with tissue collection and the preparation of samples.

Mr Khalil Uddin, Dr Richard Powell and all the members of Professor Paul Moss' team for their endless technical support. Without this wonderful team my project would not have got off the ground.

Rachel Bruton for her continued non-technical support and organisational skills which kept my project on track.

To all the patients who consented to be a part of this research I extend my greatest of gratitude.

And finally, to my family who have provided me with limitless support, encouragement and love in order for me to achieve my goals. I am forever grateful for everything they have done.

Table of Contents

List of Figures

List of Tables

List of abbreviations

APC:	Antigen presenting cell
BRAF:	B-Raf oncogene
BRCA:	Breast cancer gene
CA-125:	Cancer antigen 125
CFSE:	Carboxyfluorescein succinimidyl ester
COSHH:	Control of substances Hazardous to Health
CRS:	Chemotherapy response score
CTLA-4:	Cytotoxic T-lymphocyte associated protein 4
DAMP:	Damage-associated molecular pattern
DC:	Dendritic cell
DDS:	Delayed debulking surgery
DEG:	Differentially expressed gene
DMEM:	Dulbecco's Modified Eagle Medium
DMSO:	Dimethyl sulfoxide
DNA:	Deoxyribonucleic acid
ECM:	Extracellular matrix
EDTA:	Ethylenediaminetetra acetic acid
EGFR:	Epidermal growth factor receptor
EMT:	Epithelial-to-mesenchymal transition
EOC:	Epithelial ovarian cancer
EpCAM:	Epithelial cell adhesion molecule
ER:	Endoplasmic reticulum
FACS:	Fluorescence-activated cell sorting
FBS:	Fetal Bovine Serum
FcR:	Fragment crystallisable receptor
FIGO:	International Federation of Obstetrics and Gynaecology
G-CSF:	Granulocyte colony-stimulating factor
GEM:	Gel beads in emulsion
GFP:	Green fluorescence protein
GM:	General media

GM-CSF:	Granulocyte-macrophage colony-stimulating factor
HGS:	High-grade serous cancer
HGSOC:	High-grade serous ovarian cancer
HLA-DR:	Human Leukocyte Antigen – DR isotype
IFN:	Interferon
KRAS:	Kirsten rat sarcoma viral oncogene homologue
LDL:	Low-density lipoprotein
LOX-1:	Oxidised low-density-lipoprotein receptor 1
LPS:	Lipopolysaccharide
MACS:	Magnetic-activated cell sorting
M-CSF:	Monocyte colony-stimulating factor
MDSC:	Myeloid-derived suppressor cell
MDT:	Multi-disciplinary team
m-MDSC:	Monocytic-MDSC
NGS:	Next generation sequencing
NICE:	National Institute for Health and Care Excellence
NK:	Natural killer cells
NO:	Nitric oxide
NOS:	Nitric oxide synthase
NS:	Non-significant
OpZ:	Opsonised zymosan
PAMP:	Pathogen-associated molecular pattern
PARP inhibitor:	Poly adenosine diphosphate-ribose polymerase inhibitor
PBMC:	Peripheral blood mononuclear cell
PBS:	Phosphate buffered saline
PCA:	Principal component analysis
PCR:	Polymerase chain reaction
PD-1:	Programmed cell death protein 1
PDAC:	Pancreatic ductal adenocarcinoma
pDC:	Plasmacytoid dendritic cell
PDL-1:	Programmed cell death protein ligand 1
PDS:	Primary debulking surgery

PGE2:	Prostaglandin E2
PI:	Propidium iodide
PMA:	Phorbol myristate acetate
PMN-MDSC:	Granulocytic-MDSC
RBC:	Red blood cell
RNA:	Ribonucleic acid
ROS:	Reactive oxygen species
Rpm:	Revolutions per minute
RPMI:	Roswell Park Memorial Institute medium
scRNA:	Single cell RNA
SEM:	Standard error of the mean
SLE:	Systemic lupus erythematosus
SNP:	Single-nucleotide polymorphism
STIC:	Serous tubal intraepithelial carcinoma
TAM:	Tumour-associated macrophage
TILs:	Tumour infiltrating lymphocytes
TLR:	Toll-like receptors
TME:	Tumour microenvironment
Treg:	Regulatory T cell
UMAP:	Uniform manifold projection
UMI:	Unique molecular index
VEGF:	Vascular endothelial growth factor

Chapter 1

Introduction

1.0 Ovarian cancer

1.1.1 Epidemiology

Ovarian cancer is the seventh most common cancer affecting women world-wide (1) and has a UK incidence of over 7400 cases per year (2). The lifetime risk of developing ovarian cancer is 1 in 75 and nearly 1% of women die of this disease during their lifetime (3). Although it is the second most common gynaecological cancer after endometrial cancer, ovarian cancer causes far more deaths. More than 80% of women diagnosed with the disease are post-menopausal and the highest incidence is in women aged 85-89 (Figure 1.1).

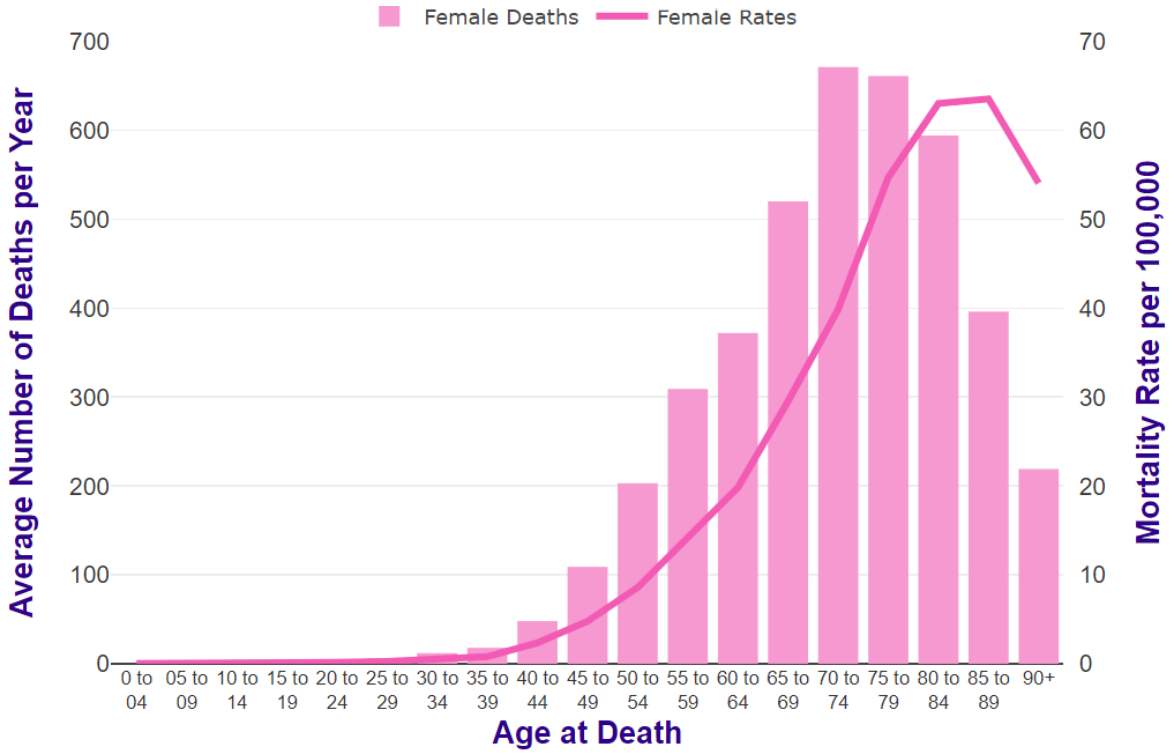

Figure 1. 1. Average Number of Deaths per Year and Age-Specific Mortality Rates per 100,000 Female Population, UK, 2017-2019 (Cancer Research UK)

Despite its poor prognosis, there has been an improvement in survival from ovarian cancer over the last 40 years (Figure 1.2). This has been attributed partly to the introduction of platinum-based chemotherapy in the 1980s as one-year survival is dependent on optimal primary therapy. Additionally, recurrent disease is now being treated more aggressively with the combination of chemotherapy and surgery able to offer a more controllable and chronic disease progression (4).

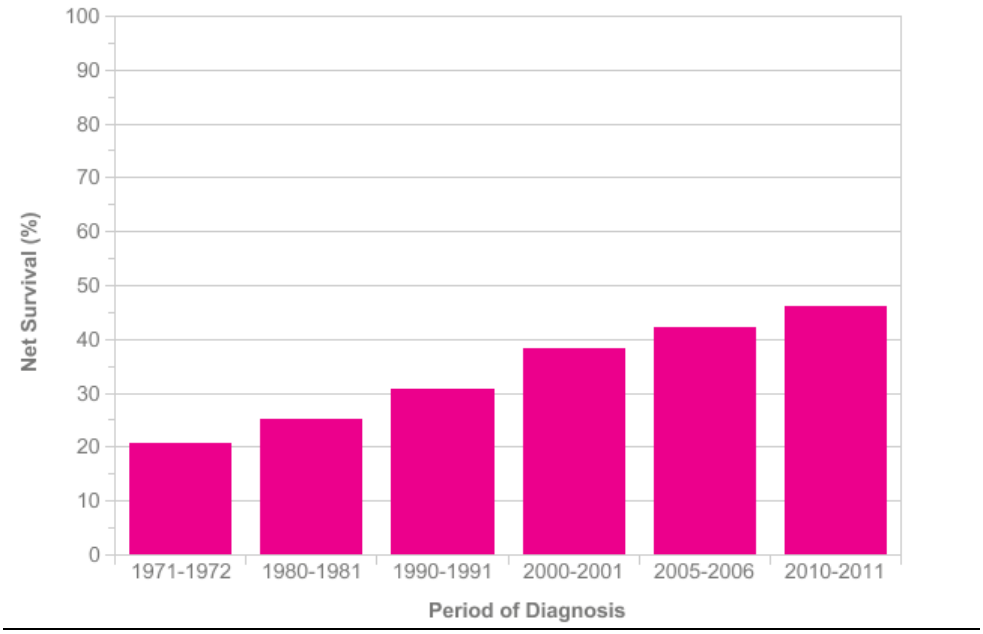

Figure 1. 2 Age-standardised five-year net survival, England and Wales 1971-2011
(Cancer Research UK).

1.1.2 The origin of epithelial ovarian cancer

Ovarian cancer is a heterogenous disorder and tumours can arise from the epithelial layer, germ cells or stroma (Figure 1.3).

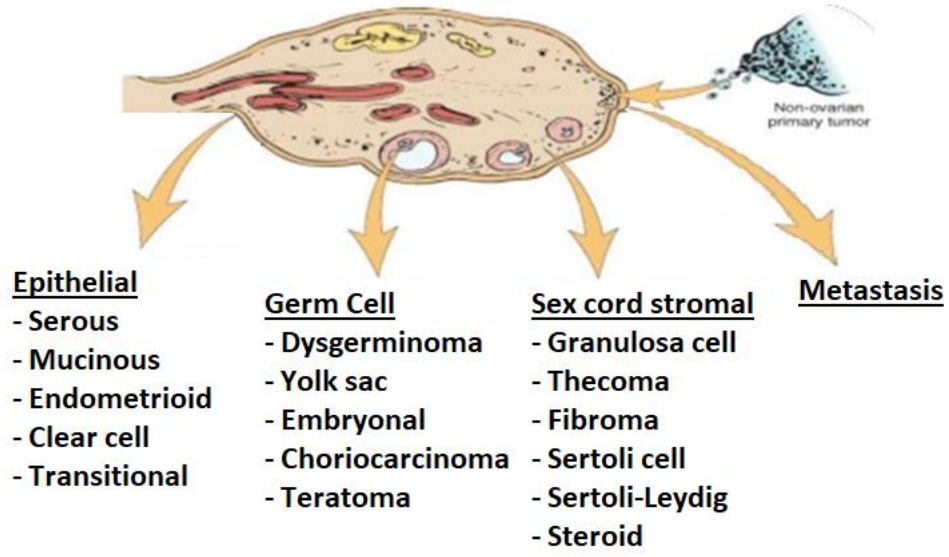

Figure 1. 3 The site of origin of the major subtypes of ovarian cancer.
Ovarian tumours may also arise as metastases from other sites, such as the gastro-intestinal tract.

The most common subtype of ovarian cancer is those of epithelial origin, comprising up to 95% of cases. This group includes high grade serous (68%), endometrioid (20%), low-grade serous (<5%), clear cell carcinoma (4%) and mucinous carcinoma (3%). The other subtypes of ovarian cancer arise from germ cell (3%) and sex cord stromal cells (2%) however, as they account for such a small proportion, the main focus is on those of epithelial origin, namely high-grade serous cancers (HGSC) (5).

There are currently thought to be three sites of origin for epithelial ovarian cancer; the single layer of epithelium covering the ovarian surface, the fallopian tube or the peritoneum mesothelium (6). Current evidence suggests the most common origin in HGSC is from the lining of the fallopian tube, especially amongst those with the *BRCA* mutation (7). Unlike many other cancers, HGSC do not have a clear precursor lesion, other than serous tubal intraepithelial carcinoma (STIC) in those women whose disease originates from the fallopian tube. Prior to a diagnosis of ovarian cancer, this is usually identified incidentally or in specimens of ovaries and fallopian tubes removed for prophylaxis in women with high-risk genetic aberrations, such as *BRCA* mutation. It has been noted that STIC, or indeed early invasive cancers, are diagnosed in 2.1% of high-risk women with unknown mutations and 8.55% of women with *BRCA* mutation undergoing a risk-reducing bilateral salpingo-oophorectomy (8). In women who presented with ovarian cancer or primary peritoneal disease, histology revealed STIC lesions in 35-47% of patients (9,10). Aside from STIC, ovarian cancers are thought to arise *de novo* from surface epithelium.

In order to further characterise ovarian malignancies according to their pathogenesis, the dualistic model for ovarian cancer was developed (11). This divides the ovarian neoplasms into two groups; type I and type II tumours. Tumours such as low-grade serous ovarian cancers are thought to develop in a stepwise fashion from borderline lesions. These cancers, which have a more predictable course of progression, are termed type 1 tumours whilst high grade serous cancer is considered a type 2 tumour. This difference is also reflected in the associated genetic aberrations as *KRAS* and *BRAF* are most commonly affected in type 1 serous cancers whilst *p53* is an important mutated gene in high grade serous disease (11).

1.1.3 Risk factors

The main theory behind the pathogenesis of ovarian cancer is the 'incessant ovulation' hypothesis. This considers that with every ovulation there is surface epithelial damage and that subsequent inaccurate DNA repair leads to a gradual accumulation of genetic mutations. Therefore, any factor that increases the number of ovulations that a women undergoes in a lifetime (such as age of menarche, age of menopause, parity, breastfeeding status) will increase the risk of developing ovarian cancer (12).

After increasing age, the single biggest risk factor for developing ovarian cancer is having a family history of the disease. First-degree relatives have a several fold increased risk of developing ovarian cancer, especially if their relatives developed the disease at an early age (13). The mean age for presentation with ovarian cancer with *BRCA1* mutation is around aged 51 and 61 in those with *BRCA2* mutation (14). This is around 10 – 15 years earlier than non-familial ovarian cancer (15). Inheritance of defined genetic mutations such as *BRCA1* or *BRCA*2 increases the lifetime risk of the disease to 44% and 27% respectively (16). Such cancer syndromes account for 36% of familial relative risk (17). A delayed menopause of 5 years is associated with an increased risk of endometrioid and clear cell tumours, whilst use of hormone replacement therapy has been associated with an increased risk of serous and endometrioid cancers (18). Ovarian stimulation used during fertility treatment is associated with an increased risk of invasive and borderline tumours.

Protective factors identified include hysterectomy, tubal sterilisation and salpingectomy. Hysterectomy can offer a reduction in risk of 30-40% (19), whilst bilateral salpingectomy can reduce the overall risk of ovarian cancer by 50% compared to unilateral salpingectomy (20).The theory behind the protective effect of tubal sterilisation lies in preventing retrograde transport of carcinogenic substances, including exfoliated cells, from the vagina and fallopian tube to the ovary and peritoneum (19).

1.1.4 Staging of ovarian cancer

The staging for ovarian cancer describes how far the disease has spread and can provide the patient and clinician with an idea of expected prognosis and treatment options. The International Federation of Gynaecology and Obstetrics (FIGO) updated their staging classification in 2014 (Table 1.1). In short, stage I disease describes disease localised to the ovaries and can offer women a five-year survival of 90%. Most tumours presenting in this stage are type I tumours, which usually have a low proliferative activity and hence also have a better prognosis, accounting for only 10% of deaths from ovarian cancer. Type II tumours, however, present in an advanced stage in more than 75% of cases and are aggressive, high grade and develop rapidly (21). This difference in disease pathobiology also accounts for the vast differences in survival at the different stages of disease.

Stage 2 disease has spread into the pelvis and includes primary peritoneal disease. The five-year survival for stage 2 disease is approximately 68%. Stage 3 includes disease that has metastasised to the retroperitoneal lymph nodes or upper abdomen and has a five-year survival of up to 27%. Finally stage 4 disease is the most advanced and displays distant metastasis, including peritoneal metastasis, and has a dismal five-year survival quoted around 14% (22–24). Despite this, the overall mortality in ovarian cancer is falling, largely due to the advent of PARP inhibitors and more aggressive surgical

cytoreduction. Between 1999 and 2019 the mortality rate has dropped from 16.5 women per 100,000 to 12.2 per 100,000 (23).

Stage	Description
Stage I	**Limited to the ovary**
IA	Limited to 1 ovary or fallopian tube, capsule intact, no tumour on external surface
IB	Limited to both ovaries or fallopian tubes, capsule intact, no tumour on external surface
IC	Tumour on surface of 1 or both ovaries or fallopian tubes with any of the following:
	IC1 – intraoperative spill
	IC2 – capsule ruptured prior to surgery or tumour on external surface
	IC3 – malignant cells present in ascites or peritoneal washings
Stage II	**Involving 1 or both ovaries with pelvic extension (below pelvic brim) or peritoneal cancer**
IIA	Extension and/or metastasis to uterus and/or tubes and/or ovaries
IIB	Extension to other pelvic intraperitoneal tissues
Stage III	**Involving 1 or both ovaries, or fallopian tubes, or primary peritoneal cancer, with cytologically or histologically proven peritoneal implants outside the pelvis and/or positive retroperitoneal lymph nodes**
IIIA1	Metastasis to retroperitoneal lymph nodes with or without microscopic peritoneal involvement outside the pelvis
	IIIA1 (i) Metastasis <10mm diameter
	IIIA1 (ii) Metastasis >10mm diameter
IIIA2	Microscopic extrapelvic peritoneal involvement with or without positive retroperitoneal lymph nodes
IIIB	Macroscopic extrapelvic disease <2cm, with or without positive retroperitoneal lymph nodes
IIIC	Macroscopic extrapelvic disease >2cm, with or without positive retroperitoneal lymph nodes
Stage IV	**Distant metastases excluding peritoneal metastases**
	IVA pleural effusion with positive cytology
	IVB metastases to extra-abdominal organs

Table 1. 1. The International Federation of Gynaecology and Obstetrics (FIGO) staging for ovarian cancer 2014.

Due primarily to a lack of definitive symptoms in early disease, only 15% of all women with ovarian cancer will present at stage 1 (3). Consequently, approximately 70% of women present at an advanced stage with evidence of metastatic disease (6,25). More than 80% of women with stage 3 and 4 disease respond to surgical debulking and chemotherapy (26) although recurrence tends to occur within 22 months and the overall 5 year survival rate is 27% (25,27).

1.1.5 Ovarian cancer screening

There is currently no approved screening available for the detection of ovarian cancer. Primary analysis of the UK Collaborative Trial of Ovarian Cancer Screening (UKCTOCS) published in 2016 did not show a benefit from screening but did show encouraging results for reduction in mortality at years 7-14 post-diagnosis. They concluded, that further evidence was required before firm conclusions could be made (28). Despite using ultrasound and cancer-antigen 125 (CA-125) monitoring, the sensitivity and specificity of screening is inadequate to justify the potentially invasive and unnecessary interventions caused by false-positive results. Currently, women at high risk of ovarian cancer, such as those who carry a *BRCA* mutation, are offered prophylactic 'risk-reducing' bilateral salpingo-oophorectomy as this is associated with improved survival (29). The UK Familial Ovarian Cancer Screening Study (UKFOCSS) originally performed a study on annual screening for women with a lifetime risk of >10%. This lacked sensitivity for early-stage disease and as such the screening interval was increased to 4-monthly. Use of the 'risk of ovarian cancer algorithm (ROCA)' was shown to be highly sensitive and was associated with a significant improvement in stage at diagnosis, however the authors only recommend it for women refusing risk-reducing bilateral salpingo-oophorectomy as a survival benefit is yet to be established (30). Additionally, it does not comment on the potential negative effects of women having to attend 4-monthly screening both psychologically for the women and financially for the NHS.

1.1.6 Treatment of primary ovarian cancer

The mainstay of treatment for ovarian cancer is a combination of platinum-based chemotherapy and cytoreductive surgery. Dependent on patient factors and presentation of disease, women may undergo primary debulking surgery followed by chemotherapy or commence treatment with neo-adjuvant chemotherapy and have interval debulking surgery after chemotherapy. There have been several randomised trials investigating the role of neo-adjuvant chemotherapy in ovarian cancer and in each of these trials the practice was to offer 3-4 cycles of neo-adjuvant therapy and this is therefore the standard (31–34). If a woman responds well to chemotherapy, surgery may therefore be performed after 3 cycles of chemotherapy, followed by further chemotherapy after surgery. If the response is sub-optimal the women may have 6 cycles of chemotherapy prior to surgery but this is not standardised practice. In addition, it has been found that despite maximal cytoreduction, patients who received 5 or more cycles of chemotherapy had a poorer prognosis compared to those who received 3-4 cycles (35). Generally speaking, women with large volume disseminated disease, pleural effusions or miliary peritoneal disease have a low likelihood of achieving complete cytoreduction and so tend to receive chemotherapy prior to surgical intervention. Complete cytoreduction is defined as complete removal of macroscopic residual disease, and is termed 'optimal debulking', whilst suboptimal debulking occurs if there is any residual tumour remaining following surgery. Two randomised trials, International Collaborative

Ovarian Neoplasm (ICON) and Adjuvant ChemoTherapy in Ovarian Neoplasm (ACTION), have demonstrated improved survival and disease-free survival when adjuvant platinum-based chemotherapy is given when women have no residual disease following primary surgery (36,37). An extension to the ICON trial demonstrated that the addition of bevacizumab was not beneficial except for women with poor-prognosis disease (38).

If a woman presents with a large but more confined ovarian tumour it is unlikely to respond well to chemotherapy due to the relatively necrotic environment so primary removal of all visible disease followed by chemotherapy to remove microscopic deposits is indicated. Both of these approaches have been shown to be equally effective (31). Optimal operative cytoreduction is associated with improved prognosis, even in those women with a large tumour burden (39). The standard chemotherapy used in ovarian cancer consists of a platinum-based compound such as carboplatin, coupled with a taxane such as paclitaxel, demonstrated to improve survival by the International Collaborative Ovarian Neoplasm 4 (ICON4) trial (40).

Poly (ADP-ribose) polymerase inhibitors (PARP inhibitors) target the PARP enzyme family, essential for DNA repair. Through its inhibition, it allows the accumulation of single-strand breaks, and consequently double-strand breaks, enabling death of tumour cells. PARP inhibitors were first trialled in 2009 in a phase I study and since have been put through phase III trials and are now incorporated into clinical practice. Although they are more efficacious in women with BRCA mutation, they still provide a significant improvement in survival when used in women without BRCA mutation (41). Initially they were reserved for women with recurrent and treatment-resistant disease, however over the last few years they have been introduced to patients newly diagnosed with ovarian cancer, following the results of the SOLO-1 trial in 2018 which demonstrated an improved progression-free survival of 3 years in women with BRCA mutation. A further analysis in 2020 demonstrated thar almost 50% of women who had been given PARP-inhibitors had not progressed after 5 years, compared to 20% in the placebo group (42). The PAOLA-1 trial combined PARP-inhibitors with bevacizumab (anti VEGF) in women with homologous-recombination deficiency (HRD) rather than just BRCA mutations and demonstrated an improved progression-free survival of just under 6 months (43). Following this and other subsequent trials, the FDA approved Olaparib (PARP-inhibitor) with bevacizumab for first-line maintenance therapy for people with HRD in April 2020 (44).

1.1.7 Management of recurrence

Recurrent disease can be identified in many ways; through an increase in CA-125 on monitoring blood tests, detection on routine imaging or when the patient presents with symptoms such as bloating or a mass.

The role of surgery in the management of recurrence is somewhat controversial. A randomised clinical trial published in 2019 comparing secondary debulking surgery in association with chemotherapy and bevacizumab or chemotherapy and bevacizumab alone without surgery demonstrated no survival benefit in women receiving surgery (45). The Desktop III trial was published in 2021 which demonstrated a survival advantage in women who underwent surgery, however there was no addition of bevacizumab within these patients so cannot be directly compared to the previous study (46). The chemotherapy of choice is dependent on the time interval from the previous platinum-containing treatment to the identification of recurrence. If this time interval is less than 6 months this is termed platinum-resistance and is associated with a 15% chance of response with re-treatment. Patients with an interval of 6-12 months are deemed partly platinum-sensitive and their response improves the further away from the last treatment the recurrence is identified. Some women may progress whilst on platinum-based treatment and this is termed platinum-resistance and these women have a particularly poor prognosis (22). Recurrence with platinum-sensitive disease offers a median survival of 3 years, whilst platinum-resistance disease has a median survival of 1 year (47). The use of PARP inhibitors in platinum-sensitive disease has been trialled in many phase III trials. The findings of the ARIEL 3 trial published in 2020, demonstrated a chemotherapy-free interval of 14.3 months in the PARP inhibitor group versus 8.8 months in the placebo group. The time to disease progression on subsequent therapy or death was 21 months in the PARP inhibitor group versus 16.5 months in the placebo group. These results demonstrate clinically-meaningful benefits to patients with platinum-sensitive recurrence (48).

1.1.8 Targeted therapy

The identification of biomarkers for ovarian cancer is extremely important as it can dictate the potential for response to immunotherapy. One such biomarker is the ‘mutational load’ expressed by the cancer. Those tumours with a greater number of somatic mutations will produce an increased number of peptide ‘neo-epitopes’ which can act as antigens to activate an immune response. As such these tumours display an improved response to immunotherapy, as also seen in solid cancers such as non-small-cell lung cancer, urothelial cancer and melanoma (49–52). This is of importance in ovarian cancer because it has been demonstrated that tumours developing in women with *BRCA* mutation with a high mutational load have a better prognosis (53). *BRCA* mutation can also affect the cell’s ability to repair DNA damage, a process termed homologous repair. Loss of this ability of self-repair results in the accumulation of mutation and cancer. Women with defects in homologous repair have a better response to the use of targeted therapy in the form of poly (ADP-ribose) polymerase (PARP) inhibitors (54) and improved platinum-sensitivity (55). To grow, tumours require adequate blood supply and recruit the formation of new blood vessels through the production of vascular endothelial growth factor (VEGF). Agents that target VEGF have been trialled in addition to conventional chemotherapy. The trials ICON7 and

GOG281 demonstrated improved survival advantage for women taking VEGF pathway inhibitors with stage III or IV disease who had residual disease following cytoreductive surgery (56,57). More recently, the addition of anti-VEGF therapy has been found to improve progression-free survival irrespective of stage or residual disease (58). This demonstrates the potential role for targeted therapy, immunotherapy and genomics in ovarian cancer.

1.1.9 Ovarian cancer progression

Whilst most cancers spread through the haematological and lymphatic route, ovarian cancer spreads through direct spread and shedding of tumour cells within the peritoneal cavity. These tumour cells deposit preferentially upon the mesothelium and omentum, and upon the serosal surface of intra-abdominal organs. An unusual feature is that the disease does not readily invade through the superficial bowel serosa so women tend to present with advanced disease with multiple metastases within the abdominal cavity. Unfortunately, despite complete cytoreductive surgery and chemotherapy, further relapse is largely inevitable. The mechanisms of relapse of ovarian cancer are largely unknown but are thought to originate from quiescent cancer stem cells becoming activated within a microenvironment primed for the development and maintenance of progeny cells (59). How these cancer cells evade immune detection is the subject of great interest, and research into how the immune system interacts with cancer is developing with the hope that this could unlock the potential for cure of disease without the systemic effects of standard chemotherapy.

1.2.0 Immune involvement in ovarian cancer

The immune response can be divided broadly into two main categories, the innate and the adaptive systems, although significant overlap and interaction occurs between these two responses. The innate immune response refers to the initial immune defence and is activated rapidly by foreign pathogens and tissue damage. This includes dendritic cells, macrophages and neutrophils. The adaptive immune response is targeted towards a specific antigen and has the capacity for ‘memory’ to allow rapid response in case of future exposure. The principal cells forming the adaptive immune response are T cells and B cells and the host immune response to cancer is of vital importance and the degree of immune cell infiltration can be correlated to prognosis and disease outcome.

Immune cell infiltration has been shown to be associated with prognosis in ovarian cancer. The 5-year survival in tumours with T cell infiltration was 38% compared to just 4.5% in those with no T cell presence. It was also predictive of whether optimal surgical debulking was achieved, with those with high T cell infiltration being more likely to achieve complete cytoreduction (60). How the different

immune populations interact is important; infiltration of CD4 regulatory T cells alongside CD8 cells worsens prognosis thus a high CD8/CD4 Treg ratio is associated with improved prognosis (61). Intraepithelial tumour-infiltrating lymphocytes (TILs) have been shown in a meta-analysis to predict outcome in ovarian cancer (62). The balance between immunosuppressive activity and immunostimulatory cells demonstrates the importance of the tumour microenvironment and immune response and how manipulation with immunotherapy may be beneficial in ovarian cancer.

1.2.1 Myeloid-derived suppressor cells

1.2.2 Nomenclature

Myeloid-derived suppressor cells (MDSC) were originally described over twenty years ago when they were identified by their ability to suppress immune function and enable tumour progression in mice (63,64). The term 'myeloid-derived suppressor cells' was coined by Gabrilovich et al in 2007 (65) to replace their previous description as 'immature myeloid cells' or 'myeloid suppressor cells'. MDSC play a role in a multitude of pathological conditions including cancer, chronic inflammation, graft-versus-host disease, infection and trauma (66).

Two main populations of MDSC have been identified; monocytic-MDSC (m-MDSC) and granulocytic-MDSC (PMN-MDSC). This nomenclature denotes their primary myeloid lineage but is likely to be greatly over simplified as MDSC represent a spectrum of alternatively differentiated myeloid cells which could lie anywhere between the common myeloid progenitor and a terminally differentiated mature and committed cell, such as a macrophage. This diversity of cell subtypes makes their identification challenging as they do not form a distinct population.

Original studies on MDSC were performed on mice where they are more readily identified through the expression of Gr-1 and CD11b (67,68). In humans, however, there is not yet a defining marker to aid their identification and, as such, a series of phenotypic features are used. The common positive markers for both m-MDSC and PMN-MDSC are CD11b, representing their myeloid lineage, and CD33 denoting their relationship to leucocytes. Monocytic-MDSC are CD14 positive, expressed mainly by macrophages but also dendritic cells, and are HLA-DR negative. This separates them from a mature antigen-presenting cells as it is the HLA-DR surface receptor that forms the MHC class II receptor and plays an important role in activation of CD4+ T cells. The absence of this receptor thus contributes to the immunosuppressive phenotype. Granulocytic-MDSC are CD15 positive (69), a protein expressed by granulocytes and monocytes and is involved in chemotaxis and phagocytosis. Recently, lectin-type oxidised low-density-lipoprotein receptor-1 (LOX-1) has been identified on the surface of PMN-MDSC (70). MDSC lack the markers for mature T-cells, B-cells and NK cells and are thus defined as 'lineage negative' or lin^- (71). It is thought that growth factors such as GM-CSF, G-CSF, IL-6 and PGE2 act

upon STAT 3 in the haematopoietic stem cell to stimulate growth and expansion and then require a second signal, such as PGE2, LPS and IFN is required to activate the cells into MDSC (72) (Figure 1.4).

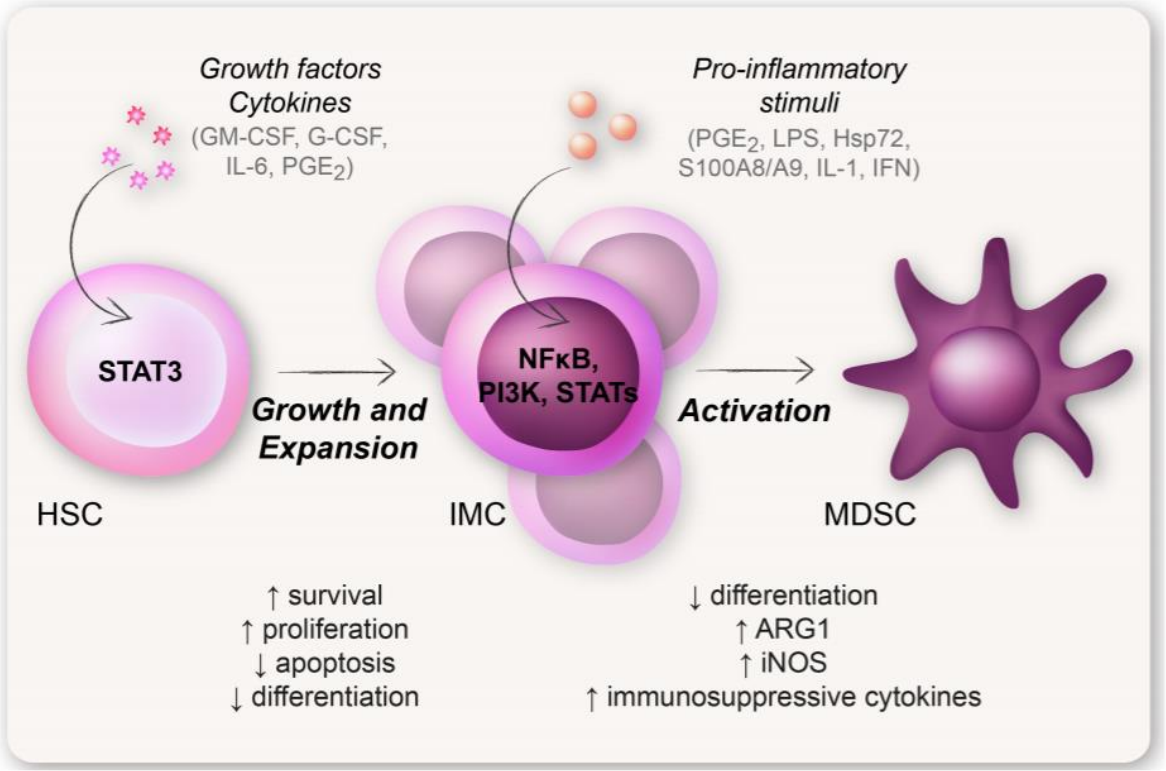

Figure 1. 4 The two-signal hypothesis of MDSC generation.
Growth factors and cytokines, such as colony-stimulating factors (G-CSF, GM-CSF), act though STAT3 to increase the production of immature myeloid cells from the bone marrow. Once stimulated by pro-inflammatory stimuli they become activated and develop the MDSC phenotype and characterisation. HSC haemopoietic stem cell, IMC immature myeloid cell. Millrud, Camilla & Bergenfelz, Caroline & Leandersson, Karin. (2016). On the origin of myeloid derived suppressor cells. Oncotarget. 8. 10.18632/oncotarget.12278.

1.2.3 Role in immune response

MDSC are emerging as a topic of particular interest due to their potential role in inhibiting immune responses and this could represent a novel therapeutic target. MDSC have been shown in a meta-analysis to hold prognostic value in patients with solid tumours such as hepatocellular carcinoma and gastro-intestinal cancers (73). Of note, ovarian cancer was not included in this study.

When an individual is exposed to an acute insult, an immune response is initiated through engagement of toll-like receptors (TLR), damage-associated molecular patterns (DAMPs) and pathogen-associated molecular patterns (PAMPs) (74,75). This enables expansion of inflammatory cells from the bone marrow into inflamed tissue, resulting in a controlled immune response which comes under control following limitation of the insult and leads to a return to homeostasis. In contrast, under the influence

of chronic stressors such as ongoing inflammation or malignancy, the immune system is continually activated and leads to overproduction of granulocyte-colony stimulating factor (G-CSF), monocyte-colony stimulating factor (M-CSF) and granulocyte-macrophage-colony stimulating factor (GM-CSF) causing expansion and proliferation of MDSC populations. This prolonged myeloid activation causes inefficient phagocytosis and the production of immunosuppressive cytokines and factors such as arginase-1, prostaglandin E2, reactive oxygen species (ROS) and nitric oxide (NO) (69). It is within this environment that tumours can flourish (Figure 1.5).

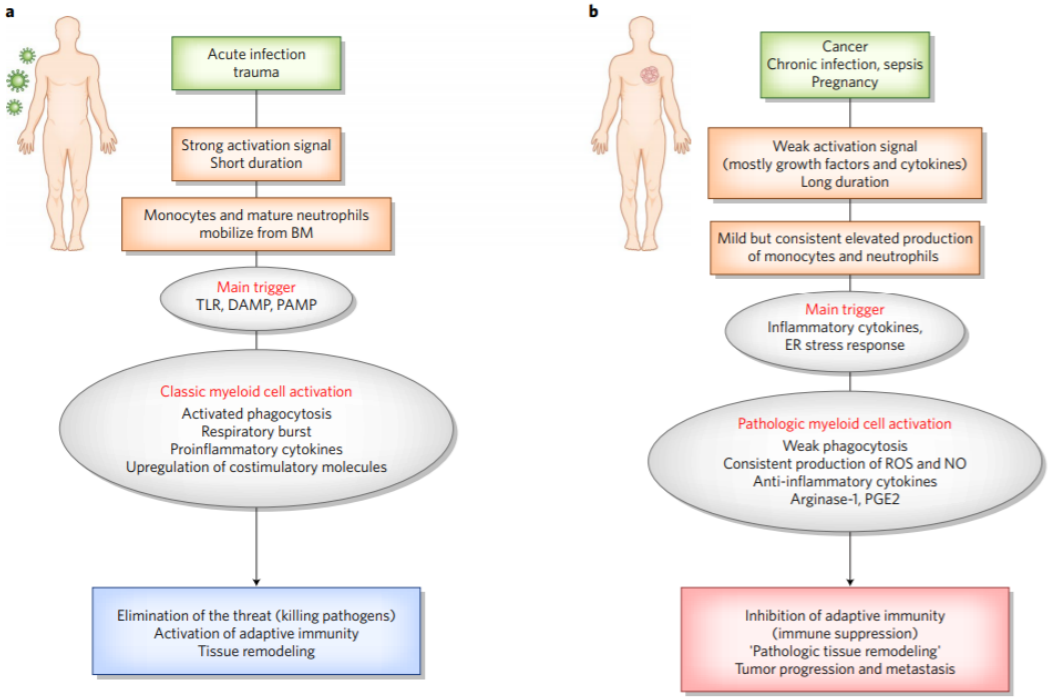

Figure 1. 5 The pathological activation of the immune response.
Source: Veglia F, Perego M, Gabrilovich D. Myeloid-derived suppressor cells coming of age. Nat Immunol. 2018 Feb;19(2):108-119. doi: 10.1038/s41590-017-0022-x. Epub 2018 Jan 18. PMID: 29348500; PMCID: PMC5854158.

MDSC manipulate the immune system through both the adaptive and innate immune systems (76). They have a direct effect on macrophages through MDSC production of IL-10, causing reduced production of IL-12 and converting them from immunocompetent tumour-attacking cells (so-called M1 response) to an immune-suppressive tumour-facilitating role (M2 response) (67). Their actions on the adaptive immune system are complex and wide-ranging and affect the function of natural killer (NK) cells, CD4 and CD8 T cells. They also have non-immunological tumour-facilitating properties, such as producing the type 4 collagenase enzyme MMP9 and the ability to differentiate into tumour-like endothelial cells, both of which support angiogenesis but also tumour invasion and metastasis (77,78).

1.2.4 MDSC in ovarian cancer

Tumour-infiltrating MDSCs have been identified within epithelial ovarian cancer and are associated with shorter disease-free interval and overall survival (79,80). M-MDSC were found to be increased in peritoneal fluid, peripheral blood and tumour tissue in comparison to healthy donors, whereas PMN-MDSC showed only a greater accumulation in tumour tissue. Both m-MDSC and PMN-MDSC were present in greater abundance in tumour rather than peripheral blood. The accumulation of m-MDSC within the tumour was associated with more advanced disease (both grade and stage of disease), however this was not seen with the PMN-MDSC population (79). MDSC have been found to increase the metastatic potential of tumours through modulation of gene transcription. They do this though increasing production of microRNA-101 which regulates cell 'stemness', their ability to self-renew and proliferate, and increases cell survival (80).

In mouse models the immunosuppressive effect in ovarian cancer has been found to occur through the production of IL-10, inducible NOS (iNOS), and arginase which act through the Stat-3 pathway, presenting another potential therapeutic target (81). However, inherited allelic variation within genes associated with MDSC function have not been found to correlate with prognosis in epithelial ovarian cancer (82).

In order to develop into invasive tumours, epithelial cells typically undergo a process of loss of epithelial markers and instead express a mesenchymal phenotype, a process known as epithelial-to-mesenchymal transition (EMT). Those cancers with greater expression of mesenchymal markers, i.e., those with greater EMT, have been associated both with increased infiltration of MDSC and reduced CD8+, and a poorer prognosis. This is mediated through the increased production of the ligands CXCL1 and CXCL2 acting upon the receptor CXCR2. CXCR2 has been found to be raised in MDSC in ovarian cancer and associated with poorer prognosis (83).

As well as research into the local tumour microenvironment, the investigation of circulating metabolites can indicate the involvement of immunosuppressive cells. Homing of immune cells, including MDSC, to the site of tumour occurs via chemotaxis controlled by factors such as vascular endothelial growth factor (VEGF) (84) and prostaglandin E2 (PGE2) (85). PGE2 is released by ovarian cancer tumours and causes migration of MDSC into ascites and the tumour microenvironment (85). VEGF has been shown to be elevated in the serum of women with serous ovarian cancer in comparison to control (86), whilst increased serum arginase has been identified in women with ovarian cancer. MDSC are a major producer of IL-10 which impacts on T cell function and mediates MDSC-related immunosuppression. IL-10 in serum and ascites is associated with worse prognosis in ovarian cancer and its blockade in mouse models has been associated with improved survival (87).

1.2.5 PMN-MDSC: activated neutrophils or a separate discrete entity?

There is increasing interest in the debate as to whether PMN-MDSC are actually tumour-associated neutrophils. Singel et al demonstrated that mature neutrophils are able to cause T cell immunosuppression through direct cell-cell communication and complement release. These neutrophils were derived from peripheral blood and ascites of patients with newly diagnosed epithelial ovarian cancer, however it was also demonstrated this effect with malignant effusions from other cancers, demonstrating its applicability in malignancy as a whole (88). The appearance of MDSC were initially thought to be 'immature' demonstrating a banded-shaped nucleus, however this has subsequently been disproved and in fact the more 'mature'-appearing neutrophils actually provide the greatest immunosuppression (89).

The markers used for the identification of MDSC are classically CD33 and CD11b, which are broad-ranging markers present on all cells of myeloid lineage and natural killer cells, whilst CD15 positivity is also expressed by both neutrophils and eosinophils. In mice, there have been dedicated markers identified, however this is yet to be the case for humans (90). Condamine et al demonstrated the marker of endoplasmic reticulum (ER) stress, leptin-like receptor for oxidised LDL (LOX-1), as a potential marker for PMN-MDSC. They demonstrated that cells with an immune-suppressive function were typically LOX-1 positive compared with primary neutrophils which were not immunosuppressive and LOX-1 negative. They identified LOX-1 positive cells representing up to 15% of circulating neutrophils and 15-50% of tumour-infiltrating neutrophils within the cancer specimens, compared with <1% in healthy donors. LOX-1 was also suggested to be a specific marker within cancer patients as those with chronic inflammatory conditions were also investigated but not found to have significantly raised LOX-1+ cell numbers (70). However a recent study by Rahman et al has shown that LOX-1 positivity on low-density granulocytes isolated from patients with systemic lupus erythematosus was associated with a heightened immune response rather than immunosuppression, demonstrating that there is further research required into the expression of LOX-1 and its potential association with immunosuppression (91).

Additionally, purified neutrophils taken from healthy donors have been shown to have MDSC activity following activation, suggesting that instead of them being a different cell population, they are the same cells along a spectrum of activation determined by their surrounding environment (90). A study by Trovato et al. on patients with pancreatic ductal adenocarcinoma recently demonstrated that although there is an increased accumulation of myeloid cells such as MDSC at the site of tumour and in circulating blood, the presence of subtypes of MDSC1, 3 and 4 did not correlate with patient survival and only MDSC2 demonstrated a poorer prognosis over a specific threshold in fresh blood. The subtypes were identified by their surface marker expression: MDSC1 was CD14+IL-4Rα+, MDSC2 was CD15+IL-4Rα+, MDSC3 was Lin−HLA-DR−CD33+ and finally, MDSC4 was identified as

CD14+HLA-DR−/low. When investigating their immunosuppressive effects, PMN-MDSC suppressed at high ratios of 1:6 (T cell:PMN-MDSC), a ratio unlikely in the tumour microenvironment, whilst m-MDSC were suppressive at ratios of 1:1. On further analysis, however, not all m-MDSC were suppressive; indeed of the 26 patients enrolled in this study, only 6 demonstrated evidence of immunosuppression at ratios of 1:3. They concluded that in those with the immunosuppressive phenotype, there was increased metastatic potential (92). This further highlights that the immunosuppression demonstrated by MDSC is somewhat patient-dependent and not a universal property heralded by all cells with the phenotypic characterisations of MDSC.

Lastly, PMN-MDSC have been described classically as low-density cells and, as such, following density centrifugation they reside in the peripheral blood mononuclear cell (PBMC) layer whilst the granulocytes collect in the high-density fraction. It has been found, that activated neutrophils can reside in the low-density fraction, whilst PMN-MDSC can be found in the high-density portion, therefore potentially providing misleading proportions of the cell populations (93). Following the potential overlap between PMN-MDSC and neutrophils, one could consider these cells as 'alternatively-activated' neutrophils. Regardless of nomenclature, their role in immunosuppression in the tumour microenvironment in cancer is a potential target for therapy and therefore is still of interest and needs further investigation.

1.2.6 Ascites

More than one third of women present with evidence of ascites (26,27,94) and unlike most malignancies, where the presence of ascites indicates advanced disease with survival of around 11% after 6 months (95), in ovarian cancer it is associated with a 5-year survival of 27% (3). This suggests that the composition and pathophysiology surrounding the accumulation of ascites in ovarian cancer is unique in comparison to other malignancies. Ascites is potentially an important mediator for the propensity for ovarian cancer to metastasise. Once tumour cells have undergone EMT and detached from their host site, they can form spheroids, which are aggregates of tumour cells. They do retain some of their epithelial phenotype enabling them to invade on to the peritoneal surface. The spheroids are less susceptible to chemotherapy due to their reduced proliferative capacity and limited drug penetration so play an important role in tumour recurrence. The ascites itself is a milieu of a multitude of chemokines and cytokines that can support tumour growth and development, such that areas of greatest contact with ascites; the pouch of Douglas, right subphrenic space and the greater omentum, are the most likely sites for metastatic deposition (26). A study performed by Elwan et al. investigated the presence of MDSC in benign versus malignant disease and in the ascites of both conditions. They examined normal subjects, patients with liver cirrhosis and patients with hepatocellular carcinoma (HCC). Their results showed a significant increase in MDSC in the peripheral blood from the control

cohort and those with cirrhosis and a further significant increase between cirrhosis and HCC. They also demonstrated low levels of MDSC in the ascitic fluid indicating they favour accumulation in peripheral blood over ascitic fluid (96). This is in contrast to the findings in ovarian cancer where it has been reported there is a great infiltration of m-MDSC within malignant ascites (85,97) with resulting poorer prognosis (98), however conflicting evidence suggests great heterogeneity within the infiltration and immunosuppressive capability of MDSC within ascites (99).

1.2.7 Chemotherapy effects on MDSC activity

The first line chemotherapy in ovarian cancer is platinum-based therapy. Oxaliplatin (usually used as first line in colorectal carcinoma) has been found to reduce the suppressive action of MDSC post-therapy through reduction in MDSC number and increased tumouricidal T cell populations such as CD8 with a reduction in immunosuppressive Tregs (100). Cisplatin has also been shown to have immune-modulating effects including the upregulation of MHC 1 expression, the recruitment, proliferation and increased lytic action of effector cells and through dampening the immunosuppressive microenvironment. These effects have been demonstrated in both pre-clinical and clinical settings (101). Cisplatin has been shown in murine models to reduce the number of MDSC's in tumour-bearing mice (102) and when used in combination with paclitaxel can also simultaneously decrease the regulatory T cell infiltration (103).

Gemcitabine has been found to have many positive immunomodulatory effects, including reducing the number of MDSC whilst increasing the M1 response in patients with platinum-resistant p53-positive tumours. There was no increase in M2 response and it reduced the number of Tregs thus reducing the immunosuppressive capacity of the tumour (104). Other effects found in pancreatic cancers include the increase of T memory cells (105), monocytes and macrophages (106). For this reason, gemcitabine has been considered as an adjunct to other immunotherapies in order to prime the microenvironment to improve the efficacy of additional agents.

1.2.9 Use of immunotherapy in ovarian cancer

Therapeutic targeting of immune checkpoint molecules has proved very successful in various cancers including bladder and renal cell cancers but this has not been demonstrated in ovarian cancer. There are multiple reasons for this including 1) tumour heterogeneity, 2) low intrinsic ability to induce an immune response and 3) plasticity in overcoming targeted immune receptor blockade (107).

Programmed cell death-1 (PD-1) is a transmembrane protein found on many immune cells including T cells, natural killer cells, dendritic cells, activated monocytes and B cells. Its ligand PD-L1 is expressed on activated immune cells as well as on tumour cells. Activation of the PD-L1/PD-1 pathway causes T

cell inertia resulting from inhibition of T cell activation and subsequent immunosuppression. Through blockade of this pathway the immune system can be re-sensitised and cause tumour cell destruction (108). PD-L1 has been found to be present in all ovarian cancer subtypes but to a greater degree in serous ovarian cancer, with over half of cases showing PD-L1-positivity (109). The expression of PD-L1 is inversely proportional to the prognosis (110–112). Agents such as nivolumab have been trialled in platinum-resistant ovarian cancer and have demonstrated safety and clinical efficacy with 45% achieving disease control (113).

Chemotherapy can alter immune function; exposure to paclitaxel caused an increased expression in PD-L1 in the tumour cell line (114), whilst cisplatin increased PD-L1 in HCC (115), therefore potentially advocating the use of combination therapy of paclitaxel with PD-L1 blockade. In an ovarian cancer mouse model it was found that paclitaxel increased infiltration of CD8+ cells and increased expression of PD-L1 thus with combined treatment with PD-L1 blockade there was an improved survival compared to paclitaxel monotherapy (116). Other immunotherapies and targeted therapies implicated in the treatment of ovarian cancer include PARP inhibitors, monoclonal antibodies against VEGF (Bevacizumab), EGFR (cetuximab) and CTLA-4 (tremelimumab and ipilimumab). Although in their infancy, research into the use of these adjuncts in combination with PD-L1 blockade have shown clinical efficacy and safety (25,108).

1.3 Future role of immunomodulation through targeting MDSC

Due to the vast heterogeneity displayed by ovarian malignancy, discovering the ‘silver bullet’ to treat it has proven very challenging. The development of cancer vaccine technologies aim to increase the host immune response to the tumour but this has been met with limited efficacy due to immunosuppressive factors such as PD-1, poor invasion of T effector cells, post-operative immunosuppression and MDSC infiltration. Immunisation followed by myeloid-depletion to reduce the MDSC population and hence immunosuppression within murine models has been shown to delay tumour progression (99).

1.4 Conclusion

Research into the role of the immune system and infiltration into the tumour microenvironment is still in its infancy, especially in ovarian cancer. Likely due to the heterogeneity displayed by ovarian cancer, the results of immunotherapy have been variable and research into the immune microenvironment has displayed some conflicting results. As such, more research is required to further interrogate the pathways of immune activation and its effect on tumour cells in order to identify novel immunotherapies

which effectively target tumour cells specifically without wide-ranging systemic effects caused by current chemotherapeutics.

This thesis sets out to further investigate the role of MDSC within the ovarian cancer tumour microenvironment and their functional role, whilst assessing their relationship with patient outcome and prognosis.

1.5 Hypothesis

The hypothesis for this project was that MDSC were present in ovarian cancer and its metastatic deposits. It was also hypothesised that the MDSC would be absent in benign disease and healthy donor specimens.

1.6 General aims and objectives

The aims of this project were:

- To identify the presence of MDSC in ovarian cancer and to compare this to benign disease and healthy donor specimens
- To demonstrate that the MDSCs have an immunosuppressive effect through reducing T cell proliferation
- To further characterise the myeloid compartment in omental metastatic disease and identify any upregulated genes that could play a role in immunosuppression.

The objectives of this project were:

- To use fresh blood and tissue samples from healthy donors and patients for analysis by flow cytometry to identify MDSC using cell surface markers
- To measure a reduction in T cell proliferation as a marker of immunosuppression following co-incubation with MDSC
- To use 10x single cell sequencing to further characterise the myeloid compartment in the omental metastasis of ovarian cancer

Chapter 2

Materials and Methods

2.0 General Laboratory Practice

All experiments were undertaken to University of Birmingham standards for safe working with chemical substances in laboratories. All standards comply with the Control of Substances Hazardous to Health Regulations (COSHH).

2.0.1 Ethical approval

All clinical samples were taken following written consent from patients in accordance with the Declaration of Helsinki as approved by the Health Research Authority and University of Birmingham (IRAS project ID 225991, protocol number RG 17-225). All samples were stored in compliance with the Human Tissue Act (2004).

2.0.2 Subjects and sample collection

Patients were approached to be included in the study if they had a diagnosis of an ovarian mass at either City Hospital Birmingham or New Cross Hospital Wolverhampton between October 2018 and March 2020. Phlebotomy was performed at the time of induction of anaesthesia into heparinised BD Vacutainer® (NJ, USA) tubes, aiming for 12ml of blood per patient. The tissue samples were taken upon surgical removal in theatre, except when the ovarian mass was contained within the ovary with no evidence of metastatic spread. In this case the specimen was taken to pathology and a small section was removed following thorough examination with the Pathologist, in order to avoid affecting the patients' clinical staging. If the capsule is breached prior to the receipt of the specimen by the pathologist, this can up-stage the patients' condition erroneously. Specimens included ovarian tumour, normal ovary, omentum and sites of metastatic spread such as the peritoneum and visceral serosal surfaces. The samples were anonymised at source, stored in basic media and transported to the laboratory as per our ethical requirements.

2.1 Cell Culture

2.1.1 Basic media

The tissue culture media used throughout the experiment is outlined below unless otherwise stated and will be referred to as 'general media' or 'GM'. Media was stored at 4°C and supplemented with antibiotics and foetal bovine serum.

RPMI 1640: 500ml bottles of sterile liquid (Gibco®, ThermoFisher Scientific, MA, USA) supplemented with 2mM L-glutamine and adjusted to pH 7.0. For general use 10% foetal bovine serum and 1% penicillin/streptomycin was added.

2.1.2 Supplements and sterile solutions

Foetal bovine serum (FBS): Sterile liquid in 500ml bottles pre-screened for viral and mycoplasma contamination (Gibco®, ThermoFisher Scientific, MA, USA). Long-term storage at -20°C. Fifty millilitres aliquots added to 500ml basic culture media.

New born Calf Serum: Sterile liquid in 500ml bottles pre-screened for viral and mycoplasma contamination (Gibco®, ThermoFisher Scientific, MA, USA). Long-term storage at -20°C.

Penicillin/Streptomycin: Sterile liquid in 100ml bottle containing 10,000 units/ml penicillin and 10mg/ml streptomycin (Sigma Aldrich, MO, USA). Five millilitres aliquots stored at -20°C. Five millilitres added to 500ml basic culture media.

Lympholyte-H: Sterile liquid in 500ml bottle stored at 4°C (Tebu-Bio, UK). Used for density gradient separation for the isolation of viable lymphocytes and monocytes from peripheral blood samples. Used at room temperature.

Red Blood Cell (RBC) Lysis Buffer: Sterile liquid in 1 litre bottle stored at 4°C (Cambridge Bioscience, UK).

Accutase cell dissociation reagent: Sterile liquid in 100ml bottle (Gibco®, ThermoFisher Scientific, MA, USA). Fifteen millilitres aliquots stored at 4°C, protected from light. Long-term storage at -20°C.

Phosphate Buffered Saline (PBS) without Ca^{2+} and Mg^{2+}: Sterile liquid 500ml bottle (Sigma-Aldrich, MO, USA). Stored at room temperature.

Ethylenediaminetetra acetic acid (EDTA) 0.5M: Sterile liquid in 100ml bottle stored at 4°C (Corning, NY, USA).

MACS buffer: Sterile liquid made with PBS (Sigma-Aldrich, MO, USA), 2% new born calf serum (ThermoFisher) and 2 millimoles of EDTA (Corning, NY, USA). Stored at 4°C.

Primocin: Sterile liquid in 1ml vial (50mg/ml) stored at -20°C (InvivoGen, CA, USA). Added to media where stated at 1:1000 concentration.

Opsonised zymosan A: 250mg powder formulation derived from Saccharomyces cerevisiae, consisting of protein-carbohydrate complexes (Sigma Aldrich, MO, USA). Stored at 4°C. Prepared by reconstituting the opsonised zymosan A powder in PBS at a concentration of 10mg/ml.

2.1.3 Antibodies and cytokines

Human FcR Blocking Reagent: Liquid in 2ml bottle stored at 4°C (Miltenyi Biotec, Germany). Fifteen microlitres used per sample to increase the specificity of staining by minimising non-specific antibody binding.

Propidium Iodide (PI): Liquid in 2ml bottle stored at 4°C (Miltenyi Biotec, Germany). To each sample, 1.5µl was added to exclude dead cells from flow cytometric analysis.

Recombinant Human Interleukin-6 (IL-6) (carrier-free): Sterile solution aliquoted on arrival to prevent multiple freeze-thaw episodes, and stored at -20°C (BioLegend).

Recombinant Human Granulocyte-Macrophage Colony-Stimulating Factor (GM-CSF): Sterile solution aliquoted on arrival to prevent multiple freeze-thaw episodes and stored at -20°C (BioLegend).

Anti-Human CD3 antibody: 500µl vial (ThermoFisher Scientific) stored at 4°C protected from light.

Anti-Human CD28 antibody: 500µl vial (ThermoFisher Scientific) stored at 4°C protected from light.

LIVE/DEAD™ Fixable Red Dead Cell Stain Kit: 10 vials of LIVE/DEAD™ stain (solid) with 500µl DMSO to be reconstituted as per protocol (ThermoFisher Scientific). Stored at -80°C.

The antibodies used for the flow cytometry panel in the identification of MDSC are shown in Table 2.1.

Target antigen	Conjugate	Supplier	Volume used per sample (microlitres)
CD3	PE Dazzle	BioLegend, CA, USA	3
CD19	PE Dazzle	BioLegend, CA, USA	3
CD56	PE Dazzle	BioLegend, CA, USA	3
CD11b	BV510	BioLegend, CA, USA	4
CD45	AF700	BioLegend, CA, USA	4
CD14	APC Fire	BioLegend, CA, USA	4
CD15	PerCPCy5.5	BioLegend, CA, USA	4
HLA-DR	BV421	BioLegend, CA, USA	4
CD163	APC	BioLegend, CA, USA	4
LOX-1	PE	BioLegend, CA, USA	5

Table 2. 1. Myeloid-derived suppressor cell antibody panel for flow cytometry

2.1.4 Cell isolation / activation products

MS Columns: Columns designed for positive cell isolation (Miltenyi Biotec, Germany) used in conjunction with MiniMACS™ separator.

EasySep™ Human T Cell Isolation Kit: Contains 2 component vials: EasySep™ Human T Cell Isolation Cocktail and EasySep™ Dextran RapidSpheres™ 50103. Both vials contain 1ml sterile liquid and are stored at 4°C (StemCell™ Technologies, Vancouver, BC, Canada).

Dynabeads® Human T-Activator CD3/CD28: superpara-magnetic, 4.5µm polymer beads coated with monoclonal antibodies against CD3 and CD28 cell surface molecules. Suspended in 2ml sterile liquid and stored at 4°C (Gibco®, ThermoFisher Scientific, MA, USA).

Invitrogen™ eBioscience™ Cell stimulation cocktail 500x: Vial containing 100µl of cell stimulation cocktail stored at -20°C protected from light (Invitrogen™, ThermoFisher Scientific, MA, USA). It contains a combination of phorbol 12-myristate 13-acetate (PMA) and ionomycin; known to activate many cell types and is used in functional assays.

Immunocult™ Human CD3/CD28 T Cell Activator: 2ml sterile vial stored at 4°C (StemCell™ Technologies, BC, Canada). Tetrameric antibody complex that activates and expands human T cells without the requirement for magnetic beads, antigens or feeder cells.

CellTrace™ Violet cell Proliferation Kit: fluorescent dye used to distinguish cell division to assess proliferation. Kit contains 9 vials of CellTrace™ Violet (lyophilised powder) and a 500µl vial of DMSO, all stored at -20°C (ThermoFisher Scientific, MA, USA). To reconstitute CellTrace™ violet

dye, 20µl of DMSO is added to violet dye desiccate and pipetted to dissolve. To use, 1µl violet dye suspension per 1 x 10^6 cells in 1ml of serum-free media.

CD15 microbeads: Two millilitres bottle containing microbeads conjugated to monoclonal mouse anti-human CD15 antibodies (Miltenyi Biotec, Germany). Stored at 4°C protected from light.

Carboxyfluorescein succinimidyl ester (CFSE): fluorescent cell permeable cell staining dye (ThermoFisher Scientific, MA, USA).

LIVE/DEAD™ Viability/Cytotoxicity Kit: two-colour assay to determine cell viability through detecting plasma membrane integrity using fluorescence (Invitrogen™, ThermoFisher Scientific, MA, USA).

2.2.0 Identification and enumeration of Myeloid-Derived Suppressor Cells

2.2.1 Preparation of whole blood

Whole blood was collected, as per our ethics approval, into sterile blood collection tubes containing sodium heparin (BD Vacutainer™) and stored at room temperature in the dark overnight. The blood samples were added to pre-warmed GM in equal volumes and mixed. The whole blood was layered over Lympholyte®-H at room temperature (same volume used as per starting volume of blood collected) and centrifuged at 2000rpm at 21°C for 30 minutes with the deceleration set at 1. The outcome of density centrifugation is shown in Figure 2.1.

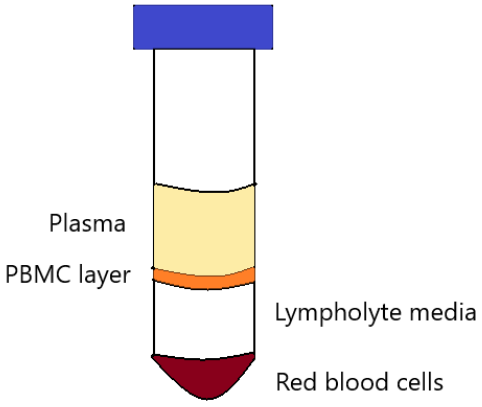

Figure 2. 1 Blood separation following density centrifugation with Lympholyte®-H.
The peripheral blood mononuclear cell (PBMC) layer contains cells with a round nucleus such as NK cells, T cell and B cells, as well as MDSC. Erythrocytes, multinucleated cells such as neutrophils, and dead cells sediment to the bottom of the tube to form a pellet. Platelets are predominantly positioned within the plasma layer.

The PBMC layer was harvested and added to a fresh tube and topped up with GM. This was centrifuged at 1500rpm for 10 minutes at 21°C. The supernatant was discarded and the pellet resuspended in 10ml GM and centrifuged at 1200rpm for 10 minutes at 21°C. The supernatant was again discarded and the pellet resuspended in 10mls GM and counted on the haemocytometer. PBMC's were identified using light microscopy by their physical characteristics, and contain lymphocytes, monocytes and dendritic cells, following exclusion of erythrocytes and granulocytes through density centrifugation. One million PBMC were removed from the sample, as calculated from the concentration of cells identified through counting using the haemocytometer, and transferred into a 5ml FACS tube and topped up to 3-4mls with PBS.

2.2.2 Preparation of tissue samples

2.2.3 Non-enzymatic tissue digestion

Tumour specimens were retrieved with patient consent as per our ethics approval. The fresh specimens were manually minced in to 2mm pieces and plated out in sterile 6-well tissue culture plates and GM was added. The specimens were then incubated at 37°C, 5% CO_2 overnight.

The following day the tissue was agitated further and the GM, enriched with immune cells, was harvested using a transfer pipette into a 50-micron filter (CellTrics, Sysmex-Partec, Germany) over a 15ml tube. The wells were washed with GM media three times to obtain any residual single cells within the filter. The sample was centrifuged at 1500rpm for 10 minutes at 21°C, the supernatant was discarded and 2ml RBC lysis buffer was added to the resuspended pellet depending on the degree of erythrocyte contamination. This was left for 10 minutes at room temperature then topped up to 10mls with GM and centrifuged again at 1500rpm for 10 minutes at 21°C. If the sample was particularly blood-stained this process was repeated. The pellet was resuspended in 5mls GM and counted using a haemocytometer. At least 1 x 10^6 cells were transferred to a FACS tube (may require further centrifugation if too few cells in 5mls) and topped up to 3-4mls with PBS.

2.2.4 Enzymatic tissue digestion

The tumour samples were collected and stored overnight at 4°C in GM. The following day they were manually minced in to 2mm pieces and placed in a GentleMACS C Tube (Miltenyi Biotec) with 500µl 10x Collagenase/Hyaluronidase in DMEM. Five millilitres of pre-warmed GM were added to the sample then it underwent initial dissociation using the GentleMACS Dissociator on 'Human Tumour Programme 1.01'. The sample was incubated in a water bath at 37°C for 30 minutes. This was followed by the second dissociation using 'Human Tumour Programme 1.02' on the GentleMACS Dissociator

and re-incubated at 37°C for a further 30 minutes. The final dissociation was performed using 'Human Tumour Programme 1.03'.

The sample was passed through an EASY-strainer™ 100-micron filter which was washed out with GM following passage of the sample to retrieve any remaining single cells. This was then passed through an EASY-strainer™ 40-micron filter and the filter was washed with GM.

The sample was centrifuged at 1500rpm at 21°C for 10 minutes, supernatant discarded and the pellet resuspended in the residual volume. To this, 2mls of RBC lysis buffer was added and left to incubate at room temperature for 10 minutes. Following incubation, it was topped up with GM and centrifuged at 1500rpm for 10 minutes at 21°C. Tubes were topped up to 3-4mls with PBS.

2.3.0 Flow cytometry

2.3.1 Patient-derived PBMC and tissue samples

Once in a single cell solution containing 1 x 10^6 cells the FACS tubes were centrifuged at 1500rpm for 5 minutes at 21°C, the supernatant discarded and the pellet resuspended in the residual volume of PBS. The samples were stained with 15µl human FcR block and incubated for 10 minutes at room temperature. The antibody panels outlined in table 1 describes the antibodies used in each sample. The samples were incubated in the dark at 4°C for 25-30 minutes then topped up with 3mls PBS, centrifuged at 1500rpm for 5 minutes at 4°C and the supernatant discarded. The pellet was resuspended in the residual PBS and topped up with a few drops of PBS, followed by 1.5µl of propidium iodide (PI) to each sample prior to flow cytometric analysis using a Gallios flow cytometer (Beckman Coulter Life Sciences, US).

2.3.2 Analysis

All MDSC samples were analysed using FlowJo™ software (Becton, Dickson & Company, Canada). Statistical analysis was performed using GraphPad Prism version 8.

2.3.3 Gating strategy for MDSC

The gates were applied using known cell clusters according to their cell surface expression. Sequential gating was used in order to identify the cells as MDSC. The gating strategy is demonstrated in Figure 2.2.

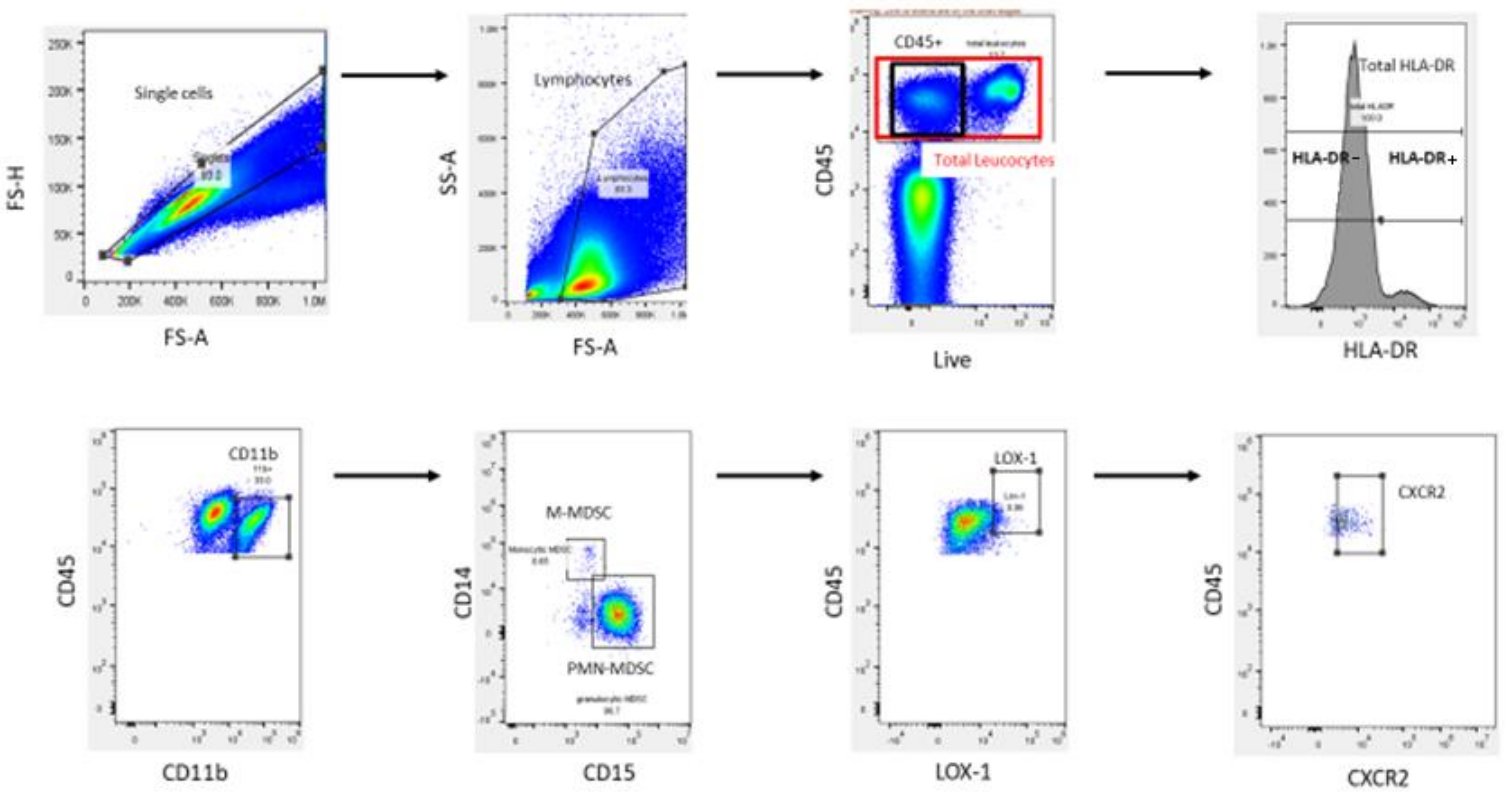

Figure 2. 2 Gating strategy to determine monocytic (M-MDSC) and granulocytic MDSC (PMN-MDSC). Sample shown in on PBMC.
Each panel is gated sequentially using the preceding panel's gate as the total population.

2.4.0 T cell Suppression Assay

Patient-derived samples

2.4.1. Isolation of CD15 positive tumour-infiltrating leucocytes (TILS) using CD15 microbeads

The TILs were obtained as described in the method above (2.2.2). The cells were centrifuged at 1500rpm for 10 minutes and resuspended in 500µl MACS buffer. Fifteen microlitres FcR block was added and incubated at room temperature for 5 minutes. TILs were washed with MACS buffer and resuspended in 250-500µl of MACS depending on cell concentration. Cells were stained with anti-CD15 microbeads as described by the manufacturer. MS Columns were washed with MACS buffer prior to use and the CD15+ labelled TILs were applied to the columns. Once the cell suspension had passed through the columns, they were washed twice with MACS buffer to remove unbound cells. The column was then inserted into a 15ml tube and 2mls of MACS was added to the column and the plunger applied. This effluent was enriched for CD15 positive cell population derived from the tumour specimen. They were centrifuged and resuspended at 1 x 10^6 / ml in GM media.

2.4.2. Preparation of PBMC as responder cells

The blood was prepared as described in 2.2.1 in order to obtain PBMC. Cells were counted and washed with PBS, then resuspended in PBS at 1 x 10^6 cells / ml. CellTrace™ Violet proliferation dye was reconstituted and used as per the data sheet. Briefly, protected from light, 20µl of DMSO was added to the purple dye and gently reconstituted. One microlitre of reconstituted dye was added per ml of PBMC and incubated for 20 minutes at 37°C. Following incubation, 5 times the volume of GM media was added to dilute excess dye and the cells were incubated for 5 minutes at 37°C, 5% CO_2 to quench the dye. The PBMC were centrifuged at 1500rpm for 10 minutes and resuspended in GM and counted using a haemocytometer. The cells were centrifuged and resuspended in media at 1 x 10^6 / ml.

2.4.3 Plating out proliferation assay

Fifty microlitres (5 x 10^4 cells) of PBMC were seeded into a 96-well flat-bottom plate to act as responder cells. To this, 50µl (5 x 10^4 cells) CD15+ TILs were added. Anti- CD3 and CD28 activating antibodies were added to the appropriate wells at a concentration of 0.6µg for CD3 and 0.4µg for CD28 per well. GM was added to each well to achieve a final volume of 200µl per well. The cells were incubated at 37°C for 4 days.

2.4.4. T cell proliferation detection

On day 4, cells were collected and each well washed out with PBS twice. The cell solution was centrifuged and resuspended in residual volume. To this, 5µg/ml anti-CD3 antibody (ThermoFisher Scientific) and LIVE/DEAD™ fixable red dead cell stain kit, reconstituted as per the data sheet, were added. Briefly, 50µl DMSO was added to a vial of LIVE/DEAD™ and mixed well. To each sample, 0.1µl of dye was added and were incubated with the anti-CD3 antibody for 30 minutes protected from light at 4°C. Three millilitres of MACS buffer was added to each sample and centrifuged at 1500rpm for 5 minutes at 4°C. The supernatant was discarded, pellet resuspended in residual volume and 1.5µl of PI was added to each sample, followed by a few further drops of MACS buffer. The sample was processed using a Gallios flow cytometer (Beckman Coulter Life Sciences) and data analysed using Kaluza analysis software (Beckman Coulter Life Sciences).

2.4.5 Gating Strategy for suppression analysis

The gating strategy was determined using Kaluza analysis software, using sequential gating to identify the target population of cells. The gating strategy is shown in Figure 2.3.

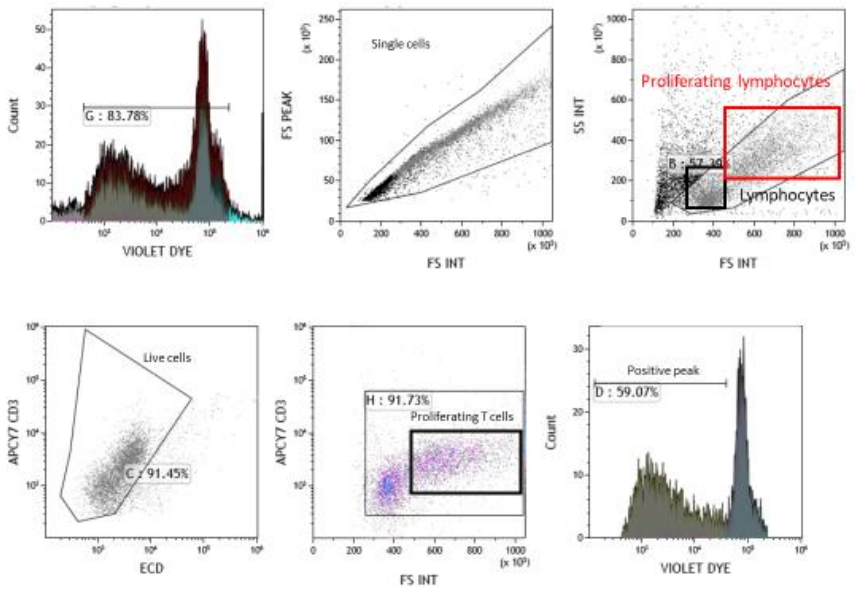

Figure 2. 3. Gating strategy for suppression assay.
Each panel is gated sequentially using the preceding panel's gate as the total population.

2.4.6 Isolating CD14+ and CD15+ TILS from tumour samples using FACS cell sorting

The PBMC responders were prepared as described above (4.1.2.).

The MDSC were prepared as described in 2.2.2. They were centrifuged and resuspended in 200-400µl of MACS buffer, depending on cell density. Fifteen microlitres of FcR block was added to the cells and incubated for 5 minutes prior to adding the following antibodies: HLA-DR BV421, CD11b BV510, CD14 APC Cy7 and CD15 PerCPCy5.5 (all BioLegend). These were incubated at 4°C protected from light for 25 minutes. The cells were topped up with MACS buffer and centrifuged at 1500rpm for 5 minutes, resuspended in 500µl MACS buffer and 1.5µl PI was added prior to sorting.

2.4.7 Cell sorting

The BD FACSMelody™ cell sorter was used to sort cells into CD15+ and CD14+ cells and CD14+ cells were further sorted into HLA-DR positive and negative into GM. The cells were centrifuged at 1500 rpm for 5 minutes and resuspended at 1 x10^6 ml. The gating strategy for sorting the cells is shown in Figure 2.4.

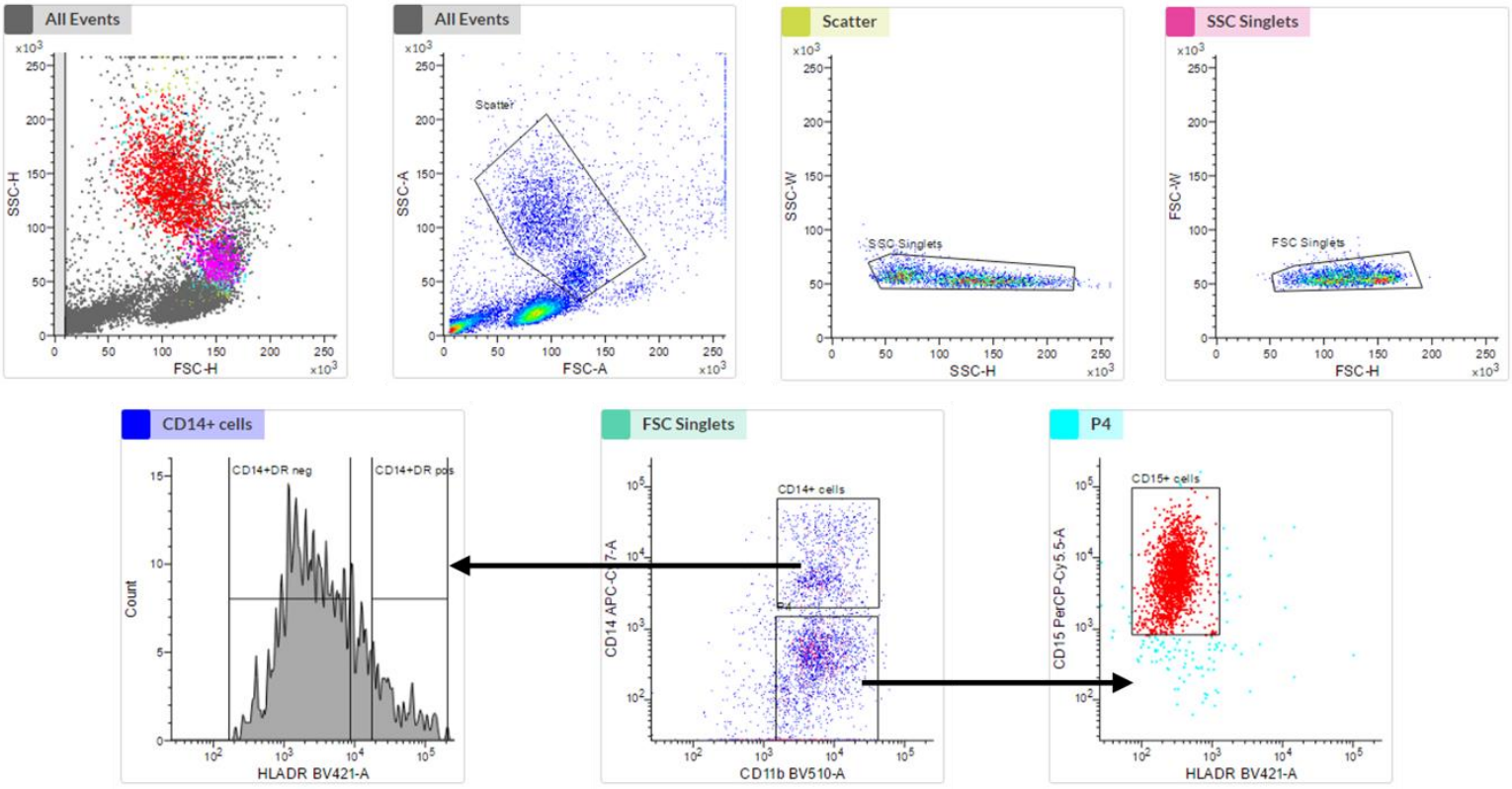

Figure 2. 4. Gating strategy for identification of m-MDSC and PMN-MDSC.
The gating used included CD15+ cells, and CD14+ cells with HLA-DR+ and HLA-DR- gates.

2.4.8 Plating out suppression assay

To a 96-well flat-bottom plate, 50µl (5 x 10^4) of PBMC were added, along with 50µl (5 x 10^4) of desired MDSC to achieve a 1:1 ratio. For ratios of 1:0.5, 1:0.25 and 1:0.1; 25µl, 12.5µl and 5µl of MDSC were added to 50µl of PBMC. The CD3 and CD28 antibodies were added at concentrations of 0.6µg and 0.4µg per well, respectively. GM media was added to each well to give a total volume of 200µl and incubated at 37°C for 4 days.

2.4.9 Harvesting cells from suppression assay

On day 4 the cells and media were aspirated from the wells and then each well was washed with PBS twice to collect any residual cells. The sample was centrifuged at 1500 rpm for 5 minutes at 4°C. Fifteen microlitres FcR block was added and incubated at room temperature for 5-10 minutes. To this the following antibodies were added: 5µl CD3 APCy7 (BioLegend), 5µl CD14 PE Dazzle (BioLegend) and LIVE/DEAD™ red stain (ThermoFisher) 0.1µl per sample. The cells were incubated at 4°C protected from light for 25 minutes then washed with MACS buffer, centrifuged and resuspended in

residual MACS and topped up with a few drops of MACS buffer prior to flow cytometry. The same gating strategy was used as described in 4.1.5.

2.5 Development of positive control for suppression assay

2.5.0 Cytokine-induced MDSC polarisation from peripheral blood

PBMC from a healthy donor was obtained and prepared as described in 2.2.1. The PBMC were counted on a haemocytometer and then centrifuged at 1500rpm for 10 minutes at 21°C, supernatant discarded, and resuspended at 2 x 10^6/ml with pre-warmed GM. The PBMC were seeded into T75 flasks (Corning®, US) with 10mls per flask (2 x 10^7 cells). To each flask, 10ng (1ng/ml) IL-6 and 10ng (1ng/ml) GM-CSF was added and the flasks were stored horizontally in the incubator at 37°C, 5% CO_2 for 7 days. The media was changed on day 3 by removing 5mls of the culture media, centrifuging at 1500rpm for 5 minutes at 21°C then discarding the supernatant. The pellet was resuspended in 5mls GM containing 20ng/ml IL-6 (BioLegend) and GM-CSF (BioLegend) to allow a final concentration of 10ng/ml when added to the remaining media in the flask.

2.5.1 MDSC harvesting and antibody staining

The T75 flasks containing *in vitro* generated MDSC were removed from the incubator following 7 days of incubation and the culture media aspirated. Non-adherent cells were collected in the GM media. The flask was washed with PBS then 5 ml of Accutase was added to each flask and incubated at 37°C, 5% CO_2 for 10 minutes. Five millilitres of GM media was added to the flask to deactivate the Accutase. This was pipetted vigorously and the cells added to the previously removed supernatant containing suspension cells. A further 5 ml of PBS was added to the flask to prevent dehydration and the flask was put on ice for a further 10 minutes. This was again pipetted vigorously to remove adherent cells and the flask reviewed under the microscope to ensure maximum yield of cells obtained from each flask. The cells were centrifuged at 1500rpm for 10 minutes at 21°C and the supernatant discarded. The pellet was resuspended in 3mls MACS buffer, transferred to a FACS tube and centrifuged at 1500rpm for 5 minutes at 21°C. Supernatant was removed and the pellet was resuspended in residual media.

Cells were stained with 15µl human FcR block incubated at room temperature for 10 minutes, followed by 4µl of CD11b (BV510, BioLegend, CA, USA), CD14 (APC Fire, BioLegend) and HLA-DR (BV421, BioLegend), and incubated at 4°C in the dark for 30 minutes. Three mililitres MACS buffer was added per FACS tube and centrifuged at 1500rpm for 5 minutes at 4°C. The supernatant was discarded and the pellet resuspended in 0.5 ml MACS buffer ready for cell sorting. Prior to sorting, 1.5µl PI was added to each sample to assess and remove non-viable cells.

2.5.2 Cell Sorting of cytokine-derived mMDSC

The cells were sorted using the FACSMelody™ (BDBiosciences, NJ, USA) cell sorting machine by creating a gating strategy to include CD11b+CD14+HLA-DR- cells (Figure 2.5). Depending on the degree of polarisation of the sample, the yield would vary between subjects. Where possible, HLA-DR positive cells were also sorted, however usually most cells were HLA-DR negative and as such insufficient cells were of HLA-DR positivity to allow for sorting. The cells were sorted into FACS tubes containing GM.

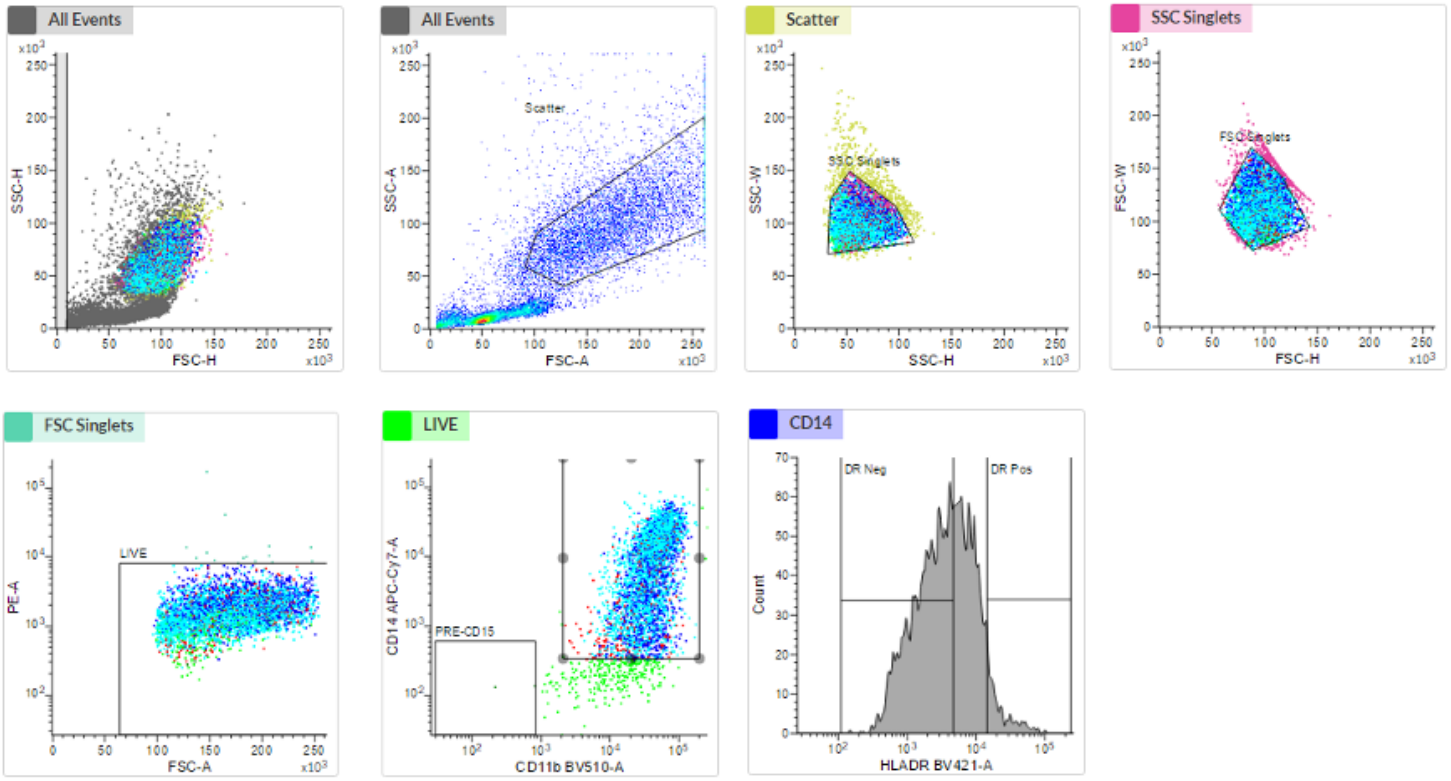

Figure 2. 5. Gating strategy for cytokine-induced m-MDSC (CD14+, HLA-DR negative).

The sorted cells were centrifuged at 1500rpm for 5 minutes at 21°C and resuspended at 1 x 10^6 cells/ml. They were seeded at 5 x 10^4 cells per well for experiments with a 1:1 ratio with activated T cells, 2.5 x 10^4 cells for a 0.5:1 ratio, 1.25 x 10^4 cells for a 0.25:1 ratio and 5 x 10^3 cells for a 0.1:1 ratio.

2.5.3 T cell enrichment

Whole blood was processed through density centrifugation as described in 2.2.1. The PBMC layer was harvested and cells washed twice in GM then resuspended in MACS buffer and transferred to a FACS tube. The sample was centrifuged at 1600 rpm for 5 minutes at 21°C. The supernatant was removed and cells resuspended at 5 x 10^7 per ml in MACS buffer. The EasySep™ T Cell Enrichment Cocktail was added at a concentration of 50µl per millilitre of sample and incubated at room temperature for 10 minutes. The EasySep™ Dextran RapidSpheres™ were vortexed for 30 seconds immediately prior to use and 40µl was used per millilitre of sample. This was added directly to the sample and left to incubate at room temperature for 5 minutes. Following incubation, MACS buffer was added to the sample to reach a total volume of 2.5ml. The tube was inserted into the magnet and left for a further 5 minutes at room temperature. The sample was then inverted and the enriched cell suspension was collected and topped up with PBS prior to centrifugation at 1600rpm for 5 minutes at 21°C. The supernatant was discarded and pellet resuspended in 2ml PBS.

The purity of the sample was stated to be over 98% on the data sheet. This was checked and confirmed by staining the T cells with CD3 FITC antibody (BioLegend, US) and flow cytometry performed using Gallios Flow Cytometer (Beckman Coulter, Life Sciences, US).

2.5.4 T cell labelling

Two microlitres of reconstituted CellTrace™ (ThermoFisher) violet dye was added to the T cells sample and incubated for 20 minutes at 37°C, 5% CO_2 protected from light. The T cells were counted using a haemocytometer then 10ml GM was added and incubated at 37°C, 5% CO_2 for 5 minutes to quench the dye. The cells were centrifuged at 1500rpm for 5 minutes at 21°C, the supernatant discarded and the cells resuspended at 1 x 10^6 cells/ml.

2.5.5 T cell stimulation using ImmunoCult™

ImmunoCult™ (StemCell™ Technologies, BC, Canada) stimulation tetramer complexes were diluted through addition of 25µl Immunocult to 225µl of GM (sufficient for 1 x 10^6 T cells (1ml)). Twenty-five microlitres of diluted Immunocult™ solution was added to 5 x 10^4 (50µl) purified T cells in the desired wells of a sterile 96-well flat-bottom plate for T cell activation.

2.5.6 T cell stimulation using anti-CD3/CD28 Dynabeads®

The Dynabeads® (ThermoFisher) were first resuspended through vortex for 30 seconds. Dynabeads® were added to a tube, sufficient for 1.6µl per well to achieve a bead-to-cell ratio of 1:1, and 1ml of PBS

was added. The tube was inserted into the magnet and left for 1 minute and the supernatant discarded. The tube was removed from the magnet and the Dynabeads® resuspended in GM (2µl per well required).

The washed Dynabeads® (1.6µl) were added to 5 x 10^4 purified T cells in a sterile 96-well flat-bottom plate for T cell activation. For the experiment where 10 times the concentration of beads was added in order to overwhelm the phagocytic capacity of the MDSC, the volume of beads was increased by a factor of 10.

2.5.7 T cell stimulation using Invitrogen™ Cell Stimulation Cocktail

The Cell Stimulation Cocktail (ThermoFisher) was diluted to a working concentration of 2µl/ml as per the product specification data sheet. This was added to each of the wells containing 5 x 10^4 purified T cells.

2.5.8 Inhibition of phagocytosis using opsonised zymosan A

The opsonised zymosan (Sigma Aldrich) was prepared by reconstituting the opsonised zymosan A powder in PBS at a concentration of 10mg/ml. This suspension was boiled for 30 minutes then incubated at 37°C for a further 30 minutes with an equal volume of fresh pooled human serum. The particles were then washed three times with PBS and finally resuspended in PBS.

2.5.9 Staining T cells with CFSE

Firstly, 18µL DMSO was added to a vial of CellTrace CFSE staining solution. It was then diluted in 20 mL of warmed PBS (37°C) for a 5 µM staining solution. 10mL of cells were added to a 50mL centrifuge tube and spun for 5 minutes at 1500rpm at 21°C, then the supernatant discarded. Cells were resuspended in 10mL CellTrace CFSE staining solution and incubated for 20 minutes in a 37°C water bath. To this, 40 mL OpTmizer T Cell Expansion SFM was added to the cells to absorb any unbound dye and incubated for 5 minutes in the dark at room temperature. The cells were then centrifuged for 5 minutes at 1500rpm and resuspended in pre-warmed OpTmizer T Cell Expansion SFM.

2.6.0 Statistical analysis

GraphPad Prism 8.0.1 software was used to perform the statistical analysis. T tests, and where applicable, one-way analysis of variance (ANOVA) were performed. The cut off for statistical significance was a p value of 0.05.

2.7.0 10X Genomics Single Cell RNA Sequencing

2.7.1 Basic media

The tissue culture media used throughout the experiment is outlined below unless otherwise stated and will be referred to as 'general media' or 'GM'. Media was stored at 4°C and supplemented with antibiotics and foetal bovine serum.

RPMI 1640: 500ml bottles of sterile liquid (Gibco®, ThermoFisher Scientific, MA, USA) supplemented with 2mM L-glutamine and adjusted to pH 7.0.

2.7.2 Supplements, enzymes and sterile solutions

MACS Tissue Storage Solution: Sterile liquid in 100ml bottle (Miltenyi Biotec Ltd., UK) validated and approved for use on human tissue, including tumour, to prevent cell modification and preserve cell function. Stored at 4°C.

Liberase™: Sterile 5mg vial containing lyophilized enzyme (Merck, Sigma-Aldrich, Germany) reconstituted in sterile conditions as per the data sheet and aliquoted into 500µl volumes. Stored at -20°C until use.

Benzonase® Nuclease: Sterile liquid ≥250 units/µl (Merck KGaA, Germany) stored at -20°C. Used to reduce clumping due to DNA release from dying cells.

10x Collagenase/Hyaluronidase in DMEM: Sterile liquid in 10ml bottle containing 3000 units/ml collagenase and 1000 units/ml hyaluronidase with Dulbecco's Modified Eagle's Medium (DMEM) (1000mg D-glucose/L) (StemCell™ Technologies, US). Aliquoted into 500µl volumes and stored at -20°C.

2.7.3 Specialist consumables

GentleMACS™ C Tubes: Sterile tubes used in conjunction with gentleMACS Dissociator to aid the digestion of tissue into single cell solution (Miltenyi Biotec Ltd., UK).

2.7.4 Antibodies

Podoplanin, AF488 FITC – Biolegend, CA, USA

CD45, BV765 – Biolegend, CA, USA

EpCAM, APC – Biolegend, CA, USA

2.7.5 10x Genomics components

Chromium Next GEM Single Cell 3' GEM, Library & Gel Bead Kit v3.1, 4 rxns – Kit obtained from 10x Genomics, CA, USA. Stored at -80°C until use.

Chromium Next GEM Chip G Single Cell Kit, 16 rxns – Kit obtained from 10x Genomics, CA, USA. Stored at -20°C until use.

Illumina® HIGH 150 cycle flow cell - NextSeq 500/550 High Output Kit v2.5 (150 Cycles) (Illumina®, CA, USA)

2.7.6 Tissue preparation

Fresh tissue samples were immediately stored in MACS Tissue Storage Solution and stored at 4°C until use (usually the following day due to the late arrival of tissue samples). The sample was finely minced and added to 5ml of pre-warmed GM in a GentleMACS C Tube. Five hundred microlitres of Liberase™, 500µl collagenase/hyaluronidase and 2µl Benzonase® was added to the C tube containing tissue and GM.

The sample underwent initial dissociation using the GentleMACS Dissociator on 'Human Tumour Programme 1.01', then incubated in a water bath at 37°C for 30 minutes. This was followed by the second dissociation using 'Human Tumour Programme 1.02' on the gentleMACS Dissociator and re-incubated at 37°C for a further 30 minutes. The final dissociation then occurred using 'Human Tumour Programme 1.03'.

The sample was passed through an EASY-strainer™ 100-micron filter which was washed out with GM following passage of the sample to retrieve any remaining cells. This was then passed through an EASY-strainer™ 40-micron filter and the filter was washed with GM.

The sample was then centrifuged at 1500rpm at 21°C for 10 minutes. The supernatant was discarded and the pellet resuspended in the residual volume. To this, 2 ml of RBC lysis buffer was added and left to incubate at room temperature for 10 minutes. Following incubation, it was topped up with GM and centrifuged at 1500rpm for 10 minutes at 21°C.

The pellet was resuspended in 4 ml of MACS buffer and centrifuged for 5 minutes at 1500rpm at 21°C. The supernatant was discarded and the pellet resuspended in the residual volume. Fifteen microlitres of human FcR blocking reagent was added and incubated at 4°C for 10 minutes. The following antibodies

were then added, each 5µl per sample: Podoplanin, CD45 and EpCAM. This was then incubated for 20 min at 4°C protected from light.

Following incubation, the sample was topped up with 3 ml MACS buffer and centrifuged at 1500rpm for 5 minutes at 4°C. The supernatant was discarded and the pellet resuspended in the residual volume. MACS buffer (500µl) was added to the sample ready for cell sorting and 1.5µl of propidium iodide was added to exclude dead cells.

2.7.7 Cell sorting

The cells were sorted into GM and the number of cells sorted was documented; CD45+ cells in one tube, EpCAM+ and podoplanin+ cells in the other. The gating strategy is outlined below in Figure 2.6.

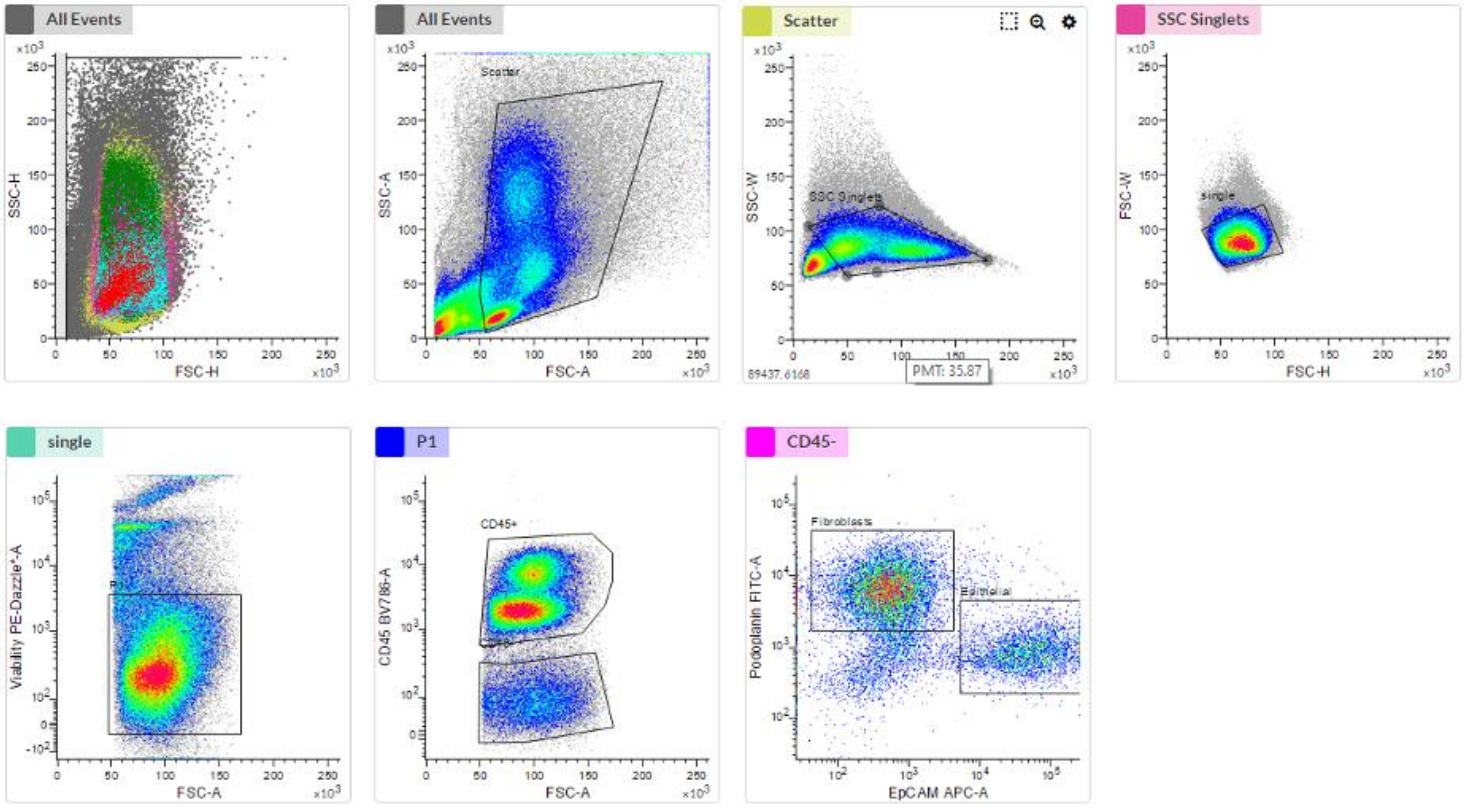

Figure 2. 6. Gating strategy for sorting cells into CD45+ and podoplanin/EpCAM+.
Sequential gating strategy was used to identify the appropriate cell populations.

The samples were combined at a ratio of 80% CD45+ cells and 20% EpCAM/podoplanin+ cells and then centrifuged at 1700rpm at 4°C for 10 minutes to ensure an adequate pellet and resuspended in appropriate volume to achieve a concentration of 1 x 10^3 cells per microlitre. The sample was stored

and transported on ice to the Genomics Birmingham Facility for single cell RNA sequencing using the 10X Genomics Platform.

2.7.8 10X Genomics single cell capture, library preparation and sequencing

Cells were processed using the 10x Genomics Chromium Controller and the Chromium Single Cell 3′ Library & Gel Bead Kit following the standard manufacturer's protocols.

In brief, around 6,000 live cells were loaded onto the Chromium controller in an effort to recover 5,000 cells for library preparation and sequencing. Gel beads were prepared according to standard manufacturer's protocols. Oil partitions of single-cell + oligo coated gel beads (GEMs) were captured and reverse transcription was performed, resulting in cDNA tagged with a cell barcode and unique molecular index (UMI). Next, GEMs were broken and cDNA was amplified and quantified using Tape station High Sensitivity.

To prepare the final libraries, amplified cDNA was enzymatically fragmented, end-repaired, and polyA tagged. Fragments were then size selected using SPRIselect magnetic beads (Beckman Coulter). Next, Illumina sequencing adapters were ligated to the size-selected fragments and cleaned up using SPRIselect magnetic beads (Beckman Coulter). Finally, sample indices were selected and amplified, followed by a double-sided size selection using SPRIselect magnetic beads (Beckman Coulter). Final library quality was assessed using Tape station High Sensitivity. Samples were then sequenced on the Illumina NEXTSeq with a target of at least 20,000 reads/cell.

2.8.0 scRNA-seq data analysis

2.8.1 Pre-processing and QC

The analysis of the scRNAseq data was kindly analysed by Dr Wayne Croft at the Centre for Computational Biology and Institute of Immunology & Immunotherapy, University of Birmingham. Raw sequencing read data were processed using Cell Ranger v5.0.1 (117). Raw read bcl files were converted to fastq and aligned to the Human reference genome GRCh38 with cellranger mkfastq and cellranger count respectively, giving a matrix representing unique molecular identifiers (UMI's) per cell barcode per gene.

The raw UMI matrices for each sample were processed using R v3.6.2 (118) with the Seurat package v3.2.0 (119). Matrices were filtered to remove cells with < 500 genes detected, > 3500 genes detected and cells with >10% of reads mapping to mitochondrial RNA. DoubletFinder (120) was used to identify doublets, which were subsequently removed from further analysis.

2.8.2 Normalisation and data integration

Seurat CellCycleScoring function was utilised to calculate a cell cycle score for each cell and the difference between G2M and S phase score quantified. Seurat SCTransform normalization procedure was applied, regressing out percentage mitochondrial mapping and G2M-S phase cell cycle score difference. Sample data integration was completed using the IntegrateData function following Seurat SCTransform integration workflow with the top 6k most variable genes.

2.8.3 Unsupervised clustering and high-level cell type annotation

The 6k most variably expressed genes were used for dimensionality reduction, firstly by principal component analysis (PCA) and subsequently by uniform manifold projection (UMAP), selecting PCs 1:20 that explained the majority of the variance observed (assessed by elbow plots). A shared nearest-neighbour graph was constructed in PCA-space using PCs 1:20 with Seurat FindNeighbors function. Clusters are identified within this graph using Seurat FindClusters function, optimising the modularity with the Louvain algorithm. The resolution parameter to control cluster granularity was set at 0.8. Cluster marker genes were identified with FindAllMarkers function using parameters: *only.pos=TRUE, min.pct=0.25, logfc.threshold=0.25, test.use="MAST".*

To guide annotation of clusters with high-level cell type, canonical cell type marker gene expression level was assessed. High-level cell type markers used to inform annotation were CD3D (T cell), MS4A1 (B cell), IGKC (Plasmablast), EPCAM (Epithelial), MKI67 (Cycling), PECAM1 and CLDN5 (Endothelial), DCN and COL1A2 (Fibroblast), LYZ (Myeloid), TPSAB1 (Mast), GNLY and GZMB (Cytotoxic) and IL3RA (pDC). Ambiguous cells that could not be clearly assigned to a high-level cell type were removed from further analysis.

2.8.4 Myeloid subset analysis

For finer grained analysis of Myeloid cells, data were subset on the "Myeloid" high-level cell type cluster for independent analysis. Using Seurat, the myeloid cell population was split back to the raw per-sample UMI matrix data and SCTransform integration procedure applied as previous. Dimensionality reduction, clustering (resolution = 0.2) and cell type annotations were then applied on this subset as previously described. Clusters were annotated with mid-level myeloid cell types: monocyte; macrophage; neutrophil and mDC based on expression of canonical marker genes and automated cell type annotation using SingleR (121).

The Neutrophil population and Monocyte + Macrophage populations were subset further and re-clustered (resolution parameters 0.2 (Neutrophils); 0.9 (Monocyte + Macrophage)) for the finer grained analysis of Neutrophils and Monocyte + Macrophage cells independently. Clusters were annotated with phenotype and main gene discriminating from other clusters wherever possible. At each iteration following sub setting and re-clustering, any cells that were carried over due to previous mis-clustering and hence assigned an incorrect cell type were removed from further analysis. Mis-clustered cells were identified by assessing expression high level cell type markers.

2.8.5 Cluster proportion comparisons

Sample wise proportions of each cluster were calculated and stratified by pre/post chemotherapy and tissue type (HGSOC, Metastasis or Normal). Wilcoxon rank sum test was applied to compare the distributions of cluster proportions observed.

2.8.6 Signature scoring

Cells were scored for signatures of interest using Seurat AddModuleScore function. This score is calculated as the average expression of the gene module per single cell minus background expression from randomly selected control features with positive scores indicating that the gene module is expressed more highly than expected given the average population expression. To identify likely MDSC cells, an established MDSC signature gene set was used (122). Neutrophil maturity signature scores were attained from Martinelli et al., 2004 (123) and TAM, M1 and M2 Macrophage signatures from Zhang et al., 2020 (124).

2.8.7 Differential expression

Genes differentially expressed in post vs pre chemotherapy sample data were identified using findMarkers with MAST option (test.use="MAST"), which uses a hurdle model tailored to scRNA-seq data. MAST is a two-part GLM that simultaneously models how many cells express the gene by logistic regression and the expression level by Gaussian distribution (115). Differential expression testing is then done using the likelihood ratio test.

Chapter 3

Phenotypic analysis of MDSC in ovarian pathology

3.0 Introduction

The immune response in the cancer microenvironment is a topic of great interest due to recent advances in immunotherapy. Infiltration of immune cells into the tumour microenvironment is associated with a better prognosis in many cancers whilst the presence of immunosuppressive cells, such as MDSC, are associated with a poorer prognosis (79,80). Altering the tumour microenvironment to favour immune cell infiltration and limit immunosuppression could help to improve survival in patients with cancer.

Myeloid-derived suppressor cells can be subdivided into two major populations based on their phenotypic characteristics and function. These are termed monocytic MDSC (m-MDSC) and granulocytic MDSC (PMN-MDSC). The phenotype of MDSC will be interrogated in this chapter, whilst assessment of their functionality will be covered in Chapter 4.

The hypotheses for this project were:

1. MDSC are present in ovarian cancer tissue, peripheral blood and sites of metastasis.
2. There is a greater presence of MDSC within cancer specimens compared to benign and normal tissue.
3. Chemotherapy reduces the population of MDSC due to its chemotoxic effects.

In order to undertake this work, blood and tissue was collected from patients undergoing treatment for ovarian cancer and from age-matched patients undergoing gynaecological procedures other than for ovarian cancer. The aims of this project were to:

1) Identify and enumerate MDSC populations in tissue from women diagnosed with high-grade serous ovarian cancer (HGSC) and compare with control tissue.
2) Compare the composition of m-MDSC and PMN-MDSC populations within the peripheral blood and tumour samples with age-matched control.
3) Compare the presence of the MDSC subtypes within different disease states, including benign ovarian disease and other ovarian cancer subtypes, to identify if their presence is unique to a malignant process.
4) Determine the effect of chemotherapy on MDSC populations within PBMC, ovarian tumour and omentum samples.
5) Correlate the presence of MDSC infiltrates with treatment outcomes in patients with ovarian cancer.

3.1 The identification of MDSC from patient samples

3.1.1 Cohort

Women undergoing surgery for confirmed and suspected ovarian cancer at either City Hospital Birmingham or New Cross Hospital Wolverhampton were approached to participate in the study. All clinical samples were taken following written consent from patients in accordance with the Declaration of Helsinki as approved by the Health Research Authority and University of Birmingham (IRAS project ID 225991, protocol number RG 17-225). All samples were stored in compliance with the Human Tissue Act (2004).

Women were either having a diagnostic operation to remove an ovarian tumour of unknown aetiology, termed 'primary debulking surgery/staging laparotomy', or had already been diagnosed with cancer and had received chemotherapy and were having residual tumour removed, termed 'delayed debulking surgery'. At the point of consent for primary debulking/staging surgery the histological diagnosis was unknown and only available 2 weeks post-operatively. All histopathology diagnoses were made by a central gynaecological oncology specialist histopathologist consultant.

Women were approached to be healthy donors if they were undergoing surgery to remove fallopian tubes and ovaries for risk-reduction surgery, in which case these patients were either known *BRCA* gene mutation carrier or previously had a diagnosis of breast cancer. Peripheral blood samples were taken from age and gender-matched healthy donors with consent.

In total, 56 women were recruited to the study between October 2018 and February 2020. This comprised 8 women who were controls; 3 women undergoing risk-reducing surgery and 5 women who were age-matched healthy donors of blood. In the cancer cohort, 33 women were diagnosed with primary ovarian cancer, 25 of which were HGSC. Of these women, 13 underwent primary debulking surgery, and therefore had not been exposed to chemotherapy (chemo-naïve), whilst 12 patients received chemotherapy followed by delayed debulking surgery. In addition, 4 women were subsequently found to have a primary endometrial cancer with involvement of the ovaries and 4 women were diagnosed with metastatic disease from other primary e.g., gastro-intestinal tumours. There were 7 women with benign disease and a summary of the patient characteristics are described below in Table 3.1.

Age at operation	Patients	Healthy donors
Median	61	51
Range	35-82	43-61
Diagnosis	Number	Percentage (%)
Epithelial ovarian cancer	33	
High-grade serous	25	75.8
Endometrioid	3	9.1
Mucinous	1	3.0
Clear cell carcinoma	1	3.0
Low-grade serous	1	3.0
Borderline	1	3.0
Carcinosarcoma	1	3.0
Benign tumour	7	
Fibroma	4	57.1
Endometrioma	3	42.9
Endometrial cancer	4	
Endometrial serous	3	75.0
Endometrioid endometrial	1	25.0
Metastasis	4	
Stage of high-grade serous ovarian cancer		
1	1	4.0
2	1	4.0
3	18	72.0
4	5	20.0
Chemotherapy exposure		
Primary debulking surgery	13	52.0
Delayed debulking surgery	12	48.0
Number of chemotherapy cycles		
3	3	25.0
4	3	25.0
6	6	50.0
Chemotherapy response score		
1	3	25.0
2	6	50.0
3	1	8.3
Not stated	2	16.7

Table 3. 1. Summary of the patient characteristics of women enrolled within the research study.

3.2.1 Identifying the presence of MDSC in women diagnosed with HGSC compared to benign specimens

To investigate the proportions of the different MDSC populations present in HGSC and benign disease, qualitative and quantitative analysis was performed on PBMC, ovarian tumour and omental samples using flow cytometry. Samples were dissociated into single cell suspensions and were stained with antibodies for 25 minutes, protected from light, in preparation for flow cytometry. The flow panel consisted of CD3, CD19 and CD56 to exclude T cells, B cells and NK cells, CD45, CD11b, CD14, CD15 and HLA-DR in order to detect the m-MDSC and PMN-MDSC cell types. Propidium iodide was added just prior to flow cytometry to exclude dead cells.

The gating strategy for the phenotypic identification of MDSC was based upon recommendations published in the literature (66) with m-MDSC identified with a CD45+/CD11b+/CD14+/CD15-/HLA-$DR^{-/lo}$ profile whilst PMN-MDSC were identified with the markers CD45+/CD11b+/CD15+/CD14-.

3.2.2 Normal ovarian tissue contained little or no MDSC

Control ovarian biopsies were obtained from 3 patients and results from flow cytometry showed that 2 of the 3 patients did not have detectable MDSC, while the third sample showed that the both m-MDSC and PMN-MDSC were present in <1% of the total leucocyte population (Figure 3.2A and B). The gating for the identification m-MDSC and PMN-MDSC in benign and malignant samples are demonstrated in Figure 3.1.

Interestingly, when a similar analysis was performed on histologically-proven microscopically ‘normal’ ovarian tissues taken from patients with either benign or malignant ovarian tumour, these tissues contained a higher proportion of MDSC when compared to tissues taken from healthy donor. The proportion of PMN-MDSC and m-MDSC in microscopically “normal” ovarian tissue were 28% and 0.2% of the total leucocyte population, respectively; while those with benign ovarian tumours had an average of 20% PMN-MDSC and 0.15% m-MDSC (Figure 3.2A and B), demonstrating the ‘microscopically normal’ ovary may not be completely normal as it has a similar infiltration as those with benign ovarian tumours.

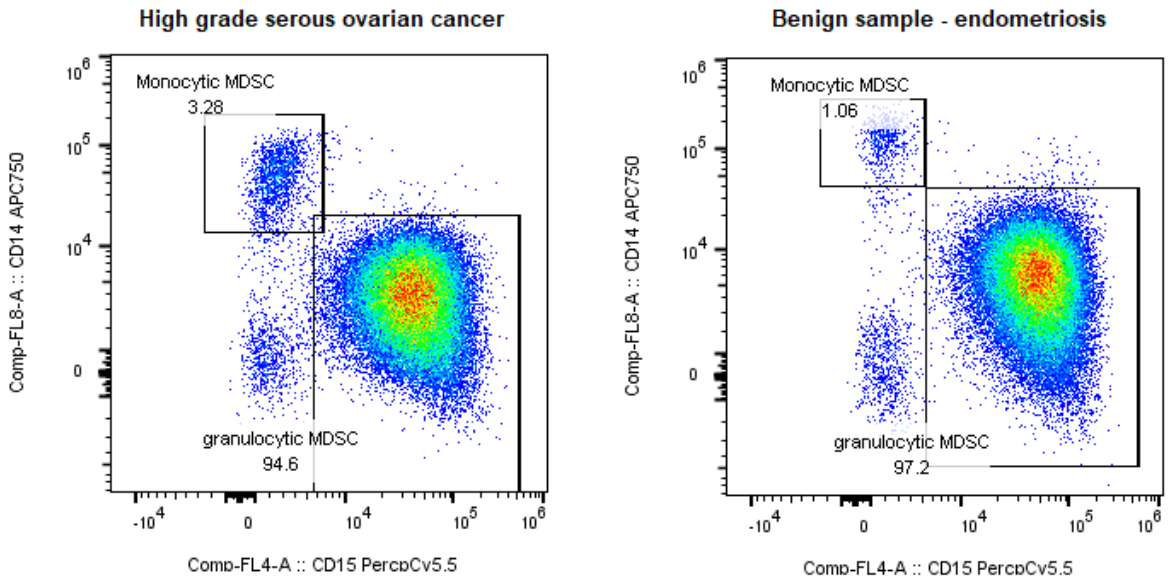

Figure 3. 1 Representative fluorescence-activated cell sorting (FACS) graphs of a single sample of HGSC (shown left) and endometriosis (shown right).
These graphs demonstrate the gating for monocytic and granulocytic MDSC in high grade serous ovarian cancer and endometriosis (benign tumour). Tissue sample demonstrated is from ovarian tumour. Percentages of each cell population are demonstrated.

The proportion of PMN-MDSC in ovarian tissues for benign and HGSC tumours were 38% and 19% of the total leucocyte population respectively, and m-MDSC were 0.16% and 0.3%, respectively (Figure 3.3A and B).

Women with a microscopically normal ovary but with a diagnosis of HGSC had the greatest percentages of both PMN-MDSC and m-MDSC with an average of 28% and 0.2% respectively, whilst those with benign ovarian tumours had an average of 20% PMN-MDSC and 0.15% m-MDSC. Although this did not reach significance, further samples may have improved the power for significance to be achieved.

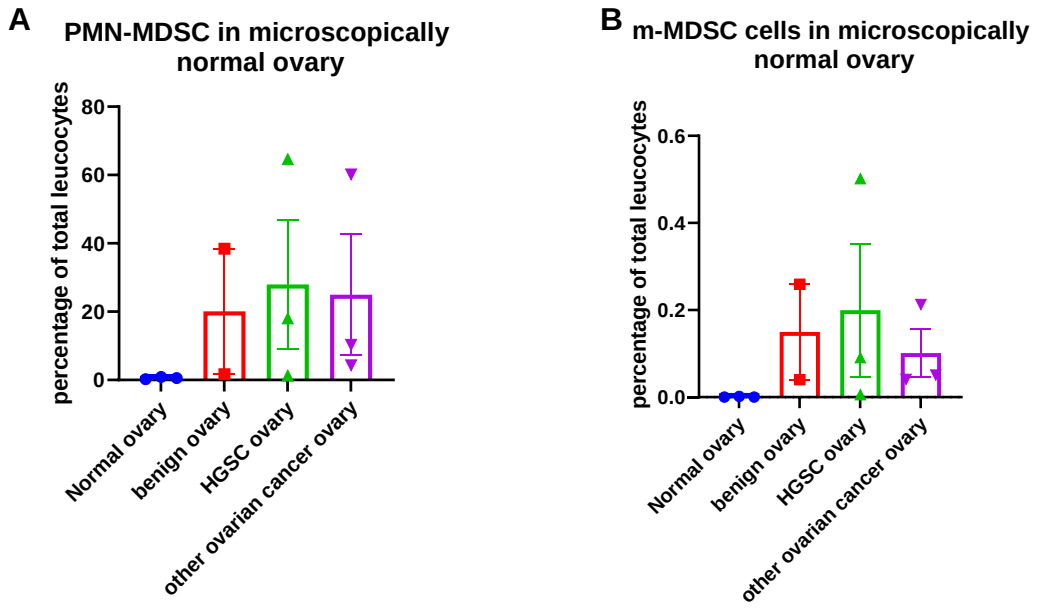

Figure 3. 2. Comparison of PMN-MDSC and m-MDSC presence in the macroscopically normal ovary in different disease states.
The percentage of A) PMN-MDSC and B) m-MDSC of the total leucocyte population in microscopically normal ovarian tissue. ANOVA: non-significance. Normal ovary n=3, benign ovary n=2, HGSC ovary n=3, other ovarian cancer ovary n=3. Bars represent mean and standard error of the mean.

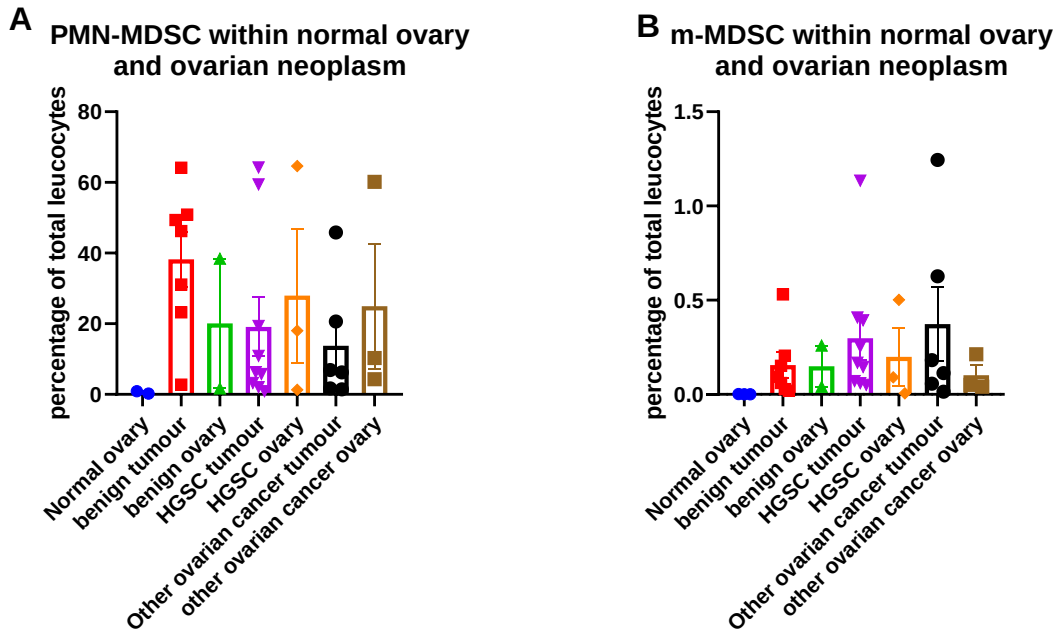

Figure 3. 3. Comparison of MDSC subsets in tumour and benign ovarian tissue.
The percentage of A) PMN-MDSC and B) m-MDSC as a proportion of the total leucocyte population in microscopically normal ovary and different ovarian tumour subtypes. ANOVA: non-significance for all results. Bars represent mean and standard error of the mean. Normal ovary n=3, benign tumour n=7, benign normal ovary n=2, HGSC tumour n=9, HGSC normal ovary n=3, other ovarian cancer tumour n=6, other ovarian cancer normal ovary n=3.

3.2.3 There is no difference in the percentage of total MDSC within the leucocyte population between benign and malignant disease.

MDSC populations were interrogated as a proportion of the total leucocyte population to determine if the MDSC population comprised a higher proportion of the total leucocyte population between benign and malignant disease and within different tissue types. PBMC analysis was also conducted on healthy donors but omental tissue wasn't available as this is not routinely excised during procedures for benign disease. It was not possible to perform omentum or tumour analyses on 5 of these women as they didn't undergo surgery, or if they did (n=2), ovarian tumour and omentum was not removed. Importantly, little or no MDSC were retrieved from normal ovary samples.

In order to perform this experiment, the total leucocyte population was identified through flow cytometry by gating on all of the CD45+ cells, following exclusion of dead cells and doublet cells. This population was then compared to the total populations of PMN-MDSC (CD45+/CD11b+/CD15+/CD14-) or m-MDSC (CD45+/CD11b+/CD14+/HLA-DR$^{-/lo}$/CD15-) as identified through multiple gating on flow cytometry.

The results showed that when MDSC were analysed as a proportion of the total leucocyte population (Figure 3.4), the proportion represented by MDSC remained consistent in benign and malignant tissues as well as in healthy donors. Within the PBMC, the MDSC accounted for 4.6% and 4.9% of the total leucocyte population in HGSC and healthy donors respectively. This increased to 7.7% and 11.2% in the other ovarian cancer group and benign disease respectively. Within the omentum, the average percentage of MDSC was very similar between the benign, HGSC and other ovarian cancers with 30%, 28% and 32% respectively. Within ovarian tumours, surprisingly the benign tumours had the highest percentage of MDSC at 38%, followed by other ovarian cancers with 28%, the HGSC with 19% and lastly normal ovarian tissue with 0.6%. These results did not achieve statistical significance. It was expected that the HGSC or other ovarian malignancies would have the greatest infiltration of MDSC but these results demonstrated that it was the benign disease that had the greatest infiltration within the tumour.

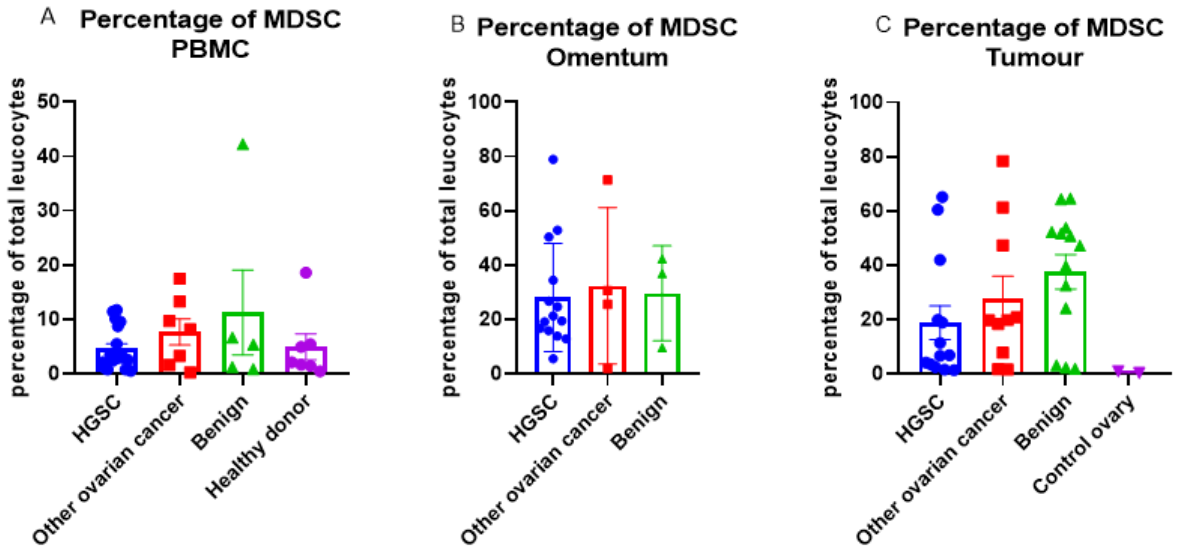

Figure 3. 4. Comparison of the percentage of MDSC of the total leucocyte population in the different disease states compared to healthy donor.
The percentage of MDSC of the total leucocyte population in a) peripheral blood samples. n= 18 HGSC, n= 7 other ovarian cancer, n= 5 benign disease, n= 7 healthy donors. b) tumour samples. n= 13 HGSC, n= 10 other ovarian cancer, n=13 benign c) omental samples. n= 14 HGSC, n=4 other ovarian cancer, n=3 benign disease. ANOVA: There was no statistically significant difference between the samples. HGSC: high-grade serous ovarian cancer. Bars represent mean and standard error of the mean.

3.2.4 The proportion of MDSCs in primary HGSC and its metastatic deposits is significantly higher compared to PBMC.

Once the ability to identify MDSC within the PBMC, ovarian tumour and omental samples was confirmed, it was investigated whether MDSC were present in higher numbers in different tissue types when compared to PBMC.

The number of MDSC was assessed as a percentage of the total leucocyte population as described above. For malignant disease, comparisons were made between PBMC and ascites, omental tissue, primary ovarian tumour and peritoneum in high-grade serous ovarian cancer. In benign disease PBMC was compared only to omental and primary ovarian tumour samples. This was because in benign disease there were no metastatic deposits on the peritoneum so it was not routinely removed and ascites was absent in benign disease.

In HGSC, the proportion of MDSC in PBMC, ovarian tumour, ascites, omental tumour and peritoneal deposits were 4.6%, 19%, 8.7%, 28% and 38%, respectively. Figure 3.5 shows that the proportion of MDSC were significantly higher in sites of metastasis, the omental and peritoneal deposits, when

compared to PBMC. Interestingly, there was no significant different in the amount of MDSC in PMBC and ascitic fluid.

In the benign tumour, the proportion of MDSC in PBMC, ovarian tumour and omental samples were 11%, 28% and 30%, respectively and the distribution was not significant across these 3 sites (Figure 3.6). This may have been due to the smaller sample size in the benign cohort.

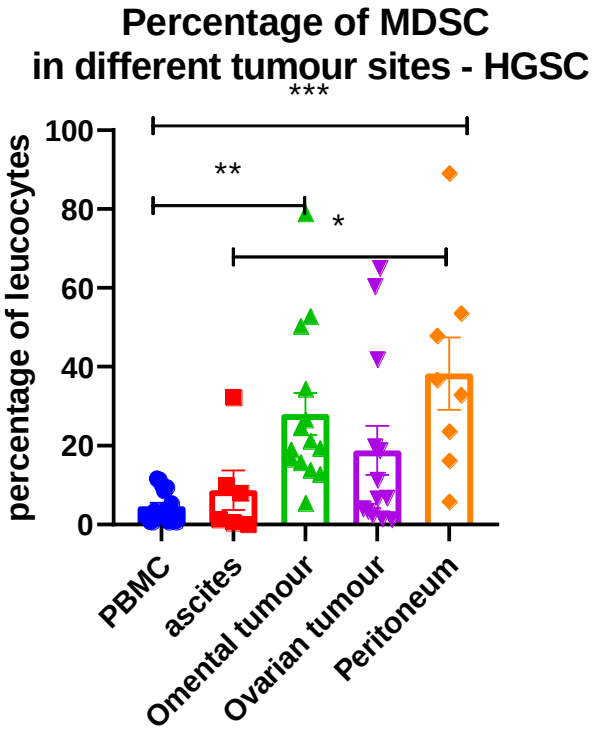

Figure 3. 5. Comparison of the percentage of MDSC of the total leucocyte population at different sites of tumour metastasis within HGSC.
Ordinary one-way ANOVA with Tukey's multiple comparisons test * = p <0.05, ** p=<0.01*** = p <0.0005. All other results non-significant. n= 18 PBMC, n= 6 ascites, n= 14 omental metastasis, n= 13 ovarian tumour, n=8 peritoneum. Bars indicate mean and standard error of the mean.

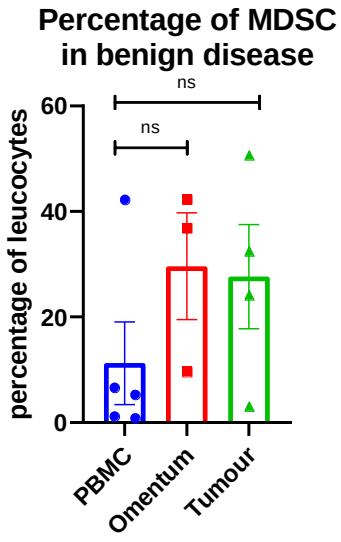

Figure 3. 6. The percentage of MDSC of the total leucocyte population in different tissues in benign disease.
ANOVA: There is no significant difference between the percentage of MDSC in the PBMC and the tumour. n= 5 PBMC, n= 3 omental samples, n= 4 tumour samples. Bars represent mean and standard error of the mean.

3.2.5 Comparison of the compositions of m-MDSC and PMN-MDSC populations within peripheral blood and tumour samples.

Having established that MDSC were present within PBMC, ovarian tumour and omentum in benign and malignant samples, the proportions of m-MDSC and PMN-MDSC within the different histological groups were interrogated. The populations were identified through the cell surface markers described above using flow cytometry.

3.2.6 Both monocytic and granulocytic MDSC are present in malignant and benign ovarian tumours and granulocytic MDSC constitute the highest proportion of total MDSCs.

From my results, it was evident that PMN-MDSC are the most prevalent MDSC population in PBMC, ovarian tumour and omentum. The percentage of m-MDSC and PMN-MDSC within PBMC in benign disease, high-grade serous ovarian cancer and in other ovarian cancer sub-types was compared and demonstrated that PMN-MDSC were the dominant sub-type regardless of the underlying diagnosis (Figure 3.7A). Similar results were demonstrated when comparing tumour and omental samples (Figures 3.8A and 3.9A). A comparison of the PMN-MDSC and m-MDSC were made in each of the tissues and demonstrated highly significant ($p=<0.0001$) differences between the different MDSC subsets in each of the tissue types and diagnoses (Figures 3.7B, 3.8B and 3.9B). On average, in PBMC the PMN-MDSC comprised 79% of the total MDSC population in high-grade serous ovarian cancer,

compared to 97% in benign disease and 98% in other ovarian cancer subtypes. In the ovarian tumour samples, the PMN-MDSC accounted for 92%, 99% and 97% in the high-grade serous ovarian cancer, benign and other ovarian cancer subtypes, respectively. Finally, in the omental samples the PMN-MDSC made up 98% in the high-grade serous group, whilst they consisted of >99% of the population in both the benign and other ovarian cancer subtypes. Statistical analysis did not find any significant differences between any of these results (Figure 3.10).

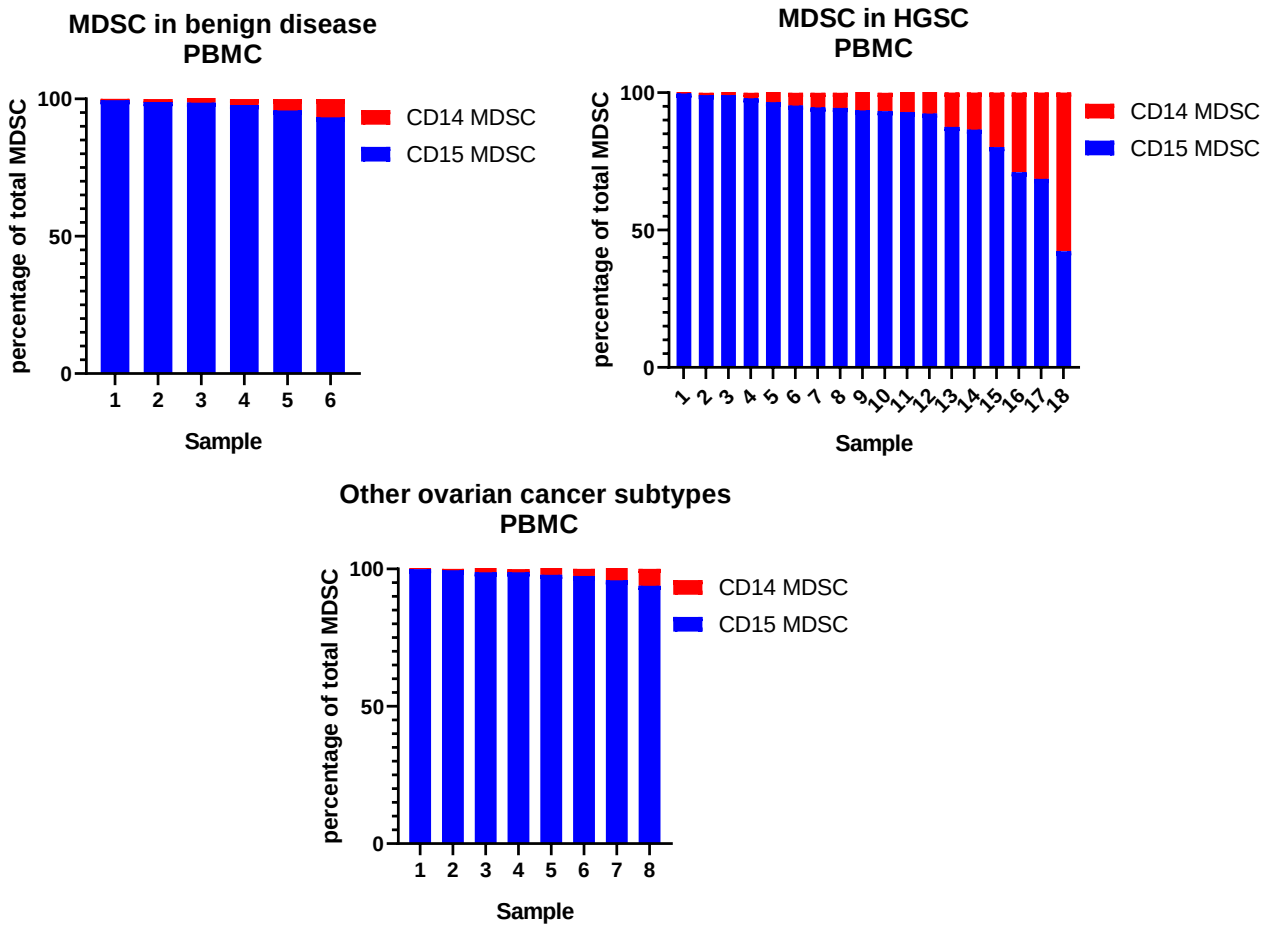

Figure 3.7 A. Comparison of the proportions of granulocytic and monocytic MDSC comprising the total MDSC population within PBMC samples in benign disease, high-grade serous ovarian cancer and in other ovarian cancer subtypes.

HGSC: high-grade serous ovarian cancer. CD14 MDSC: m-MDSC, CD15 MDSC: granulocytic MDSC. n=6 for benign disease, n=18 for HGSC and n=8 for other ovarian cancer subtypes.

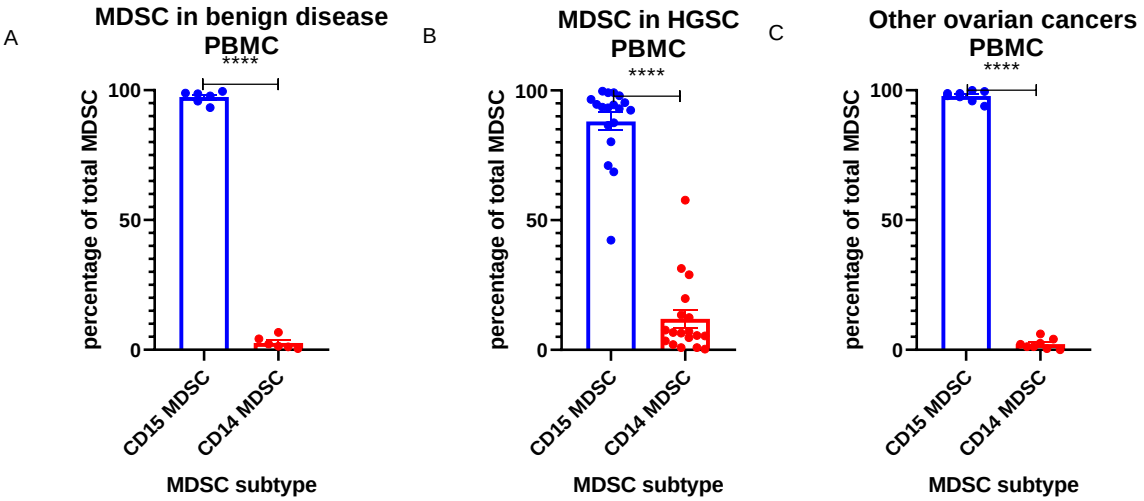

Figure 3.7 B. Comparison of the proportions of PMN-MDSC and mMDSC of the total MDSC population in the PBMC of A) benign disease, B) HGSC and C) other ovarian cancers.
HGSC: high-grade serous ovarian cancer. CD14 MDSC: m-MDSC, CD15 MDSC: granulocytic MDSC. n=6 for benign disease, n=18 for HGSC and n=8 for other ovarian cancer subtypes. T Test performed **** p = <0.0001. Bars depict mean and standard error of the mean.

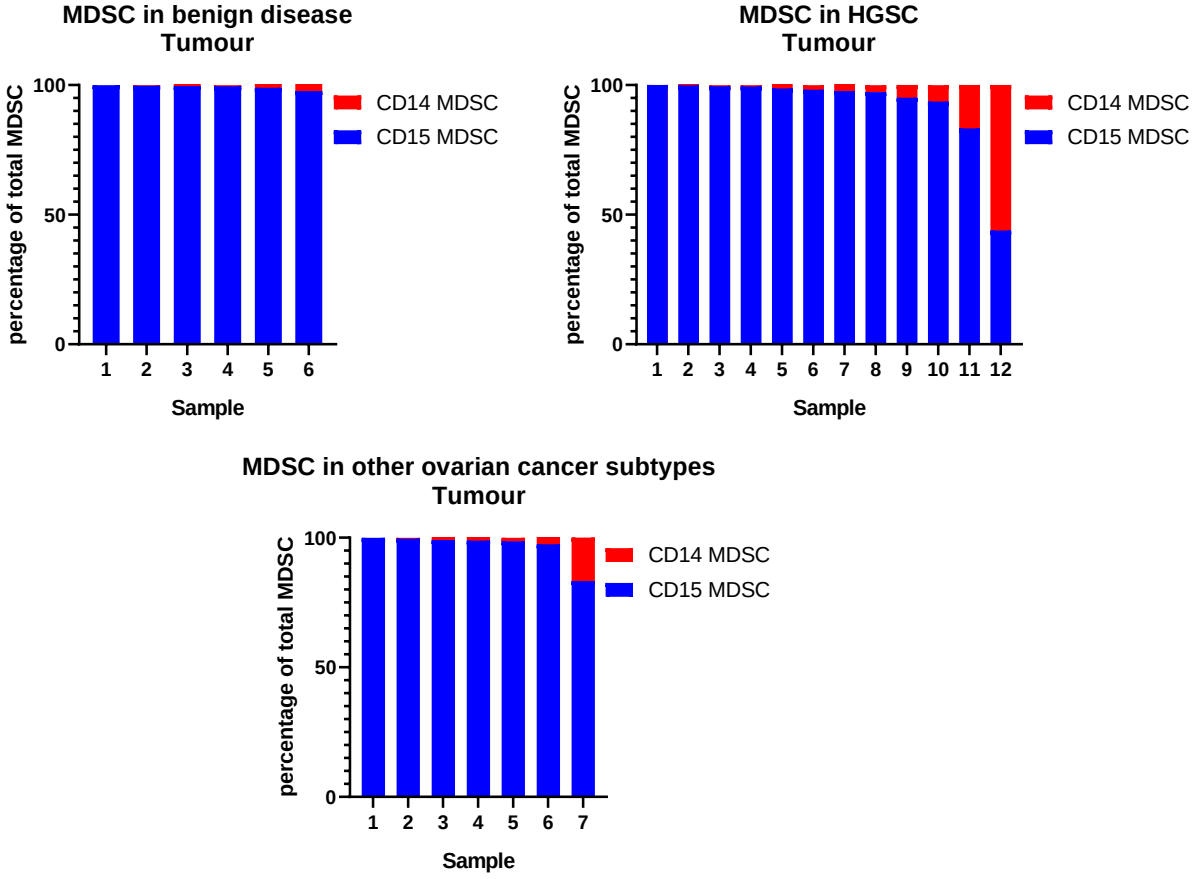

Figure 3.8 A. Comparison of the proportions of granulocytic and monocytic MDSC comprising the total MDSC population within tumour samples in benign disease, high-grade serous ovarian cancer and in other ovarian cancer subtypes.

HGSC: high-grade serous ovarian cancer. CD14 MDSC: m-MDSC, CD15 MDSC: granulocytic MDSC. n=6 for benign disease, n=12 for HGSC and n=7 for other ovarian cancer subtypes.

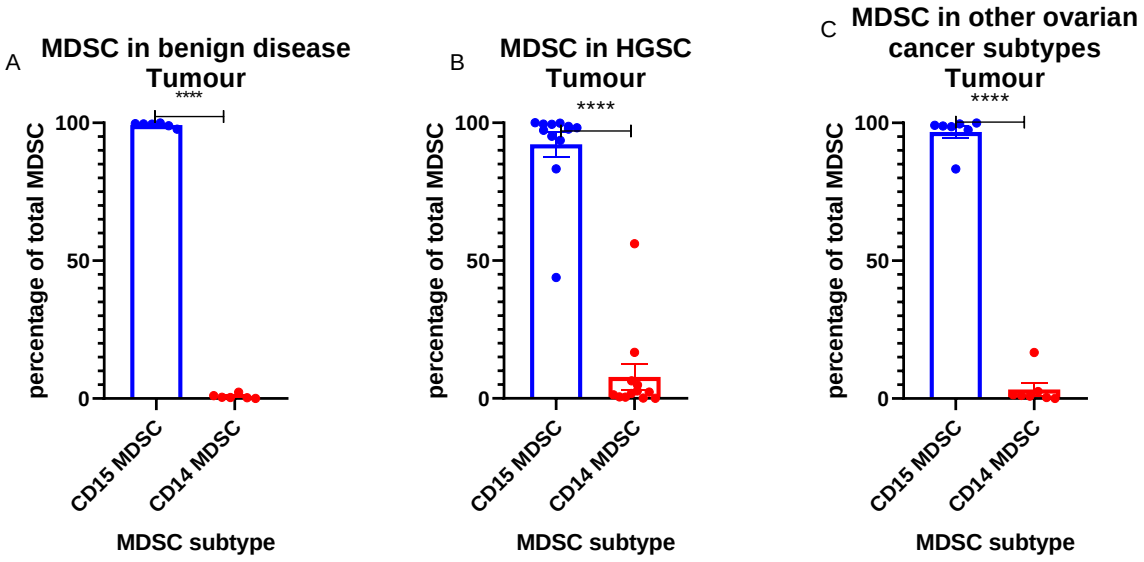

Figure 3.8 B. Comparison of the proportions of PMN-MDSC and m-MDSC of the total MDSC population in the tumour of A) benign disease, B) HGSC and C) other ovarian cancers.
HGSC: high-grade serous ovarian cancer. CD14 MDSC: m-MDSC, CD15 MDSC: granulocytic MDSC. N=6 for benign disease, n=12 for HGSC and n=7 for other ovarian cancer subtypes. T test performed. **** = p=<0.0001. Lines depict mean and standard error of the mean.

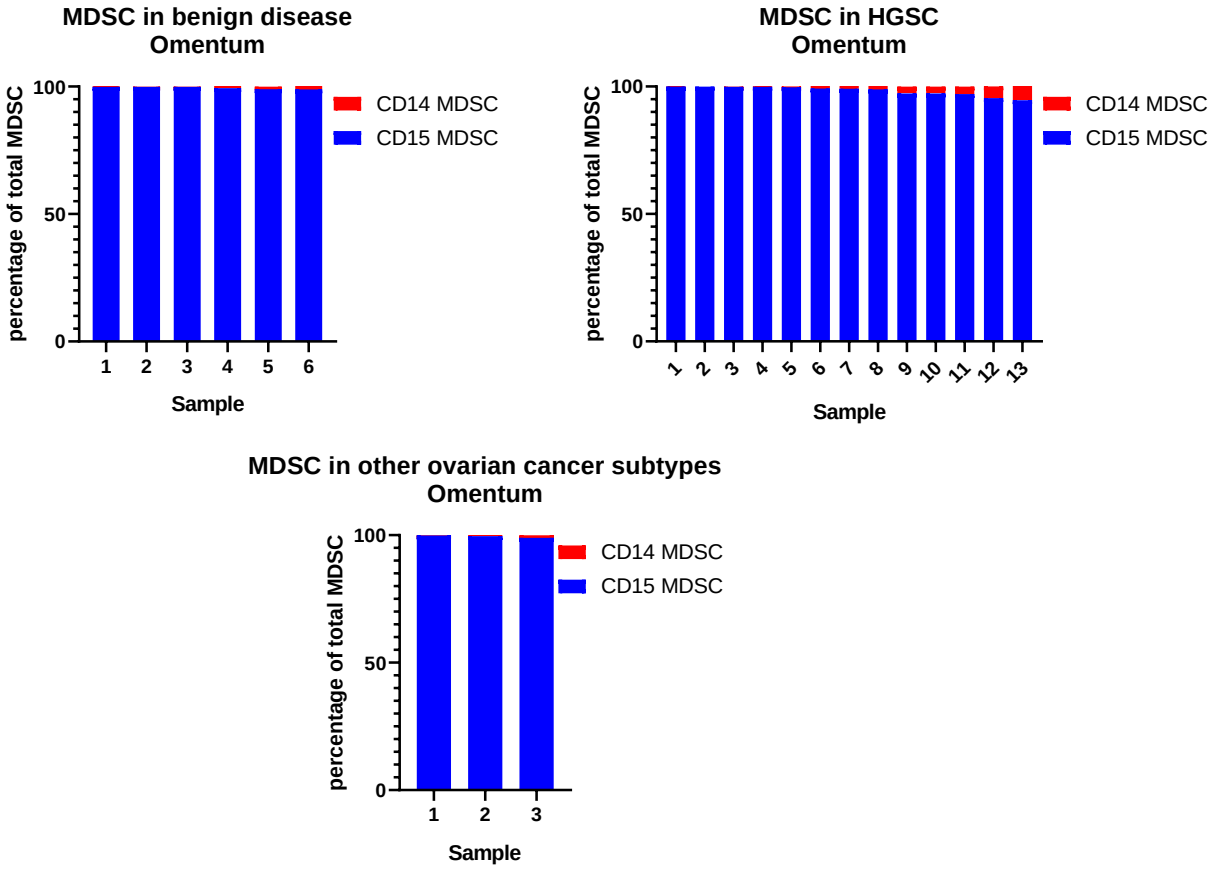

Figure 3.9 A. A comparison of the proportions of granulocytic and monocytic MDSC comprising the total MDSC population within omental samples in benign disease, high-grade serous ovarian cancer and in other ovarian cancer subtypes.
HGSC: high-grade serous ovarian cancer. CD14 MDSC: m-MDSC, CD15 MDSC: granulocytic MDSC. n=6 in benign disease, n=13 in HGSC and n=3 in other ovarian cancer subtypes.

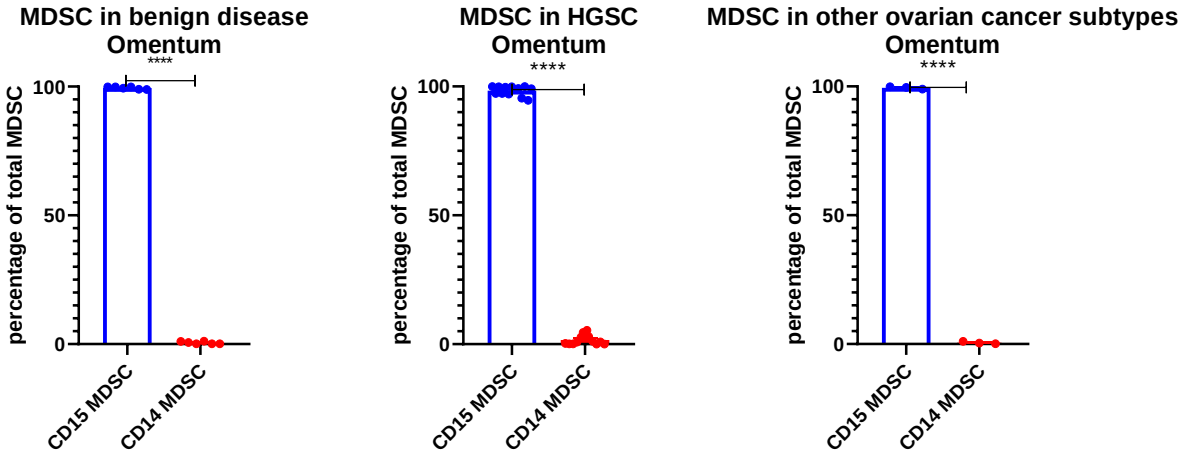

Figure 3.9 B. Comparison of the proportions of PMN-MDSC and m-MDSC of the total MDSC population in the omentum of benign disease, HGSC and other ovarian cancers.

HGSC: high-grade serous ovarian cancer. CD14 MDSC: m-MDSC, CD15 MDSC: granulocytic MDSC. n=6 in benign disease, n=13 in HGSC and n=3 in other ovarian cancer subtypes. T test performed. **** = p=<0.0001. Lines depict mean and standard error of the mean.

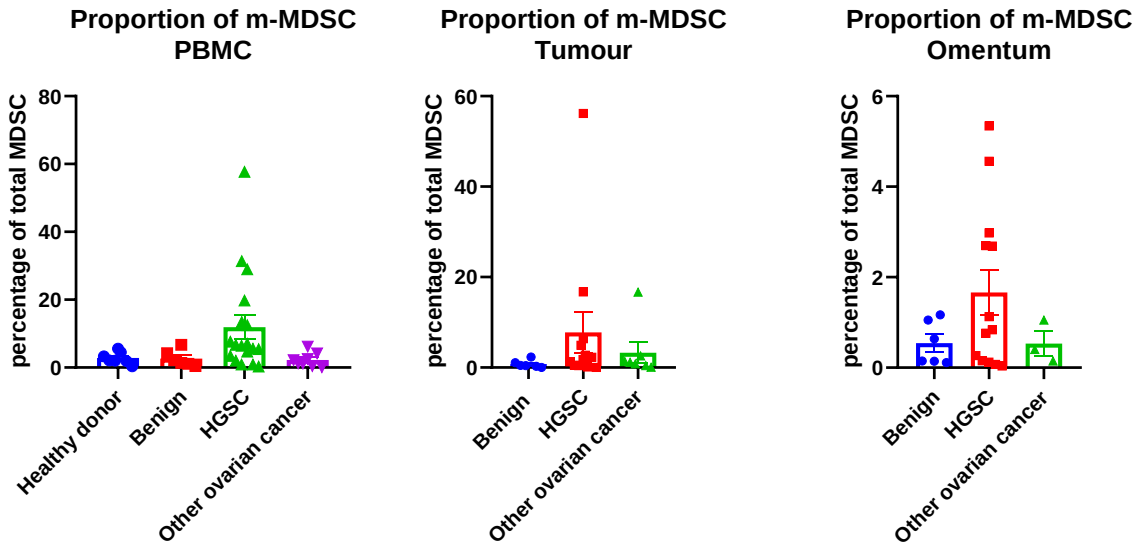

Figure 3.1 0. A comparison of the percentage of m-MDSC of the total MDSC population within the PBMC, tumour and omentum.
ANOVA: all results non-significant. Bars represent mean and standard error of the mean. PBMC: n=6 for benign disease, n=18 for HGSC and n=8 for other ovarian cancer subtypes. Tumour: n=6 for benign disease, n=12 for HGSC and n=7 for other ovarian cancer subtypes. Omentum: n=6 in benign disease, n=13 in HGSC and n=3 in other ovarian cancer subtypes.

3.2.7 Determining the effect of chemotherapy on the presence of MDSC within PBMC, tumour and omentum samples

Chemotherapeutic agents, such as oxaliplatin, have been found to regulate the presence of MDSC by reducing the population of MDSC, especially the monocytic subtype (100). The most commonly used chemotherapy agents in ovarian cancer are platinum-based chemotherapy, primarily carboplatin, which can be used as a single-agent or in combination with a Taxane, such as paclitaxel. These are typically administered for 3 cycles before delayed debulking surgery. Chemotherapy used in this fashion is termed ‘neo-adjuvant chemotherapy’. Whether women undergo primary debulking surgery or neo-adjuvant chemotherapy with subsequent delayed debulking surgery is dependent on the disease burden, the general fitness of the patient and clinician preference (125). It is, however, a decision that is ultimately made by a multi-disciplinary team following discussion and review of imaging and histology results.

In order to investigate the effect of chemotherapy on the MDSC populations the cohort of women who underwent delayed debulking surgery were selected and their results compared to those women who had not received chemotherapy, termed 'chemotherapy-naïve'.

3.2.8 Exposure to chemotherapy reduces the proportion of MDSC within tumour but not in the omentum or peripheral blood.

The percentage of MDSC reduced at the primary site of tumour following chemotherapy but did not appear to change within the PBMC or in the omental samples. Within PBMC, the chemotherapy naïve patients had an average of 6% MDSC, whilst those exposed to chemotherapy had an average of 3.3%. Within the omentum there was a non-significant difference of just over 6% with the chemotherapy naïve patients having an average of 26% compared to 34% in those who had received chemotherapy. Within the ovarian tumour there was a significant difference of over 3-fold reduction in MDSC population with an average of 33% in those unexposed to chemotherapy compared to 10% in the exposed cohort ($p<0.05$) (Figure 3.11). As previously described, the percentage of MDSC within the PBMC of both the chemotherapy-exposed and naïve patients is much less than in the tumour and omental sites. In both the PBMC and ovarian tumours the MDSC appeared to reduce following chemotherapy, whilst it increased non-significantly within the omentum. This could be due to chemotherapy being potentially less able to penetrate the omental metastases in comparison to PBMC or ovarian tumours, or could be due to the post-chemotherapy change in the immune microenvironment that has been created within the omental metastasis; perhaps increasing the secretion of factors such as GM-CSF to increase infiltration of MDSC to these sites.

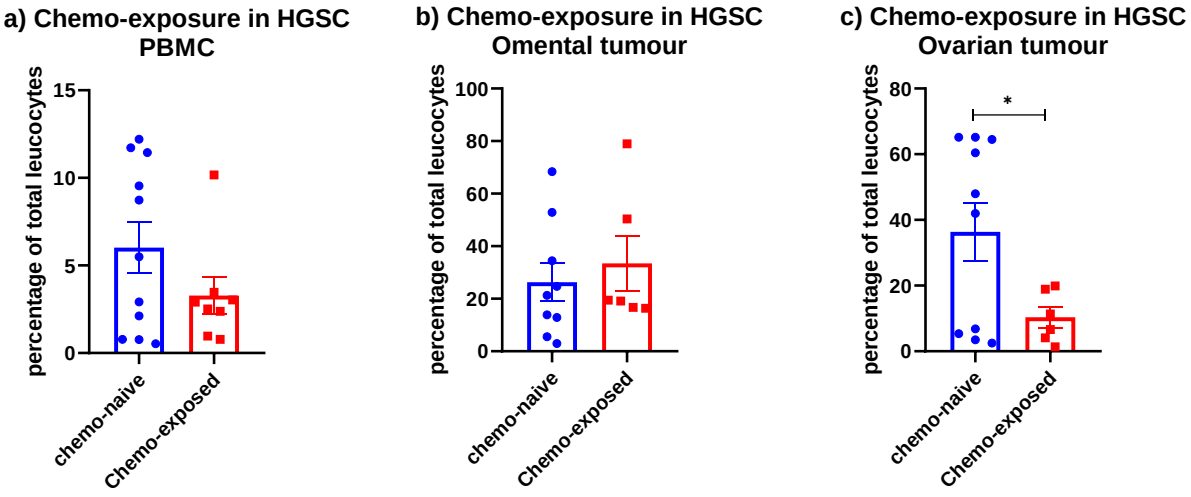

Figure 3.1 1. A comparison of the percentage of MDSC in women exposed to chemotherapy versus those who were not.

Samples taken from the a) peripheral blood, n= 11 in the chemo-naïve cohort, n= 8 in the chemo-exposed cohort, b) omentum, n= 9 in the chemo-naïve cohort, n= 6 in the chemo-exposed cohort and c) primary tumour n= 10 in the chemo-naïve cohort, n= 6 in the chemo-exposed cohort. T test performed. There is a statistically significant difference between the groups in the ovarian tumour samples but not in the peripheral blood or omentum. * = p <0.05. Bars depict mean and standard error of the mean.

A non-significant trend was observed towards an increased proportion of m-MDSC within the chemotherapy-exposed cohort in both the omentum (p=0.15) and tumour samples (p=0.1), but not PBMC, compared to those who were naïve to chemotherapy (Figure 3.13). A representative FACS graph for a chemotherapy-exposed and chemotherapy-naïve patient demonstrating the MDSC populations is shown in Figure 3.12. There is no significant difference in PMN-MDSC between the chemotherapy exposure groups in either the PBMC, omentum or tumour samples (Figure 3.14).

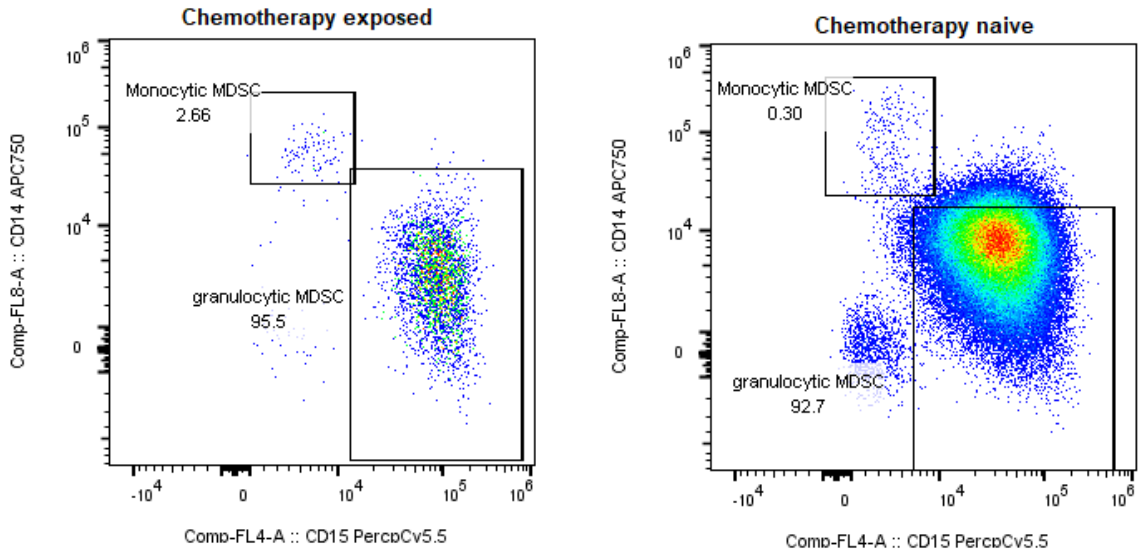

Figure 3.1 2. Representative FACS plots demonstrating the MDSC populations in high grade serous ovarian tumours in a chemotherapy-exposed and chemotherapy-naïve patient.
Tissue shown here is ovarian tumour. Percentages are labelled on the graphs. Much greater numbers of cells were retrieved from the chemotherapy-naïve patients, but proportionately there were more m-MDSC in those exposed to chemotherapy.

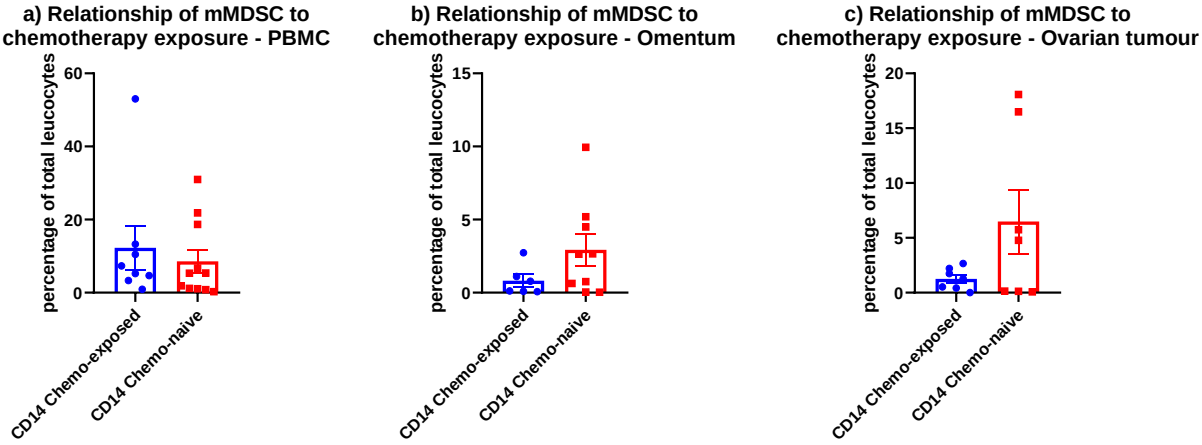

Figure 3.1 3. The percentage of m-MDSC of total leucocyte population in the omentum and ovarian tumour pre- and post-chemotherapy exposure.
a) PBMC. n=8 chemo-exposed, n=11 chemo-naïve b) omentum. n= 6 chemo-exposed, n= 9 chemo-naïve, T test demonstrates non-significance. c) ovarian tumour. n= 7 chemo-exposed, n= 7 chemo-naïve. T test demonstrated non-significance. Bars represent mean and standard error of the mean.

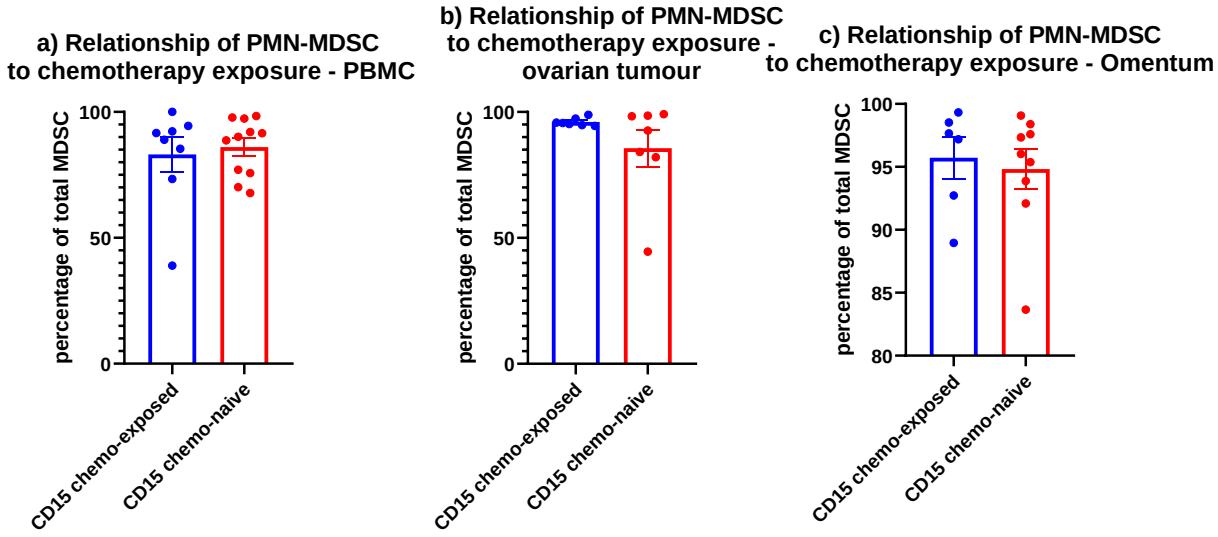

Figure 3.1 4. The percentage of PMN-MDSC of total leucocyte population in the omentum and ovarian tumour pre- and post-chemotherapy exposure.
a) PBMC. n=8 chemo-exposed, n=11 chemo-naïve b) omentum. n= 6 chemo-exposed, n= 9 chemo-naïve, T test demonstrates non-significance. c) ovarian tumour. n= 7 chemo-exposed, n= 7 chemo-naïve. T test demonstrated non-significance. Bars represent mean and standard error of the mean.

3.2.9 Correlation of the presence of MDSC infiltrates with treatment outcomes in patients with ovarian cancer

It was evident that MDSC were present within ovarian cancer and that the granulocytic population was the major population within all tissue and PBMC samples. To investigate if there was any clinical

correlation between the presence of MDSC and outcome, the percentage of MDSC within the total leucocyte population were compared to various outcome measures. The chosen outcome measures were the ability to achieve complete cytoreduction and the chemotherapy response score (CRS) as both of these factors are known to impact on prognosis (39,126). It was not possible to measure mortality or recurrence data due to the short length of follow up.

3.3.0 Women who achieved complete cytoreduction had a trend to fewer MDSC in their tumour samples.

Cytoreduction is measured according to the amount of tumour visible following surgery. If all visible tumour is removed, this is termed 'R0' or complete cytoreduction (127). If there are tumour deposits less than 1 cm remaining following debulking surgery this is classed as R1, and greater than 1 cm is termed R2. If the patient has a large volume of disease infiltrating the small bowel mesentery, the coeliac axis, the porta hepatis or the surface of the stomach it is unlikely that R0 can be achieved as these are essential structures and cannot be entirely surgically removed.

The results demonstrate a trend to increased MDSC infiltration in tumour specimens in those women with a poorer surgical outcome with a cytoreduction score of 1 or 2 (Figure 3.15). In particular, in those achieving complete cytoreduction (R0) there was more than 50% reduction in MDSC within their tumour samples compared to those who did not, at 14% and 35%, respectively. The MDSC within the PBMC remained similar between the 2 cohorts, at 4.9% and 4% for R0 and R>=1 respectively. When analysing the difference between the MDSC in the PBMC and tumour samples, there is almost a 9-fold difference between the MDSC in the PBMC compared to tumour within the R>=1 cohort, compared to less than 3-fold increase in those with optimal cytoreduction.

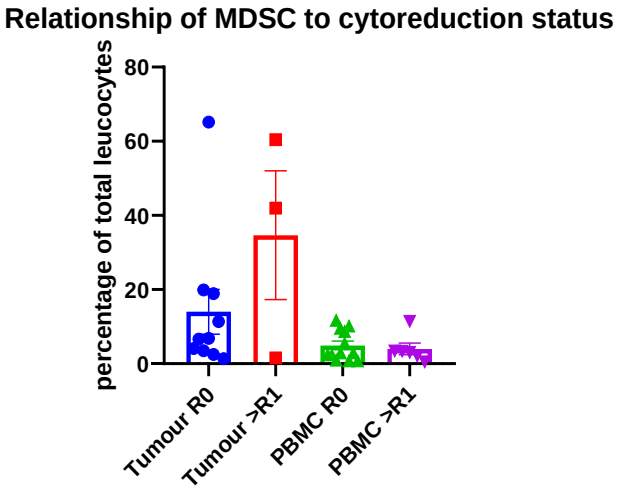

Figure 3.1 5. The percentage of MDSC of the total leucocyte population in both the peripheral blood and tumour of those women achieving complete cytoreduction (R0) compared to suboptimal cytoreduction (R≥1).
There is a trend (p=0.17) to a greater infiltration of MDSC seen in those with suboptimal cytoreduction. n= 10 tumour R0, n= 3 Tumour >R1, n= 12 PBMC R0, n= 6 PMBC >R1. T test: All results non-significant. Bars depict mean and standard error of the mean.

3.3.1 Women achieving optimal histological response to chemotherapy (CRS3) had a trend to fewer MDSC present in their peripheral blood, tumour and omental samples.

The chemotherapy response score (CRS) is a three-tiered scoring system based on histological findings to assess the response to chemotherapy in high-grade serous tubo-ovarian cancer. Analysis of the omentum has been found to be associated with progression-free survival, with those achieving a CRS 1-2 having a poorer progression-free survival than those with a CRS3 (126,128). The score is provided on the histopathology report following completion of histopathology analysis.

The results show that there appears to be a trend to greater accumulation of MDSC within the tissue of women with a poorer CRS score (CRS1-2) compared to the patient achieving a CRS score of 3 (Figure 3.16). Within the PBMC the percentage is relatively constant between those with CRS1 or 2 and those with CRS 3 at 3.5% and 2.4% respectively. This is similar to the findings described above for women achieving complete cytoreduction. Within the omentum however, there is more than 2-fold difference in MDSC between the CRS3 and CRS 1 and 2 groups at 16% and 37% respectively. This increase is further demonstrated within ovarian tissue whereby MDSC represent 1.4% of total leucocytes in the patient with CRS3 versus 17.1% in those with CRS 1 and 2. Whilst there is actually a 50% decrease in MDSC within the ovary compared to PBMC samples in the woman with CRS3, there is an 8-fold increase in MDSC accumulating at the ovarian tumour in the women with a poorer CRS score.

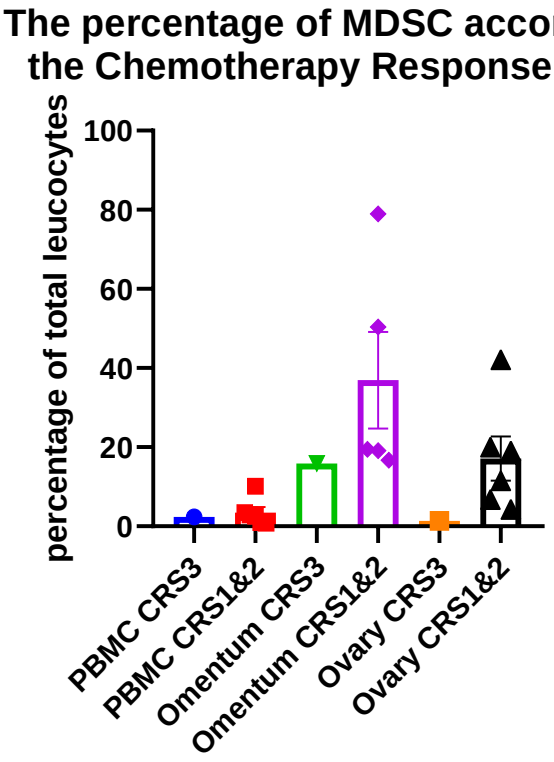

Figure 3.1 6. The percentage of MDSC of the total leucocyte population in those with a good response to chemotherapy (CRS 3) and a suboptimal response to chemotherapy (CRS 1-2). No statistical tests performed as only one sample in CRS 3 category. n= 1 PBMC CRS 3, n= 6 PBMC CRS 1&2, n= 1 omentum, CRS 3, n= 5 omentum, CRS 1&2, n= 1 ovarian tumour CRS 3, n= 6 ovarian tumour CRS 1&2. All samples are HGSC. Bars depict mean and standard error of the mean.

3.3.2 Increased monocytic MDSC was associated with a poorer treatment response, despite accounting for only a small proportion of total MDSCs.

Having determined that MDSC may play a role in subsequent treatment response, it was hypothesised that it may be influenced greater by either the granulocytic or monocytic populations.

Although the monocytic MDSC were the minority cell population, their presence was found to be associated with a poorer prognosis in terms of the ability to achieve complete surgical cytoreduction and their response to chemotherapy, as demonstrated by the CRS score (Figure 3.17). The results show that the PBMC of healthy donors has a percentage of m-MDSC of 0.6%, similar to that of the woman achieving CRS 3, who had and m-MDSC population 0.9%. In comparison to those with CRS 1 or 2 this is a greater than 10-fold difference compared to healthy donor with an m-MDSC population of 7% ($p=<0.0001$). In those achieving optimal cytoreduction, the percentage of MDSC was 6.7% compared to 15% in those with incomplete cytoreduction. This was compared to the m-MDSC within the healthy donors and was significantly greater in those with R0 disease ($p<0.05$). However, this did not achieve statistical significance in those with R>=1 due to the wide standard deviation within the results and a

good response to chemotherapy demonstrated significantly fewer m-MDSC than in those with a worse response to chemotherapy.

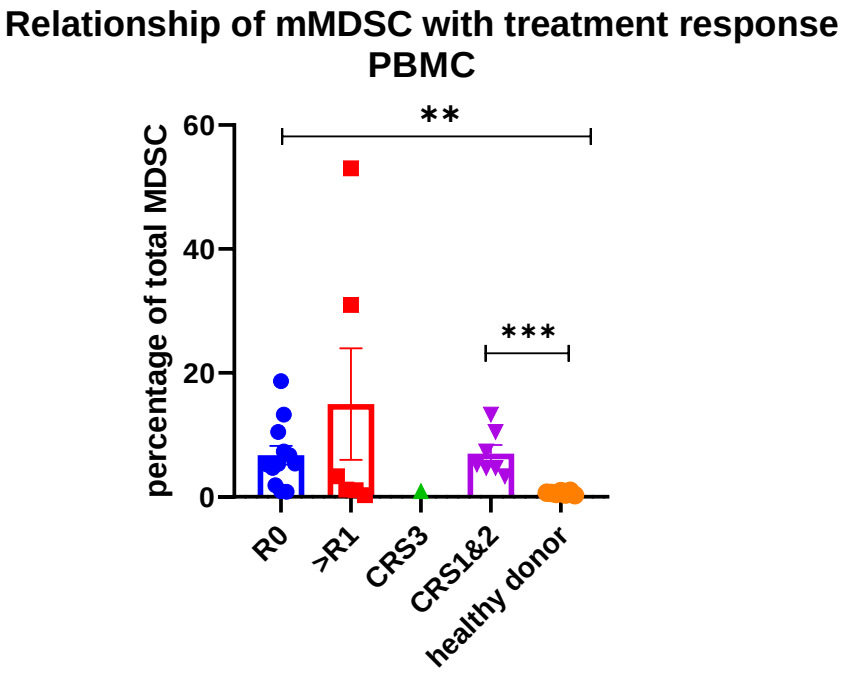

Figure 3.1 7. The relationship of m-MDSC with treatment response in the circulating blood samples of patients.
There appears to be an increased accumulation of m-MDSC in women with worse prognostic indicators (CRS 1-2, R≥1) compared to those with R0 and CRS3 and healthy donors. ANOVA: ** = p=0.01, *** = p = <0.0005 n= 12 R0, n= 6 >R1, n= 1 CRS 3, n= 7 CRS 1&2, n= 7 healthy donors. Bars depict mean and standard error of the mean.

There was a 3-fold greater percentage of monocytic MDSC in the omentum of women with residual disease following cytoreduction compared to those achieving complete cytoreduction, at 1.3% and 3.8% respectively. MDSC are known to be potent immunosuppressors and as such a 3-fold difference in their number could have a functional effect, however further study is required to characterise this effect fully. There was a 10-fold reduction in m-MDSC in the woman with CRS3 compared to those with CRS 1 or 2 with 0.1% and 1% respectively. This relationship between m-MDSC and prognosis was not apparent when investigating the site of primary tumour (Figure 3.18A and B).

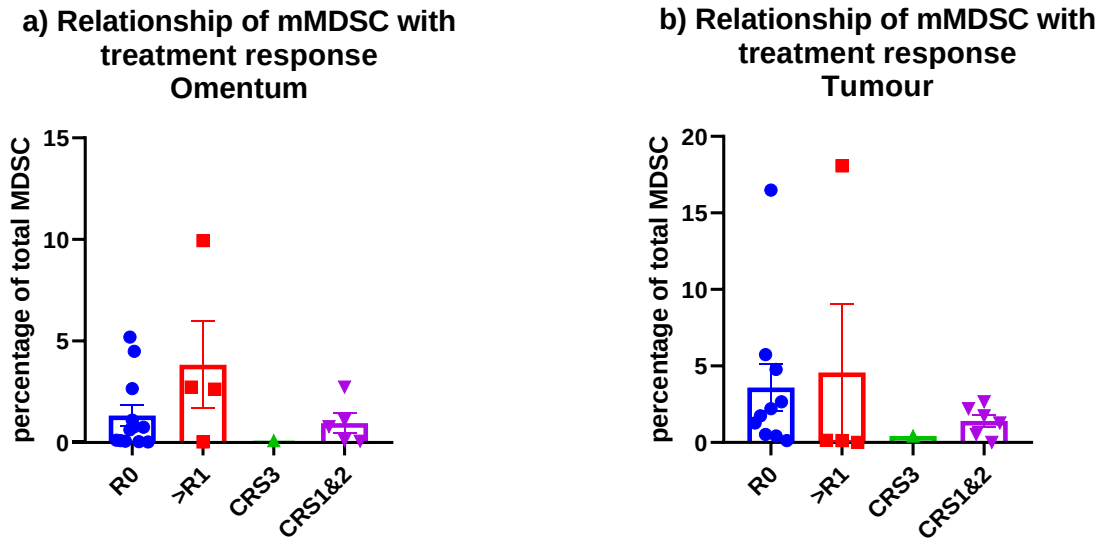

Figure 3.1 8. The relationship of m-MDSC with the chemotherapy response score and the achievement of complete cytoreduction in a) the omentum and b) the tumour.
There is a trend to greater m-MDSC in those with R≥1 (p=0.1) compared to those with complete cytoreduction and a trend to fewer m-MDSC in the patient with optimal response to chemotherapy (CRS 3). Bars depict mean and standard error of the mean. n= 12 R0, n= 4 >R1, n= 1 CRS 3, n= 5 CRS 1&2. T test: no statistical significance achieved.

3.3.3 The presence of granulocytic MDSC has no prognostic significance.

To calculate the proportion of PMN-MDSC for this analysis the population of PMN-MDSC was divided by the total MDSC population. The results comparing CRS1 and 2 with CRS 3 need to be interpreted with caution due to the limited cohort size of one in the CRS3 group. Further cases are needed to investigate these relationships further. The results show that whilst the PMN-MDSC were present in greater numbers in all specimens, their presence had no overall bearing on the response to treatment. In PBMC the percentage of PMN-MDSC in women achieving complete cytoreduction was 87% compared to 82% in women with incomplete cytoreduction. Women with a CRS score of 1 or 2 had an 88% population of PMN-MDSC compared to almost a 100% in the woman with CRS3. None of these results demonstrated any significance (Figure 3.19a). These results remained true for the omentum (Figure 3.19b) and tumour samples (Figure 3.19c).

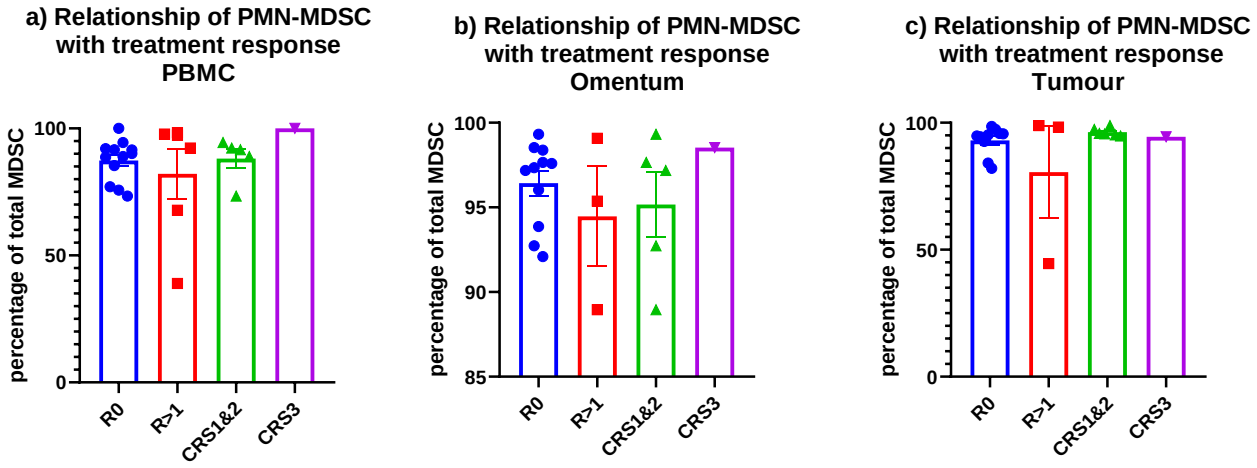

Figure 3.1 9. The percentage of granulocytic MDSC present within samples grouped according to treatment outcomes.
Samples taken from the a) peripheral blood n= 12 R0, n=6 R>1, n=5 CRS 1&2, n=1 CRS 3, b) omentum n= 11 R0, n= 3 R>1, n= 5 CRS 1&2, n= 1 CRS3, all results non-significant c) tumour n= 10 R0, n= 3 R>1, n= 6 CRS 1&2, n= 1 CRS 3. T tests performed between R0 and R1 in each of the tissues and PBMC. Unable to perform statistical analysis on CRS 3 due to only having 1 sample. All results non-significant. Bars represent mean and standard error of the mean.

3.3.4 The ratio of PMN-MDSC to m-MDSC in peripheral blood is greater in benign disease and healthy control compared to ovarian cancer

The ratio of PMN-MDSC to m-MDSC was then investigated, to determine if this held any significant prognostic value in determining benign versus malignant disease or predicting treatment outcome. Those samples with a greater number as their ratio have a greater infiltration of PMN-MDSC for every m-MDSC whereas those with a lower number have a comparatively greater infiltration of m-MDSC.

Greater numbers of PMN-MDSC within the PBMC of healthy donors were seen in comparison to women with high-grade serous ovarian cancer, as demonstrated by almost a 1000-fold increase in the ratio (p=0.002) in the healthy donor cohort (1:7048 in healthy donors versus 1:9 in HGSC) (Figure 3.20b). This effect was also seen with benign disease but to a much lesser degree, with a ratio of 1:49 in benign disease, some 145 times less than the healthy donors (Figure 3.20a). The results demonstrate that there is also a significant difference between benign tumours and high-grade serous ovarian cancer (p=0.0004) with average ratios 5 times greater in benign disease than in HGSC, at 1:9 and 1:49 respectively (Figure 3.20c).

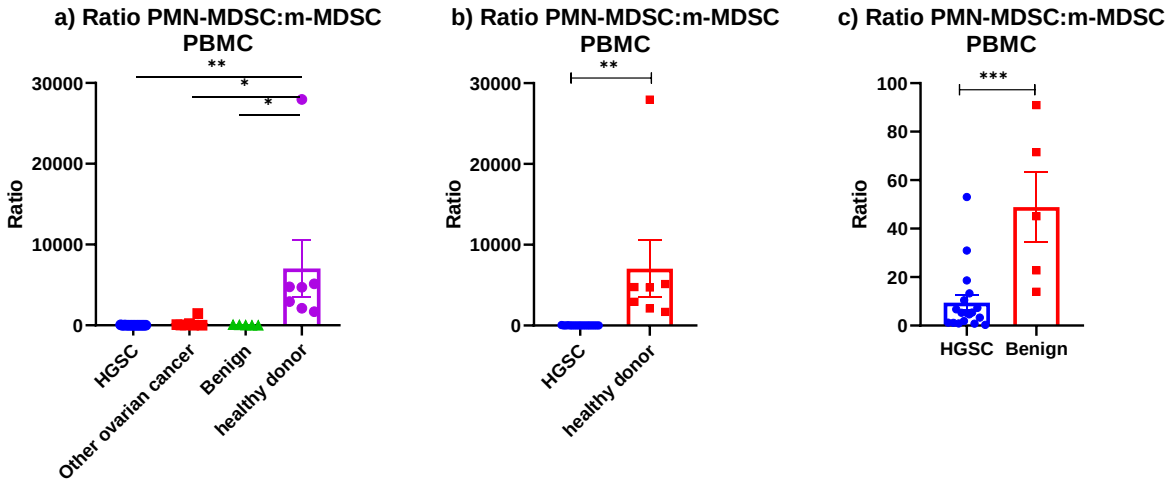

Figure 3.2 0. A comparison of the ratio of PMN-MDSC to m-MDSC within peripheral blood of healthy donors versus ovarian neoplastic disease.
The greater the value, the more PMN-MDSC are present per m-MDSC. a) Comparison between high-grade serous ovarian cancer, other ovarian cancer subtypes, benign tumours and healthy donors. n= 18 HGSC, n= 5 other ovarian cancer, n= 7 benign tumour, n= 7 healthy donor. One-way ANOVA: ** p = <0.01 * p < 0.05. b) Comparison between HGSC and healthy donor. T test ** p = <0.01 * p < 0.05. c) Comparison between HGSC and benign disease. T-test: *** p = <0.0005. Bars determine mean and standard error of the mean.

3.3.5 A trend towards a greater ratio of PMN-MDSC:m-MDSC is seen in women with CRS3 than with CRS1/2

A CRS score of 3 is associated with an improved response to chemotherapy and therefore represents an improved treatment outcome. Any observations made using the data from the CRS3 cohort need to be interpreted with caution as there was only one patient in this group and as such further work is required in order to confirm these findings. The ratio of PMN-MDSC:m-MDSC was greater in the sample which had achieved a CRS score of 3 compared to those with a CRS of 1 or 2 (Figure 3.21). This is consistent with the findings above that benign disease is associated with a greater ratio as here it is associated with an improved response to chemotherapy. The results show that in PBMC the women with a poorer response to chemotherapy (CRS1 or 2) had a ratio of 1:15 compared to 1:109 in the woman with CRS3, a 7-fold difference. No statistical analysis can be performed on any of these results due to the fact there is only 1 result for CRS3. In the tumour, the ratio was 1:78 versus 1:223 for CRS1&2 and CRS3 respectively, almost a 3-fold increase, whilst in the omentum the ratios were 1:490 and 1:1012 for CRS1&2 and CRS3 respectively - almost a 2-fold increase.

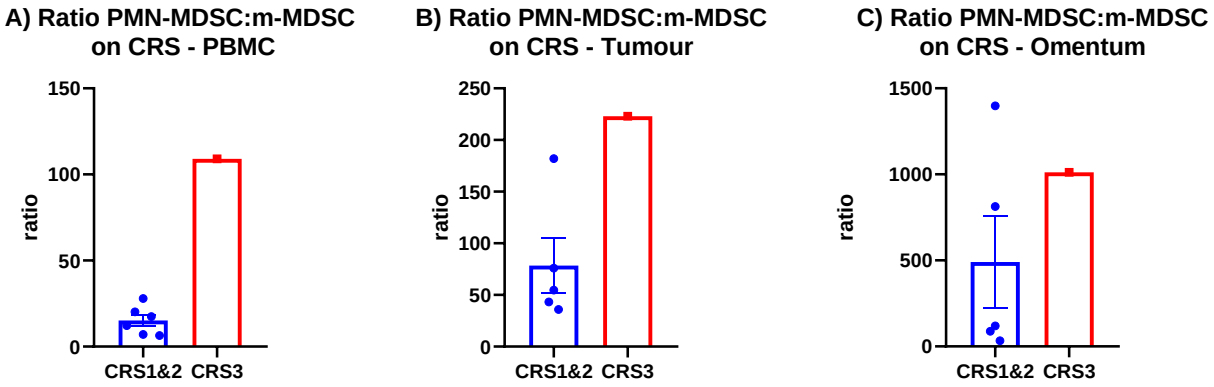

Figure 3.2 1. Graphs depicting the ratio of PMN-MDSC:m-MDSC in women achieving a CRS score of 1 or 2 compared to the sample achieving a CRS score of 3.
a) PMN-MDSC:m-MDSC in peripheral blood. CRS1&2 n= 6, CRS3 n=1. b) PMN-MDSC:m-MDSC in tumour samples. CRS1&2 n=5, CRS3 n=1. c) PMN-MDSC:m-MDSC ratio in omental samples. CRS 1&2 n=5, CRS 3 n=1. Bars depict mean and standard error of the mean. Samples are taken from interval surgery patients as they have all been exposed to chemotherapy.

3.3.6 Chemotherapy changes the populations of MDSC to favour increased accumulation of m-MDSC

Following chemotherapy, although the MDSC populations appeared to reduce in terms of overall number within the PBMC and ovarian tumour (Figures 3.11a-c), the ratio of monocytic to granulocytic MDSC changed to include a greater ratio of monocytic to granulocytic MDSC following chemotherapy (Figure 3.22). Within the PBMC there was a 6-fold increase in the ratio in the patients naïve to chemotherapy at 1:13 in the chemotherapy-exposed group and 1:78 in the chemotherapy-naïve group, however this did not reach statistical significance. The ratio in the tumour samples had a 3-fold difference of 1:102 and 1:360 in the chemotherapy exposed and naïve patients respectively. Again, these results were not statistically significant potentially due to limited patient number in each group. Similarly to the results demonstrated in Figure 3.11b above, the difference between ratios were non-significant within the omentum with a ratio of 1:490 in the chemotherapy exposed compared to 1:793 in the chemotherapy naïve patients. The combined ratios for all tissues are represented in Figure 3.23 on a logarithmic scale to demonstrate the difference in ratios between the PBMC, ovarian tumour and omentum.

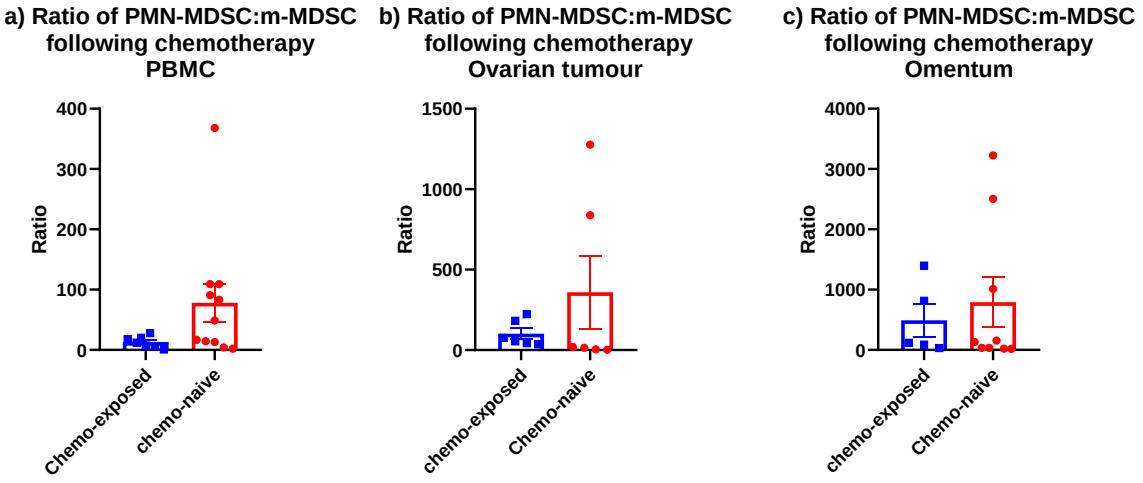

Figure 3.2 2. A comparison of the ratio of PMN-MDSC to m-MDSC prior to and following chemotherapy.
a) peripheral blood n= 7 chemo-exposed, n= 11 chemo-naïve b) ovarian tumour n= 6 chemo-exposed n= 6 chemo-naive c) omentum n=5 chemo-exposed, n= 9 chemo-naive. T test demonstrated non-significance; bars represent mean and standard error of the mean.

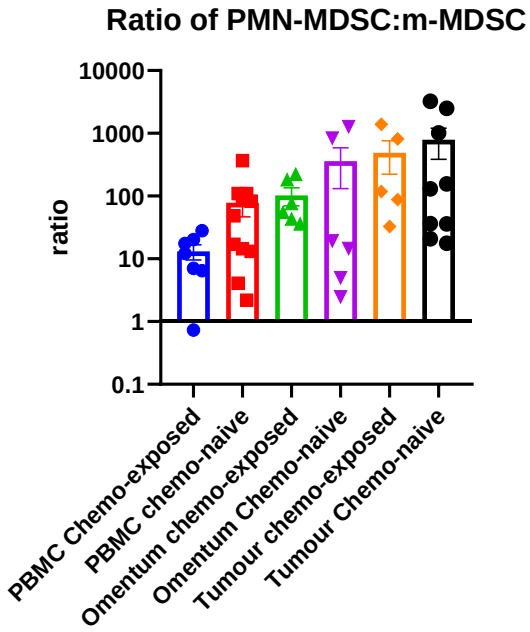

Figure 3.2 3. Summary of the effect of chemotherapy on the PMN-MDSC:m-MDSC ratio in different tissue types.
Bars represent mean and standard error of the mean.

3.3.7 No significant difference was seen in LOX-1 expression on PMN-MDSC between benign and malignant disease, and no correlation was seen with outcome

LOX-1 has been identified as a potential marker for granulocytic MDSC. It was found to be increased in low-density neutrophils (PMN-MDSC) and has been used as a surrogate marker for their presence. The identification of LOX-1 positive cells was performed by flow cytometric staining for surface LOX-1 expression. Following identification of the PMN-MDSC using the previously described gating strategy, a further gate was added in order to determine LOX-1 expression. A representative graph of the gating for each histological group is demonstrated in Figure 3.24.

These results did not find any statistically significant difference in LOX-1 expression in benign or malignant disease, the biggest difference was between HGSC and healthy donor but this did not quite attain statistical significance (p=0.08) (Figure 3.25). The LOX-1 expression in HGSC was 50%, compared to 30% in healthy donors. There was a large range in the HGSC results, however, with some subjects having as low as 19% expression, while others had up to 87% in the PBMC. Within the PBMC of healthy donors, however, the range was very narrow, between 25% and 33% (Figure 3.25A). Within the ovarian tumour the results were very similar between the different diagnoses with the average percentages of LOX-1 expression ranging from 40-54% (Figure 3.25B). In the omental samples, those with malignancy were very similar; HGSC had an expression of 45% and the samples from other ovarian cancers had an average of 43%. This was in comparison to 77% in benign disease (Figure 3.25C). There was no difference in the expression of LOX-1 between the different tissue types in HGSC (Figure 3.26).

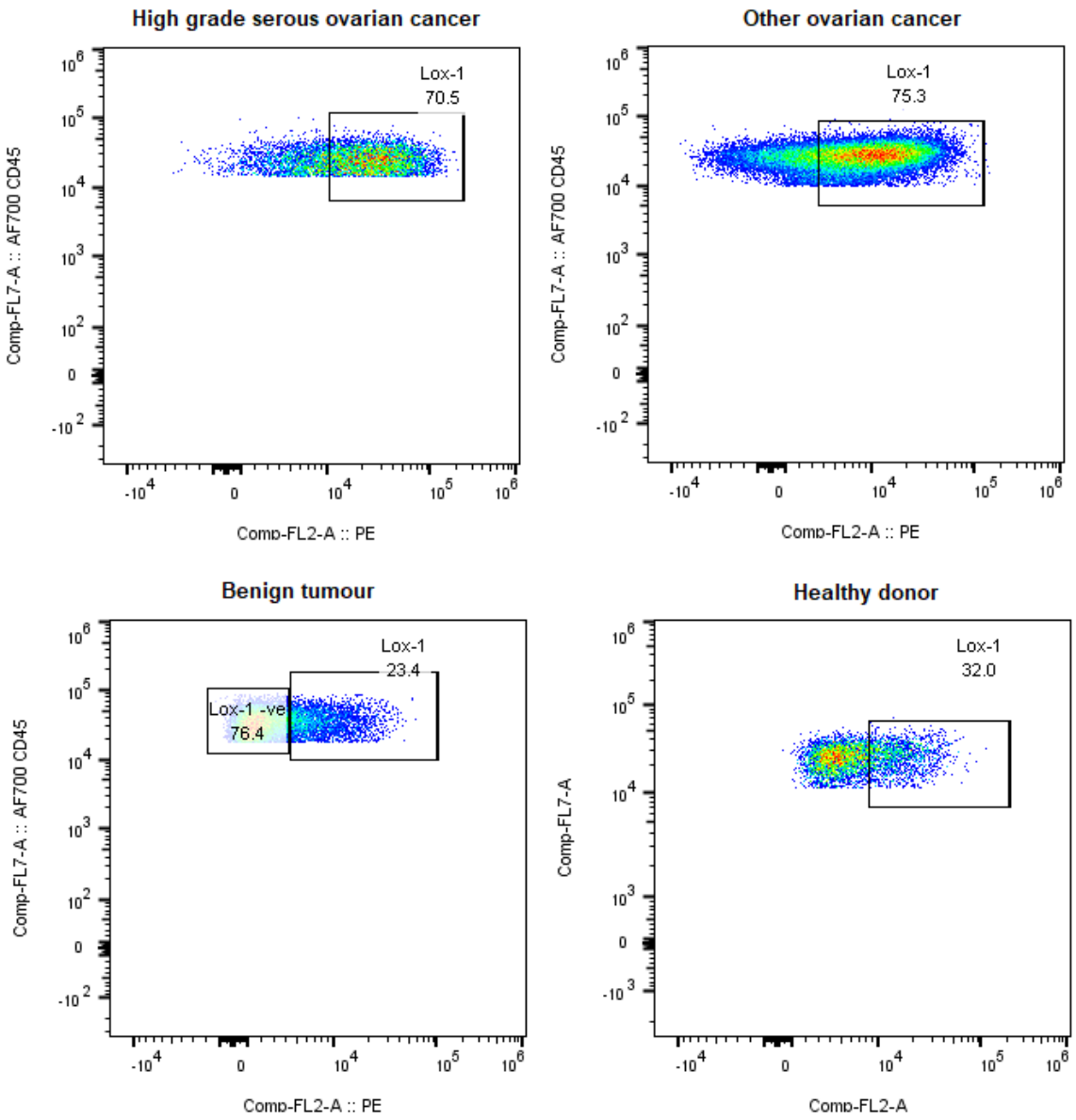

Figure 3.2 4. Representative FACS plots of LOX-1 expression in high grade serous ovarian cancer, endometrioid ovarian cancer (other ovarian cancer), benign tumour and healthy donor in PBMC.

There was a non-significantly greater presence of LOX-1 in the malignancy patients in comparison to the benign and healthy donor patients. LOX-1 expression is expressed as a percentage on the graphs.

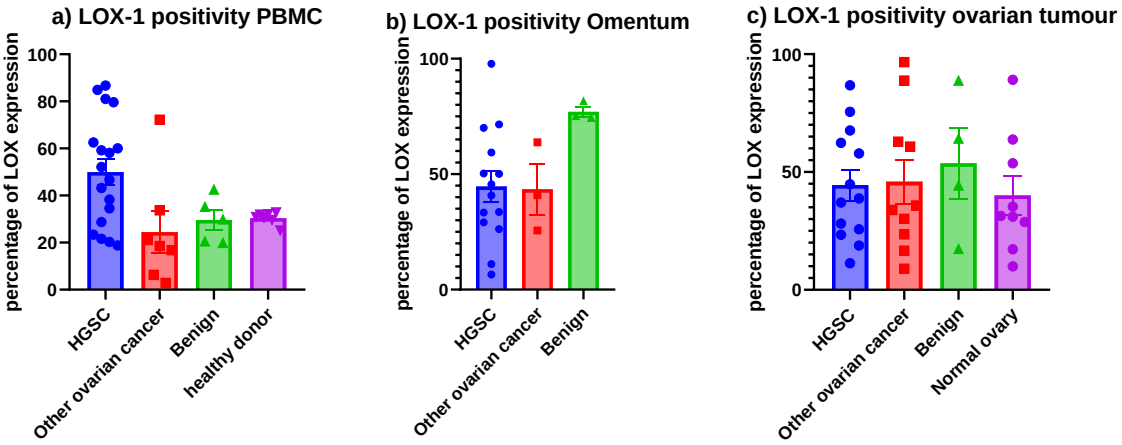

Figure 3.2 5. The percentage of LOX-1 positivity in high-grade serous ovarian cancer compared to other types of ovarian cancer, benign disease and healthy donor.
Samples taken from A) PBMC. HGSC n=18, other ovarian cancer n=7, benign n=5, healthy donor n=7, B) omentum. HGSC n=14, other ovarian cancer n=3, benign n=3 and C) ovarian tumour. HGSC n=13, other ovarian cancer n=10, benign n=4, normal ovary n=9 Statistical test – one-way ANOVA demonstrated non-significance for all results. Bars represent mean and standard error of the mean.

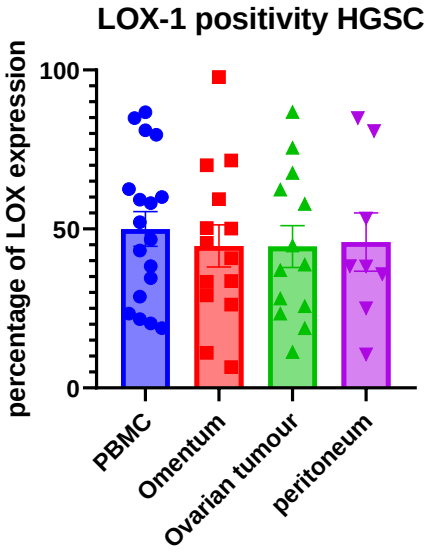

Figure 3.2 6. LOX-1 expression in different tissue types within high-grade serous ovarian cancer samples.
ANOVA: There is no statistically significant difference in its expression. n= 18 PBMC, n= 14 omentum, n= 13 ovarian tumour, n= 8 peritoneum. Bars signify mean and standard error of the mean.

The expression of LOX-1 did not correlate with diagnosis or treatment outcome measured by either CRS or cytoreduction. Within the PBMC, omentum and tumour samples there was no statistically significant difference between the CRS score or the degree of cytoreduction (Figure 3.27). The greatest difference between samples was seen in the LOX-1 positivity within tumour samples between CRS1&2

patients and the patient with CRS3, with 50% and 19% respectively. Statistical analysis was not possible due to the fact that there was only one sample with CRS3.

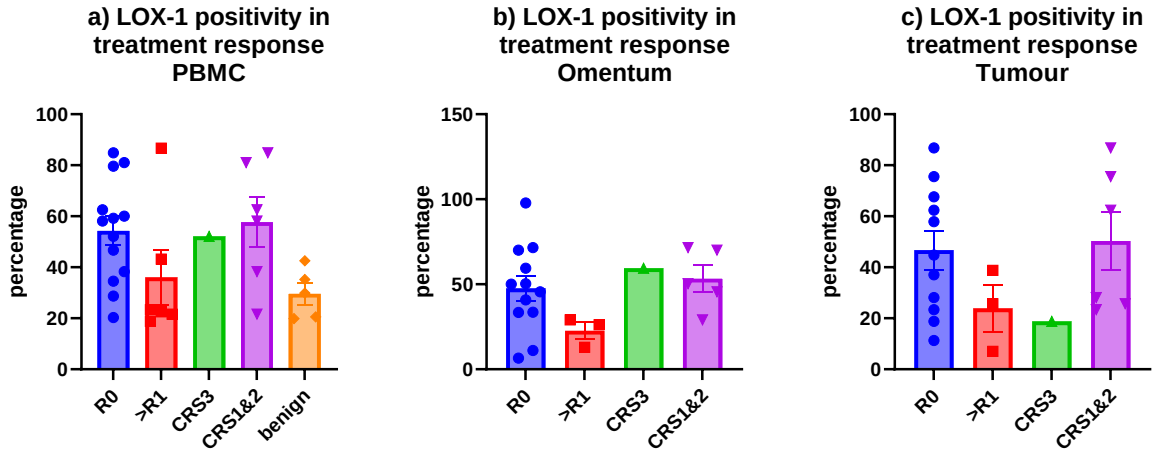

Figure 3.2 7. The percentage of LOX-1 expression compared with measurements of treatment response (degree of cytoreduction achieved and the chemotherapy response score).
Samples taken from a) PBMC n= 13 R0, n= 6 >R1, n= 1 CRS 3, n= 4 CRS 2, n= 2 CRS 1, n= 5 benign b) omentum n= 12 R0, n= 3 R>1, n= 1 CRS 3, n= 5 CRS 1&2 and c) tumour n= 11 R0, n= 3 R>1, n= 1 CRS 3, n= 3 CRS 2, n= 3 CRS 1. ANOVA: There is no statistically significant difference in their expression of LOX-1. Bars represent mean and standard error of the mean.

3.4.0 Chapter Summary

In this chapter, MDSC have been confirmed in ovarian cancer, benign disease and the PBMC of healthy donors, however, MDSC were not present in 'healthy donor' (patients diagnosed with BRCA mutation attending for risk-reducing surgery with no macroscopic or microscopic evidence of malignancy) ovarian tissue. When scrutinising the differences between benign and malignant disease further, it was found that the percentage of total MDSC within the leucocyte population remained constant, regardless of the underlying diagnosis of the patient. The potential hypothesis for this is that MDSC are accumulating at sites of inflammation, not just malignancy, and as such would be present in benign conditions, such as endometriosis, which are known to be associated with a significant inflammatory response. The presence of MDSC cannot determine whether a lesion is benign or malignant. In ovarian cancer, there was a greater accumulation of MDSC at sites of metastasis compared to circulating blood. In benign disease, this trend was not seen so may suggest the MDSC are migrating to sites of metastasis in malignant disease.

The majority of MDSC infiltrating tissue were the PMN-MDSC subtype, regardless of the tissue type or diagnosis.

Within ovarian cancer the mainstay of treatment is through surgery and chemotherapy. The degree of cytoreduction is graded from R0, meaning complete removal of all visible disease, R1 denoting deposits less than 1 cm remaining and finally R2, where disease remaining measured greater than 1 cm. R0 is associated with the best prognosis. The chemotherapy response score (CRS) grades women's response to chemotherapy by analysing the histopathological features of omental deposits. This is graded from 1 to 3, where 1 represents a poor response and 3 represents optimal response to chemotherapy. Women with CRS3 have a better prognosis than those with CRS1 or 2 (129).

Chemotherapy appeared to reduce the overall percentage of MDSC within the primary tumour but did not significantly affect MDSC within the PBMC or omental samples. The treatment outcomes, the cytoreduction score and CRS, were analysed and women who achieved complete cytoreduction had a tendency to fewer MDSC in their tumour samples. Women with a CRS3 had a trend to fewer MDSC in their PBMC, tumour and omental samples. Overall, it was found that the m-MDSC population correlated with treatment outcomes with a higher proportion of m-MDSC being associated with the poorer outcomes of CRS1 or 2 and R2 or 3. The PMN-MDSC were not correlated to these outcomes. Chemotherapy appeared to favour the accumulation of m-MDSC as there was proportionally a greater number of m-MDSC in samples post-chemotherapy than in pre-chemotherapy samples.

To investigate the relationship between PMN-MDSC and m-MDSC with treatment outcome, the ratios of PMN-MDSC:m-MDSC were analysed and demonstrated that the ratio was greater in healthy women (age- and sex-matched controls) or in women with benign disease compared to those with ovarian cancer. The ratio was influenced by an increase in m-MDSC rather than a reduction in PMN-MDSC. The ratio was able to determine benign from malignant disease with over a 5-fold difference between these groups. There was found to be a greater ratio in women with CRS3 than women with CRS1 or 2, potentially raising the possibility of using this in a blood test to assist the clinicians in predicting the histological diagnosis and perhaps longer-term outcomes such as risk of recurrence, prognosis or response to targeted therapies or immunotherapies.

These results have confirmed that MDSC are present in both benign and malignant ovarian pathology, but also that they are present in healthy donors. Their presence in neoplastic disease demonstrated an impact on treatment outcome, ultimately impacting on clinical prognostic significance.

3.5.0 Chapter Discussion

It has previously been published that in most malignancies PMN-MDSC predominate over the m-MDSC population (130) and these results echo this. In general, PMN-MDSC contributed to the majority of the MDSC population within ovarian cancer, benign ovarian disease and healthy donor cohorts.

These results demonstrated that MDSC are present in benign and malignant ovarian tumours, and importantly m-MDSC appear to have a prognostic relationship in women with HGSC. This fits with current literature showing m-MDSC to be the more potent immunosuppressor and is associated with poorer outcomes in other malignancies (131). The ratio of PMN-MDSC:m-MDSC demonstrated a higher number of PMN-MDSC in healthy donors and those with benign disease compared to those with HGSC, who had proportionally more m-MDSC within their tissue and blood samples. In healthy donor PBMC, the ratio was almost 15000 PMN-MDSC to every 1 m-MDSC, compared to up to 20 PMN-MDSC for every 1 m-MDSC in high-grade serous ovarian cancer.

Benign diseases, such as ovarian fibroadenoma or endometriosis, caused an increase in the proportion of m-MDSC in circulating blood so this was not unique to HGSC. Although these results demonstrate that MDSC are present in areas of benign inflammation, the ratio specifically may be able to differentiate between malignancy and inflammation. There was a statistically significant difference between the ratios of benign and HGS of over 5-fold and as such could present a new method for screening women with an ovarian mass. Currently, women presenting with an ovarian mass have imaging and blood tests to measure tumour markers. The most commonly used tumour marker for ovarian cancer is cancer antigen 125 (CA-125), which is a high molecular weight glycoprotein expressed by epithelial ovarian cancers. It is increased in a range of benign and malignant medical and surgical disorders and was only raised in 50% of stage I ovarian cancers, likely due to the fact that they are usually type 1 tumours and so tend to be more indolent, therefore has very poor sensitivity and specificity (132). CA-125 and imaging provide a score reflecting their risk of malignancy. The National Institute for Health and Care Excellence (NICE) recommends women with a risk of malignancy of greater than 250 be managed in a tertiary specialist centre. Women with a score less than this can be managed in a non-specialist unit as their risk is perceived to be low. Due to the intrinsic errors with using CA-125, there will be women who are erroneously managed in a tertiary centre, whilst women with an underlying diagnosis of cancer will be managed in a non-specialist unit, where the likelihood of achieving complete cytoreduction is less. A potential avenue for a new screening tool could be the ratio between PMN-MDSC:m-MDSC, however this would need further investigation and prospectively collected at the time of diagnosis and correlated with surgical and histopathological findings and ultimately clinical outcome.

The experiments in this chapter demonstrated that normal ovarian tissue had few MDSC present and could not be used as a control for further experiments. Perhaps further studies on the healthy fallopian

tube could represent an alternative appropriate control, seeing as many ovarian cancers are thought to originate from the fallopian tube itself. When microscopically normal ovaries were removed from women with a diagnosis of cancer or benign disease, there were MDSC present within these specimens; evident to a greater extent in those women with a diagnosis of ovarian cancer. This may suggest that MDSC have a potential role in facilitating metastasis or in the initiation of early disease, not yet macroscopically or microscopically visible. Although they may appear macroscopically 'normal' there may be a molecular abnormality present which could influence the tumour microenvironment.

The comparison between benign, HGSC and other ovarian cancers was a novel angle to investigate because within the literature, patients with ovarian cancer had only been compared to the blood of healthy controls, rather than those with other ovarian pathology.

It is appreciated that comparing benign and malignant disease is not a like-for-like comparison because despite the term 'benign', these ovarian neoplasms are associated with a great deal of inflammation, especially those with a background of endometriosis (133). This makes it difficult to tease apart immune infiltration secondary to malignancy or to an inflammatory process. An ideal comparison would be to use women with a pre-malignant condition, such as serous tubal intraepithelial carcinoma (STIC), and those with ovarian cancer, however samples identifying STIC are extremely rare. They are usually identified incidentally in women who are undergoing prophylactic bilateral salpingo-oophorectomy for a high-risk gene mutation, such as *BRCA*. One recent study has identified the prevalence of STIC within this cohort of patients as 2.3% (134). Other malignancies with a defined pre-malignant phase, such as adenomas in colon cancer, have been studied with respect to their MDSC infiltration. It was found that patients with pre-malignant disease had a greater number of MDSC in their PBMC compared to healthy controls but were present to a lesser extent than those with colon cancer. These results were also seen in pancreatic cancer. In addition, impaired T cell function within the pre-malignant conditions were able to be reversed, a characteristic not replicated in malignant disease, where T cells had undergone exhaustion and remained dysfunctional (135). This suggests that MDSC play a role in initiating an immunosuppressive microenvironment enabling the progression of pre-malignant disease states to cancer. If MDSC were targeted in the pre-malignant phase, this could subsequently affect the ability to restore T cell function and reduce the immunosuppressive microenvironment created favouring malignant progression. Within ovarian cancer, however, identification of such a pre-malignant condition remains complex.

The results demonstrated no significant difference in MDSC in benign or malignant disease and this remained true in PBMC, omentum and primary tumour. These findings are in contrast to other literature, where MDSC are not present in healthy individuals (136) but there is no evidence regarding their presence in benign or inflammatory ovarian disease. The identification of MDSC within benign disease may be a true finding, secondary to inflammation, or it may also be due to the method of obtaining the

MDSC; the blood was rested overnight at room temperature due to constraints present with retrieving the specimens late following theatre. This may have caused contamination of the PBMC by neutrophils that have undergone degranulation and therefore become low-density granulocytes rather than true MDSC.

There were proportionally lower numbers of MDSC in the peripheral blood in comparison to the site of primary tumour and metastatic disease in HGSC. Interestingly, the sites of greatest accumulation of MDSC were the metastatic sites of the peritoneum and the omentum, greater than those found within the primary tumour. These results suggest that perhaps MDSCs are being recruited to and sequestered at the sites of metastasis from the peripheral blood, potentially playing a role in initialising and maintaining a metastatic niche. This was not seen in benign disease, where the MDSC were increased at the tumour site but not in the omentum. In benign disease there are no peritoneal deposits thus the peritoneum is not surgically removed so could not be compared to malignant disease. This may present an avenue for further research to determine if the peritoneum plays a part in potentiating a pro-metastatic niche, particularly important in cases of primary peritoneal cancers.

These novel findings, have limitations due to the size of the benign group. Although there appears to be a difference between MDSC within the PBMC, tumour and omentum in this group, it did not attain statistical significance, likely due to low sample numbers.

The relationship between MDSC and ovarian cancer has been previously explored and shown to be associated with a shorter disease-free interval and survival (80,137). In ovarian cancer surgery, the ability to achieve complete cytoreduction (removal of all visible tumour) is integral as it has been found to have the greatest impact on survival (138,139). Currently there is no method of predicting which patients will achieve complete cytoreduction prior to commencing surgery, potentially submitting unsuitable candidates for invasive and extensive surgery.

The rates of achieving complete cytoreduction vary from 20-90%, largely explained by the level of expertise performing the surgery; in specialist units the rates are up to 90% whilst those performed by non-specialist surgeons are as low as 20% of cases (127). This can also be as a result of patient selection, with units with greater rates of cytoreduction being better able to select patients suitable to undergo such extensive surgery. Within the Pan Birmingham Gynaecology Cancer Centre (the main source of tumour samples) the rates of complete cytoreduction are approximately 80% as it is a tertiary referral unit with specialist gynaecology oncology surgeons.

There are many other factors implicated in the ability to achieve complete cytoreduction, including patient's pre-operative fitness, patient selection for debulking surgery and the patient's response to chemotherapy. Women with unresectable disease, tend to have a different disease distribution, affecting areas such as over the small bowel serosa and its mesentery, extensive porta hepatis and coeliac axis involvement, extensive stomach surface disease or invasion of the lesser omentum. Despite there being

multiple factors implicated in the ability of achieving complete cytoreduction, it appeared that fewer MDSC were associated with R0. This would fit with the sentiment that it is due to disease biology, whereby a lack of MDSC may be associated with less aggressive disease allowing for a better surgical or treatment response. To further this theory of tumour biology it would be pertinent to investigate the genomics of the tumour and its microenvironment to identify if there is a genetic difference between those achieving R0 and those who did not. This poses the question that if therapy aimed at reducing MDSC was administered prior to debulking surgery in those with a high tumour burden or disease load, would this improve the surgical debulking rate? At present, there is an anti-MDSC agent, Entinostat, which has been trialled within ovarian cancer and not found to be associated with improved survival. It was not used as an adjunct prior to surgery and as such this could be a potential use for this therapy within ovarian cancer. It has been found to be effective in immune editing of tumour neo-antigens, causing a more effective anti-tumour response (140) so if any residual disease (microscopic or macroscopic) is remaining following cytoreduction, then Entinostat may aid in its identification and destruction by the host immune response.

The effect of platinum-based chemotherapy on MDSC has been evaluated in colorectal cancer and murine models and found to reduce the presence of MDSC and their immunosuppressive capacity following chemotherapy (100,101). My results showed that in malignant ovarian tumours the MDSC were reduced following chemotherapy. This is interesting as ovarian cancer tumours are often necrotic and poorly penetrated by chemotherapy due to their hypoxic environment. Regardless of this, there were significantly fewer MDSC present following chemotherapy compared to those who had not received chemotherapy. This may be due to reduced accumulation and differentiation of MDSC due to fewer viable tumour cells secreting factors such as G-CSF and GM-CSF or it may be secondary to increased MDSC cell death following chemotherapy exposure. If it were the latter, however, one would expect widespread reduction in MDSC throughout all tissue samples rather than in the primary tumour site alone. This effect was not seen in the omental deposits where there were similar numbers of MDSC in the chemo-exposed and chemo-naïve patients. This may show that the omentum is not subject to the same chemotherapy toxicity, perhaps due to its relative vasculature, or that the MDSC are able to survive in this relatively immune-privileged site, potentially providing a site for tumour development and chemotherapy-resistance.

Chemotherapy has been shown in murine models to reduce the number of m-MDSC (102) and has been shown to reduce their immunosuppressive nature (100). My results showed that exposure to chemotherapy reduced the number of m-MDSC present, however when the ratio of m-MDSC to PMN-MDSC was studied it showed that following chemotherapy there was a proportional increase in representation of m-MDSC. This is an interesting point and demonstrates how chemotherapy could alter the tumour microenvironment, potentially allowing the preferential accumulation of the more potent m-MDSC which may play a role in further chemotherapy resistance and enabling of disease recurrence.

Murine models have demonstrated an improvement in immune response in those with an intact immune system when the anti-MDSC agent entinostat was used in ovarian cancer models (141). When trialled clinically in combination with a checkpoint inhibitor, there was no improved outcome and in fact led to increased toxicity (142). As such there is no current evidence to suggest reducing MDSC improves outcome in patients managed with immunotherapy.

The finding that the number of MDSC appears to be lower in those achieving a CRS3 would be fitting as it suggests a reduced immunosuppressive tumour microenvironment allowing the host to form an immune response to the tumour and therefore have a better prognosis. The results also demonstrated a 2-fold increase in MDSC present in the omentum of women with a poorer CRS score and in the woman with CRS3, there was a decrease in MDSC within her ovarian tumour sample. If these findings were replicated in a larger cohort, it could be incorporated into the CRS scoring system and perhaps help to predict prognosis more accurately.

The m-MDSC had the greatest prognostic significance, and if an increased cohort of patients demonstrated this relationship further, it may predict response to chemotherapy and therefore who may benefit from either a longer chemotherapy course or perhaps a different combination of chemotherapeutic agents. These results could suggest that either the m-MDSC were more resistant to the chemotherapeutic effects than PMN-MDSC, or that following administration of chemotherapy, the remaining viable tumour cells preferentially recruit m-MDSC rather than PMN-MDSC and perhaps then create a suitable immunosuppressive microenvironment for the development of recurrence and perhaps chemotherapy resistance.

LOX-1 has been heralded as a potential marker for PMN-MDSC and although important in other malignancies, this was not the case for my results. LOX-1 is a potential marker for PMN-MDSC, there is no equivalent in the m-MDSC population and I would not expect to find a great difference in LOX-1 expression between the differential diagnoses and response to treatment as this would mirror my findings on PMN-MDSC.

The omentum is a large fatty apron varying in size from approximately 300 cm^2 to 1500 cm^2, which drapes from the lower border of the stomach, covering the abdominal contents. The omentum is a complex organ containing high densities of mononuclear cells within ‘milky spots’ and a complex vascular system. It is a frequent site of metastasis, especially in ovarian cancer, often with malignant cells penetrating the milky spots and setting up metastatic nodules. The potential for angiogenesis is great and as such can support extensive neoplastic infiltration (143). The omentum was of interest to study within ovarian cancer because of its use to formulate the CRS.

With such a large organ does come disadvantages for tissue sampling and tumour heterogeneity. It is highly possible, and probable, that when taking omental samples for experimentation, areas harbouring

malignant cells are not sampled as they are not necessarily visible to the naked eye and the area is so vast that it may be missed.

Although the aim was to get a sample from the blood, primary tumour and omentum for each patient, this was not always possible. The tissues received were heterogenous due to the surgical needs of the patient.

3.5.1. Limitations associated with MDSC

MDSC are considered to be along a spectrum of alternatively differentiated/activated myeloid cells distinct from their terminally differentiated counterparts, macrophages and neutrophils. Owing to fact they are upon a spectrum there is considerable heterogeneity and therefore, there is no single identifying marker to detect these cells and they are identified by their phenotypic, molecular and functional characteristics. The phenotypic identification of m-MDSC relies on their cell surface marker expression of CD11b+/CD15-/CD14+/HLA-DR$^{-/lo}$ whilst PMN-MDSC must be CD11b+/CD15+/CD14-. Both populations must be negative for CD3, CD19, CD56 to exclude other immune cells such as T cells, B cells and NK cells. This set of cell surface markers represents the minimum requirement to detect these cells through flow cytometry. Despite this complex series of cell surface markers, they cannot distinguish between neutrophils and PMN-MDSC. Currently the only method available to separate these cell populations is through density centrifugation; the neutrophils are of greater density and therefore aggregate at the bottom of the pellet, whilst PMN-MDSC are of lower density and therefore are within the PBMC layer. There are accepted limitations with this technique, however without a unique identifying cell surface marker, identification of these cells is not possible from unseparated peripheral blood samples (66).

It is recognised that the preparation and storage of samples may affect the results with MDSC experiments as it is known that PMN-MDSC are very sensitive to many laboratory techniques, including freezing (144) and even using density centrifugation (145). Overnight incubation of blood can cause considerable contamination of the PBMC layer by neutrophils (145) and may have affected the results. This would not account for the finding of MDSC in benign tumour tissue, however this could be explained by the recruitment of MDSC to a site of chronic inflammation, which may be present in a neoplasm, regardless of its malignancy status.

To identify MDSC, the ‘grow-out’ method was used where the MDSC were incubated at 37°C overnight to allow migration out of the tissue. This method was used to avoid cellular stress due to prolonged enzymatic digestion and potential granulocyte activation. Most studies use a digestion protocol in order to retrieve MDSC which may have affected the populations retrieved compared to others using digestion. M-MDSC may be more resistant to migration out of tissues and as such a higher proportion of cells may have been retained within the tissue samples. Initially, digestion versus grow-out methods

were investigated to determine which produced more reliable results. It was found that digestion increased the cell yield but there was significant contamination of non-viable cells and cellular debris compared to the grow-out method, however the cell proportions retrieved were comparable. Using digestion affected the cell surface marker expression, thought to be due to cleavage of the antigen during the digestion process. This was verified by subjecting the PBMC to the same digestion protocol and it demonstrated the same alterations of cell surface markers, therefore it was decided to use the grow-out method rather than the digestion method.

It is conceivable that the gating strategy may not be able to identify subtle differences between samples, which perhaps is a limitation of flow cytometry. The well-recognised problem with the identification of MDSC is the lack of a specific cell surface markers requiring an extensive gating strategy on flow cytometry. To improve this, CyTOF (mass cytometry) was considered, where the antibodies are labelled on metal ions rather than fluorochromes and their time-of-flight mass spectrometry measured. This technique allows for over 40 different antibodies to be used simultaneously due to the low spectral cross-over compared to using standard fluorochromes. This technique may have been able to differentiate more accurately between the m-MDSC and PMN-MDSC cell populations and other myeloid cell types. Unfortunately, this was beyond the limitations of my funding and available resources but may be considered for future experiments.

These results have added to the literature to suggest that MDSC are present in benign disease as well as in women with cancer so have highlighted their role in alternative disease aetiologies. MDSC are present within healthy donors, suggesting laboratory preparation and processing of samples may affect results. This may not suggest a technical error, more present as a factor to be aware of when investigating MDSC and highlights the need for consistency of methodology to define MDSC and the surface markers used to identify this population. The finding of the PMN-MDSC:m-MDSC ratio is novel and adds to the increasing knowledge on MDSC and may present as a topic of interest to be studied in different malignancies and different cohorts to identify if this finding remains true.

3.5.2 Strengths and limitations of this research

This is a prospective study and is representative of real-life clinical scenarios where samples were taken from all women with ovarian masses and therefore diagnoses were blinded and could not influence the findings. With this strength, is the limitation caused by the heterogeneity of patients and the samples obtained for each case. Because the underlying pathology was unknown, it could not be guaranteed what specimens would be retrieved and those obtained would be reliant on the patients' needs during the surgery. Some tissue was not sampled as it appeared macroscopically normal or a sample was taken at random from an area for research. Although there may have been microscopic disease present on

final histology, it is impossible to say that the sample received for laboratory analysis did or did not contain any evidence of microscopic disease.

This research is a novel approach to reviewing MDSC in patients with ovarian cancer; most papers concentrate on comparing healthy donors to women with cancer but very few have compared the presence of MDSC within benign and malignant disease. Only one study was identified where peripheral blood was taken from patients with a range of ovarian pathologies, including benign and malignant disease, and compared the outcome. It was found that women with malignancy had a more immunosuppressive profile than women with benign disease (146).

An additional strength to this work is the access to multiple tissue specimens so that primary, metastatic, chemotherapy-naïve and exposed samples can be compared. This is rarely investigated so provides insight into the tumour microenvironments existing within primary and metastatic disease. The chemotherapy status of women is an interesting angle because we know that a proportion of ovarian cancer initially responds well to chemotherapy but tends to recur within 18 months. Investigating women pre- and post-chemotherapy provides information on how the immune milieu changes in response to chemotherapy, which is necessary to understand and overcome the process of chemotherapy resistance.

The major weakness with this research lies in the low patient numbers recruited, especially women who had CRS3. Very few women achieve CRS3 or have a cytoreduction score of R1 or 2, therefore a very large population would be required to identify sufficient numbers. Finally, tissue collection was limited from February 2020 due to coronavirus. Although the official lockdown commenced March 23rd 2020, there was a reduction in operating prior to this to prepare for COVID. Women were managed differently during the coronavirus outbreak as more women had 6 cycles of chemotherapy prior to surgery rather than 3 cycles in order to reduce the number of women requiring surgery during the peak of the coronavirus. This meant fewer women were approached to take part in the research project. Following the announcement of the lockdown, the University closed and I was required to return to clinical practice. Unfortunately, this remained the case until the end of my MD. I was anticipating increasing my cohort within this 6-month period in order to improve the quality of the data but was unable to do so.

To further this work, I would focus on increasing my patient numbers to determine if the preliminary results I have found within this research remain true. In particular, I would focus on the m-MDSC population and their correlation with CRS and ability to achieve complete cytoreduction as well as the role of the ratio in predicting the final histology of women presenting with an ovarian mass of unknown diagnosis. I would need to validate my findings through including patients from another cancer centre to ensure the results I have achieved are not biased to the studied sites. The potential areas for bias would lie in the local MDT decision regarding preferred treatment modality given to patients, primary

debulking surgery versus interval debulking surgery, and the surgical approach taken by surgeons in other units.

This prospective study did not allow me to evaluate the progression-free survival or the overall survival due to the time constraints, however this would be a consideration for future work.

An interesting angle would be to perform *BRCA* testing because *BRCA* mutations tend to have a better prognosis (147) thought to be secondary to the pathophysiology of their disease. *BRCA* encodes for DNA mis-match repair genes involved in homologous repair and are particularly sensitive to chemotherapy and PARP inhibitors. Whether this affects their immune profile is to be determined. *BRCA* testing has become universal in the Pan-Birmingham Gynaecology Cancer Centre but is not widespread therefore I was unable to retrieve this information on sufficient patients. Going forward, this should be available for all patients recruited from this site.

In conclusion, these results have found that MDSC are present in age- and sex-matched PBMC of healthy donors, micro- and macroscopically normal ovaries taken from patients at high risk of developing ovarian cancer, benign disease, other ovarian cancer subtypes and in high-grade serous ovarian cancer. Most interestingly, the PMN-MDSC:m-MDSC ratio may be of value to predict disease and its subsequent response to treatment. Although these results show some interesting findings, further samples are required in order to validate these findings and improve their power.

Chapter 4

Interrogation into the technique of measuring T cell suppression

4.0 Introduction

MDSC are defined by their phenotypic cell surface marker expression and more importantly their functional ability to supress T cell function. This is most typically demonstrated by their ability to inhibit T cell proliferation when co-incubated with activated T cells. In the previous chapter, PMN-MDSC and m-MDSC were present in primary ovarian neoplasms and sites of metastasis.

Following on from this, it was necessary to confirm that the identified cells did indeed display immunosuppressive properties. To effectively measure the degree of immunosuppression caused by MDSCs, inhibition of T cell proliferation was used as a marker of MDSC function (88). T cells activated *in vitro* proliferate and undergo multiple proliferation cycles, however if they are co-cultured with an immunosuppressive agent, such as MDSCs, this should impede subsequent T cell expansion. Following 4 days of co-incubation, the number of T cells proliferating are measured using flow cytometry.

Different techniques have been employed to analyse the immunosuppressive function of MDSC. The main methods of MDSC isolation include: 1) magnetic bead sorting (148), 2) magnetic bead enrichment followed by cell sorting by flow cytometry (149) and 3) flow cytometry sorting (150). Following isolation, the MDSC are then co-cultured with activated T cells. The T cell activation process is also non-standardised and is largely performed using anti-CD3/CD28 antibodies in the context of 1) magnetic polymer beads such as Dynabeads® (150), 2) plate-bound and soluble antibody (88) or 3) antigen-specific activation (151). This chapter describes the experiments performed to investigate the immunosuppressive function of MDSC isolated from ovarian cancer tissue samples and interrogates multiple methods for demonstrating immunosuppression.

The hypotheses for this chapter were:

1. MDSC demonstrate an immunosuppressive function, shown by their reduction in T cell proliferation
2. The method of stimulation of T cell proliferation does not impact the immunosuppressive result of incubation with MDSC.
3. The cells identified as MDSC in Chapter 3 can be confidently described and characterised as MDSC through their demonstrable T cell suppressive function.

4.0.1 Aims of experiment

1. To determine if MDSC identified in benign and malignant ovarian tumour possess immunosuppressive property.
2. To identify a reliable method for performing suppression assays with minimal artefactual influence.

4.1.0 Chapter Results

The immunosuppressive capability of MDSC was investigated using MDSC derived from tumour and PBMC samples. Following this experiment, the requirement for a reliable positive control became evident. Furthermore, due to the heterogeneity of techniques to perform suppression assays within the literature, a number of experimental methods were performed in order to determine the most reliable method whilst limiting artefactual results.

Initially, PMN-MDSC were chosen to perform the suppression assays as they were present in greater numbers in the samples and had been demonstrated within the literature to have a suppressive effect.

4.1.1 *Ex vivo* MDSC suppression assays using CD15+ magnetic beads to isolate PMN-MDSCs

4.1.2 Cohort

Patient samples (n=2) were used for the initial CD15-magnetic bead suppression assays. The patient characteristics used for the experiments in this chapter are described in Table 4.1. The patients used for these experiments were not the same patients used for the initial MDSC phenotypic experiments in order to maximise the cells available for the suppression analysis. The manner in which the patients were recruited, and the method of specimen collection was the same as previously described.

Patient	Ethnicity	Age	Diagnosis	Stage	Chemotherapy
CD15+ magnetic beads					
1	White British	69	Borderline serous ovarian cancer	1a	nil
2	White British	65	Ovarian fibroma	Benign	nil
Cell sorter					
3	White British	65	High-grade serous ovarian cancer	3c	nil
4	Asian	46	High-grade serous ovarian cancer	4a	4 cycles neo-adjuvant chemotherapy

Table 4. 1. Patient characteristics of samples used for CD15+ magnetic beads isolation suppression assays (n=2) and samples using the cell sorter to identify MDSC populations (n=2).

4.1.3 No T cell suppression was identified when PMN-MDSC were identified using CD15+ magnetic microbeads

Initially, magnetic isolation microbeads for CD15 isolation were used for both tumour and blood (n=2 for each). The CD15+ cells were magnetically labelled from both PBMC and tumour samples and then isolated from the cell suspension using magnetic columns. The columns were then washed twice to

remove all isolated cells and the CD15-enriched cell solution was used for the suppression assays. The purity was examined using flow cytometry and appeared to be approximately 50% for PMN-MDSC. Autologous PBMC were used as the responder cells for these experiments. The CD15 positive cells were co-incubated in a flat-bottom 96-well plate with PBMC activated with Immunocult™ to stimulate T cell proliferation. Immunocult™ is an antibody complex which binds to CD3 and CD28 to stimulate T cell activation. They were co-incubated at ratios of 0.2:1 up to 2:1 (CD15+ 'MDSC':PBMC) at 37°C for 4 days and then the degree of proliferation was examined using flow cytometry following staining the sample with CD3 antibody to detect T cells. Live T cells were gated to demonstrate T cell proliferation (Figure 4.1). The experiment was repeated twice with cells retrieved from 2 different patients.

This experiment was only repeated twice due to the fact the purity achieved was so low. A different method was sought in order to improve this as any result could not be relied upon as the result may have been due to contamination. **Figure 4. 1. *Ex vivo* CD15+ cells derived from tumour samples were incubated with PBMC as responders and stimulated with ImmunoCult™ to elicit T cell proliferation.**

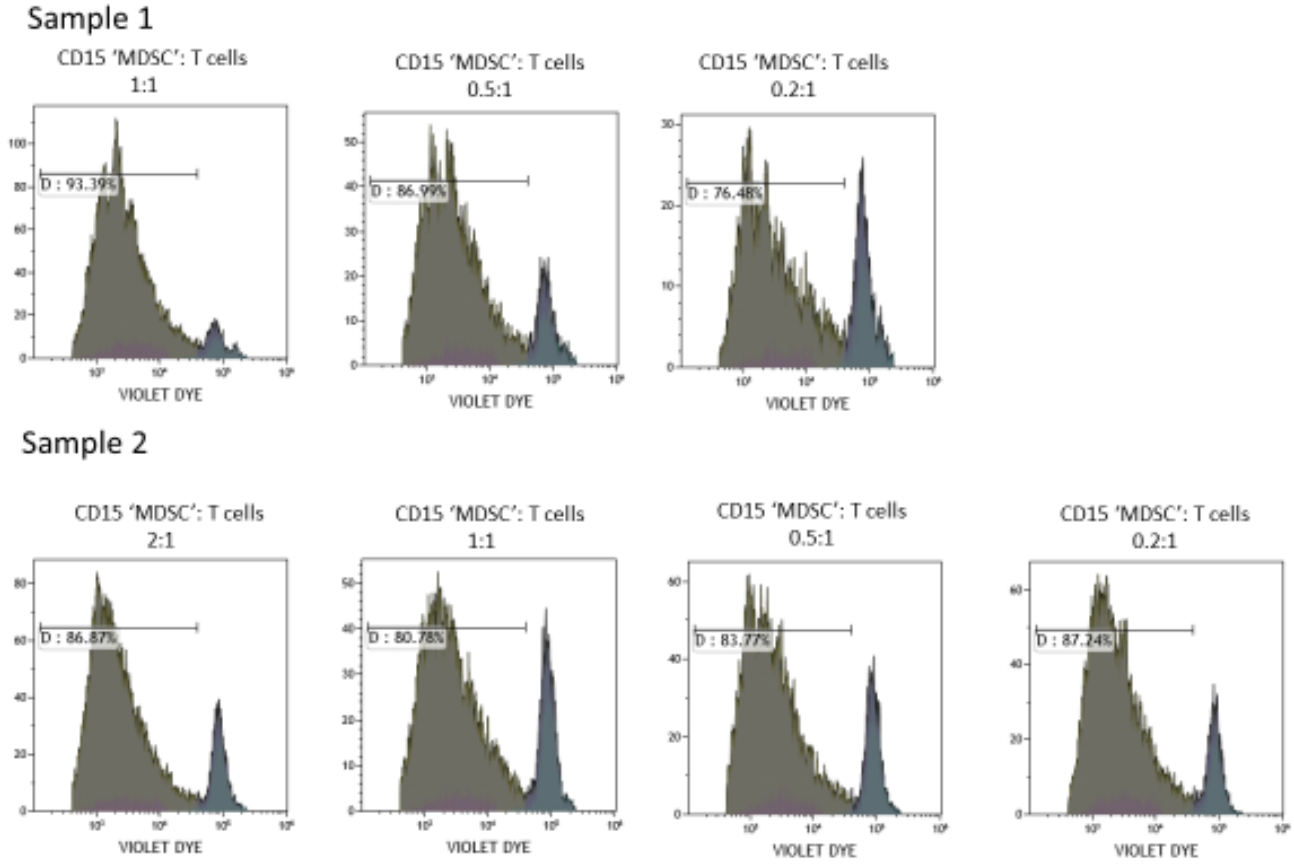

The histograms demonstrate the dilution of CSFE as a marker of T cell proliferation. Different ratios were used to identify the potency of the immunosuppressive effect. n=2.

4.1.4 No T cell suppression was observed using e*x vivo* MDSC suppression assays following FACS sorting of CD15+ PMN-MDSC

Due to the poor purity of PMN-MDSCs (approx. 50%) following CD15+ bead enrichment, and the inability to use m-MDSCs as suppressor cells, a method was optimised using the BDFACS Melody cell sorter, which provided over 98% purity for each population of interest. The cells were sorted on CD14 positive and CD15 positive cells, with the CD14 population being further sorted into HLA-DR negative and HLA-DR positive.

Despite tissue digestion and multiple attempts of optimisation it was not feasible to get sufficient CD14+ HLA-DR negative cells from the tumour samples. As such only the CD15+ granulocytic MDSC were taken for these experiments. The cohort is described in Table 4.1 above.

For the PBMC samples, sufficient cells were identified to sort on the monocytic MDSC population. For these experiments, the T cells were isolated from the PBMC using a T cell isolation kit, rather than using PBMC as responders. Equal numbers of T cells were plated with MDSC into a flat-bottom 96 well plate. CSFE labelling was chosen to assess T cell proliferation, and T cells were stimulated with ImmunoCult™ as before. Figure 2 shows a representative sample demonstrating the proliferation cycles of T cells in the presence of CD14+ and CD15+ MDSC. The top row depicts the m-MDSC co-incubated with T cells and demonstrates that the CD3-stained T cells have undergone multiple proliferation cycles, despite being co-incubated with m-MDSC. At ratios of 1:1, 0.5:1 and 0.2:1 (m-MDSC:T cells) the percentage of T cells undergoing proliferation was 79.2%, 76.2% and 74% respectively. The bottom row demonstrates the proliferation of T cells incubated with PMN-MDSC at the ratios of 1:1, 0.5:1 and 0.2:1 (PMN-MDSC:T cells). Here the proliferation was found to be 65.8%, 72.1% and 71% respectively. The multiple spikes in each of the graphs demonstrate the T cells undergoing multiple proliferation cycles, unaffected by the presence of MDSC (Figure 4.2).

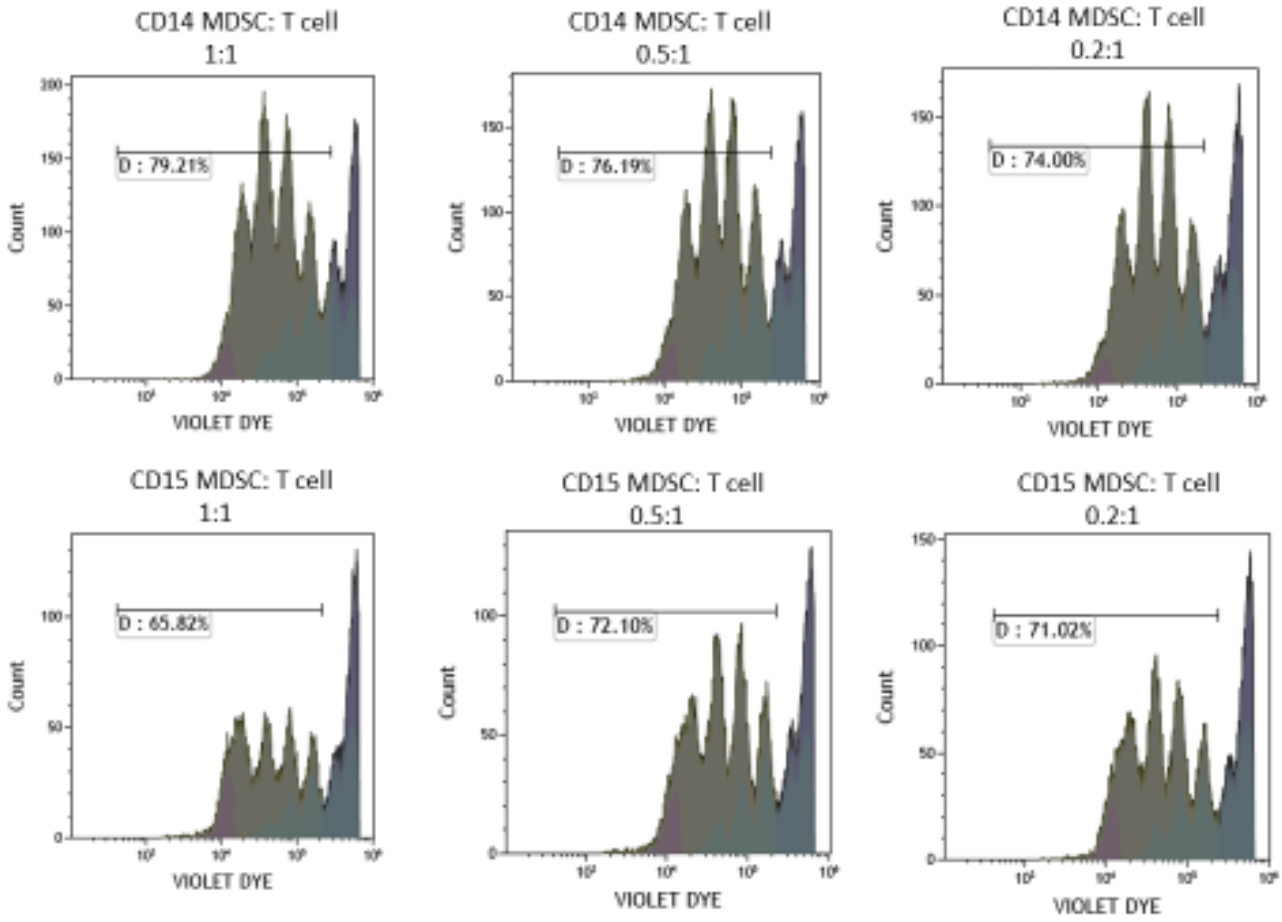

Figure 4. 2. Proliferation cycles demonstrated using ImmunoCult™ to stimulate T cell activation in the presence of CD14 MDSC and CD15 MDSC at reducing ratios.
Sample is from PBMC from a patient with ovarian cancer and sorted using flow cytometry. n=2 patients.

Despite amending the method of cell sorting from the use of CD15 isolation beads to using flow cytometry to improve the cell purity, the results remained consistent; immunosuppression did not occur using *ex vivo* m-MDSC or PMN-MDSC. This result was corroborated when comparing malignant (n=3) and benign (n=1) disease. The results from the cells isolated using CD15 isolation beads were unreliable due to their contamination, however, those taken from the cell sorting were highly pure and therefore present more reliable data.

Following this, a positive 'immunosuppressive' control was sought to demonstrate a reduction of T cell proliferation. This was needed to enable valid comparison to be made between the patient samples and the positive control and to interpret the results accurately.

4.2.0 Development of a positive control

Due to the lack of immunosuppression demonstrated in initial studies, a reliable positive control was required to ensure that these observations did not reflect a technical fault with my suppression assay. From the literature, MDSC derived from PBMC cultured with IL-6 and GM-CSF provided a good positive control (148) so these cells were developed for use in the suppression assay. Additionally, it seemed as though it was the monocytic population that had the most prognostic significance and as such this proved to be a potentially interesting subtype to concentrate upon.

4.2.1 m-MDSC were derived from healthy donor PBMC through incubation with IL-6 and GM-CSF

As described in the Methods section, following 7 days of culturing with IL-6 and GM-CSF, healthy donor PBMC were differentiated into m-MDSC, evidenced by their loss of HLA-DR and CD14 positivity on flow cytometry. This confirmed the technique for the differentiation of m-MDSC.

4.2.2 *In vitro* m-MDSC did not cause immunosuppression when T cells were stimulated with ImmunoCult™

ImmunoCult™ is a tetrameric CD3/CD28 T cell activator and does not require beads, feeder cells or antigens. The literature suggests that m-MDSC should cause T cell suppression at ratios as low as 0.25:1 (m-MDSC:T cells) (98,152) so the titration commenced at 0.1:1 (m-MDSC:T cells) in order to demonstrate a suppression curve (Figure 4.3). Ratios of 0.1:1, 0.25:1, 0.5:1 and 1:1 were used, depending on the number of m-MDSC retrieved following cell sorting. The average percentage of proliferation was 78% when T cells were incubated with Immunocult™ alone. When incubated with monocytes (identified by CD14+/HLA-DR+ antibody staining through flow cytometry) the average proliferation was 85.8%, an increase of over 7% compared to incubating T cells with Immunocult™ alone. When co-incubated with m-MDSC at ratios of 0.1, 0.25, 0.5 and 1 the average proliferation was 74.2%, 84.7%, 82% and 69.4% respectively. None of these results demonstrated a statistically significant change from the baseline of proliferation achieved with T cells incubated with Immunocult™ alone ($p>0.91$).

The percentage change was calculated using T cells incubated with ImmunoCult™ as a comparator to monocytes (CD14+/HLA-DR+) and m-MDSC (CD14+/HLA-DR-) at differing ratios (Figure 4.4). This demonstrated an average percentage change of 0.13% for monocytes, -17.3% for m-MDSC at 1:1 ratio and 9.2% for m-MDSC at a ratio of 0.5:1. This suggests that at lower ratios the m-MDSC can actually improve T cell proliferation rather than reduce it. The proliferation profiles of m-MDSC co-cultured with T cells and ImmunoCult™ and T cells stimulated with ImmunoCult™ alone demonstrate no difference in proliferation cycles when analysed on flow cytometry software (Figure 4.5).

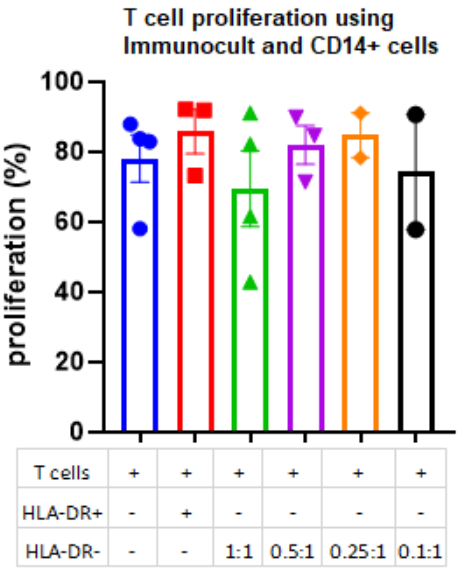

Figure 4. 3. Graph depicting the percentage proliferation of T cells with ImmunoCult™ when co-cultured with CD14+ cells at differing ratios.
HLA-DR+ denotes monocytes (CD14+/HLA-DR+); HLA-DR- denotes m-MDSC (CD14+/HLA-DR-) in the ratios of 1:1, 0.5:1, 0.25:1 and 01:1 (m-MDSC:T cells). Bars depict mean and standard error of the mean. n=4 T cells with ImmunoCult™, n= 3 T cells with ImmunoCult™ and monocytes, n=4 T cells with ImmunoCult™ and m-MDSC in 1:1 ratio, n=3 T cells with ImmunoCult™ and m-MDSC in 0.5:1 ratio, n= 2 T cells with ImmunoCult™ and m-MDSC in 0.2:1 ratio, n= 2 T cells with ImmunoCult™ and m-MDSC in 0.1:1 ratio. One-way ANOVA demonstrated non-significance for all results.

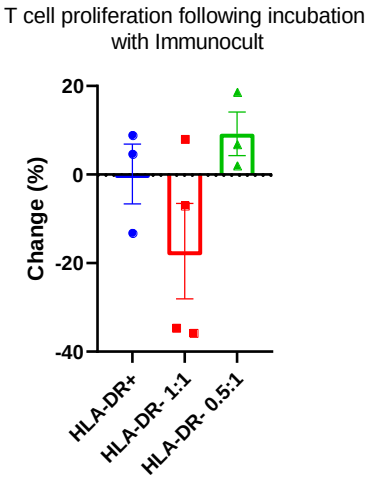

Figure 4. 4. The percentage change from the baseline of T cells incubated with ImmunoCult™ compared to the proliferation achieved when cultured with monocytes (HLA-DR+) or m-MDSC (HLA-DR+) at varying concentrations of 1:1 and 0.5:1.
One-way ANOVA demonstrated non-significance between results. Bars depict mean and standard error of the mean. n= 4 monocytes, n= 3 m-MDSC 1:1, n= 3 m-MDSC 0.5:1.

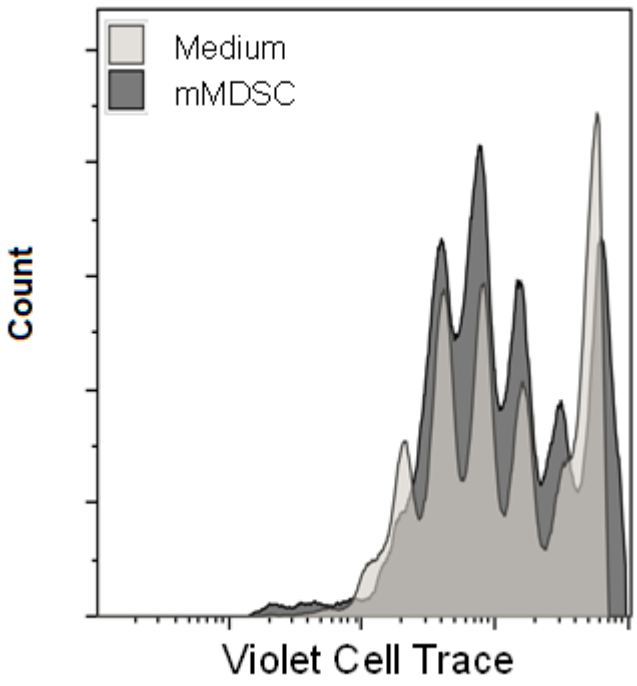

Figure 4. 5. T cells from patient 1 (Table 2) were stained with Violet Cell Trace and activated with ImmunoCult™ in the presence (dark grey curve) or absence (light grey curve) of autologous m-MDSC.
T cell proliferation was evaluated by measuring the dye dilution within the cells at day 4.

4.2.3 *In vitro* m-MDSC demonstrated immunosuppression when T cells were activated with Dynabeads®

After failing to demonstrate immunosuppression using ImmunoCult™, the protocol was modified to use Dynabeads® as this has been widely cited in the literature for T cell activation in MDSC suppression assays in both previous and ongoing studies (153–157). The MDSC were isolated using flow cytometry, as this proved to be a reliable method of cell isolation, and the T cells continued to be isolated from autologous whole blood using a T cell isolation kit. The MDSC and T cells were plated out in differing ratios as described above. The Dynabeads® were washed and prepared as per manufacturers' protocol and added to each of the wells in a 1:1 ratio with the T cells. A control experiment was performed using T cells and Dynabeads® alone. The cells were co-incubated for 4 days at 37°C and the subsequent T cell proliferation was assessed through flow cytometry as described above.

The average proliferation of T cells incubated with Dynabeads® alone was 91%, superior to the 78% achieved using Immunocult™. The Dynabeads® provided reliable T cell proliferation with results ranging from 82-99%. When co-incubated with m-MDSC at a ratio of 1:1 the results demonstrated a

statistically significant T cell suppression, with an average proliferation of 62.7% ($p<0.05$). One experiment at 1:1 ratio failed to produce any immunosuppression and had a proliferation of 98.98%, which affected the overall results. Without this result the average was 54% (range 38.5-63.9) when co-incubated with m-MDSC. When the ratio of MDSC:T cells was reduced to 0.5:1, this immunosuppressive effect was lost and the average proliferation was 88.1% ($p=0.52$) (Figure 4.6). In addition to these results, the proliferation profiles were analysed and demonstrated an obvious reduction in proliferation cycles when the m-MDSC were co-incubated with the T cells (red curve) compared to the multiple proliferation cycles demonstrated with T cells and Dynabeads® alone (green curve) (Figure 4.7).

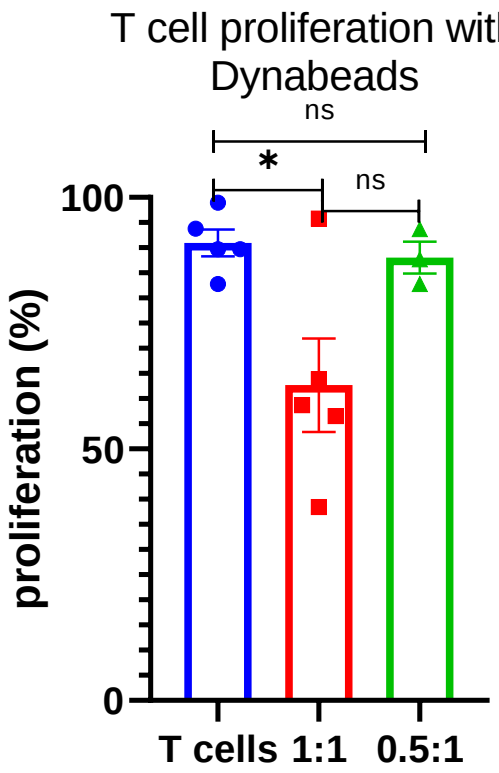

Figure 4. 6. T cells were incubated with 1:1 Dynabeads® and their proliferation assessed after 4 days.
T cells and Dynabeads® were co-cultured with m-MDSC at a ratio of 1:1 and 0.5:1 (m-MDSC:T cells) and proliferation assessed after 4 days. T cells and m-MDSC:T cells 1:1 ratio experiment repeated 5 times, 0.5:1 ratio repeated 3 times. * $p<0.05$. ns = non-significant. Bars depict mean and standard error of the mean.

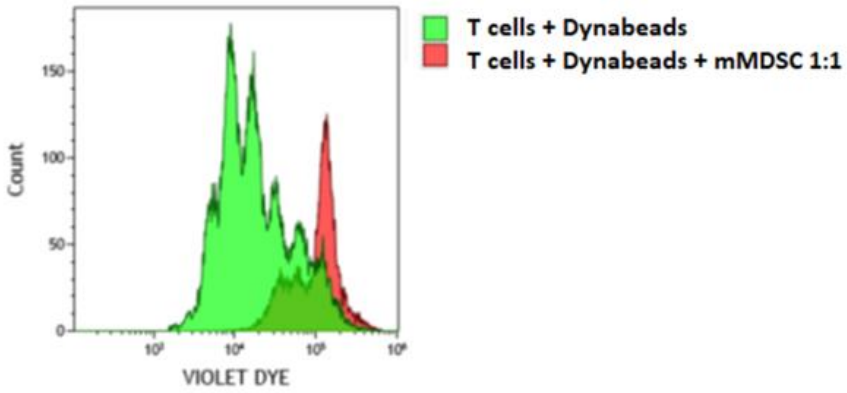

Figure 4. 7. Proliferation profiles of T cells when incubated with Dynabeads® (green) and following co-incubation with m-MDSC at 1:1 ratio (red).

4.2.4 Monocytes pre-incubated with Dynabeads® did not induce a reduction in T cell proliferation

The experiment was then repeated using monocytes (CD14+/HLA-DR+) to investigate if the above effect was unique to m-MDSC alone. Monocytes were co-cultured with T cells and Dynabeads® as in the previous experiment. The monocytes did not have the same propensity to reduce T cell proliferation as that demonstrated by m-MDSC (Figure 4.8).

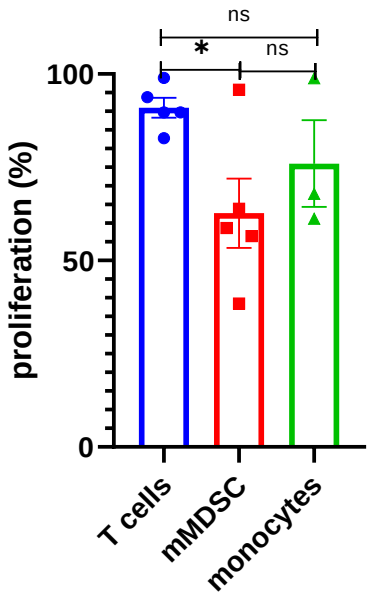

Figure 4. 8. Monocytes (CD14+/HLA-DR+) were co-cultured with T cells and Dynabeads® in 1:1 ratio, n= 3. M-MDSC were co-cultured in 1:1 ratio with T cells and Dynabeads® n= 5.
*p<0.05, ns = non-significant. Bars depict mean and standard error of the mean.

4.2.5 *In vitro* m-MDSC-induced reduction in T cell proliferation is secondary to phagocytosis of Dynabeads®

It was hypothesised that the mechanism behind this apparent immunosuppression was m-MDSC phagocytosing the beads. Photomicrographs were taken serially in order to investigate potential phagocytosis. The proportion of m-MDSC which had phagocytosed beads and the number of phagocytosed beads per cell both increased during culture (Figure 4.9A and B) such that at the end of incubation some m-MDSC were completely engulfed with beads (Figure 4.9D).

T cell activation mediated by anti-CD3/CD28 beads reaches a plateau after 6 hours (158) so we allowed up to 18 hours for the identification of any differences in the groups. It is therefore possible that m-MDSC-mediated phagocytosis can markedly reduce the number of CD3/CD28 Dynabeads® available for T cell activation. Indeed, the proportion of T cells bound to beads was reduced by over three-fold during co-incubation with m-MDSC (Figure 4.9C).

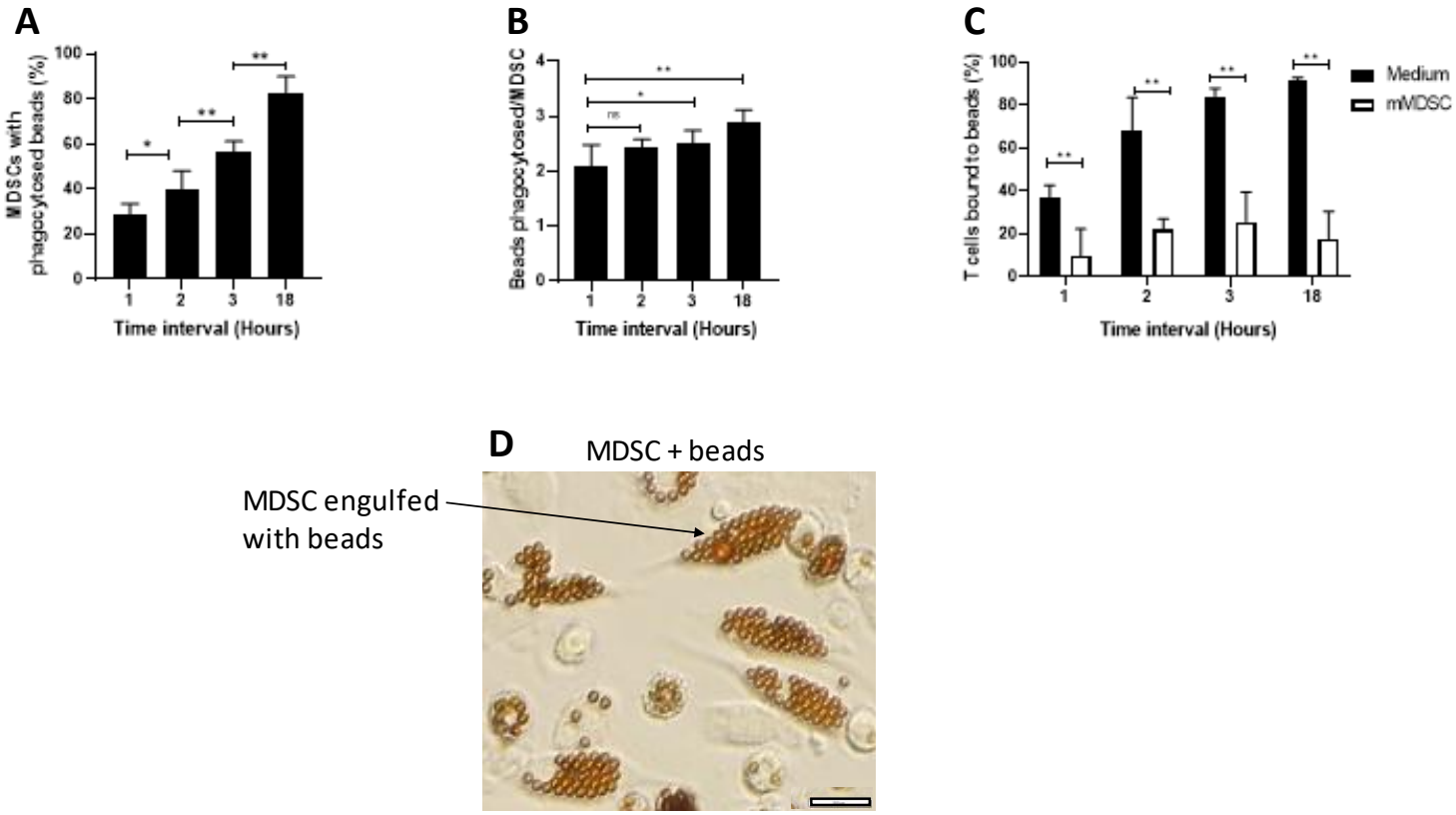

Figure 4. 9. *In vitro* differentiated m-MDSC were incubated with Dynabeads and photomicrographs were taken at different time intervals to evaluate bead-to-cell binding. ns=non-significant, *p=<0.05, **p=<0.01. Bars show 1 standard deviation. A) The percentage of m-MDSC which had phagocytosed beads as a percentage of the total number of m-MDSC. Experiment performed in triplicate. B) The number of beads phagocytosed per m-MDSC. Experiment performed

in triplicate. C) The percentage of T cells bound to beads in the absence or presence of m-MDSC. D) Photomicrograph of m-MDSC after 18-hour incubation with beads. Scale bar (bottom right) represents 500µm.

To improve accuracy of results and discriminate between m-MDSC and T cells the latter cells were stained with CFSE. This causes fluorescence of the T cells when visualised under a GFP filter enabling differentiation of T cells and m-MDSC (Figure 4.10). Serial photomicrographs were taken at 1-hour intervals to document the phagocytosis of the beads following co-incubation with m-MDSC (Figure 4.11).

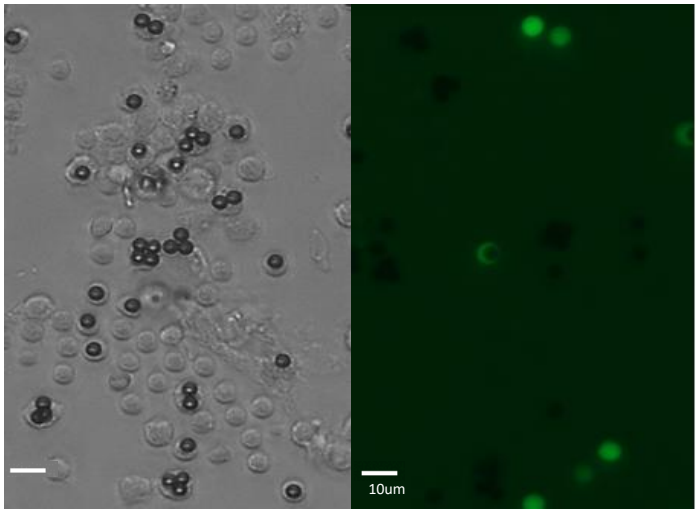

Figure 4. 10. Photomicrograph of co-cultures of m-MDSC and T cell in presence of Dynabeads® at 2 hours.
T cells were stained with CFSE. Left panel shows normal light, right panel fluorescence with green fluorescence protein (GFP) filter. Experiment performed in triplicate.

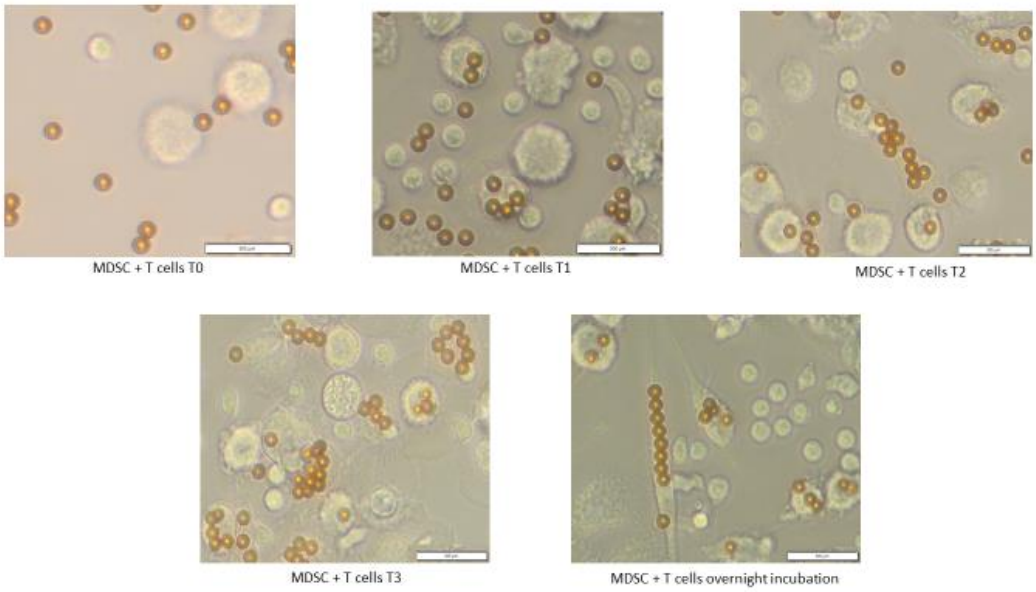

Figure 4. 11. Serial photomicrographs of m-MDSC co-cultured with Dynabeads® taken at 1-hour intervals and finally overnight incubation.
Scale bar represents 500µm.

4.2.6 Both *in vitro* and *ex vivo* m-MDSC demonstrate phagocytosis of Dynabeads®

To investigate whether these findings are unique to m-MDSC generated *in vitro* or might also be related to m-MDSC isolated *ex vivo* (patient-derived), circulating m-MDSC were enriched from two patients with high-grade serous ovarian cancer (Table 4.2). These patients were approached and consented as described previously and were not used in any of the previous experiments. Interestingly, *ex vivo* isolated m-MDSC demonstrated an enhanced capability to phagocytose beads within the first three hours compared to cells generated *in vitro* (Figure 4.12 A, B).

Patient	Ethnicity	Age	Diagnosis	Stage	Chemotherapy
1	White British	58	HGS cancer	4b	4 cycles neo-adjuvant chemotherapy
2	White British	65	HGS cancer	3c	nil

Table 4.2. Patient characteristics for ex-vivo isolated m-MDSC.
HGS cancer: high grade serous ovarian cancer.

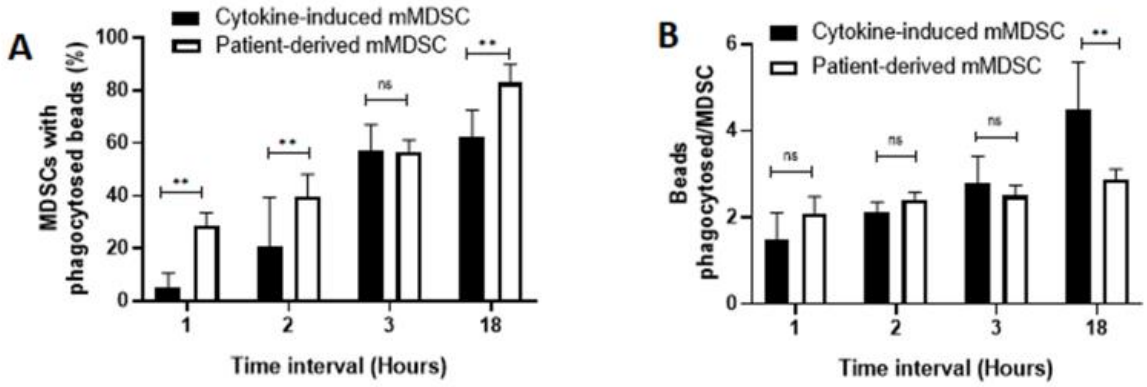

Figure 4. 12. Enriched circulating m-MDSC from two patients with high-grade serous ovarian cancer were co-cultured with Dynabeads® and serial photomicrographs were taken to assess the degree of phagocytosis of the beads.
A) The number of m-MDSC which had phagocytosed the beads as percentage of the total number of m-MDSC using both *in vitro* differentiated and *ex vivo* enriched m-MDSC. Data are from 2 experiments each performed in triplicate. B) The number of beads phagocytosed per m-MDSC for both *in vitro* differentiated and *ex vivo* enriched m-MDSC. Data are from 2 experiments each performed in triplicate. Bars depict 1 standard deviation.

4.2.7 Overwhelming the phagocytic capability of m-MDSC and pre-incubating T cells with Dynabeads abrogated the perceived immunosuppressive effect of m-MDSC on T cell proliferation

In order to assess if m-MDSC-mediated Dynabead® phagocytosis was sufficient to account for a drop in T cell proliferation, more beads were made available to T cells by increasing the amount of CD3/CD28 Dynabeads® by 10-fold. Importantly, the m-MDSC-dependent inhibition of T cell proliferation that was clearly apparent at the standard 1:1 T cell:bead ratio was not present at the 1:10 ratio (Figure 4.13A).

Moreover, when T cells were pre-incubated with CD3/CD28 Dynabeads® for 1 hour, in order to induce T cell proliferation before the addition of m-MDSC, the inhibition of T cell proliferation was largely abrogated (Figure 4.13B). The average proliferation achieved with T cells and m-MDSC alone was 93.3% and this was significantly reduced to an average of 65% in the presence of 1:1 Dynabeads® ($p=0.0003$). When the T cells were pre-incubated for 1 hour with Dynabeads® to allow T cell activation to occur, the average percentage proliferation was 83.5%, a non-significant reduction from the T cells and Dynabeads® control experiment ($p=0.13$). This also showed a significant reduction in the average proliferation achieved between the experiments where the m-MDSC were added immediately, compared to when they were added after 1 hour ($p<0.05$).

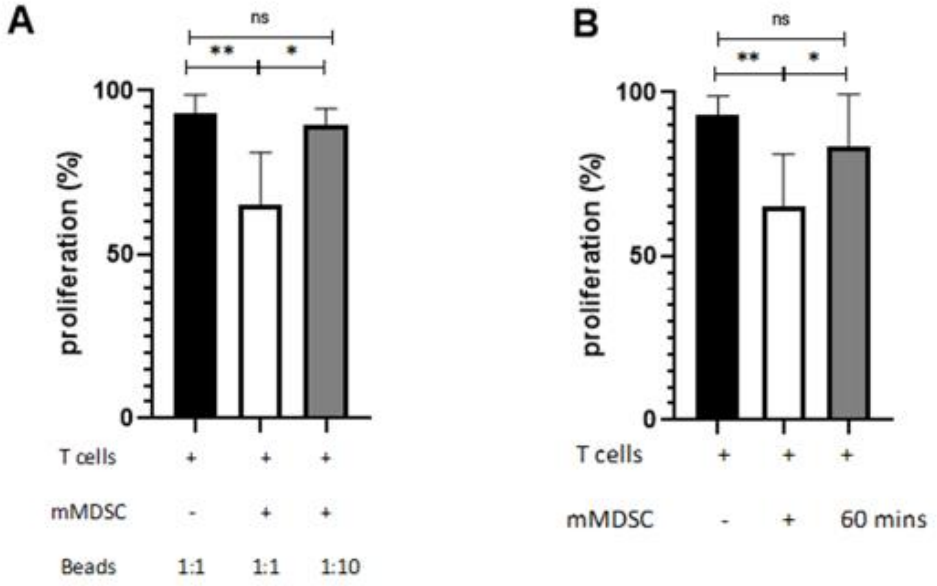

Figure 4. 13. T cell proliferation following differential stimuli in the presence or absence of m-MDSC.
Proliferation was measured by flow cytometry enumerating the cells displaying reduced CellTrace staining. ns=non-significant, * p=<0.05, ** p=<0.01. Bars depict 1 standard deviation. A) The number of Dynabeads® was increased ten-fold to augment the availability of beads for T cell activation. Data are from 8 experiments at a concentration of 1:1 and 5 experiments at 1:10. B) T cells were pre-incubated with Dynabeads® for 1 hour prior to adding m-MDSC or added together with m-MDSC. Data are from 8 experiments with immediate addition and 6 experiments with delayed addition of m-MDSC. ns=non-significant, * p=<0.05, ** p=<0.01.

4.2.8 Overwhelming the phagocytic ability of m-MDSC with opsonised zymosan inhibits reduction in T cell proliferation

Opsonised zymosan was used to overwhelm the phagocytic ability of m-MDSC by co-incubating them with these phagocytosable particles. As such, m-MDSC were pre-incubated with an excess of opsonized Zymosan A (OpZ) for 1 hour. Serial photomicrographs demonstrated a lack of phagocytosis of the Dynabeads by the m-MDSC (Figure 14A). OpZ was also seen to completely block m-MDSC-dependent inhibition of CD3/CD28 Dynabeads®-induced T cell proliferation (Figure 4.14B).

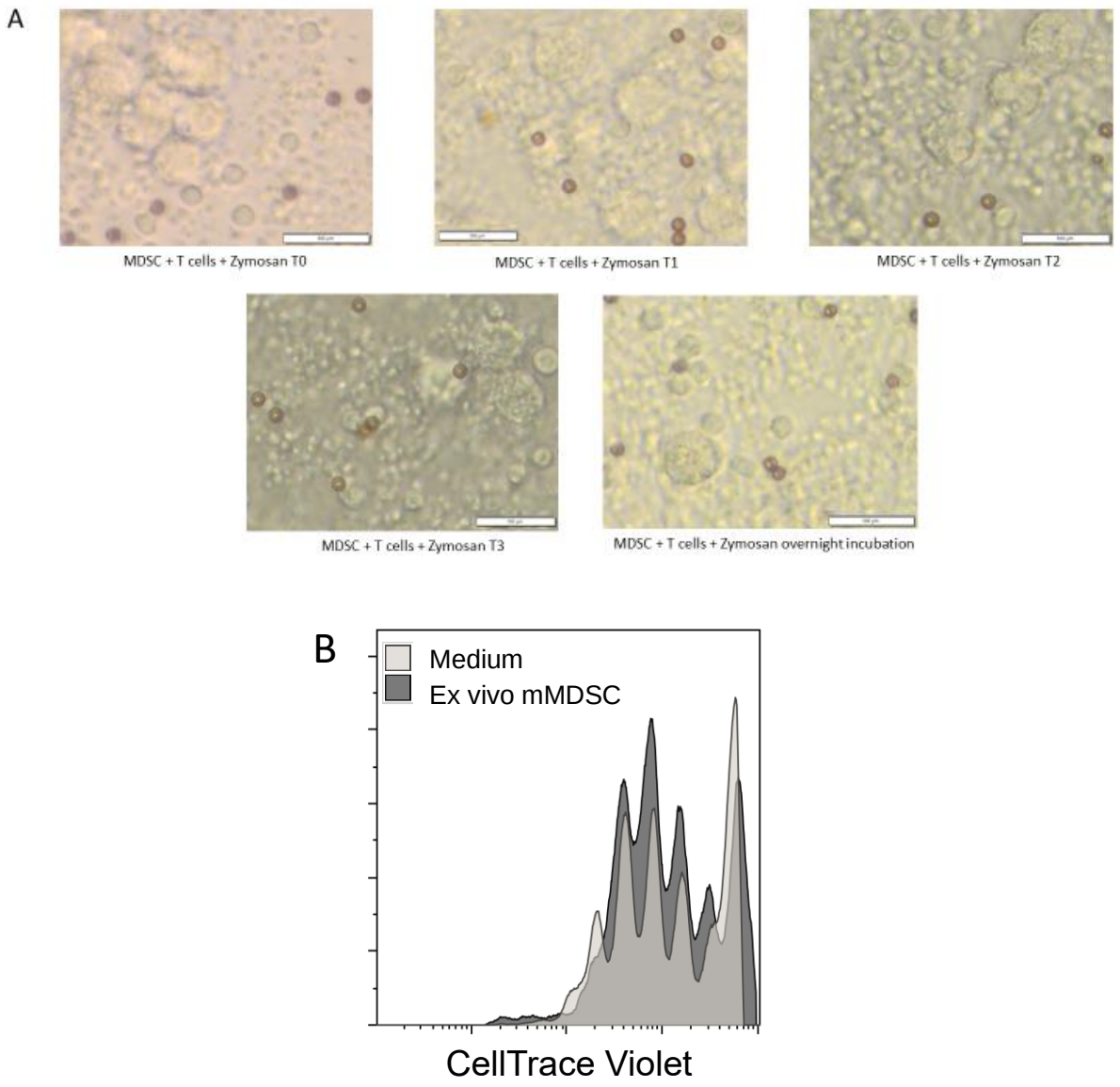

Figure 4. 14. Opsonised Zymosan was co-cultured with m-MDSC and T cells with Dynabeads®. A) Serial photomicrographs of m-MDSC co-cultured with Dynabeads® taken at 1-hour intervals (T1, T2 and T3 taken 1, 2- and 3-hours following incubation respectively) and finally overnight incubation. Scale bar represents 500µm. B) T cells were activated with Dynabeads® in the presence or absence of m-MDSC pre-incubated for 1 hour with OpZ prior to the addition. Superimposed flow cytometry profiles. Single experiment.

4.3.0 m-MDSC co-cultured with non-phagocytosable T cell stimuli did not induce inhibition of T cell proliferation

Since phagocytosable stimuli appeared to artefactually influence the results of m-MDSC immunosuppression assays, the effect of non-phagocytosable soluble stimuli were investigated in the same assays. m-MDSC were incubated with autologous T cells in the presence of ImmunoCult™, a soluble tetrameric antibody complex that activates and expands human T cells. Under these conditions neither *in vitro* differentiated nor *ex vivo* enriched m-MDSC induced inhibition of T cell proliferation (Figure 4.15A). The T cells were stimulated with PMA plus ionomycin, which activate T cells through

bypassing the T cell receptor complex. Of note, the addition of m-MDSC not only failed to produce immunosuppression but actually led to an enhancement in T proliferation (Figure 4.15B).

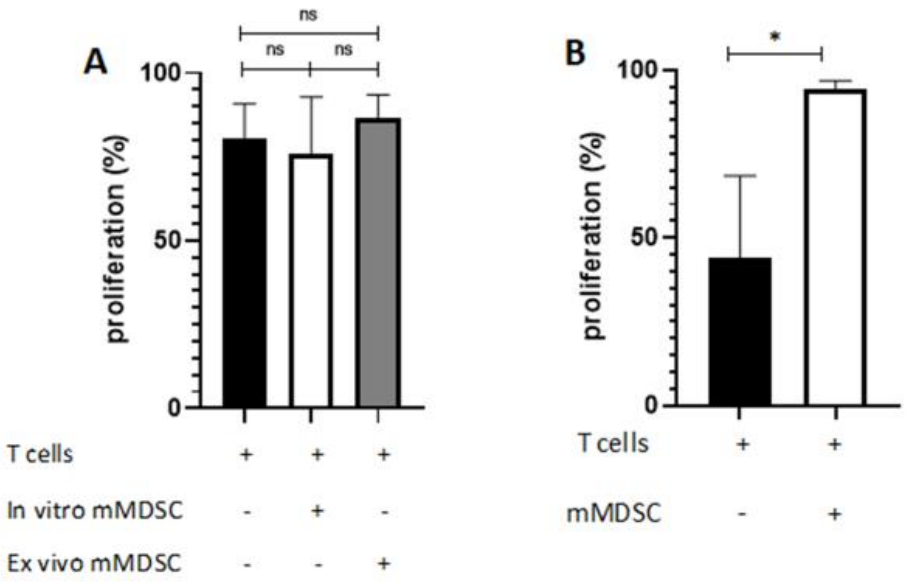

Figure 4. 15. Non-phagocytosable stimuli were used to elicit T cell proliferation and co-incubated with m-MDSC in 1:1 ratio.
A) ImmunoCult™ was used to induce T cell proliferation in co-culture with *in vitro* differentiated or *ex vivo* enriched m-MDSC. Data are from 7 experiments using cytokine-induced m-MDSC and 3 using patient-derived (*ex vivo*) m-MDSC. B) T cells were incubated with PMA plus ionomycin in the presence or absence of *in vitro* differentiated m-MDSC. Data are from 3 experiments. ns= non-significant, *$p<0.05$. Bars depict 1 standard deviation.

4.3.1 Plate-bound anti-CD3 antibody did not demonstrate reliable immunosuppression when co-cultured with m-MDSC

The role of plate-bound CD3 with soluble CD28 was then investigated as this method has also been published within the literature (98). This was investigated in 2 different ways; firstly, by plating the m-MDSC first and secondly by plating the T cells first to investigate if m-MDSC could interfere with T cell activation by steric hindrance (Figure 4.16). The plate was gently spun to allow the cells to adhere to the bottom of the plate then the m-MDSC were added to the T cells plate and T cells were added to the m-MDSC plate. The results showed no reduction in proliferation when either the m-MDSC or T cells were plated first and they did not demonstrate any immunosuppression. However, it could be argued that the number of proliferation cycles achieved by the T cells exposed to the CD3 directly was greater than those achieved by the T cells when the MDSC were plated first.

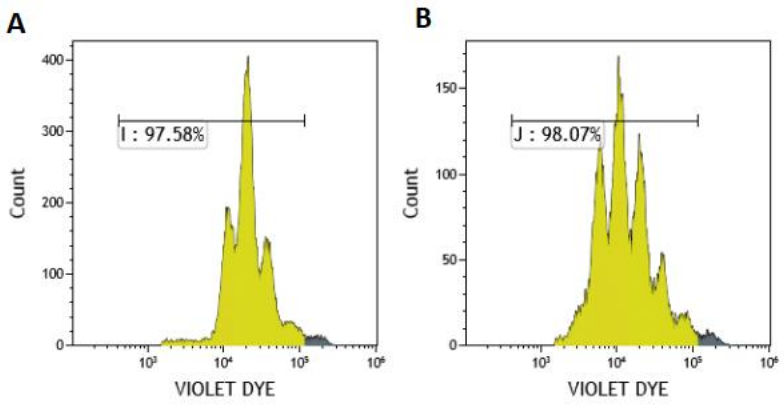

Figure 4. 16. m-MDSC were incubated with T cells stimulated with plate-bound CD3 and soluble CD28.
A) The proliferation of T cells when m-MDSC were plated first B) The proliferation achieved when T cells were plated first. Experiment performed in triplicate.

4.4.0 Conclusion

The results demonstrate that *in vitro* and *ex vivo* m-MDSC do not reliably cause immunosuppression when activated with non-phagocytosable stimuli such as ImmunoCult™, ionomycin/PMA and plate-bound/soluble antibody. It was found that CD3/CD28 Dynabeads® generate artefactual results in immunosuppression assays involving m-MDSC. As such, non-phagocytosable stimuli should be used in order to activate T cells in this setting.

The absence of any observable inhibition of T cell proliferation when soluble stimuli were used to perform the suppression assay challenges the concept that m-MDSC exert a significant suppressive activity on T cell proliferation. This possibility deserves further investigation as m-MDSC have been considered widely as the most potent immune suppressive subset within the myeloid lineage (69).

4.5.0 Summary of results

The results demonstrated no evidence of immunosuppression when *ex vivo* PMN-MDSC were identified using CD15+ microbeads or flow cytometry and were cultured with T cells activated with ImmunoCult™. As such, *in vitro* MDSC were used to investigate the reliability of the suppression assays and multiple methods for T cell activation were examined. Firstly, no immunosuppression was identified when *in vitro* MDSC were incubated with T cells stimulated with ImmunoCult™ so the method of T cell activation was changed to Dynabeads®, which demonstrated significant T cell suppression when incubated with *in vitro* MDSC. This effect was abrogated when the Dynabeads® and T cells were co-incubated with monocytes, demonstrating this was unique to MDSC. This method was further interrogated to use *in vitro* and *ex vivo* MDSC and demonstrated that both populations caused

immunosuppression, highlighting this was not a methodological artefact with the *in vitro* polarisation of MDSC. It was considered that the method behind this immunosuppression was artefactual and was secondary to the phagocytosis of the Dynabeads® by the MDSC. As such, the phagocytic capability was overwhelmed by increasing the concentration of Dynabeads® by 10-fold and through co-incubating them with phagocytosable particles to inhibit the phagocytosis of the beads. In addition, the T cells were pre-activated for 1 hour prior to the addition of MDSC to investigate if this affected the immunosuppressive capacity. It was found that all these interventions abrogated the immunosuppressive effect of MDSC, demonstrating the mechanism behind the perceived immunosuppression was secondary to the phagocytosis of Dynabeads®.

In conclusion, the use of non-phagocytosable stimuli for T cell activation did not demonstrate any immunosuppression when co-incubated with MDSC. Dynabeads® when used in the investigation of MDSC for suppression assays produce artefactual immunosuppression and are unreliable.

4.6.0 Chapter Discussion

Immunosuppression has been one of the pillar stones for the definition of MDSC. Their ability to suppress T cell proliferation is what sets them aside from ordinary monocytes, macrophages and neutrophils. Despite this, there is no consistent method described to measure T cell proliferation when co-incubated with MDSC for the purposes of determining their immunosuppressive function.

The experiments performed in this chapter demonstrated that *ex-vivo* MDSC derived from patients with both benign and malignant disease did not demonstrate immunosuppression, following the isolation of MDSC with magnetic beads or using cell sorting techniques. When using magnetic beads for the isolation of CD15+ cells the purity was poor and highly contaminated and were likely to be unreliable. When the purity was improved through changing the technique to FACS sorting, there was still no evidence of immunosuppression. It was then shown that *in vitro* m-MDSC were able to demonstrate reliable T cell suppression but only in the presence of Dynabeads® used for T cell activation. This was demonstrated to be secondary to phagocytosis of the beads rather than due to true immunosuppression, a result replicated using *ex vivo* samples. Despite multiple attempts to demonstrate reliable immunosuppression using non-phagocytosable stimuli, these experiments failed to show reliable reduction in T cell proliferation, on the contrary, in some instances an increase in proliferation was demonstrated.

Furthermore, the 'immunosuppressive' effect was abrogated when the T cells were pre-stimulated with Dynabeads® for 1 hour prior to the addition of MDSC and when the phagocytic capability of the MDSC was overwhelmed by increasing the Dynabeads® concentration 10-fold. These results corroborate with previous findings that the first hour of T cell activation is crucial (138) and if MDSC impair this, the whole assay may be flawed.

4.6.1 Potential pitfalls encountered during suppression assays

There is no standardised approach to performing suppression assays and methods vary widely within the literature. Performing these experiments in human samples is fraught with difficulty due to many reasons. Firstly, the identification of human MDSC is still debated due to the lack of a clear identifying cell surface marker, unlike in murine models. Secondly, it is difficult to obtain sufficient cells from human samples to run effective proliferation assays, therefore they are often performed on peripheral blood or ascites (88,98) from cancer patients or MDSCs are derived from healthy donor blood and polarised to MDSC *in vitro* (159).

4.6.2 Isolation of PBMC from whole blood

MDSC are isolated using density centrifugation where whole blood is layered over a density gradient medium and centrifuged to separate the cells of varying densities. Granulocytes and erythrocytes have a higher density so when using a density centrifugation media, such as Lympholyte®, they sediment through the media and form a pellet. The PBMC form a layer above the Lympholyte®, due to their lower density, and contain the mononuclear cells.

Neutrophils are very delicate cells and can undergo degranulation with minimal stimulation. It has been shown that neutrophil activation can occur when density centrifugation is performed with dextran, Ficoll (160) or Percoll (161). Rahman et al demonstrated that low-density granulocytes taken from systemic lupus erythematosus (SLE) patients showed increased expression of degranulation markers (CD63 and CD107a) and reduced intracellular arginine-1 (Arg1) when compared to autologous normal-density granulocytes, demonstrating their increased activation status. The low-density granulocytes were also found to have increased LOX-1 expression, the marker of expression used to distinguish low-density neutrophils from PMN-MDSC. Interestingly, in studies of immunosuppression, both low-density and normal-density granulocytes taken from healthy donors did not cause immunosuppression and only normal density granulocytes from systemic lupus erythematosus (SLE) patients caused immunosuppression (91). Whether the effect of density centrifugation itself alters the granulocytes through degranulation and thereby affects the function on PMN-MDSC remains to be seen as this has not been investigated, but its potential effects need to be borne in mind.

The purity of the cells within the PBMC layer is also a factor for consideration because Negorev et al demonstrated considerable contamination of CD15+ conventional neutrophils within the PBMC layer in blood subjected to overnight incubation, cooling and separation over a membrane or gel (145). Many experiments, are performed following overnight incubation due to the issue of the time at which the specimens are received in the laboratory, and as such could be subject to considerable contamination.

4.6.3 Isolation of MDSC from patient samples

There are many methods described; using flow cytometry cell sorting (150), magnetic beads isolation with anti-CD33 beads only (without sorting for HLA-DR positivity) (159) and magnetic beads isolation with anti-CD15 and anti-CD14 beads (162).

4.6.3.1 Magnetic bead sorting

This method is popular as it is the simpler approach, focusing on sorting CD33 positive cells (159), CD11b depletion (149), CD11b positive cells (85), CD14 (m-MDSC) or CD15 (PMN-MDSC) cell populations (162). Some describe a two-step sorting protocol where they sort for HLA-DR and either CD33 (163) or CD14 (164). Most protocols sort on CD11b or CD33, without the addition of HLA-DR

sorting. This subsequently means this population includes mature cells such as monocytes and macrophages which can affect T cell proliferation; monocytes can increase T cell proliferation, whilst macrophages may phagocytose the beads if subsequent bead activation is used therefore inhibiting T cell proliferation.

4.6.3.2 Magnetic bead enrichment and flow cytometry sorting

Following isolation of PBMC by density centrifugation, the PBMC are sorted according to their CD11b and CD14 positivity (CD14+CD11b+ signifies m-MDSC whilst CD14-CD11b+ signifies PMN-MDSC). They are enriched and sorted either with magnetic beads (165) or FACS sorting. Similarly to above, this method can only sort on a few markers and there is a high risk of contamination with other cell types. Due to the poor results seen in the first experiment performed, it was decided to instead try a method with greater accuracy without using magnetic beads as they had been shown to interfere with results on neutrophils (145).

4.6.3.3 Flow cytometry sorting (FACS)

This is the most accurate way of sorting cells as multiple cell surface markers can be identified using peripheral blood (150) and ascites (98). This method can detect both PMN-MDSC and m-MDSC populations with minimal contamination.

Experiments on neutrophils have shown that flow cytometry sorting does not alter neutrophil activation or chemotaxis, measured by CD11b and CD62L expression, shape change and intracellular calcium flux (166). It can be inferred that this is a reliable method of sorting for MDSC populations. There have been studies demonstrating that FACS sorting of cells can affect their metabolome and oxidation state so in theory could impact on future function, however to date this has not been identified as a cause of irregularities within suppression assays (167).

The major drawback with the use of flow cytometry cell sorting is that due to its high purity, very few cells may be obtained, especially from patient tissue samples. In my experience, cell sorting was able to clearly identify both PMN-MDSC (CD11b+/CD15+) and m-MDSC (CD11b+/CD14+/CD15-/HLA-DR-) cell types, however there were limitations on the number of cells retrieved from patient tissue samples, especially of m-MDSC. In the process of cell sorting, cell loss is inevitable so more cells than required are necessary to account for this. In addition, the high-pressure nature of FACS sorting may affect cell viability and function.

4.6.4 T cell activation

The main methods employed include using magnetic beads coated with CD3 and CD28 (150,159,162), antibodies for CD3 and 28 (either plate-bound (88,168) or soluble (98)) and, in murine models, pulsed

dendritic cells are used to provide a T cell activation through specific antigen presentation upon the T cell receptor (81).

There are considerations required regarding the choice of T cells used for the proliferation assay; should they be autologous i.e., derived from the same patient as the MDSCs are, or allogeneic and taken from a healthy donor? The arguments to support autologous T cells is that it prevents an artefactual proliferation due to HLA-incompatibility, however as they are taken from a pathological specimen there is the argument that they may not respond in the same manner as healthy donor T cells, due to T cell exhaustion for example. This may affect the T cells' ability to proliferate and therefore affect the assay.

On the other hand, a healthy donor's 'normal' T cells may proliferate even in the presence of immunosuppression secondary to the incompatibility reaction. If using *in vitro* polarised m-MDSC as a positive control, the use of autologous samples is not practically possible when using patient samples as PBMCs are incubated for a week with GM-CSF and IL-6 in order to differentiate them into m-MDSC and that would require venepuncture of the patient on 2 separate occasions 7 days apart. Therefore, autologous samples were chosen in this study, which was technically more demanding as the donor had to be bled twice, a week apart, but guaranteed T cell proliferation was not secondary to any HLA-incompatibility reaction.

4.6.4.1 Magnetic beads - Dynabeads®

Dynabeads® can be used to capture and isolate cells and for cell expansion and have been used in studying the immunosuppressant effects of MDSC (150,152,159,162,165). Dynabeads® are symmetrical, 4.5µm in size - similar to that of antigen-presenting cells - and made from polystyrene bound by antibodies and do not require the addition of antigen-presenting cells (APCs), feeder cells, mitogens or antigens. They bind CD3 and CD28 antigens on T cells and initiate the signalling pathway inducing proliferation, causing a more physiological activation. Antibodies are formed from amine and carboxyl groups. The importance of this is that a study by Makino et al have demonstrated that alveolar macrophages phagocytose polystyrene microspheres and had a greater propensity to do so when primary amine and carboxyl groups were present. The optimal size of microsphere for phagocytosis was 1µm, however phagocytosis still occurred with microspheres up to 10µm in size (169). This suggests that Dynabeads® have the desired properties to enable phagocytosis by macrophages and thereby prevent activation of T cells by inhibiting their contact with the beads. T cell activation with anti-CD3/CD28 beads has been found to occur with 1 hour and reaches a plateau after 6 hours (158) and, should the MDSC impair this initial activation, their ability to cause T cell proliferation will be somewhat dampened. This phagocytic activity has not been demonstrated within MDSC experiments to date.

My results showed that m-MDSC have the ability to phagocytose Dynabeads®, whether they are *in vitro* or *ex vivo* derived cells and therefore can cause artefactual immunosuppression therefore caution should be taken when using Dynabeads®.

4.6.4.2 Plate-bound antibody

T-cell receptor-specific antibodies such as CD3 are essential for the initial T cell activation signal, however T cell proliferation is dependent on a co-stimulation signal provided by CD28. The initial signal through the T cell receptor via the peptide or MHC is antigen-specific, causing the cell to enter the cell cycle, whilst the co-stimulation is required for T cell cytokine production and proliferation. Soluble antibodies do not provide sufficient cross-linking of the T cell receptor to cause activation of down-stream signalling which is why they are usually immobilised in the form of attachment to a bead, the plate or accessory cells (158). The anti-CD28 is usually soluble as this does not require the cross-linking to the T cell receptor. Both soluble anti-CD3 and CD28, however, have been used in the study of MDSC and demonstrated adequate T cell proliferation (98). A potential mechanism for the disruption of the interaction between plate-bound anti-CD3 and the T cell receptor is that the MDSC may adhere to the bound anti-CD3 and form a physical barrier over the top of it preventing access by T cells. They may subsequently undergo frustrated phagocytosis due to the inability to phagocytose the anti-CD3 and thus release the contents of their phagolysosome into the surrounding environment. Such contents include reactive oxygen species, which have been implicated as part of the mechanism of MDSC suppression. The limited experiments I performed on plate-bound antibody did not show any evidence of immunosuppression whether the T cells or MDSC were plated first, however more experiments are required to investigate this fully. In addition, it may be required to measure and quantify cell contents in the cell culture media, such as reactive oxygen species, to identify if frustrated phagocytosis is indeed the mechanism underlying any demonstrated ‘false' immunosuppression.

4.6.5 Measuring T cell proliferation

The method to measure T cell proliferation varies between using thymidine and carboxyfluorescein succinimidyl ester (CFSE) labelling. There has been a study demonstrating that neutrophils can actively secrete thymidine which affects subsequent measured labelled thymidine uptake and therefore can erroneously demonstrate T cell suppression (170). Although this has not been demonstrated in PMN-MDSC, they are phenotypically similar to neutrophils and so it is not inconceivable that this may occur when using thymidine in MDSC suppression assays. I opted to used CellTrace™, a CSFE-based product, to avoid any potential false results.

4.6.6 Plating out the suppression assay

The use of flat- vs round-bottom plates is varied in the literature between different authors. Flat-bottom plates tend to be used for plate-bound antibody (162) as this provides an even surface for adherence whilst round-bottom plates provide increased opportunity for cell-cell interaction which has been shown to be important in T cell suppression (159). Many studies do not state whether a flat- or round-bottom plate was used suggesting that this is not of great significance or importance. Flat-bottom plates were used in this study to provide equal distribution of beads or antibody to the T cells.

4.6.7 Developing a positive control

As I was unable to demonstrate immunosuppression in the original *ex vivo* MDSC experiments, I set about identifying a control in the form of *in vitro* m-MDSC, derived from PBMC incubated with IL-6 and GM-CSF over 7 days. This was a published method of producing MDSC with strong and reliable immunosuppressive potential and therefore would be a useful way to identify if suppression assays were working, and the patient-derived MDSC cells were truly not suppressive or whether there was an intrinsic error in the assay setup.

Lechner et al. published a study on the *in vitro* polarisation of PBMC into MDSC through the use of IL-6 and GM-CSF. The resulting MDSC demonstrated significant immunosuppressive properties when MDSC were in direct contact with T cells, an effect abrogated by the use of a transwell membrane (159), demonstrating their need for direct cell contact. Interestingly, however, Chomarat et al have shown that IL-6 and GM-CSF are required to differentiate monocytes into a macrophage phenotype (171). Macrophages are highly phagocytic cells and usually express HLA-DR, which differentiates them from MDSC. This close association of MDSC and macrophages may suggest that MDSC have a similar phagocytic potential and may behave in a similar fashion, or that cells are differentiating into macrophage or monocyte derivatives rather than MDSC. The markers used to identify m-MDSC were CD14 and HLA-DR, with HLA-DR being the discriminating factor; it should be positive in monocytes and macrophages but negative in m-MDSC. As has been extensively discussed, however, multiple markers are required to identify MDSC and without a specific identifying surface marker, being sure on their phenotypic identification is very difficult.

4.6.8 The potential of inter-subject variability

Despite testing multiple methods for T cell activation, only when using Dynabeads® was any reliable immunosuppression demonstrated and we found this to be due to phagocytosis of the beads rather than true immunosuppression. With each method, varying titrations of MDSC and T cells were used from

0.1:1 (MDSC:T cells) to 1:1 (MDSC:T cells) and found that it was only in the higher ratio of 1:1 that any suppression was seen. Ratios greater than this were not investigated because it was thought that this was not representative of the tumour microenvironment and as such was going to produce intrinsically biased and not clinically relevant results.

One healthy donor did show evidence of immunosuppression with Immunocult™ with a reduction in proliferation of 25%, however this was not replicated in the other 4 donors, potentially showing that the immunosuppressive nature of these cells is variable between subjects. It was thought that even with this one result, a decrease of 25% at a 1:1 ratio of m-MDSC:T cells did not represent reliable or sufficient immunosuppression to warrant further investigation.

A recent publication by Trovato et al. demonstrated the presence of MDSC within patients with pancreatic ductal adenocarcinoma (PDAC). They investigated the immunosuppressive capability of MDSC isolated from patient samples and found that whilst m-MDSC had a greater ability to supress T cell proliferation, this was only achieved at a ratio of 1:1 with PBMC. Immunosuppression was only achieved in PMN-MDSC at ratios of up to 6:1 (PMN-MDSC:PBMC). Furthermore, they performed an additional experiment inclusive of 26 patients whereby they separated their cohort into 'suppressive PDAC', if their m-MDSC could suppress at ratios of 1:3, and 'non-suppressive PDAC' if no suppression was seen. There were only 6 patients who qualified for the 'suppressive PDAC' cohort demonstrating that immunosuppression is not a reliable and reproducible functionality demonstrable *in vitro* (92). The results demonstrated by Trovato et al. correlate with those found in this study; m-MDSC cannot reliably suppress T cell function in *in vitro* studies and whilst some degree of immunosuppression may be seen in a small proportion of subjects (one donor out of 5 demonstrated mild suppression in experiments without Dynabeads® in this study) it is not a universal finding. Whilst there are so many methods for performing suppression assays and with the emergence of these later studies, it appears there needs to be a more precise and reliable method for detecting true immunosuppression, rather than immunosuppression caused through laboratory technique and alteration of cell function *in vitro*.

It is becoming apparent that there may be flaws in the *in vitro* investigation of immunosuppression, supporting the findings in both *ex vivo* m-MDSC and *in vitro* m-MDSC in this study. Negorev at al. demonstrated that suppressive PMN-MDSC were present in patients with lung cancer, depression/anxiety and also in healthy donors, which may suggest that PMN-MDSC are of no clinical significance if they are indeed present or that the methods of extraction are affecting the results and are erroneously showing them to be present. They further investigated whether there could be an alternative explanation for the demonstrated immunosuppression. They showed that this was an artefact when using beads to activate PMN-MDSC as immune-suppression did not occur when using plate-bound or soluble anti-CD3/28. They also demonstrated a small increase in T cell proliferation when co-cultured

with MDSC, a finding consistent with our results, considered to be due to an MLR. They only managed to demonstrate immunosuppression when using bead-based stimulation assays. Even when taking neutrophils from the pellet following Ficoll gradient separation, these neutrophils were also found to be 'immunosuppressive' when incubated with beads, highlighting that this was not just a phenomenon unique to MDSC. They considered this to be due to phagocytosis, however discounted this theory based on examination of their cytospins and deemed the size of the beads (4.5µm) too large for phagocytosis. They identified that the CD15+ cells were forming rosettes around the beads precluding T cell binding and that this occurred to a greater extent when blood was used the day after collection. Additionally, the CD15 cells were cleaving the CD3 antibodies from the beads which prevented T cell activation (145). My study found that the cells formed clusters or rosettes around the beads initially but after prolonged exposure m-MDSC would phagocytose them. Whilst neutrophils were not able to demonstrate phagocytosis, the m-MDSC were behaving in a fashion not dissimilar to macrophages and monocytes and therefore may have a superior ability to phagocytose this size of particle.

4.7.0 Potential future experiments

As described above, there are a multitude of problems with performing suppression assays *in vitro*. Another drawback to performing suppression assays in this fashion is that you remove the cells from their original tissue localisation and so may lose their *in vivo* function. Additionally, when cells are mixed into a single cell suspension their spatial context is lost so cells that were proximal to the tumour may behave differently to those that were in an area unaffected by malignancy, but this cannot be differentiated using an *in vitro* suppression assay.

The use of histopathological slides with immunofluorescence imaging acts as a snapshot to focus in on the precise tumour microenvironment and assess the potential cell interactions. This identifies the immune infiltration *in situ* and allows comparisons to made to their location within the tumour specimen. Due to the lack of a clear cell surface marker for MDSC, conventional immuno-histochemistry or immunofluorescence is not able to adequately define this population. Newer techniques, such as multi-spectral imaging, are now available which can stain multiple surface markers concurrently allowing rigorous spatial statistics to be performed to analyse cell interactions. Si et al identified MDSC within human cancer tissue and investigated their effect on T cell proliferation and cytotoxic potential through measuring K-i67 and granzyme B (GrzB) respectively. They showed that in areas of high prevalence of MDSC (denoted by CD66b+ and either expressing LOX-1, arginase or MPO) there were fewer proliferating or cytotoxic T cells. They demonstrated the importance of LOX-1 positivity in the immunosuppressive function of MDSC by showing reduced proliferation of both CD4 and CD8 T cells in areas of high LOX-1 positivity and reduced production of GrzB when T cells were in conjugation with these MDSC (172).

To further this work on MDSC, multidimensional imaging using multispectral imaging (Vectra Polaris) was hoped to be performed to identify tumour cells, T cells and MDSC on ovarian tumour and omental metastases. This would have enabled measurement in an *in-situ* model of T cell proliferation was being dampened by MDSC as one would expect fewer proliferating T cells (denoted by Ki-67) surrounding MDSC than in other areas of tumour. There remains the limitation of the number of surface markers that can be stained, however. At present with the Vectra Polaris the upper limit is 8 different markers concurrently and potential markers that could be used include: CD3 and Ki67 to detect T cell proliferation, EpCAM to detect ovarian epithelial cancer cells, CD14 and HLA-DR to identify m-MDSC and perhaps CD15 and LOX-1 to identify PMN-MDSC. Unfortunately, I was unable to continue my work due to limitations secondary to restrictions with COVID-19, however feel this would be the most accurate way to pursue this topic further.

4.8.0 Conclusion

The use of suppression assays in the experimentation of MDSC has been an integral part of publication. This is in part due to the difficulty in identification of MDSC through cell surface markers alone; their presence has been required to be proven through their immunosuppressive activity. As described above, the investigation of the immunosuppressive activity of MDSC has been achieved in a multitude of ways with great inconsistencies. Potential flaws are present with most methods of experimentation, which need to be borne in mind when undertaking these experiments. Adequate control experiments are required to identify true immunosuppressive effects rather than simply demonstrating artefactual results.

Following these experiments, it has been demonstrated that m-MDSC have the capacity to phagocytose Dynabeads® with subsequent effect on T cell proliferation which may be erroneously perceived as immunosuppression.

The observations highlighted in chapter 3 were that *ex vivo* studies on m-MDSC appeared to demonstrate an association with treatment outcomes and therefore may have a prognostic implication. Subsequently in chapter 4, *in vitro* experiments were performed which did not demonstrate the immunosuppression as hypothesised, whether this was due to a technical fault with the suppression assays or failure to isolate pure MDSC is unknown. To further this work transcriptomic analysis can be used to identify myeloid cells, including MDSC, more accurately within the ovarian tumour microenvironment and through identifying their gene expression signature, it may provide an insight into their potential functionality. This will be discussed further in chapter 5.

Chapter 5

RNA profiling of immune cell phenotypes in ovarian cancer

5.0 Introduction

In ovarian cancer as a whole, response to immunotherapy has been varied and somewhat disappointing (107). This variation in clinical response has been attributed to the tumour heterogeneity but also potentially the heterogeneity of immune cell infiltration. This poses the questions of what composition of immune cells are present within ovarian cancer?

5.1.0 RNA sequencing

5.1.1.1 Transcriptome

Ribonucleic acid (RNA) is a single-stranded polymeric chain of nucleotides that serves in essential cell functions. There are many forms of RNA molecules providing different functions; from protein-coding messenger RNA transporting nucleic information to the ribosome, to non-coding regulatory RNA which can regulate gene expression. Up to 98% of RNA is non-protein-coding or 'non-coding' and this is integral to gene expression and ultimately contributes to the phenotypic variation observed between humans (173). The transcriptome encompasses all RNA transcripts, including both coding and non-coding within an organism or cluster of cells.

5.1.1.2 Measuring the transcriptome

There are two main methods to quantify the transcriptome, either through DNA Microarray or through RNA-sequencing. DNA microarray is restricted to measuring expression of pre-defined transcripts and genes, whilst RNA-sequencing can perform full sequencing of the whole transcriptome-level expression (174). RNA sequencing is a technique that allows identification of the quantity and sequences of RNA within a sample, through analysis of the transcriptome (175). It provides information on the activation status of genes and their level of expression (176). There are several different analyses that are commonly applied to extract information from RNA sequencing data including single-nucleotide polymorphism (SNP) identification, transcriptional profiling, differential gene expression analysis and functional enrichment analysis (177).

RNA-sequencing can be performed on two different levels – bulk or single cell sequencing. Bulk sequencing is able to analyse large populations of cells largely by computing the averaged gene expression across thousands of cells, whilst single cell can identify heterogeneity between cells in a small population. Bulk sequencing may have the limitation of averaging out biologically significant

heterogeneity within a sample and may contain averages of cells considered as contamination thus affecting the result. The analysis of single-cell sequencing can be more challenging due to the potential contamination of the sample by high level of background 'noise' and considerable heterogeneity owing to it analysing each individual cell (178) therefore the desired output needs to be carefully considered prior to commencing these techniques. The sequencing platforms used to gather the data is important as this can affect the data interpretation. The major differentiating factor is whether DNA ligase or primase is used to control their sequencing reaction; Roche 454, Illumina, PacBio and Helicos use the latter, whilst SOLiD and Complete Genomics use the former. Illumina offers a greater sequencing depth enabling detection of low expressed transcripts whilst maintaining a low sequencing error rate of <1% (179). This forms the basis of choice of this product for the study of the immune cells in the ovarian microenvironment.

In order to perform RNA sequencing, firstly the RNA needs to be isolated from the sample and reverse transcribed into cDNA fragments. Upon preparation of the library platform-specific adapter sequences are added and PCR-amplified before being sequenced through next generation sequencing (NGS). This can be either single-read or paired-end sequencing; the former involves sequencing from one end of the cDNA fragment, whilst the latter sequences from both ends. Paired-end sequencing is consequently more in-depth but is also costly and time-consuming (180).

Further differences in techniques in RNA sequencing involve strand-specific and non-strand specific protocols. Strand-specific protocols provide further information and tend to be preferred as they retain information about which DNA strand was transcribed.

5.1.1.3 Single cell transcriptional profiling

The key point with scRNA is that the single cells are isolated from the sample and then the RNA is extracted rather than the RNA being extracted from all of the cells within the sample. There are several single cell isolation methods that can be used, including laser-capture microdissection (LCM) and microfluidic approaches. LCM allows the user to select particular cells of interest under direct vision to create histologically pure enriched cell populations and can utilise fresh frozen samples and formalin-fixed paraffin-embedded tissues (181), which allows for storage of the tissue for use at a later date. The remaining tissue can also be stored and used for future experiments where necessary, allowing maximum use of the sample. The microfluidic approaches include techniques such as drop-seq and 10X techniques, whereby small volumes of sample are passed through channels filled with fluid, such as reaction media or buffers and this separates the cells through altering the size of the channel height and width. The advantages of this technique include low reagent consumption which is more cost-effective and it has a high surface to volume ratio allowing maximal exposure to surfaces which may be necessary to facilitate reactions with surface immobilised enzymes or sensing applications. It offers a high spatio-temporal resolution allowing for individual cells to be studied over time and due to the fact it requires

only small volumes and can run parallel reactions, there is a high throughput available with each run (182). 10x Genomics is currently the leading microfluidics platform and provides a solution for immune profiling and as such, this option was decided for this research.

5.1.1 10 x Genomics

This method of RNA sequencing allows transcriptome sequencing at a single cell level through incorporating a unique barcode within each individual cell through the creation of 'GEMs' – Gel bead in Emulsion partition. Here the cells are individually encapsulated in droplets along with barcoded gel beads and reverse transcriptase reagents, enclosing a central functionalised gel bead (Figure 5.1). This system allows high throughput and can analyse up to 8 separate samples simultaneously. In addition, owing to each transcript having cell-specific barcodes, the data can be demultiplexed to assign reads to their source cell post sequencing.

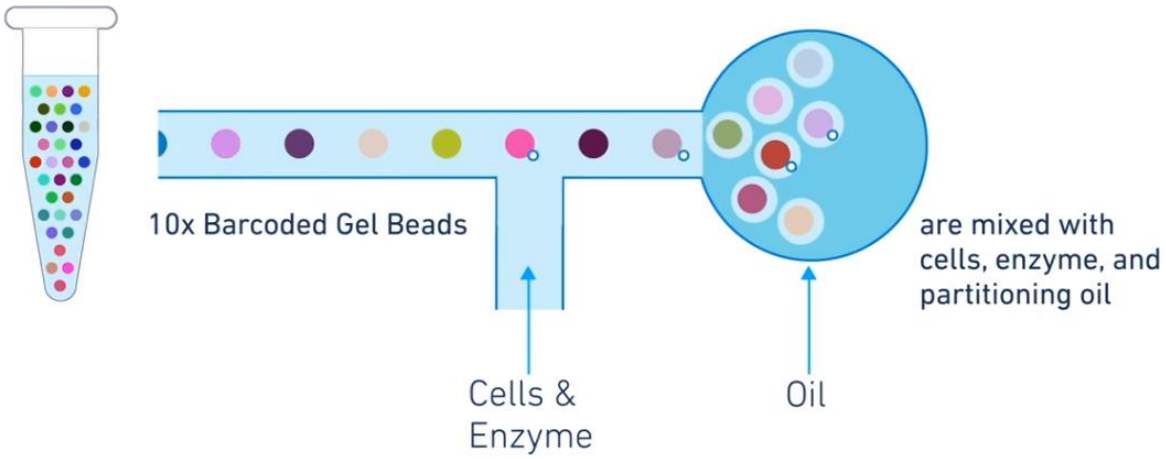

Figure 5. 1. The formation of the barcoded gel beads.
The gel beads are combined with the cell and encapsulated with reverse transcription reagents in solution within a partitioning oil. Image reproduced from the Chromium Next GEM Single Cell 3' Reagents Kit v3 User Guide. Document number CG000204.

Following this, the gel bead is dissolved, primers are detached and the cell is lysed to release the genetic material. The cell lysate is combined with reverse transcription enzymes, producing barcoded cDNA. This cDNA is then amplified using PCR and primers are added to each end of the cDNA for Illumina® (CA, USA) bridge amplification. This can then be used for sequencing (Figure 5.2). This method is therefore a paired-end, strand-specific method of RNA sequencing.

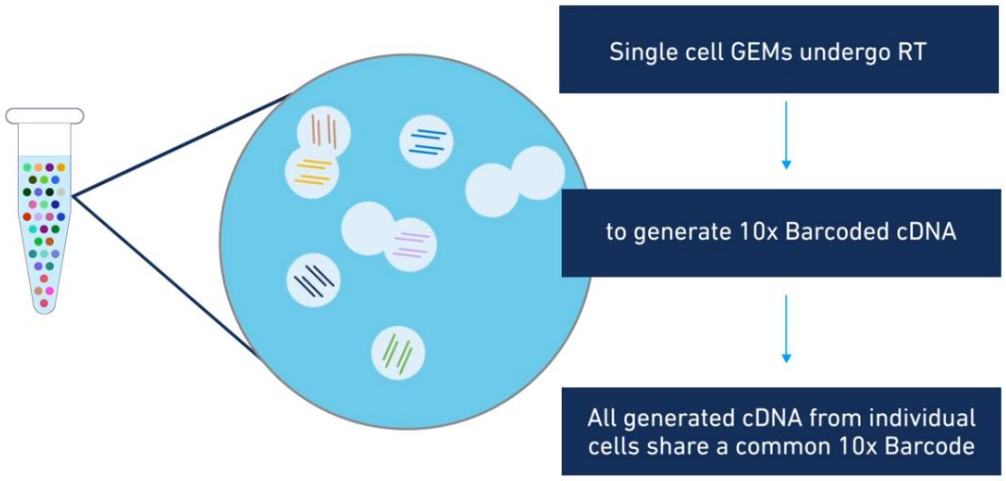

Figure 5. 2. The generation of barcoded cDNA.
The gel bead is dissolved and the primers are detached to allow reverse transcription. Barcoded cDNA is then generated. Image reproduced from the Chromium Next GEM Single Cell 3' Reagents Kit v3 User Guide. Document number CG000204.

5.1.2 Single cell RNA sequencing in cancer

The identification of a novel cancer therapy, free from treatment resistance and which is tumour-specific has been plagued with difficulties due to heterogeneity within the tumour, the immune cell infiltration and the interactions within the host tumour microenvironment. As alluded to previously, bulk sequencing can have the effect of averaging out important heterogeneity and this is where single cell sequencing offers a big advantage within a cancer setting. Using scRNA sequencing analysis, it is now possible to explore in finer detail the immune cell subsets present within tumours and provide a snapshot in time detailing the various stages of differentiation that the immune cells are undergoing in response to the tumour microenvironment and can therefore identify intra- and inter-tumoural heterogeneity. This method allows analysis of the genetic signature of cells as opposed to relying upon expression of a restricted set of cell surface marker proteins, which can be falsely altered in response to laboratory techniques. Additionally, some pre-selected markers may be differentially expressed when exposed to different environments such as inflammation, making characterisation via genetic signature more reliable and accurate. Single cell sequencing to characterise a number of tumour microenvironments, including breast tumours (183), melanoma (184) and hepatocellular carcinoma (185) whereby significant heterogeneity of immune cells and their activity has been identified, as well as identification of markers of immune cell exhaustion which has helped in mapping the immune landscape within neoplasms. Kim et al demonstrated variability in the activation of drug target pathways between the primary and metastatic tumours of renal cell carcinoma taken from a patient with multi-resistant disease. This would help to dictate most effective combination therapy in order to improve outcome thus demonstrating the role of single cell sequencing in advancements towards personalised medicine (186).

Additionally, single-cell sequencing has been used to identify paclitaxel resistance in breast cancer cells and demonstrated that they behaved differently in unexposed, stressed and drug-tolerant cell groups, with RNA variants existing in genes associated with microtubules, cell adhesion and cell surface signalling (187).

The TME in one distinct area has the potential to influence and dictate the microenvironment at other sites through migration of cells to other metastatic sites or to lymph nodes. This was shown in a study on hepatocellular carcinoma which demonstrated the dynamic relationship of myeloid and lymphoid cell subsets between tumour, adjacent liver, lymph nodes, blood and ascites (188). Prior to single cell sequencing, it was believed that T cells differentiated efficiently into their stable mature states such as Treg, effector, memory or exhausted T cells. Instead, it demonstrates T cell differentiation occurring along a continuum of cellular states which can be pathogenic or non-pathogenic. A large proportion of this diversity lies within the activation status of the T cell receptor and this, along with unique gene expression, distinguishes the discrete state of the T cell. In comparison to this spectrum of activation that exists within the T cell population, myeloid populations tend to demonstrate more discrete delineations in differentiation. This does not suggest a black and white delineation of myeloid subsets as it was shown that in macrophages, the expression of both M1 and M2 genes were frequently co-expressed so suggest that macrophages sit among a spectrum somewhere between the M1 and M2 states. Interestingly, there appeared to be greater patient-specific variation within the myeloid lineages in comparison to the T cells (183).

Changes in the immune cell function have been identified to occur as early as in stage 1 disease, with a reduced CD8+ T effector:Treg ratio being apparent compared to normal lung, as well as depleted CD141 dendritic cells, reduced CD16+ monocytes and increased expression of PPARγ macrophages, known to be associated with immunosuppression. All of these alterations depict an early establishment of an immunosuppressive microenvironment ideal for tumourigenesis (189).

5.1.3 Transcriptional analysis in Ovarian cancer

Single cell RNA sequencing is of importance in ovarian cancer because heterogeneity is the major challenge for treatment and relapse. Many papers have investigated bulk sequencing of RNA in high grade serous ovarian cancer and attempted to categorise based upon the expression patterns identified into mesenchymal, differentiated, immunoreactive and proliferative subtypes (190–193). This categorisation did offer some clinical relevance as it did correlate with response to antiangiogenic treatment with bevacizumab (194). However, when this was interrogated on a single cell level, it was identified that all such subtypes were present within one patient sample, further demonstrating the existing heterogeneity within ovarian cancer samples and how this may be hidden in bulk sequencing (192). On a single-cell level, Winterhoff et al identified 2 major subsets of cells within HGSOC characterised by stromal (genes associated with epithelial-to-mesenchymal transition) or epithelial

(genes associated with oxidative phosphorylation and MYC activity) gene expression, which showed the majority of stromal cells fell into the 'mesenchymal' group, whilst the epithelial cells fell largely into the 'proliferative' group (194). Significant heterogeneity has been also identified in the malignant ascites of ovarian cancer patients; however, the majority expressed the 'differentiated' subtype, whilst the non-malignant cells, comprising of cancer-associated fibroblasts and immune cells were of 'mesenchymal' and 'immunoreactive' subtypes respectively. This work suggests that the majority of cells within the 'mesenchymal' subtype are indeed cancer-associated fibroblasts rather than malignant cells themselves (195). Malignant fibroblasts have been found to be critical for ovarian cancer development and drug resistance evidenced by increased gene expression of genes involved in the metabolic pathway, DNA replication and repair and drug resistance (196). It is unsurprising, therefore, that the mesenchymal subtype of ovarian cancer is associated with a worse prognosis out of the 4 subtypes (197). It has been suggested that mesenchymal high grade serous cancer is simply a marker of advanced disseminated intraperitoneal disease rather than a distinct subtype of ovarian cancer, as it is found in upper abdominal/peritoneal metastases irrespective of the ovarian tumour subtype (198). Interferon alpha inducible protein 6 (IFI6) has been identified through scRNA sequencing as a potential gene in carcinogenesis and cisplatin resistance (199) and the hope is that with further work, more common targets will be identified to direct treatment.

A further study investigating the genetic aberrations in ovarian cancer demonstrated that 80% of primary HGSOC had TP53 mutation, whilst 40% of those with recurrence had this, demonstrating heterogeneity within the same patient and tumour evolution. It demonstrated that the BRCA mutation is effectively controlled following therapy as they were not present in the recurrence specimens, but tumours without the BRCA mutation exhibited recurrence (200). This may help to predict response to immunotherapies to deliver more personalised medicine in future. Much of the scRNA sequencing work that has been performed to date in ovarian cancer has focused upon the tumour cells and therefore removed immune populations from the sample.

5.1.4 Myeloid subsets in Ovarian cancer

The myeloid population are subject to great heterogeneity and serve as a potential target for immunotherapy, especially through inhibition of immunosuppressive subsets such as tumour associated macrophages and MDSC. As such, the use of scRNA sequencing lends itself well to the identification and phenotyping of myeloid subsets within cancer. Shih et al identified that cells of myeloid lineage or fibroblasts secreted more factors than the primary epithelial tumour itself and when investigating metastatic sites, found that the fibroblasts increased their production of essential factors to promote metastatic growth. Once the metastatic niche was established, few epithelial cells were required to maintain it as it was largely maintained by invading lymphocytes (201). These results demonstrate the importance of the immune response to cancer and more specifically that the myeloid subset play an

integral role in maintaining the primary site tumour. Looking at cancer more generally, scRNA sequencing has been able to identify multiple myeloid cells based on transcriptional similarity, including mast cells, plasmacytoid dendritic cells, conventional dendritic cells, monocytes and macrophages in a study investigating myeloid populations in the top 15 most common cancers. It was shown that there is significant heterogeneity within the tumour-associated myeloid cells and identified a specific cancer type with the potential to respond to mast cell-targeted immunotherapy. In addition, it was identified that a specific sub-population of macrophage was associated with tumour angiogenesis and was linked with poor prognosis in 8 different tumour types (202). This demonstrates that although there exists significant heterogeneity, single cell sequencing does have the potential to identify possible commonalities in order to help guide future therapy, and that targeting the myeloid population may be key in doing this.

Further work into the infiltration of myeloid cells into the tumour microenvironment have discovered a subtype of macrophage known as SPP1, which are associated with worse prognosis in non-small cell lung cancer and colorectal cancer and do not fit into the standard categorisation of M1/M2 macrophages (203,204). Potential future avenues for therapy could include targeting these subsets of macrophages to improve myeloid-targeted immunotherapy.

5.1.5 Modification of the tumour microenvironment by chemotherapy

There is limited research on the chemotherapy effects on the transcriptional profiles of immune cells in ovarian cancer. Within cervical cancer, however, it has been shown that post-chemotherapy the P13K/AKT and MAPK signalling pathways were enriched in epithelial, T and B cells in women with chemotherapy resistance (205). No studies on the transcription profiles of myeloid cells specifically were noted.

Whole exome sequencing and RNA expression data have been used within ovarian cancer to determine how a primary site tumour differs from its metastatic sites following treatment with chemotherapy in one patient. They found that the primary site tumour had little or no immune cell infiltration, whilst metastases to the liver and right upper quadrant peritoneum were infiltrated largely by CD4 and CD8 T cells. Those areas infiltrated with T cells showed evidence of regression with therapy, whilst those without infiltration progressed during therapy (206). Although this is of interest, it is based on a single patient so further work is required within ovarian cancer to evaluate the effect of chemotherapy to identify methods of overcoming relapse and resistance to therapy.

5.2.0 Aims of project

There are no current studies that identify and phenotype the myeloid cell populations in ovarian cancer in response to chemotherapy. We sought to:

1. Identify the immune cell infiltration in women with high-grade serous ovarian cancer pre- and post-chemotherapy using 10 x Genomics (CA, USA) technology.
2. Compare this to cancer of a different origin (metastatic adenocarcinoma) and normal tissue.

We have focussed analysis on the myeloid subset of cells as these cells remain less studied than T lymphocytes, however their presence has been associated with patient survival and may be implicated in facilitating metastasis (207). As such, it is important to further characterise the contexture of infiltrating myeloid cells in HGSC.

RNA profiling of immune cells in ovarian cancer

5.3.0 Results

As discussed previously in this thesis, the immune microenvironment of a tumour can potentially influence its propensity to invade and metastasise. As previously alluded to, however, the detection of these immune cells, especially MDSC, can be variable depending on the surface marker selected and the laboratory technique used. Therefore, to identify the immune cells present within cell populations and the tumour microenvironment (TME), single cell RNA sequencing was utilised.

In this chapter, using omentum tumour samples obtained from women with ovarian masses removed during their debulking surgery, the aims were to:

1) Further characterise the contexture of immune cells within the omental metastases of women with ovarian cancer.
2) Characterise sub-populations of Myeloid cells.
3) Identify suppressive genes upregulated within these cells which could contribute to an immunosuppressive environment.
4) Investigate the extent to which chemotherapy affects the composition of cells within the TME.

5.3.1 The isolation and immune profiling of immune cells in ovarian metastases

5.3.2 Patient cohort selection

Women undergoing tumour debulking surgery in either City Hospital, Birmingham or New Cross Hospital, Wolverhampton were approached to participate in the study as granted by our ethics approval. Women were either having primary surgery, where the histology result was unknown and there was no exposure to chemotherapy, or delayed debulking surgery, where the women had a previous biopsy performed to confirm their diagnosis of high grade serous ovarian cancer and had subsequently received chemotherapy for this. All diagnoses were confirmed by a specialist gynaecology histopathologist.

In total, 10 women were approached to participate in the study. Four of these women had delayed debulking surgery (DDS) and as such had been exposed to chemotherapy and five women were identified as primary debulking surgery (PDS) and therefore their diagnoses were not confirmed and they had not received chemotherapy. There was one normal omentum included in the cohort. The omentum was selected as the site of tissue sampling as invariably it is a site of metastasis if the ovarian cancer has metastasised, so it provided a consistent tissue to sample. In addition, I found through previous work using ovarian tissue and various metastatic sites that the metastases within the omentum tended to be less necrotic and therefore contained more quality cells within the sample. In total, 8 of the

samples were confirmed to be high grade serous ovarian cancer; 4 were primary debulking surgery and 4 were delayed debulking surgery. One woman from the primary debulking cohort was subsequently diagnosed with a metastatic gastric adenocarcinoma rather than a primary ovarian tumour and one of the samples was proven to be normal, free from any macroscopic or microscopic disease. The patient characteristics are described below in Table 5.1.

AGE AT OPERATION	
MEDIAN	65
RANGE	42-78
DIAGNOSIS	**Number of patients**
HGS	8
METASTASIS	1
NORMAL	1
STAGE OF HGS DISEASE	
1	0
2	0
3	4
4	4
CHEMOTHERAPY EXPOSURE	
DDS	4
PDS	5
NUMBER OF CHEMOTHERAPY CYCLES	
3	1
4	2
6	1
CRS	
1	0
2	2
3	1
NOT STATED	0

Table 5. 1. Patient characteristics of women enrolled into the study.
HGS: high grade serous ovarian cancer. PDS: primary debulking surgery. DDS: delayed debulking surgery. CRS: chemotherapy response score.

5.3.3 Identification of the immune cells within the tumour microenvironment of omental metastasis characterised through single-cell RNA sequencing

To isolate immune cells from the sample, the tissue underwent a process of digestion to form a solution containing single cells and these cells were then stained with antibodies for podoplanin (to identify fibroblasts), CD45 (to identify immune cells) and EpCAM (to isolate epithelial cells) as per the

manufacturer's guidance. The cells were then sorted using flow cytometry into 2 separate populations; CD45 positive and podoplanin/EpCAM positive cells. To ensure sufficient numbers of Immune cells for an immune-focussed analysis, the sample was then reconstituted to contain 80% CD45+ cells and 20% podoplanin/EpCAM+ cells. The sample was then transferred to Genomics Birmingham for library preparation and RNA sequencing. The total number of cells sequenced per patient was in the range 2271 – 6355, whilst the Normal sample returned a greater number at 20492 cells (Table 5.2).

Cells numbers retrieved per patient sample

Patient number	Diagnosis	Chemotherapy	Number of cells
Pt1	HGS	Post	5244
Pt2	HGS	Pre	2271
Pt3	HGS	Post	3174
Pt4	Metastasis	Pre	5366
Pt5	Normal	Nil	20492
Pt6	HGS	Post	6284
Pt7	HGS	Pre	4352
Pt8	HGS	Post	5764
Pt9	HGS	Pre	4062
Pt10	HGS	pre	6355

HGS: high grade serous cancer

Table 5. 2. The diagnosis of patients included in the study with their chemotherapy status and the number of cells sequenced in each sample.

5.3.4 Single cell profiling identifies the high-level cell types present in the tumour microenvironment

RNA single cell transcriptome data across all samples were integrated and unsupervised clustering applied in order to identify groups of cells (clusters) with similar transcriptional profiles. 8 Distinct clusters were realised and identified as T and NK cells, stromal, myeloid, B cells, plasmacytoid dendritic cells (pDC), plasmablast, endothelial and cycling cells (Figure 5.1A).

5.3.5 The T and NK cell group account for the greatest proportion of CD45+ cells within the samples

Of the CD45+ cell types identified (T_NK, cycling, Myeloid, B, plasmablast and pDC) the T_NK cell group are the dominant cell type, whilst the myeloid cells are the second biggest contributor. The cells were labelled by their sample number to visualise the extent of consistency cell-type populations across all samples. This indicates that there is a relatively even spread of cells from each of the patient datasets, with the only exception being a particularly high number of B cells present within Patient 6, who was a post-chemotherapy HGS cancer patient (Figure 5.3B). The data was analysed depending on the

exposure to chemotherapy in the HGS samples and this was compared to the metastatic adenocarcinoma and normal sample (Figure 5.3C).

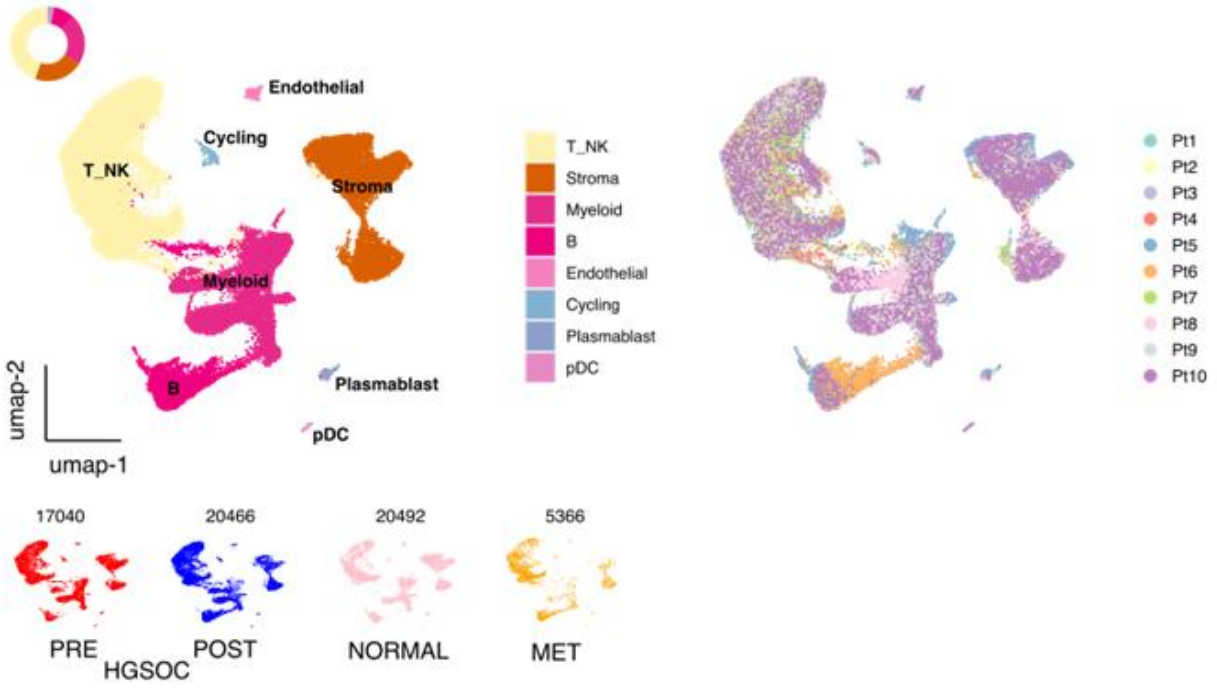

Figure 5. 3. High-level cell type ATLAS of High Grade Serous Ovarian Cancer.
UMAP embedding overlaid with cluster cell type annotations (A) and originating sample label (B). Donut chart of proportions of all cells (A inset). (C) UMAP embeddings split by chemotherapy treatment and tissue type. Total cell number indicated above plot.

The high-level cell types were identified by canonical cell-type marker gene expression (Figure 5.4). The T_NK cluster showed high expressions of the T-cell glycoprotein CD3D (forms part of the T cell receptor/CD3 complex so is involved in T cell activation) and a likely cytotoxic/NK subset expressing granulysin (GNLY). Granzyme B (GZMB) was highly expressed in this cluster and is known to be expressed by cytotoxic T cells and NK cells, whilst B cells were identified through the expression of the B-lymphocyte antigen MS4A1 and IGKC (immunoglobulin kappa constant) commonly found on plasma cells. Lysozyme (LYZ) forms part of the immune barrier produced by the monocyte-macrophage system so aids in the identification of the myeloid cells. Mast cells, which are a subset of the myeloid cluster, were identified through TPSAB (tryptase alpha-1 and tryptase beta-1), which is a gene coding tryptases, known to be associated with mast cell function (208). The cells undergoing proliferation (cycling) are denoted by MKI67 as this gene codes for Ki-67, a prominent marker for highly proliferative and neoplastic cells (209). Plasmacytoid dendritic cells were identified through IL3RA, a marker which has been used previously in single-cell RNA sequencing (210) and CDH1 (cadherin 1), which is involved in cell-cell adhesion and is known to be expressed by dendritic cells such as Langerhan's cells (211). The endothelial cells have been identified using PECAM1 (platelet

and endothelial cell adhesion molecule 1) and CLDN5 (Claudin 5). PECAM1 is also known as CD31 and is unique to blood and vascular cells and forms part of the vascular barrier (212), whilst claudins are integral membrane proteins serving as a barrier to prevent free movement of solutes and water through epithelial or endothelial cells. Decorin (DCN) is a component of the extracellular matrix and a marker for stromal cells along with the collagen COL1A20. In addition, EpCAM (epithelial cellular adhesion molecule) is involved with cell adhesion of epithelial cells and is present in a subset of a stromal cluster.

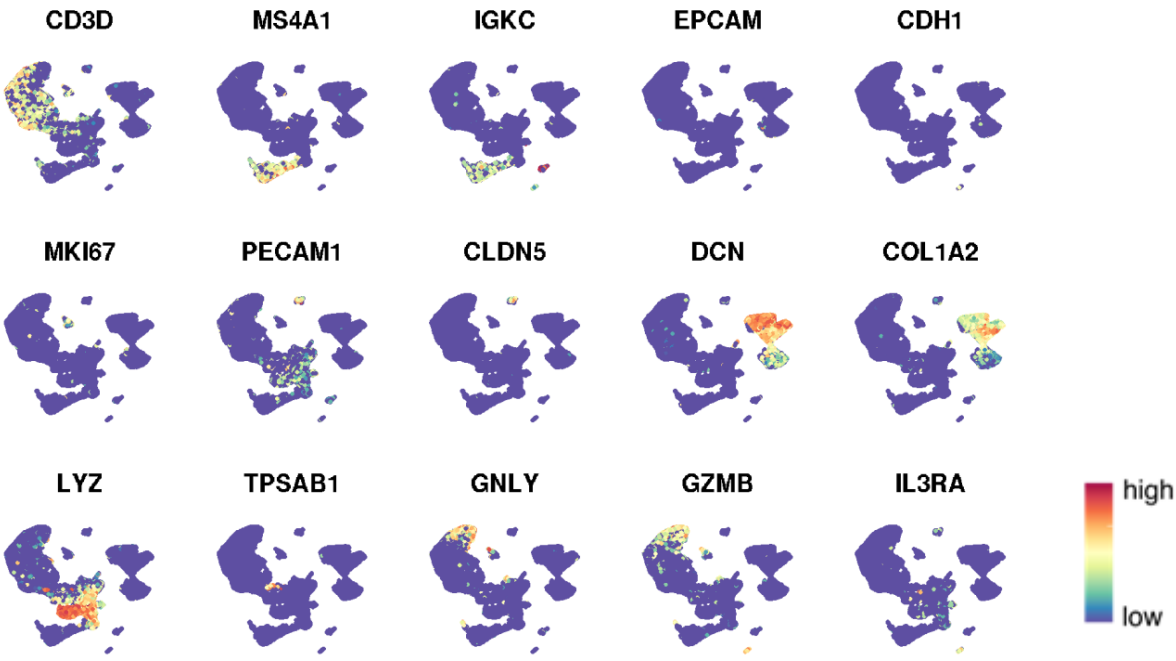

Figure 5. 4. The identification of the major cell types. UMAP embeddings overlaid with expression of canonical high-level cell type marker genes

Comparisons between HGSOC (high grade serous ovarian cancer) and MET (metastasis) or NORM (normal) (Figure 5.5) are limited due to the sample size of one in each of the MET and NORM cohorts. Noteworthy observations, however, include a greater proportion of T/NK and B cells within the metastasis compared to the HGSOC. In addition, there was a higher proportion of stromal cells in the normal tissue compared to the other diagnoses. There were similar proportions of myeloid cells within the high grade serous ovarian cancer and normal tissue, which were both considerably greater than the metastasis sample. Within the gastric adenocarcinoma sample there tended to be a greater presence of T/NK and B cells but lower influence of myeloid cells.

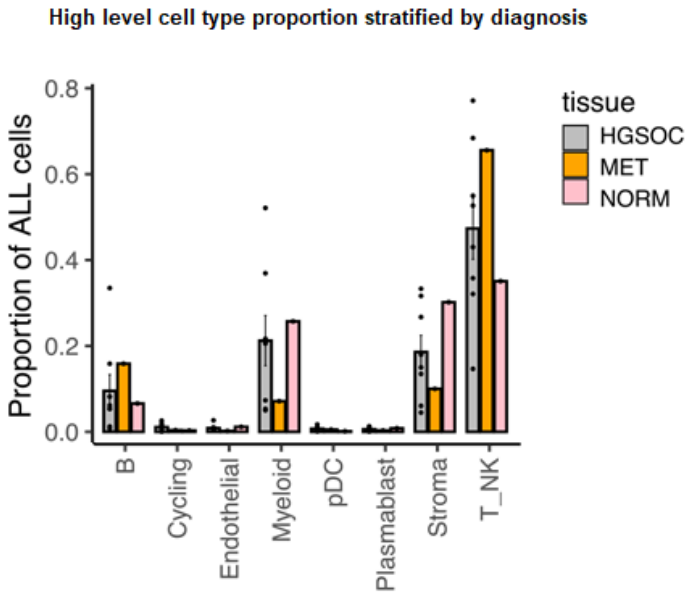

Figure 5. 5. A depiction of the proportion of all cells represented by each cell type in the various tissue types.

High level type proportion stratified by diagnosis. Comparison of cell type proportion in High Grade Serous Ovarian Cancer (HGSOC), Metastasis from GI tract (MET) and Normal Omentum (NORM) tissue samples. Bars represent mean ± SEM.

5.3.6 Modulation of high-level cell type proportion by chemotherapy treatment

The data was then analysed depending on the exposure to chemotherapy and this was then compared to the normal and metastatic adenocarcinoma samples. Trends were observed in chemotherapy increasing the proportion of T/NK cells but reducing the myeloid, stromal and endothelial cell groups (Figure 5.6).

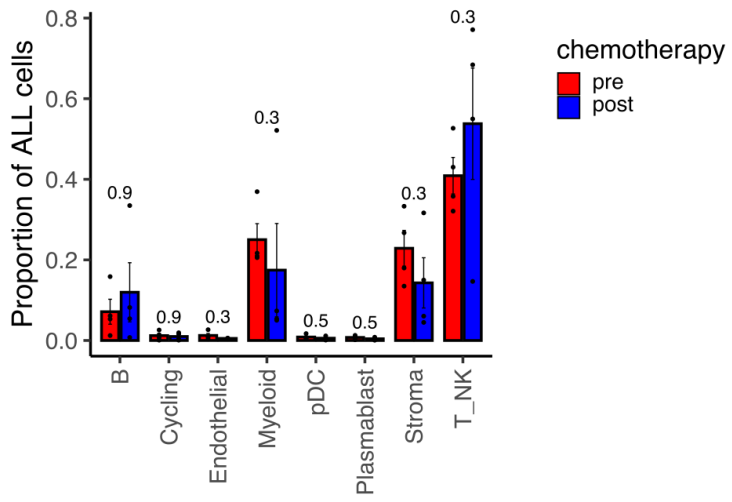

Figure 5. 6. Chemotherapy modulation of immune cell subtypes in ovarian cancer.
Comparison of cell type proportion in High Grade Serous Ovarian Cancer (HGSOC) tissue samples pre vs post chemotherapy. Points represent within-sample cluster proportion of total cells and p values determined by Mann-Whitney test. Bars represent mean ± SEM.

5.3.7 Modulation of myeloid sub-populations dependent on the underlying diagnosis and the exposure to chemotherapy

The myeloid subset of cells was then focussed upon to look in finer detail at the different cell subtypes within this group. Myeloid cells only were subset from the data and unsupervised clustering on these identified the major myeloid sub-populations.

5.3.8 The major myeloid subsets identified were monocytes, macrophages and neutrophils with a small group of monocytic dendritic cells present

The 3 major subgroups identified within the myeloid population were monocytes, neutrophils and macrophages (Figure 5.7A). When the UMAP embedding was overlaid with patient label there was generally consistent contribution to each of the cell groups from each of the patients, except for Patient 8 (Pt8) who seemed to have a greater proportion of neutrophils within the sample (Figure 5.7A, 5.7B). The monocytes formed the largest subgroup, whilst the monocytic dendritic cells were the smallest.

Within the high-grade serous cohort, there was a greater proportion of neutrophils compared to the metastatic adenocarcinoma and normal samples. Chemotherapy altered the immune microenvironment by causing a greater proportion of neutrophils and subsequently smaller proportion of macrophages within the post-chemotherapy cohort.

5.3.9 Identification of major myeloid sub-populations by canonical marker gene expression

The identification of the myeloid subgroups was made depending on the expression of key marker genes, including CD14, ITGAM (integrin subunit alpha M), HLA-DQA1, HLA-DRA, FCER1A (Fc receptor epsilon 1A), CD68, CD163 and S100A8. The HLA genes form the proteins for the major histocompatibility complex class 2, which typically are expressed by monocytes and macrophages and have demonstrated high expression within this subgroup of cells, aiding in their identification as such. CD163 is expressed by macrophages, so has helped differentiate between the macrophage and monocyte subgroups, whilst CD68 is largely expressed by monocytes. S100A8 is involved in neutrophil chemotaxis and adhesion so has differentiated this subset of cells (Figure 5.7C). CD14 is mainly expressed by macrophages but can also be expressed monocytes and, by a far lesser degree, by neutrophils. ITGAM is required for the adherence of monocytes and neutrophils to activated epithelium. The expression profiles of both ITGAM and CD14 are consistent with the literature in identifying the major myeloid subsets (Figure 5.7C). The subset of cells expressing moderate expression for FCER1A are likely to represent the cDC population. The top markers identified by differential expression analysis to be overexpressed in each of the myeloid sub-populations indicate distinct transcriptional profiles (Figure 5.7D).

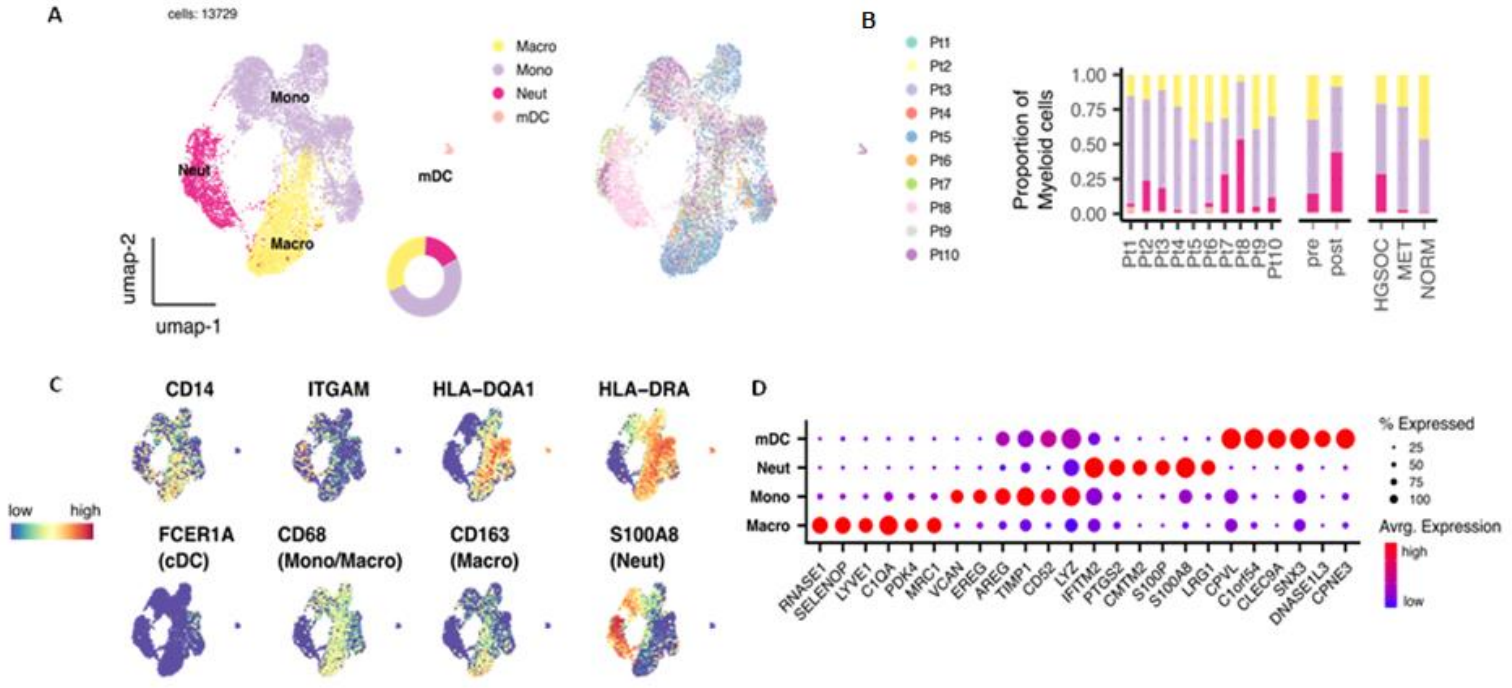

Figure 5. 7. The identification of the cell types through their gene expression.
A) UMAP embedding overlaid with cluster cell type annotations (left) and sample label (right). Donut chart proportion of total cells (inset). B) Breakdown of cluster proportions by sample, pre/post chemotherapy treatment and tissue type. C) UMAP embeddings overlaid with expression of canonical high-level Myeloid cell type marker genes. D) Average expression profile dotplot of top cluster marker genes. Dot size indicates percentage of cells expressing the gene.

The top cluster marker genes aided in the identification of different cell subsets, with specific cluster markers being indicative of particular cell types. Marker genes such as RNASE1, SELENOP, LYVE1, C1QAPDK4 and MRC1 are highly expressed in macrophages but not in any of the other myeloid subsets (Figure 5.7D). Meanwhile, CPVL, C1orf54, CLEC9a, SNX3, DNASE1L3 and CPNE3 were highly expressed in mDC but not in any other subset.

5.4.0 Macrophage proportion trends towards being reduced post chemotherapy treatment

Although only a single normal tissue was included in the data, making statistical comparisons unfeasible it was noted that there was a greater proportion of macrophages within the normal tissue compared to the HGS and adenocarcinoma metastasis (Figure 5.8A). There was a trend to a decrease in macrophage infiltration post-chemotherapy compared to pre-chemotherapy. Chemotherapy also trends towards an increase both in the monocytes and monocytic dendritic cells in the high grade serous ovarian cancer samples (Figure 5.8B). There was an apparent increase in neutrophils in the HGSOC compared to the metastasis and normal tissue (Figure 5.8A) and this population remained relatively stable following chemotherapy (Figure 5.8B).

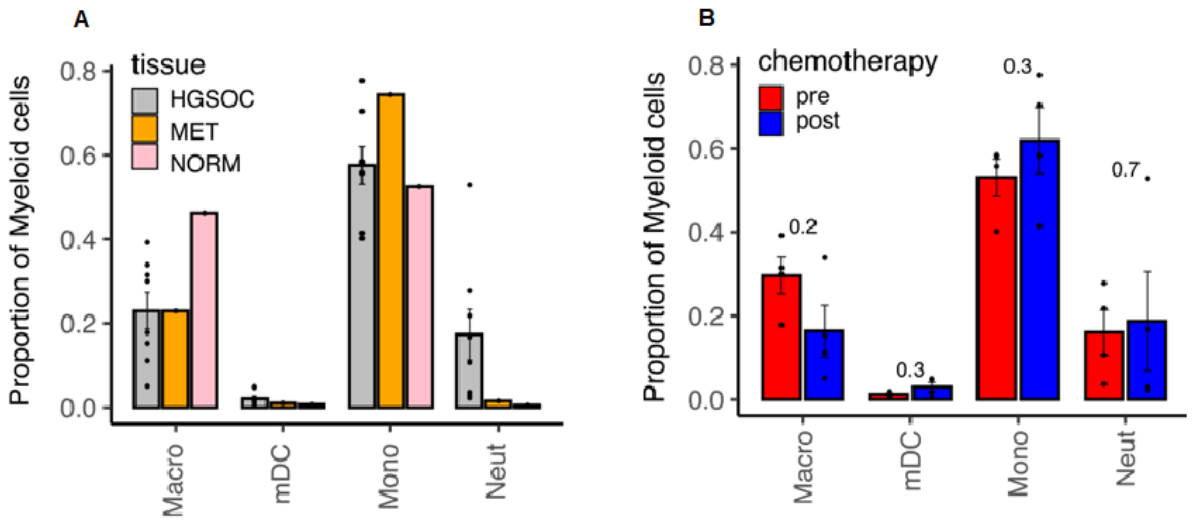

Figure 5. 8. The proportional infiltration of the different subsets of myeloid cells within the samples.
A. Comparison of cell type proportion in High Grade Serous Ovarian Cancer (HGSOC) vs Metastasis from GI tract (MET) vs Normal Omentum (NORM) tissue samples. B. Comparison of cell type

proportion pre vs post chemotherapy HGSOC samples. Points represent within-sample cluster proportion of total cells and p values determined by Mann-Whitney test. Bars represent mean ± SEM

5.4.1 Transcriptional changes post chemotherapy are apparent within myeloid cells

The expressed genes from the pre-and post-chemotherapy specimens were compared to demonstrate those that were differentially up- or downregulated following chemotherapy (Figure 5.7A). Transcriptional divergence upon chemotherapy treatment in terms of the number of DEGs identified was most apparent in Macrophage, Monocyte and Neutrophil cells whilst very few DEGs were identified in the mDC population. There were striking changes in expression of 4 of the genes in particular, the MHC class II beta chain HLA-DRB5 and APOE (apolipoprotein E) were greatly downregulated in macrophages and monocytes, whilst FOLR3 (folate receptor 3) and LAIR2 (leucocyte associated immunoglobulin-like receptor 2) were upregulated in neutrophils and monocytes respectively (Figure 5.9A, 5.9B). These data suggest substantial modification of transcriptional profiles in monocytes, macrophages and neutrophils following chemotherapy.

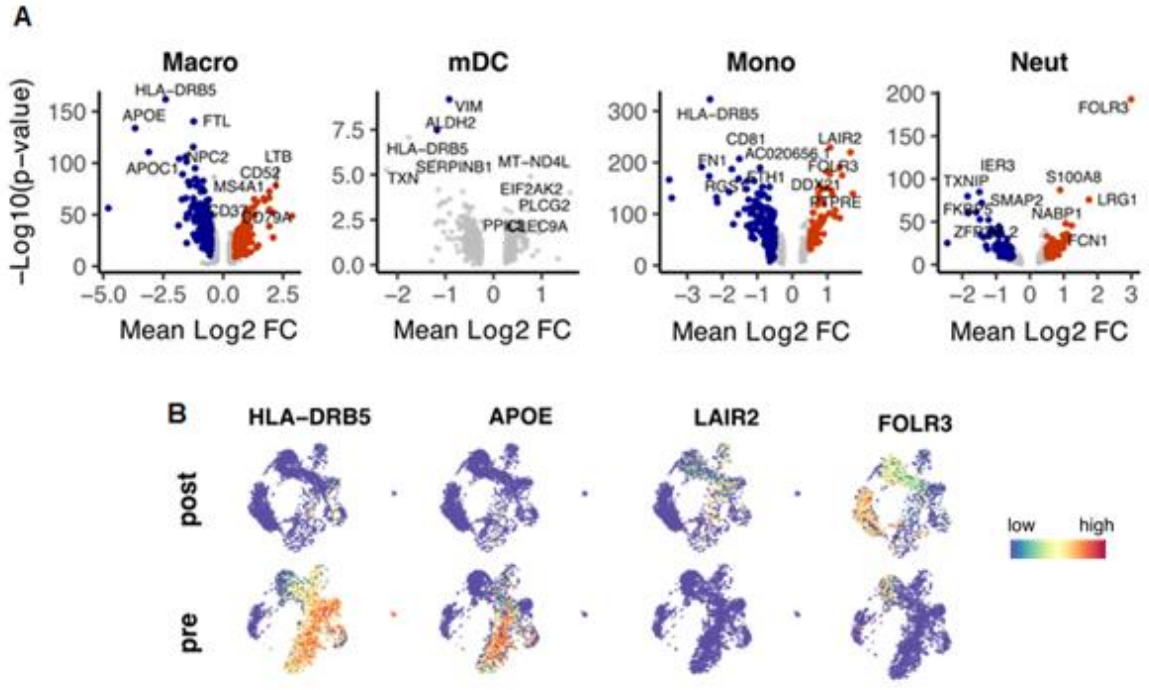

Figure 5. 9. The relative change in gene expression pre- and post-chemotherapy within the myeloid subsets.
A. Differentially expressed genes upregulated (red) and downregulated (blue) in post-chemotherapy compared to pre-chemotherapy samples within each cluster. B. UMAP embeddings overlaid with expression profile of selected differentially expressed genes from A.

5.4.2 The MDSC populations potentially increase post-chemotherapy

The MDSC were identified using an established MDSC signature set previously published (213). Scoring this signature highlighted probable MDSC or MDSC-like cells that were not evident within the adenocarcinoma metastasis and not widespread in the normal tissue but were strongly present in the high-grade serous cancer samples (Figure 5.10). Qualitatively, the MDSC signature score was increased and more widespread in the post-chemotherapy cohort compared to the pre-chemotherapy cohort.

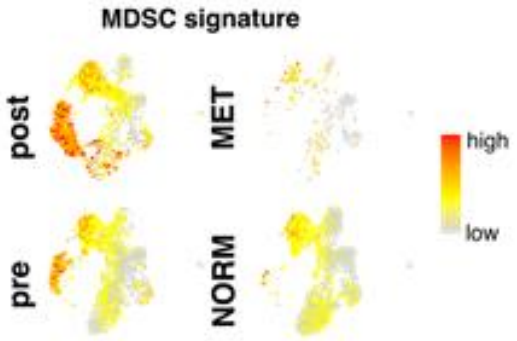

Figure 5. 10. MDSC gene expression signature score pre- and post-chemotherapy in high grade serous ovarian cancer, adenocarcinoma metastasis and normal tissue.
UMAP embeddings overlaid with Myeloid Derived Suppressor Cell (MDSC) signature score.

5.4.3 Finer grained analysis of Neutrophil contexture highlights patient-specific neutrophil populations

The neutrophil contexture was subsequently analysed in the context of pre- and post-chemotherapy and 3 major sub-populations were identified following unsupervised clustering (Figure 5.11A). Clusters were labelled by their most definitive marker gene: NEAT1 (nuclear paraspeckle assembly transcript 1), ARG1 (arginase 1) and CXCR4 (C-X-C chemokine motif receptor 4) dominant populations. Assessing cluster proportions by patient (Figure 5.11A, 5.11B), it was evident that the vast majority of NEAT1 neutrophils were derived from Patient 8, whilst ARG1 subsets were dominant in Patients 1-4 (3 HGSOC - 2 post-chemotherapy, and the metastasis) and CXCR4 subsets had a dominant cluster in Patients 5, 6, 9 and 10 (3 HGSOC – 2 pre and 1 post-chemotherapy, and the normal sample). Following chemotherapy, a greater proportion of NEAT1 neutrophils was observed compared to pre-chemotherapy samples, however this could be heavily skewed by the inclusion of patient 8. Proportion of N CXCR4 cells also appeared greatly reduced post chemotherapy. Within the metastasis there were no CXCR4 neutrophils, whilst in the normal tissue the majority were of CXCR4 subtype

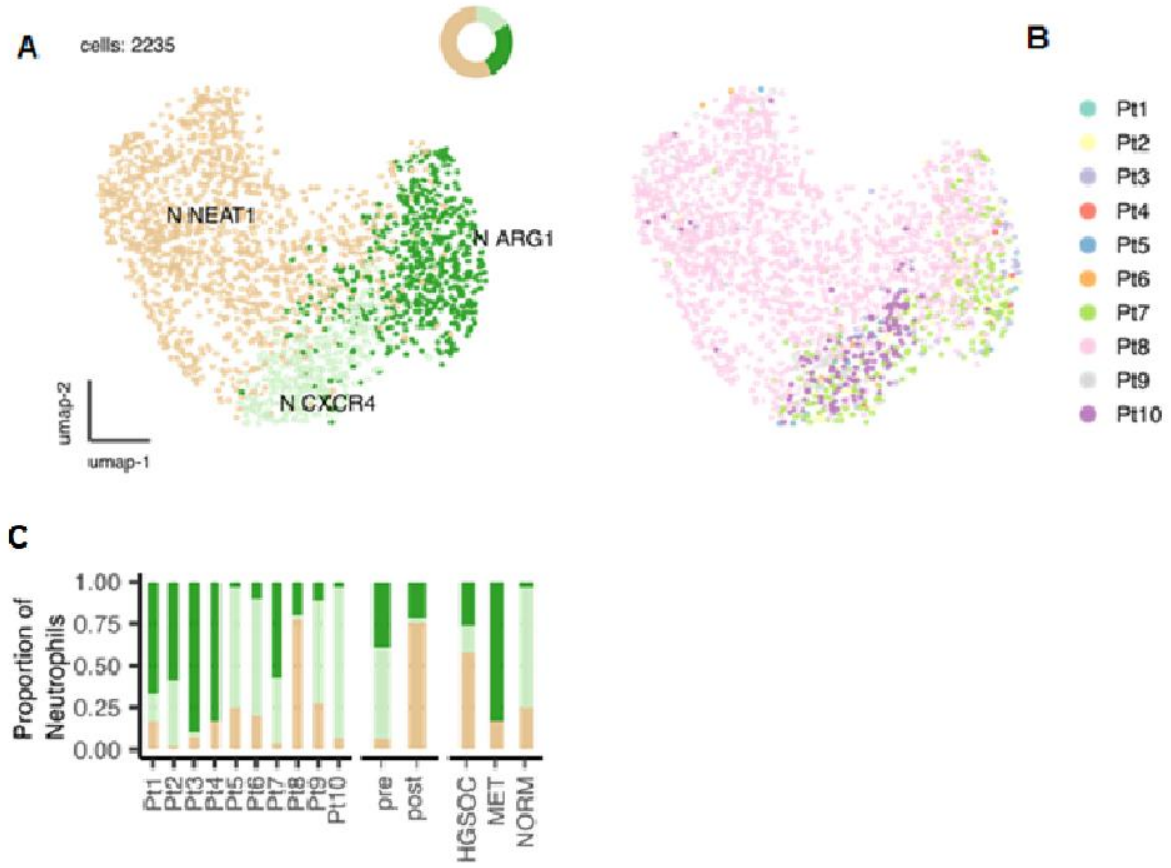

Figure 5. 11. The contexture of neutrophils in ovarian cancer.
A. UMAP embedding overlaid with cluster cell type annotations (left) and sample label (right). Donut chart proportion of total cells (inset) B. Breakdown of cluster proportions by sample, pre/post chemotherapy treatment and tissue type. C. Proportion of neutrophils represented by sample, the chemotherapy status and by the diagnosis. HGSOC: high grade serous ovarian cancer MET: metastasis NORM: normal

5.4.4 Expression profiles in ovarian cancer neutrophil sub-populations

The top marker genes overexpressed in each of the neutrophil subsets were identified (Figure 5.12A) to further characterise the cells within these clusters. High expression of NEAT1, MALAT1, CSF3R and PLEK are consistent with the NEAT1 neutrophil subset, whilst positivity for CXCR4, FTH1 and FOS were indicative of the CXCR4 neutrophil subset. The ARG1 population was characterised by high expression of arginase 1 and calcium binding proteins S100A12/A9/A6 and A6 (Figure 5.12A, 5.12B). Interestingly, the ARG1 subset are present in greater proportion in the metastasis and high-grade serous cancer (both neoplastic) specimens compared to the normal sample (Figure 5.12C). Arginase 1 is known to cause immunosuppression and has been associated with MDSC suppressor function. There is a trend to a greater proportion of NEAT1 subset post-chemotherapy compared to pre-chemotherapy and trend towards reduction in CXCR4 neutrophils post-chemotherapy (Figure 5.12C). Neutrophil maturity signature scores (123) suggest that the NEAT1 and CXCR4 subsets are comprised of more mature neutrophils, whilst the ARG1 subset tends to consist of more immature profile (Figure 5.12D).

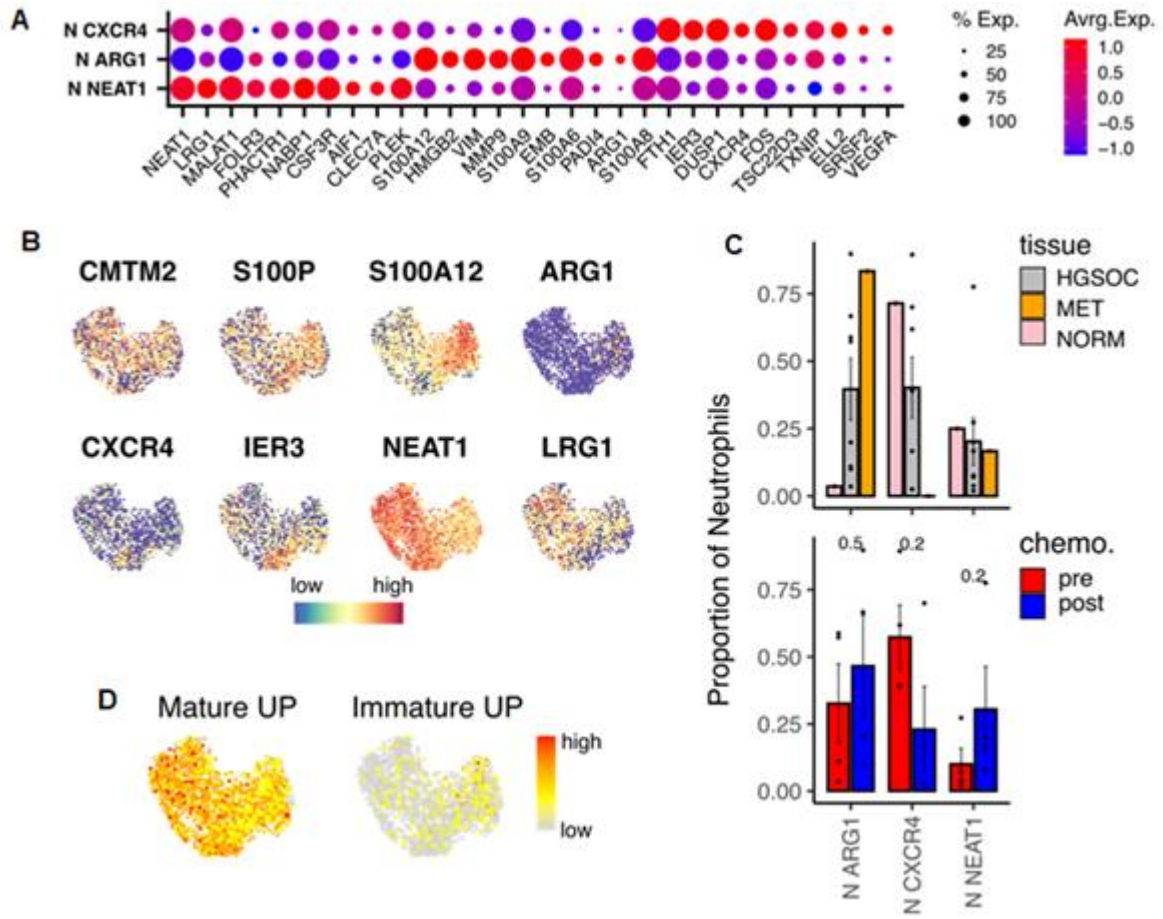

Figure 5. 12. The markers used for the identification of the neutrophil subsets and the presence of these subsets within the different cohorts.
A. Average expression profile dotplot of top cluster marker genes. Dot size indicates percentage of cells expressing the gene. B. UMAP embeddings overlaid with expression of selected Neutrophil cluster marker genes. C. Comparison of cell type proportion in High Grade Serous Ovarian Cancer (HGSOC) vs Metastasis from GI tract (MET) vs Normal Omentum (NORM) tissue samples and pre vs post chemotherapy HGSOC samples. Points represent within-sample cluster proportion of total cells and p values determined by Mann-Whitney test. D. UMAP embeddings overlaid with signature score from genes upregulated in mature/immature human neutrophils (from mature vs immature comparison).

5.5.5 Post vs pre-chemotherapy differential expression analysis reveals SMAP2 and FOLR3 expression to be modified in Ovarian cancer neutrophils

Post vs pre- chemotherapy treatment differential expression analysis was performed within the ARG1 and CXCR4 subsets (Figure 5.13A). Gene expression was most modulated by chemotherapy treatment within the N ARG1 population as evident by a large number of differentially expressed genes identified within this population. In particular the folate receptor FOLR3 was strikingly upregulated and SMAP2 (Stromal Membrane-Associated GTPase-Activating Protein 2) was downregulated in N ARG1 cells following chemotherapy (Figures 5.13A and 5.13B).

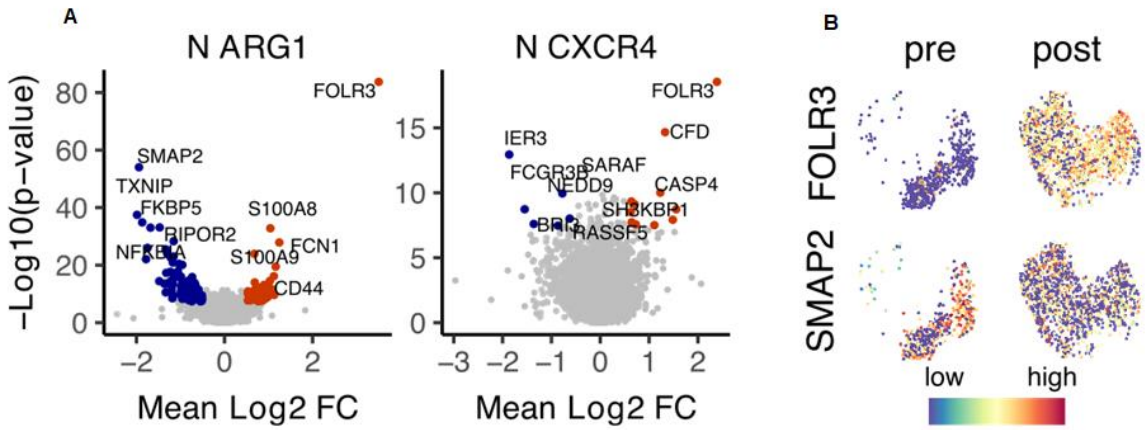

Figure 5. 13. The gene expression in the neutrophil subsets pre- and post-chemotherapy.
A. Differentially expressed genes upregulated (red) and downregulated (blue) in post-chemotherapy compared to pre-chemotherapy samples within N ARG1 and N CXCR4 Neutrophil clusters. B. UMAP embeddings overlaid with expression profile of selected differentially expressed genes from A.

5.5.6 Finer grained analysis of Monocyte and Macrophage composition identified 1 classical dendritic cell (cDC), 4 macrophage, 3 monocyte and 2 tumour associated macrophage (TAM) subsets

The monocyte and macrophage population was subset and unsupervised clustering was initially applied solely on these cells to identify 11 clusters based on their transcriptional profile (Figure 5.14A). Following this, marker genes for key clusters were identified (Figure 5.15) then each cluster was annotated using both the cell type marker gene and the marker gene expressed that is most uniquely distinguishable for that specific subset. The largest cluster identified was the SELENOP macrophages. The distribution of the cells within the patient samples (Figure 5.14B) was relatively consistent across all patients, although Pt5 was noted for an increased proportion of the Mac SELENOP subset (Figure 5.14B). The canonical expression of the genes used to identify the subsets (Figure 5.14C) demonstrates that a large proportion of the macrophages are M2 macrophages due to their CD163 positivity. The monocytes and macrophage clusters were also identified through their expression of top marker gene profiles (Figure 5.15).

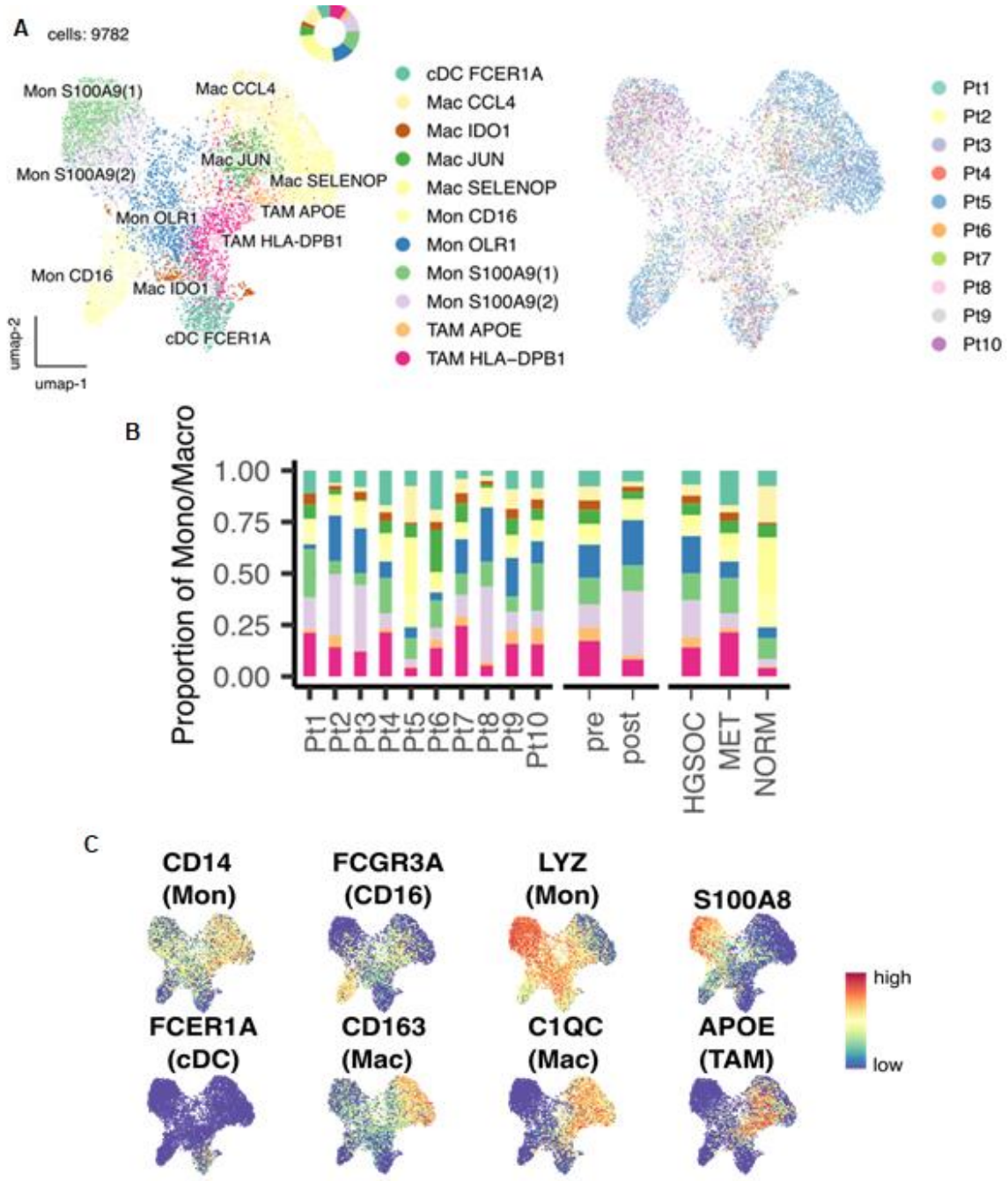

Figure 5. 14. Monocytes and macrophage contexture in HGSOC.
A. UMAP embedding overlaid with cluster cell type annotations (left) and sample label (right). Donut chart proportion of total cells (inset) B. Breakdown of cluster proportions by sample, pre/post chemotherapy treatment and tissue type. C. UMAP embeddings overlaid with expression of canonical monocyte and macrophage cell type marker genes.

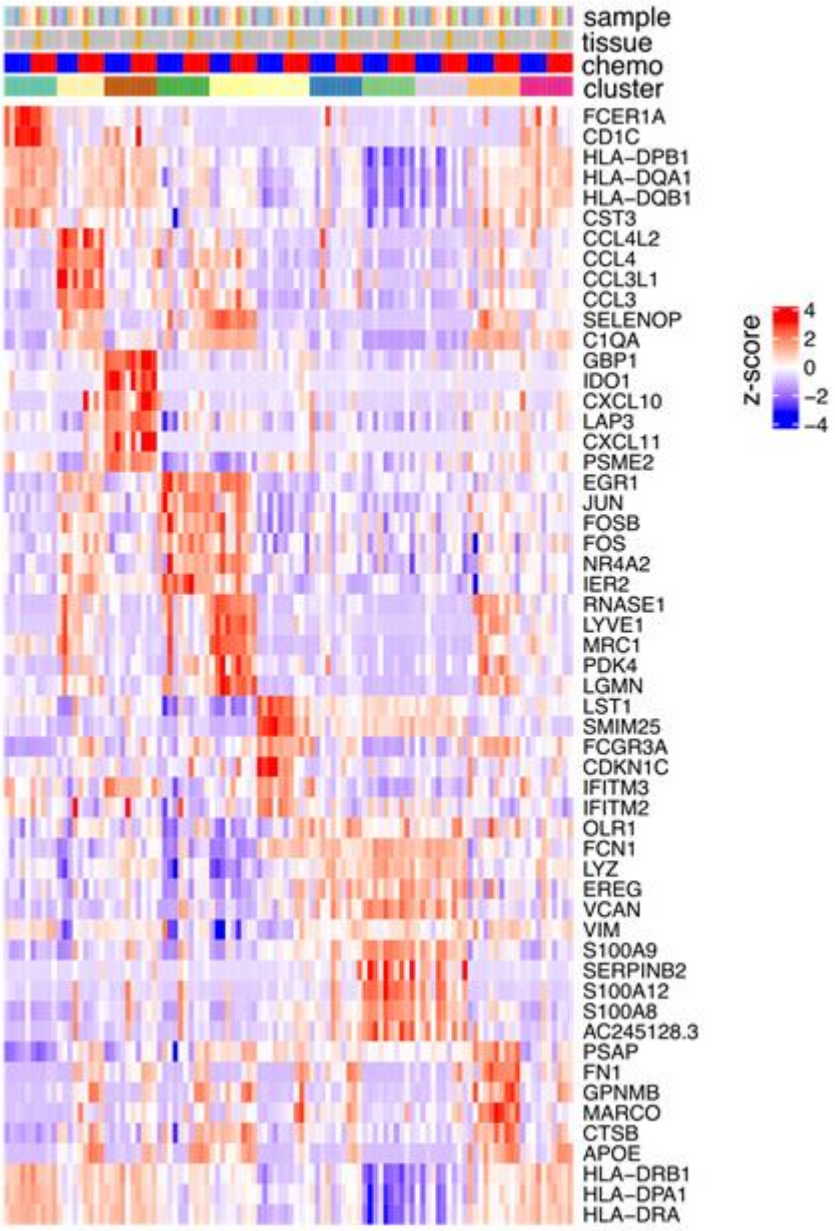

Figure 5. 15. Monocyte and macrophage populations marker gene expression profile.
Gene expression profile of the top cluster marker genes identified to be over expressed in each of the monocyte and macrophage clusters identified by unsupervised clustering. Expression is represented as the scaled average within sample-cluster raw RNA molecule count.

5.5.7 Chemotherapy alters the monocyte and macrophage milieu in HGS cancer

The monocyte and macrophage contexture were next compared, stratifying by tissue type and chemotherapy treatment (Figure 5.16). Observations made comparing the malignancy (n=9) to the normal (n=1) samples are made with caution due to the limited sample size. However, malignancy increased the presence of tumour-associated macrophages (TAM) APOE and TAM HLA-DPB1, whilst decreasing the CCL4 positive macrophages (Figure 5.16A). There was a greater infiltration of S100A9

monocytes in malignancy compared to normal tissue. Interestingly comparatively fewer cells were retrieved from the metastatic adenocarcinoma sample. Following the administration of chemotherapy, the monocyte and macrophage contexture was altered, showing more S100A9 (2) monocytes and CD16 positive monocytes post chemotherapy whilst pre-chemotherapy samples trended towards more APOE/HLA-DPB1 TAMS. There was also a greater proportion of CCL4 positive macrophages in the pre-chemotherapy samples. M2 macrophages are thought to have an immunosuppressive phenotype. When scoring for expression of published gene signatures for MDSC (122), TAM, M1 and M2 (124), it is evident that there is a high proportion of MDSC within the samples (Figure 5.16C), which mainly aligns with the S100A9 monocyte populations and is further demonstrated by their S100A8 positivity. Interestingly, the presence of this population does not seem modified by chemotherapy treatment; there is a similar density and proportion identified pre-and post-chemotherapy (Figure 5.16A, 5.16B). There was a general reduction in some of the macrophage populations with chemotherapy, particularly the TAMs (TAM APOE and HLA-DPB1), and M2 macrophages (Mac CCL4), whilst the CD16 monocytes were increased post-chemotherapy. This increase, however, was still below that of the normal sample.

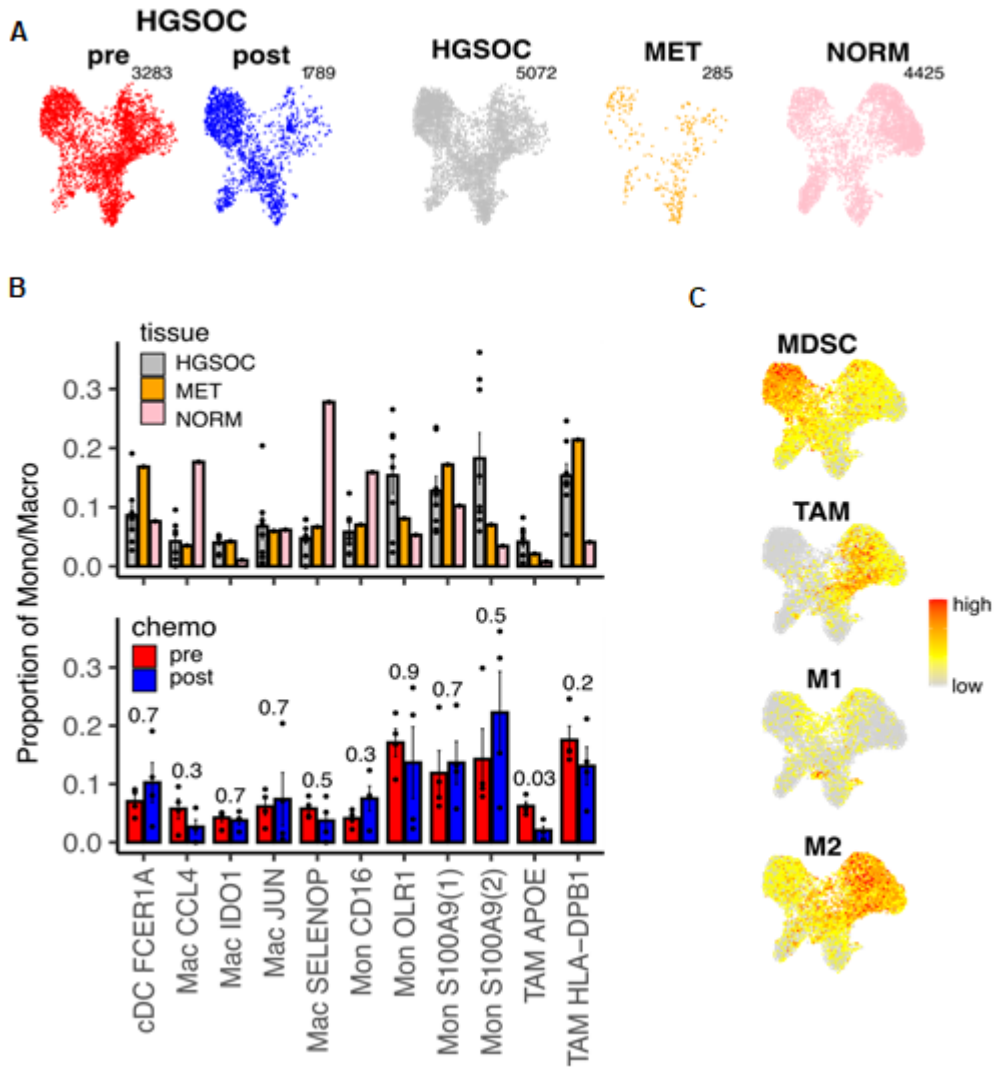

Figure 5. 16. The expression of genes denoting monocyte and macrophage subtypes in high grade serous cancer pre and post chemotherapy, as well as in metastatic adenocarcinoma and normal tissue.
A. UMAP embeddings split by chemotherapy treatment and tissue type. Total cell number indicated above plot. B. Comparison of cell type proportion in High Grade Serous Ovarian Cancer (HGSOC) vs Metastasis from GI tract (MET) vs Normal Omentum (NORM) tissue samples and pre vs post chemotherapy HGSOC samples. Points represent within-sample cluster proportion of total cells and p values determined by Mann-Whitney test. C. UMAP embeddings overlaid with published signatures of Myeloid Derived Suppressor Cells (MDSC), Tumour Associated Macrophages (TAM) and M1/M2 type Macrophages.

Upon differential expression analysis on the different monocyte and macrophage subtypes comparing chemotherapy treatment, it is evident that a high degree of transcriptional divergence is seen within the Mon OLR1 subgroup of monocytes (Figure 5.17A). The OLR1 gene encodes the protein better known as LOX-1, which is known to play a role in all aspects of neoplastic development from progression and invasion to metastasis and neo-angiogenesis. Highlighted genes of interest that were significantly upregulated in response to chemotherapy include IFITM2, MDSC-associated gene S100A9, the peptidase from the C1 family CTSS, the folate receptor FOLR3, versican (VCAN) and CD55. IFITM2 is associated with the interferon pathway and promotes an anti-tumour environment, whilst VCAN is a proteoglycan associated with the ECM and CD55 has a role in the complement cascade. Those that were downregulated post-chemotherapy are the cell growth and motility regulating tetraspanin CD81 and ferroptosis suppressor gene FTH1 (Figure 5.17B).

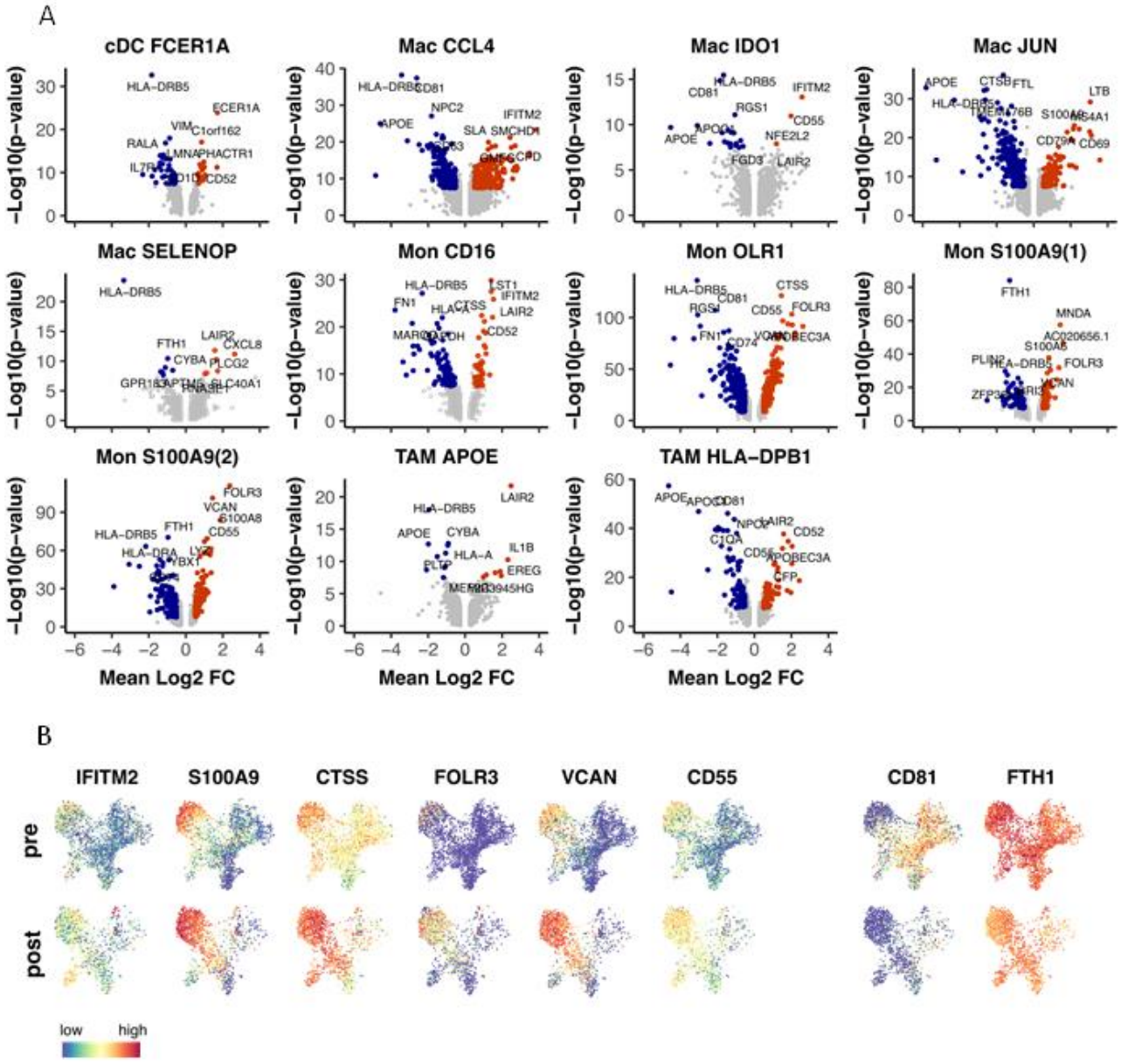

Figure 5. 17. Chemotherapy Modulation of transcription within Monocyte and Macrophage sub-populations.

A. Differentially expressed genes upregulated (red) and downregulated (blue) in post-chemotherapy compared to pre-chemotherapy samples within Monocyte and Macrophage clusters. B. UMAP embeddings overlaid with expression profile of selected differentially expressed genes from A.

5.6.0 Discussion

This chapter has sought to further characterise populations of cells, more specifically myeloid cells, present in the ovarian cancer microenvironment, making comparisons of the cellular compositions from pre- and post-chemotherapy treatment. The contexture of cells present in HGSOC was further compared to a gastric adenocarcinoma metastasis and normal tissue. We used scRNA-seq to cluster populations by their transcriptional profile and identified genes overexpressed in each cluster to characterise in detail, the immune cells present. This was aiming to overcome issues faced in previous chapters regarding the various expression of cell surface markers and the reliability of using these to phenotype complex cell subsets such as MDSC.

The results have revealed the contexture of immune cell subsets present, including likely MDSC populations that have been identified through their expression of MDSC transcriptional signatures.

5.6.1 Principal findings

5.6.2 Identification of the immune cell landscape

The major immune cell groups identified were the T/NK, myeloid, B cells, plasmacytoid dendritic cells and plasmablasts. The largest group were the T/NK cells followed by the myeloid subset. Chemotherapy appeared to have differing effects on these subsets, with T/NK cells being proportionately increased, whilst myeloid cells were proportionally decreased. The finding of increased T/NK cells following chemotherapy is consistent with a previous study in matched samples thought to be due to the effect of chemotherapy unmasking or inducing neoantigens in the patient (214). The response of immune cells following chemotherapy has been investigated due to its importance for introducing immunotherapy post chemotherapy to improve prognosis. Chemotherapy is associated with myelosuppression and therefore an immediate short-term neutropenia, however has lasting effects on many immune subtypes. In general, CD8 T cells fall during the first cycle of therapy, followed by a rapid expansion, particularly of T effector cells, but then return to baseline by 3 months post-chemotherapy (215). In addition, the CD8+ T memory cells were found to be particularly resistant to treatment, thus contributing to re-forming the T cell memory population following chemotherapy exposure. The response of CD4 T cells to chemotherapy was less consistent, however was largely found to become more depleted following chemotherapy, postulated to be due to thymic destruction following treatment (215). NK cells have an unpredictable response to chemotherapy, with conflicting results evident depending on chemotherapy used and the underlying diagnosis. Overall, the population is usually restored on completion of treatment. Chemotherapy seems to significantly reduce T regulatory cell numbers, causing a reduction in an immunosuppressive TME (215). It has been found that monocyte counts increase during chemotherapy, however long-term data is not available. This may be contrary to my results because the

proportions of cells were measured and if the T_NK cells proportionately increased to a greater degree, it can appear as a relative decrease in myeloid cells rather than a true depletion. Short-term effects of chemotherapy on MDSC have been noted to reduce their numbers within 14 days of treatment completion. In addition, this was using circulating blood rather than tumour or metastasis tissue samples so may be a very different reflection on what is happing directly in the TME (215).

The number of tumour-infiltrating lymphocytes (TILs) present following chemotherapy in breast cancer is associated with prognosis; a greater number is associated with a larger and more aggressive tumour and with greater numbers of nodal metastases (216). The research on this is not unanimous, as it has been shown within breast cancer that an increase in stromal TILs on residual cancer following neoadjuvant therapy is associated with improved recurrence-free survival (217). This demonstrates conflicting opinions on the prognostic significance of TILs with chemotherapy even within the same cancer type, therefore more research is required to improve our knowledge and understanding. Whether the chemotherapy alters their function rather than simply their number within a tumour would be interesting to determine because this then has the capacity to change a TME into pro- or anti-tumoural, regardless of how many are physically present.

5.6.3 Myeloid cells

Within the myeloid population, clear subgroups of monocytes, macrophages and neutrophils were identified through their gene expression profiles. Interestingly, a large group of MDSC were identified within the neutrophil population using an established gene expression signature for MDSC (122). This suggests that MDSC are present within ovarian cancer, identified through their transcriptional gene expression profiles and so was not reliant on their cell surface marker expression. This confirms the findings of my flow cytometry work that MDSC are present in the metastatic tumours of ovarian cancer. When pre- and post-chemotherapy samples were compared, the proportions of MDSC remained constant, whilst in general the proportions of other myeloid cells tended to reduce following chemotherapy administration. This perhaps could be due to the TME created around MDSC; secreting chemokines and factors to prevent further immune cell infiltration to ultimately cause immunosuppression and a reduction in myeloid cell presence, whilst remaining largely protected from the cytotoxic effects of chemotherapy. Also, it may be due to increased recruitment of MDSC into the tumour following chemotherapy, as has been found following administration of 5-fluorouracil in hepatocellular cancer mouse models (218). Additionally, the effect could be greater in the omentum than in the site of the primary tumour because the TME is very different in sites of metastases, with fewer tumour cells present at metastatic sites and cancer-associated fibroblasts and stromal cells playing key roles in maintaining the metastatic niche (195). There is potentially less cell death and neo-antigens present in metastases and so may not attract such an infiltration of inflammatory cells. In the third

chapter of this thesis, it was found that exposure to chemotherapy reduced the MDSC in the primary tumour but not in the peripheral blood or omentum, which corroborates with this finding.

Chemotherapy was observed to have the greatest effect on macrophages and seemed to have a negligible impact on the neutrophil population, appearing to slightly increase it as a proportion of the total myeloid population. Although proportionally there was not a great change in the populations, there was a large chemotherapy effect on the proportional differential expression analysis of genes within the neutrophil, monocyte and macrophage population, ultimately affecting their transcriptional profile. This may suggest that even if they are present in terms of number, their functionality within the immune response could be modified by chemotherapy, which may not be appreciated if assessed solely upon absolute numbers of cells present.

5.6.4 Chemotherapy-induced modulation of gene expression in Myeloid cells

Chemotherapy has been shown in breast cancer patients to induce an inflammatory response, with infiltration of CD4 and CD8 T cells (219). The greater the infiltration of inflammatory cells, the better the response to immunotherapy, thus presenting a 'window of opportunity' to administer immunotherapy. The residual tumours became immune-cell deplete, with low numbers of immunostimulatory cells and higher proportions of immunoregulatory cells, such as M2 macrophages, therefore immunotherapy is better to be timed immediately after the initial chemotherapy (219). Within ovarian cancer this is pertinent because often women are exposed to multiple rounds of chemotherapy as their disease becomes increasingly resistant, so finding an effective immunotherapy to administer following chemotherapy may be key to the management of women with ovarian cancer.

From differential expression analysis on post vs pre chemotherapy data, 4 genes of interest were highlighted in particular due to their striking significant difference: FOLR3 (folate receptor 3), LAIR2 (Leukocyte Associated Immunoglobulin Like Receptor 2), HLA-DRB5 and APOE (apolipoprotein E). The former two were upregulated in monocytes and neutrophils, whilst the latter two were downregulated in macrophages following chemotherapy. The observed increase in FOLR3 and LAIR2 and decrease in HLA-DRB5 could potentially be linked to alteration in cell metabolism, T cell exhaustion and impaired antigen presentation which could encourage dysregulated cell growth without in the absence of a healthy immune surveillance.

5.6.4.1 FOLR3 – Folate Receptor 3

FOLR3 forms part of the folate receptor and consists of 4 members (FOLR1-4). It is known that FOLR2 is over-expressed in M2-TAMS and tumour cells and has been demonstrated to be a potential target in chemotherapeutics (220). Within ovarian cancer, FOLR1 has been shown to have a better sensitivity, specificity and positive predictive value than the commonly used tumour marker ca-125 (221–223) so is of potentially great significance within ovarian cancer. Following chemotherapy there was a large

increase in expression of FOLR3 on the tumour-associated monocytes and neutrophils. Increased expression of FOLR3 has been found to be associated with chemotherapy-insensitivity in laryngeal squamous cell carcinoma (224). This may be a factor contributing to the chemotherapy resistance experienced by most women with ovarian cancer. There are many mechanisms for chemotherapy resistance, however, so a multi-faceted approach is ultimately required to overcome this problem. Whether inhibition of FOLR3 would help prevent chemotherapy resistance is unknown but could present as an avenue for further research.

5.6.4.2 LAIR-2 - Leukocyte Associated Immunoglobulin Like Receptor 2

Expression of LAIR-2 was observed to be increased primarily on monocytes and has a role in collagen synthesis in the extracellular matrix (ECM). The ECM is a complex non-cellular structure, most abundantly supported by proteins such as collagen. The ECM provides more than just architectural support, it regulates cell growth and survival, migration, angiogenesis and immune function. Ovarian cancer is associated with a dense ECM and it has been found that the proportion of collagen is inversely proportional to survival (225–227). The abnormal collagen within the ECM impairs an effective immune response and also provides a physical barrier to immune cells and therapy to prevent tumour destruction (228). LAIR-1 binds to collagen which inhibits immune cell function, including B cells, NK cells, dendritic cells, monocytes and T cells, causing cell exhaustion (229). Activation of LAIR-1 therefore causes an immunosuppressive microenvironment. The function of the closely related gene LAIR-2 is a little less clear and remains contested. It has been proposed that LAIR-2 is a naturally occurring homolog of LAIR-1, but has an antagonistic role in order to promote immune function. Increasing LAIR-2 presence has been identified as a possibility for therapy (230). However, despite these results, LAIR-2 has also been highlighted as a potential marker for T cell exhaustion in pancreatic ductal cancer (231). It was found to be present on regulatory T cells and CD8+ cells, which corroborates an exhaustive T cell microenvironment. Increased LAIR-2 expression was associated with a worse prognosis in cholangiocarcinoma and poorly differentiated thyroid cancer (232). It is difficult to comment on how these results affect prognosis in our samples as long-term patient data is not available, however in general ovarian cancer is associated with a poor prognosis so the likelihood is that there will be relapse and unfortunately demise secondary to the cancer. As such, the upregulation of FOL3 is unlikely to be a survival advantage so one could postulate that in this circumstance, FOL3 upregulation may be associated with T cell exhaustion and immunosuppression. Further work would need to be done investigating markers of T cell exhaustion in the presence of upregulated LAIR2 within ovarian cancer samples to identify if hypothesis holds true.

5.6.4.3 HLA-DR5 and APOE - Apolipoprotein E

There was a considerable downregulation of HLA-DRB5 on monocytes, macrophages and mDC's post chemotherapy whilst downregulation of APOE was observed on macrophages in particular. HLA-DRB5 is a gene encoding the major histocompatibility complex class 2 (MHC2) and as such is involved in antigen presentation. With this gene being heavily targeted and downregulated it may suggest that chemotherapy could possibly result in impairment of antigen presentation of cancer antigens to the immune system, therefore blunting the immune response. Bulk tissue profiling in colorectal cancer showed HLA-DRB5 downregulation to be associated with greater propensity for metastasis (233), with similar effects also identified for other members of the MHC class 2 group and a survival advantage to those who demonstrate its upregulation (234,235).

Contradictorily, APOE is a lipoprotein implicated in the metastasis, growth and angiogenesis of cancers and its upregulation has been associated with poor outcome in cancers such as colorectal (where tumour tissue was isolated) and pancreatic cancer (PBMC and plasma cells used) (236,237). Its inhibition has been shown to improve sensitivity of lung cancer cell lines to cisplatin in lung cancer (238), therefore its downregulation post chemotherapy could potentially be providing a beneficial effect.

5.6.5 Chemotherapy-induced modulation of gene expression in neutrophils

Unsupervised clustering identified three main sub-populations of neutrophil cells: N NEAT1 (nuclear enriched abundant transcript 1), N ARG1 (arginase 1) and N CXCR4 (C-X-C receptor 4). The population of NEAT1 neutrophils appeared to be primarily patient-specific as it largely came from patient 8. There is a suggestion in the literature that NEAT1 is associated with chemoresistance and oncogenesis in ovarian cancer through its action upon several microRNA's (239) and through functional cloning technique. NEAT1 has been associated with both tumour-suppressor and tumour-promoting properties. It has been implicated in inhibiting apoptosis thus favouring oncogenesis, as well as stabilising miRNA concentrations within the tumour cells allowing them to withstand multiple mutations and enabling resistance to apoptotic chemotherapy. Conversely it has a role as a downstream regulator of p53 so may also be involved in tumour regulation, however it is postulated that the overall effects of NEAT1 are to favour tumour progression (239). This patient had been exposed to chemotherapy and as such it would be interesting to compare prognosis to the rest of the cohort as this neutrophil contexture was markedly different to all the other samples.

When investigating neutrophil maturity signatures, it was found that the N NEAT1 and N CXCR4 neutrophil populations were more mature, whilst the ARG1-producing neutrophils showed markers of immaturity. When MDSC's were initially discovered, it was thought that MDSC's were 'immature neutrophils' as they displayed markers of immaturity, however it was later demonstrated that they were functionally mature (90). MDSC's are commonly cited to utilise arginase 1 (69) to facilitate their immunosuppression, which would fit with the findings of this research. Immature neutrophils are seen more commonly within a cancer setting and are considered to have an altered functional capacity

thought to influence tumour progression (240). This is consistent with the observation that the N ARG1 neutrophils are present at greater proportions in the ovarian cancer and adenocarcinoma metastasis compared to the normal tissue.

There was a reduction in CXCR4 neutrophils following chemotherapy which may be a positive marker as CXCR4 neutrophils have been implicated in tumour progression and metastasis through their control of neutrophil chemotaxis. It has been hypothesised that CXCR4 signalling is involved in neutrophil motility and immune-tumour cell interactions promoting tumour development in the early phase of metastasis (241). CXCR4 expression has been found to be associated with a worse tumour prognosis in triple negative breast cancer, however has been associated with improved recurrence-free survival and fewer distant recurrences when given adjuvant chemotherapy. There have been few studies focusing on the impact of CXCR4 in the context of chemotherapy so this warrants further exploration (242).

Following chemotherapy there appears to be an upregulation of FOLR3, similar to that described for the macrophages above. FOLR3 originates from secretory granules of neutrophil granulocytes and has anti-neoplastic effects through deprivation of natural folates (243). Whether this proves to anti-neoplastic in ovarian cancer is yet to be determined.

5.6.6 Chemotherapy-induced modulation of the monocyte and macrophage contexture

In total, unsupervised clustering resulted in 1 classical dendritic cell, 4 macrophage, 3 monocyte and 2 tumour-associated macrophage sub-populations. Following chemotherapy, the proportion of TAM populations was reduced and, as expected, they were barely evident at all in the normal tissue. Within ovarian cancer, neo-adjuvant chemotherapy has been found to alter the balance of pro- and anti-tumoural responses in favour of anti-tumour immunity, with increased infiltration of CD3 and CD8 TILs and CD68 macrophages following treatment. This has been shown to potentiate their cytotoxicity but unfortunately did not have impact on prognosis (244). It was unclear if the tissue used for this study was primary tumour or metastasis but if it was primary tumour, this may be why my results have shown a reduction in myeloid infiltration as the tumour composition and TME is different in metastatic sites versus primary site.

5.6.6.1 CD16+ monocytes

Post chemotherapy, there was a trend towards a proportional increase in CD16 positive monocytes. There are 3 major subsets of monocytes described in the literature; the classical ($CD14^{high}$ $CD16^{neg}$), intermediate ($CD14^{high}$ $CD16^{low}$) and non-classical ($CD14^{low}$ $CD16^{high}$). The most common subtype are the classical monocytes, accounting for 85% of the total monocyte population in the peripheral blood of healthy donors, followed by the non-classical, accounting for 10% and then the intermediate make

up 5% (245). An increase in CD16^{high} monocytes has been linked to increased tumour size (246), metastasis (247) and poor response to immunotherapy (248). The intermediate monocytes have been found to be expanded in ovarian cancer patients and contributed to immunosuppression in the tumour microenvironment and ovarian cancer progression. The CD16 positive cells were found to be in a similar proportion of the total monocyte population in the chemotherapy-naïve cohort to the healthy donors, however their absolute number was greater within the cancer patients (245). This would suggest that the presence of increased CD16+ monocytes may be associated with a poorer outcome.

5.6.6.2 IDO+ macrophages

Gene signature analysis indicated that a large proportion of the macrophages were of M2 lineage, highlighting their potential role in forming an immunosuppressive tumour microenvironment. Differentiation of monocytes to M2 macrophages is driven by the COX-regulated mediators IL-6 and PGE2. This process causes chemoresistance and has been associated with the administration of cisplatin and carboplatin in ovarian cancers. The addition of COX-inhibitors has thus been suggested as a mechanism of overcoming resistance (249).

The IDO+ macrophages remained largely unchanged pre- and post-chemotherapy and were only present in small proportions in the malignant specimens, with an even smaller proportion in the normal tissue. They have an M1 phenotype, so are associated with immunogenic response, however this has been contested. The presence of tumoural IDO has been associated with improved prognosis within many solid tumours as it is associated with CD8+ immune cell infiltration, however it has also been linked with immunosuppressive cells such as MDSCs, Tregs and causing T cell exhaustion (250). Within the tumour microenvironment it has been found that IDO-producing monocytes and macrophages are activated through interaction with T cells to create an environment favourable for tumour progression (251). This would suggest that the macrophages within our samples are largely immunosuppressive due to the majority being M2 lineage but also with the potential for T cell exhaustion caused by the IDO-expressing macrophages.

5.6.6.3 S100A8/9

Cells positive for the classical MDSC signature corresponded to the population positive for S100A8/9. This has been cited widely in the literature as a mechanism for accumulation of MDSC (252–254). Similarly to the results found within the neutrophil MDSC population, the Mon S100A9 populations did not change greatly following chemotherapy. This is interesting because it is one of the few populations of monocytes and macrophage that did not trend towards a decrease following chemotherapy administration. As mentioned previously, the myeloid cells were particularly sensitive to the effects of chemotherapy, however, these cells may have a degree of resilience to its effect.

In non-small cell lung cancer, chemotherapy was found to reduce CD14+/CD15- m-MDSC but had no effect on CD14+/CD15+ m-MDSC or PNM-MDSC. Functionally however, they were altered by the chemotherapy as the production of immunosuppressive iNOS was increased within the m-MDSC sub-populations. Prognosis was found to be better in those who had lower percentages of m-MDSC (255). In addition, chemotherapy has been found to expand myeloid suppressor cells, which increased the risk of progression and reduced long-term tumour control (256).

It has been proposed that MDSC are increased post-chemotherapy in order to regulate the immune response to a chemical insult, to prevent a catastrophic immune response, as their numbers were shown to be increased post-chemotherapy in the absence of primary neoplasm (257). This could be a potential explanation for the findings of this study.

5.6.6.4 OLR+ (oxidised low-density lipoprotein receptor) macrophages

The MAC OLR1 macrophage population showed a high degree of transcriptional divergence compared to other monocyte and macrophage populations upon chemotherapy treatment. As mentioned previously, OLR1 is an important gene as it is involved with the production of the protein LOX-1. OLR-1 has been found in cancer to promote cell proliferation and angiogenesis, whilst LOX-1 has been identified in many different cancers including colorectal (258), pancreatic (259), breast (260), lung (261) and bone (262). Its function is in fat metabolism and has been found to increase production of free radicals, known to be associated with carcinogenesis. It is hoped that it may present a marker of tumour progression to identify early disease resurgence (263).

5.7.0 Notable differentially expressed genes (DEGs) post chemotherapy

In total, 6 DEGs were highlighted to be greatly upregulated post chemotherapy. These were: IFITM2, S100A9, CTSS, FOLR3, VCAN and CD55. In addition, there were 2 DEGs that were downregulated in response to chemotherapy; CD81 and FTH1. Given what is currently known about the functionality of these genes and their potential roles in cancer, the overall effect may enable an environment favouring tumour progression, metastasis and chemotherapy resistance.

5.7.1 IFITM2 (interferon-induced transmembrane protein 2)

IFITM2 was shown to be upregulated largely in the region represented by the monocytic subsets (CD16, S100A9 and S100A8) and with this, chemotherapy increased the expression in CD16 monocytes in particular compared to the pre-chemotherapy samples. The CD16 monocytes are also known as non-classical monocytes and are pro-inflammatory, secreting inflammatory cytokines in response to infective stimuli (264). It may be possible that these have a slightly greater presence following chemotherapy due the cell damage and subsequent release of factors and cytokines, that occurs from the cytotoxic effect of chemotherapy. In an infective environment of chronic hepatitis B, IFITM2 was

found to be upregulated and associated with reduced interferon-alpha expression. IFITM2 inhibited dendritic production of interferon-alpha and these patients had a sub-optimal response to interferon-alpha treatment (265). Within an oncological environment, interferon-alpha is associated with many functions including inhibiting proliferation of tumour cells through downregulation of oncogenes and upregulation of tumour suppressor genes and promotes an anti-tumour response from the host immune system (266). Although I was unable to find any direct literature on the effect of IFITM2 on the cancer immune microenvironment, it forms part of the interferon signalling pathway and so it may suggest that upregulation of IFITM2 may regulate interferon-alpha which may support an anti-tumour microenvironment.

5.7.2 S100A9

S100A9 was identified as being upregulated largely amongst the monocytic S100A9 (1) subset pre-chemotherapy, however, post chemotherapy it was shown to be upregulated in the monocyte S100A9 (2) and OLR1 population. In cervical cancer, upregulation of this gene in particular has been found to reduce the apoptosis of cervical cancer cells to cisplatin therapy (267). On immune cells, it has been found that S100A9 inhibits the differentiation of macrophages and increases the accumulation of MDSC (252) thus promoting an immunosuppressant microenvironment. The analysis on MDSC's within my samples also demonstrated an accumulation of MDSC in the patients exposed to chemotherapy so this corroborates this finding. The upregulation and more widespread expression of S100A9 is therefore likely to be promoting a pro-tumoral niche.

5.7.3 CTSS (cysteine cathepsin protease S)

CTSS was found to be upregulated in a similar pattern to that of S100A9, with the S100A9 monocytes and OLR monocytes demonstrating high expression, largely following chemotherapy administration. Prior to chemotherapy, largely the S100A9 (1) subset are showing increased expression, much like the pattern of expression in S100A9 above. The cysteine cathepsin proteases have been found to be dysregulated within the neoplastic setting by favouring tumour progression, invasion and metastasis. The upregulation of CTSS has been associated with poor prognosis and tumour progression and may present as a biomarker for prediction of response to chemotherapy (268,269). These findings may suggest that the environment post-chemotherapy is pro-tumoural and may be supportive of micrometastases and therefore relapse following therapy.

5.7.4 VCAN (versican)

Versican was upregulated post-chemotherapy within the monocyte subgroups, namely S100A9 (1) and (2) and OLR1, whilst prior to chemotherapy it was only modestly expressed. It has been implicated in carcinogenesis and tumour progression of pancreatic cancer. Its inhibition was shown to improve the

chemosensitivity to gemcitabine (270). This implies it may facilitate chemoresistance and tumour growth, much like with CTSS and S100A9.

5.7.5 CD55

This was increased post-chemotherapy in the monocyte subtypes S100A9 and OLR1 but also CD16. Its upregulation was not as striking as VCAN, CTSS and S100A9 but there is still observable upregulation post-chemotherapy. CD55 is a glycoprotein involved in the regulation of the complement cascade. It has been shown to be associated with a worse prognosis in breast cancer, with chemoresistance occurring through inhibition of B cell induction (271) and through promoting self-renewal in endometrioid cancers (272). This cluster of genes with similar functions all being upregulated post-chemotherapy (S100A9, CTSS, VCAN and CD55) to the same cell types demonstrates that chemotherapy is having a significant effect on the monocyte populations and that this is likely to be a pro-tumoural environmental effect. To treat with immunotherapy immediately post chemotherapy to eliminate these populations may help to reduce the likelihood of relapse.

5.7.6 CD81

CD81 was highly expressed on the macrophage subtypes (CCL4, JUN, SELENOP, TAM, IDO1) pre-chemotherapy but this expression was almost entirely lost post chemotherapy. CD81 molecule is a cell surface protein and member of the tetraspanin family, which have a role in cell development, activation, growth and motility. Within oncology, CD81 has been shown to regulate tumour growth, migration and invasion and facilitating metastasis (273). Inhibition of CD81 in acute lymphoblastic leukaemia promotes chemosensitivity (274) and it also has a role in modulation of Tregs and MDSC leading to reduced tumour growth and metastasis due to an impaired suppressive function of MDSC and Tregs (275). The downregulation noted within my specimens may therefore produce a favourable effect of promoting response to chemotherapy.

5.7.8 FTH1 (ferritin heavy chain 1)

FTH1 demonstrated a global upregulation in the pre-chemotherapy samples, spanning across the monocyte, macrophage and dendritic cell populations. Following chemotherapy administration, the expression was globally reduced but still was overexpressed, however expression was disproportionately lost over the macrophage populations. FTH1 functions as an iron-storage protein and is a negative regulator of ferroptosis (276). Ferroptosis is an iron-dependent mechanism of programmed cell death. It has been found to be overexpressed in acute myeloid leukaemia and head and neck cancer and contributed to treatment resistance (277,278). As a consequence of it being generally observed to be downregulated across all monocyte and macrophage populations, this may potentially increase iron-mediated cell death and have a beneficial effect on prognostic indicators.

5.8.0 Key discoveries on MDSC through single cell transcriptome profiling

Two distinct populations of MDSC were identified from the scRNA-seq dataset; a neutrophil-like population, likely granulocytic-MDSC, and a monocyte-like group, likely monocytic-MDSC. This work has identified them without the requirement for surface markers, therefore overcoming some of the problems encountered in previous chapters.

Their genetic signatures corroborate with the literature and show upregulation of ARG1 and S100A8 in particular. This could suggest an immunosuppressive function through the genes upregulated and therefore proteins produced. The finding that the proportions of these populations did not change following chemotherapy is particularly interesting because it may suggest their role in setting up a niche that is conducive for metastasis or disease recurrence to develop. These findings on MDSC proportions following chemotherapy were also identified through my work with flow cytometry, suggesting that the surface markers used for their identification in previous chapters may have been identifying the same cells as those identified as MDSC through gene sequencing. Overall, the myeloid cells appear to be relatively chemosensitive, therefore the question remains as to what is happening within these MDSCs to make them relatively resistant to its effects? Would specifically targeting the MDSC populations in combination with chemotherapy be beneficial in preventing recurrence and death?

When flow-sorting cells in preparation for RNA sequencing, the cells were separated into fibroblasts, epithelial cells and immune cells using the markers podoplanin, EpCAM and CD45 respectively. When performing the cell sort, and from subsequent characterisation of high-level cell types, it was evident that there were few EpCAM positive cells present. Initially it was thought that this was perhaps an issue with our EpCAM antibody or sorting, however Shih et al found that in omental metastatic sites there were very few cancer cells leading them to conclude that once the cancer had metastasised, few cancer cells are required to maintain the tumour, with the focus being on the immune cell infiltration to maintain the metastatic microenvironment (279).

There is currently a large, multicentre project ongoing with collaborators throughout Europe and the UK looking to characterise through RNA sequencing high-grade serous ovarian cancer. The aim is to identify potential solutions to treatment resistance (280). With collaboration and further study, we hope to identify potential targets to overcome treatment resistance, or even treat ovarian cancer.

5.9.0 Future work

To further this work on phenotyping of the myeloid cells in ovarian cancer omental metastases, a functional characterisation analysis could be pursued to identify what functional roles these cell subsets play within the TME. Pathway level analysis of the transcriptome data could identify enrichments of relevant signalling pathways and gene sets of interest within the cell subset-specific marker genes to highlight the pathways most associated with specific cell populations. Subsequently comparing pre-

and post-chemotherapy samples and also ovarian cancer versus the normal and metastatic adenocarcinoma samples could highlight key pathways and gene sets that are altered. This may help to further identify any suppressive role for the MDSC-like subtype to demonstrate their role in immunosuppression via pathway level analysis rather than relying on interpretation from gene-level expression profiling. In addition, it may identify further subgroups which have relevant and significant functional roles, enabling further work to be performed within these subsets for potential future targets.

Further work could also be completed to validate protein level expression of the highlighted genes of interest identified by single cell RNA-sequencing and subsequent functional assays would be required to interrogate the effects modulating the level or activity of these proteins might have on the tumour microenvironment.

Chapter 6

General discussion and future work

In Chapter 3, the aim was to identify if MDSC were present in HGS tumours, their metastases and the peripheral blood of patients. The hypothesis was that MDSC are present in blood and tumour in greater numbers in malignant compared to benign tumours with minimal or no MDSC present in healthy donors. Both PMN- and m-MDSC were identified in benign and malignant tissue but also in healthy donors. There was no difference in percentage of MDSC present in the benign or malignant tumour tissue.

The m-MDSC had a greater prognostic value than PMN-MDSC and the circulating numbers of m-MDSC within healthy controls was very low. When represented by a ratio, it was evident that m-MDSC in peripheral blood may be able to stratify the disease into malignant, benign and healthy better than percentages of either PMN-MDSC or m-MDSC alone. Further analysis using ROC curves would be required in order further assess this relationship and proven to hold true, could have the potential to provide a screening tool for ovarian malignancy. This could improve patient outcomes as it would stratify patients by who needs to be operated on in a specific tertiary cancer unit by a specialist Gynae-oncologist and who could be managed in their local district general hospital for a tumour presumed to be of benign origin. Women with cancer who are not managed within a tertiary referral unit are known to have poorer outcomes (281) so improving this from the start of the patient journey may have the potential to improve their prognosis.

In the following chapter, the aim was to identify the immunosuppressive capacity of the cells identified as 'MDSC'. What was quickly evident was there are currently multiple techniques in use to prove immunosuppressive effects of 'MDSC' and there was no consensus on the methodology. As the quest for a reliable technique demonstrating T cell suppression (through reduction of T cell proliferation in the presence of stimulation) began, it became apparent that there were multiple potential laboratory-induced flaws associated with the methods used to demonstrate immunosuppression. The main technique investigated here involved co-culturing T cells stimulated with anti-CD3/CD28 beads to promote T cell proliferation with or without MDSCs. A reduction in T cell proliferation was expected if these cells were truly functional MDSC populations. The results showed the MDSC were highly phagocytotic and were ingesting the beads destined for activation of T cells so the T cells were being deprived of the necessary activation, rather than being suppressed due to factors released by MDSC. This made it difficult to determine whether the cells identified as 'MDSC' were in fact immunosuppressive, which is integral to their nomenclature.

Due to the findings of the work noting the lack of a robust immunosuppressive functional assay for the identification of MDSC, an alternative approach of identification was sought. ScRNA sequencing was chosen as this was not reliant on the expression of a single cell surface marker. This chapter identified the high-level cell types present in the TME, including T/NK cells, myeloid, B cells, plasmacytoid dendritic, plasmablast, endothelial, various stromal and cycling cells. The major myeloid subgroups identified were monocytes, macrophages, neutrophils and monocytic dendritic cells. MDSC were identified within the myeloid cell compartments and were found to be highly prevalent in HGSC samples but were rarely evident in metastatic and normal tissue, confirming the presence of MDSC within ovarian cancer. Flow cytometric analysis demonstrated MDSC in PBMC of healthy donors and omental samples in benign disease. There may be several reasons for this: 1) Although unlikely, there may have been erroneously high numbers of so-called MDSC in the PBMC samples due to handling of cells – excessive manipulation can cause neutrophils to degranulate and become low-density (and sit within the buffy layer with lymphocytes), and therefore present as 'MDSC' when in reality they are simply activated neutrophils 2) the omental samples taken as 'normal' may not have been completely normal as omentum is not routinely removed during an operation unless there is ovarian pathology, so even 'benign' samples with be subject to a degree of inflammation and likely immune response due to the underlying disease process.

Finer grained scRNAseq analysis of macrophages revealed multiple distinct subsets, including two tumour-associated macrophage (TAMs) subsets. These were increased in the malignant specimens (ovarian cancer and adenocarcinoma metastasis) but not in the normal sample. Noteworthy was that this was reduced following chemotherapy. This may demonstrate that chemotherapy has a beneficial effect as TAMs are associated with a generally poorer prognosis (282).

Interestingly, the ARG1 positive subset of neutrophils was increased in adenocarcinoma and HGS cancer. Arginase has been speculated as one of the main mechanisms of immunosuppression by MDSC and may suggest they are immunosuppressive in function and may confirm that the cells identified through flow cytometry were MDSC. Whether this means that MDSC are a separate cell entity is another question, as they have been argued to be on the spectrum of neutrophil or monocyte differentiation or maturation. There remains to be reliable markers to identify MDSC as a separate group of cells distinct from tumour-associated neutrophils or monocytes and until this is identified, MDSC research will continue to be plagued by uncertainties.

Further work is required to identify unique identification markers for MDSC enabling consistent and reliable studies to be performed to guide potential future therapies. To further this work, it would be prudent to perform functional analyses based on the transcriptional data obtained by performing pathway enrichment analyses so the functionality can be associated with the various identified clusters. This may provide clues as to which pathways or functions might be most influenced by chemotherapy

and which could be followed up on as a potential target for future therapy. In addition, more patients need to be investigated as the power and significance of the results limited the findings, especially relating to samples investigating the response to chemotherapy as only one sample had a CRS3 so statistical analysis was not possible and only inferences could be made.

Once removed from a patient, cells undergo varying degrees of degeneration and the cellular response to this may result in a shift of the subsequent expression of cell surface markers ultimately affecting their phenotypic appearance and/or function. As such, it is of upmost importance to try to maintain the tumour microenvironment as optimally as possible during the transport of the sample from the surgical field to the laboratory. The results on the functionality of MDSC demonstrated that MDSC isolated from ovarian cancer did not cause suppression of T cell function. This may be a limitation of *in vitro* suppression assays, but may also be because the cells taken from the sample were no longer subject to the tumour or TME-derived factors which may influence their overall function. In addition, the MDSC geographically closer to the tumour (or at the leading edge) may behave in a different fashion to those MDSC within the tumour core. When MDSC are removed and put into a single cell solution, this spatial profile is lost. Using techniques such as the multispectral IHC e.g. Vectra Polaris or imaging mass cytometry would help overcome this by producing a detailed *in situ* analysis of the TME. Perhaps another technique to identify MDSC by their proximity to tumour would be to use laser-capture microdissection techniques, where only tissue that is either adjacent to or within the tumour would be included. The benefit of this would be that the samples could be stored as paraffin blocks and only when the histology is confirmed would the experiment be performed. It would also be possible to return to the blocks at a later date should interesting data become apparent.

The presence of MDSC is associated with poorer prognosis in many malignancies and this has been echoed within this thesis. This work has identified MDSC within benign and malignant disease on flow cytometric analysis and highlighted the complexity of demonstrating T cell suppression *in vitro*. Through scRNA sequencing, the myeloid cell compartment in the TME of ovarian cancer omental metastasis has been phenotyped and MDSC found to be evident more specifically to ovarian cancer samples. What is difficult to accurately ascertain is whether the MDSC are cause or consequence of aggressive disease: does a greater presence of MDSC facilitate more aggressive disease to develop or does more aggressive disease produce factors to increase the accumulation of MDSC to further facilitate its growth and increase the tumour burden? By inhibiting the recruitment of MDSC could we reduce tumour growth and therefore progression or recurrence? Or should the focus be on the removal of all visible tumour in the first instance to reduce the subsequent infiltration of MDSC, despite the finding that women with greater infiltration of MDSC are less likely to achieve complete cytoreduction? One potential way to investigate this further would be to identify those women with a high accumulation of MDSC within their tissue samples and those with a low infiltration of MDSC. Genetic sequencing or proteome analysis of the tumours could then be performed to identify if any genes involved in

chemotaxis or recruitment of MDSC are upregulated in those with the greatest infiltration. Clinically, this could help to better inform the surgical team as to the best approach to manage these women by offering individualised management of chemotherapy regime and surgery dependent on their intrinsic tumour biology at the time of diagnostic biopsy.

References

1. Reid BM, Permuth JB, Sellers TA. Epidemiology of ovarian cancer: a review. Cancer Biology and Medicine. 2017.
2. Cancer Research UK [Internet]. [cited 2018 Sep 14]. Available from: https://www.cancerresearchuk.org/health-professional/cancer-statistics/statistics-by-cancer-type/vulval-cancer#heading-Zero
3. Howlader N, Noone AM, Krapcho M, Garshell J, Miller D, Altekruse S, et al. National Cancer Institute SEER Cancer Statistics Review 1975-2012. Natl Cancer Inst. 2015;
4. Kitchener HC. Survival from cancer of the ovary in england and wales up to 2001. Br J Cancer. 2008;
5. Kuhn E, Meeker AK, Visvanathan K, Gross AL, Wang TL, Kurman RJ, et al. Telomere length in different histologic types of ovarian carcinoma with emphasis on clear cell carcinoma. Mod Pathol. 2011;
6. Lengyel E. Ovarian cancer development and metastasis. Am J Pathol. 2010;177(3):1053–64.
7. Kindelberger DW, Lee Y, Miron A, Hirsch MS, Feltmate C, Medeiros F, et al. Intraepithelial carcinoma of the fimbria and pelvic serous carcinoma: Evidence for a causal relationship. Am J Surg Pathol. 2007;
8. Manchanda R, Abdelraheim A, Johnson M, Rosenthal AN, Benjamin E, Brunell C, et al. Outcome of risk-reducing salpingo-oophorectomy in BRCA carriers and women of unknown mutation status. BJOG An Int J Obstet Gynaecol. 2011;
9. Carlson JW, Miron A, Jarboe EA, Parast MM, Hirsch MS, Lee Y, et al. Serous tubal intraepithelial carcinoma: Its potential role in primary peritoneal serous carcinoma and serous cancer prevention. J Clin Oncol. 2008;
10. Roh MH, Kindelberger D, Crum CP. Serous tubal intraepithelial carcinoma and the dominant ovarian mass: Clues to serous tumor origin? Am J Surg Pathol. 2009;
11. Shih I-M, Kurman RJ. Ovarian Tumorigenesis. Am J Pathol. 2004;
12. Casagrande JT, Pike MC, Ross RK, Louie EW, Roy S, Henderson BE. "INCESSANT OVULATION" AND OVARIAN CANCER. Lancet. 1979;
13. Negri E, Pelucchi C, Franceschi S, Montella M, Conti E, Dal Maso L, et al. Family history of cancer and risk of ovarian cancer. Eur J Cancer. 2003;39(4):505–10.
14. Kotsopoulos J, Gronwald J, Karlan B, Rosen B, Huzarski T, Moller P, et al. Age-specific ovarian cancer risks among women with a BRCA1 or BRCA2 mutation. Gynecol Oncol. 2018 Jul;150(1):85–91.
15. Niederhuber JE, Armitage JO, Kastan MB, Doroshow JH, Tepper JE, editors. Abeloff's Clinical Oncology. Sixth. 2020.
16. Ford D, Easton DF, Bishop DT, Narod SA, Goldgar DE. Risks of cancer in BRCA1-mutation carriers. Breast Cancer Linkage Consortium. Lancet (London, England). 1994;
17. Bahcall OG. ICOGS collection provides a collaborative model. Nature Genetics. 2013.

18. Wentzensen N, Poole EM, Trabert B, White E, Arslan AA, Patel A V, et al. Ovarian Cancer Risk Factors by Histologic Subtype: An Analysis From the Ovarian Cancer Cohort Consortium. J Clin Oncol [Internet]. 2016 Jun 20;34(24):2888–98. Available from: https://doi.org/10.1200/JCO.2016.66.8178

19. Cibula D, Widschwendter M, Zikan M, Dusek L. Underlying mechanisms of ovarian cancer risk reduction after tubal ligation. Acta Obstetricia et Gynecologica Scandinavica. 2011.

20. Falconer H, Yin L, Grönberg H, Altman D. Ovarian cancer risk after salpingectomy: a nationwide population-based study. J Natl Cancer Inst. 2015 Feb;107(2).

21. Kurman RJ, Shih I-M. The Dualistic Model of Ovarian Carcinogenesis: Revisited, Revised, and Expanded. Am J Pathol. 2016 Apr;186(4):733–47.

22. Jayson GC, Kohn EC, Kitchener HC, Ledermann JA. Ovarian cancer. The Lancet. 2014.

23. Cancer Research UK. CancerStats: Cancer Statistics for the UK. Online Source www.cancerresearchuk.org/cancer-info/cancerstats/. 2012;

24. Cancer Research UK. Ovarian cancer incidence statistics. 2015. 2015;

25. Giornelli GH. Management of relapsed ovarian cancer: a review. SpringerPlus. 2016.

26. Ahmed N, Stenvers KL. Getting to Know Ovarian Cancer Ascites: Opportunities for Targeted Therapy-Based Translational Research. Front Oncol. 2013;3(September):1–12.

27. Kipps E, Tan DSP, Kaye SB. Meeting the challenge of ascites in ovarian cancer: New avenues for therapy and research. Nature Reviews Cancer. 2013.

28. Jacobs IJ, Menon U, Ryan A, Gentry-Maharaj A, Burnell M, Kalsi JK, et al. Ovarian cancer screening and mortality in the UK Collaborative Trial of Ovarian Cancer Screening (UKCTOCS): A randomised controlled trial. Lancet. 2016;

29. Berek JS, Crum C, Friedlander M. Cancer of the ovary, fallopian tube, and peritoneum. Int J Gynecol Obstet. 2015;

30. Rosenthal AN, Fraser LSM, Philpott S, Manchanda R, Burnell M, Badman P, et al. Evidence of stage shift in women diagnosed with ovarian cancer during phase II of the United Kingdom familial ovarian cancer screening study. J Clin Oncol. 2017;

31. Kehoe S, Hook J, Nankivell M, Jayson GC, Kitchener H, Lopes T, et al. Primary chemotherapy versus primary surgery for newly diagnosed advanced ovarian cancer (CHORUS): An open-label, randomised, controlled, non-inferiority trial. Lancet. 2015;

32. Onda T, Satoh T, Saito T, Kasamatsu T, Nakanishi T, Nakamura K, et al. Comparison of treatment invasiveness between upfront debulking surgery versus interval debulking surgery following neoadjuvant chemotherapy for stage III/IV ovarian, tubal, and peritoneal cancers in a phase III randomised trial: Japan Clinical Oncology Group Study JCOG0602. Eur J Cancer. 2016 Sep;64:22–31.

33. Vergote I, Tropé CG, Amant F, Kristensen GB, Ehlen T, Johnson N, et al. Neoadjuvant Chemotherapy or Primary Surgery in Stage IIIC or IV Ovarian Cancer. N Engl J Med [Internet]. 2010 Sep 2;363(10):943–53. Available from: https://doi.org/10.1056/NEJMoa0908806

34. Fagotti A, Ferrandina G, Vizzielli G, Fanfani F, Gallotta V, Chiantera V, et al. Phase III randomised clinical trial comparing primary surgery versus neoadjuvant chemotherapy in advanced epithelial ovarian cancer with high tumour load (SCORPION trial): Final analysis of peri-operative outcome. Eur J Cancer. 2016 May;59:22–33.

35. Liu YL, Zhou QC, Iasonos A, Chi DS, Zivanovic O, Sonoda Y, et al. Pre-operative

neoadjuvant chemotherapy cycles and survival in newly diagnosed ovarian cancer: what is the optimal number? A Memorial Sloan Kettering Cancer Center Team Ovary study. Int J Gynecol Cancer [Internet]. 2020; Available from: https://ijgc.bmj.com/content/early/2020/10/25/ijgc-2020-001641

36. Colombo N, Guthrie D, Chiari S, Parmar M, Qian W, Swart AM, et al. International collaborative ovarian neoplasm trial 1: A randomized trial of adjuvant chemotherapy in women with early-stage ovarian cancer. J Natl Cancer Inst. 2003;

37. Trimbos JB, Vergote I, Bolis G, Vermorken JB, Mangioni C, Madronal C, et al. Impact of adjuvant chemotherapy and surgical staging in early-stage ovarian carcinoma: European organisation for research and treatment of cancer-adjuvant chemotherapy in ovarian neoplasm-trial. J Natl Cancer Inst. 2003;

38. Oza AM, Cook AD, Pfisterer J, Embleton A, Ledermann JA, Pujade-Lauraine E, et al. Standard chemotherapy with or without bevacizumab for women with newly diagnosed ovarian cancer (ICON7): Overall survival results of a phase 3 randomised trial. Lancet Oncol. 2015;

39. Zivanovic O, Sima CS, Iasonos A, Hoskins WJ, Pingle PR, Leitao MMM, et al. The effect of primary cytoreduction on outcomes of patients with FIGO stage IIIC ovarian cancer stratified by the initial tumor burden in the upper abdomen cephalad to the greater omentum. Gynecol Oncol. 2010;

40. Parmar M, Ledermann J, Colombo N, du Bois A, Delaloye J, Kristensen G, et al. Paclitaxel plus platinum-based chemotherapy versus conventional platinum-based chemotherapy in women with relapsed ovarian cancer: The ICON4/AGO-OVAR-2.2 trial. Lancet. 2003;361(9375):2099–106.

41. Foo T, George A, Banerjee S. PARP inhibitors in ovarian cancer: An overview of the practice-changing trials. Genes Chromosom Cancer. 2021;60(5):385–97.

42. Banerjee S, Moore KN, Colombo N, Scambia G, Kim B-G, Oaknin A, et al. 811MO Maintenance olaparib for patients (pts) with newly diagnosed, advanced ovarian cancer (OC) and a BRCA mutation (BRCAm): 5-year (y) follow-up (f/u) from SOLO1. Ann Oncol [Internet]. 2020 Sep 1;31:S613. Available from: https://doi.org/10.1016/j.annonc.2020.08.950

43. Ray-Coquard I, Pautier P, Pignata S, Pérol D, González-Martín A, Berger R, et al. Olaparib plus Bevacizumab as First-Line Maintenance in Ovarian Cancer. N Engl J Med [Internet]. 2019 Dec 18;381(25):2416–28. Available from: https://doi.org/10.1056/NEJMoa1911361

44. Makin S. What's next for PARP inhibitors? Nature. 2021;600(7889):S36–8.

45. Coleman RL, Spirtos NM, Enserro D, Herzog TJ, Sabbatini P, Armstrong DK, et al. Secondary surgical cytoreduction for recurrent ovarian cancer. N Engl J Med. 2019;

46. Harter P, Sehouli J, Vergote I, Ferron G, Reuss A, Meier W, et al. Randomized Trial of Cytoreductive Surgery for Relapsed Ovarian Cancer. N Engl J Med [Internet]. 2021;385(23):2123–31. Available from: https://doi.org/10.1056/NEJMoa2103294

47. Griffiths RW, Zee YK, Evans S, Mitchell CL, Kumaran GC, Welch RS, et al. Outcomes after multiple lines of chemotherapy for platinum-resistant epithelial cancers of the ovary, peritoneum, and fallopian tube. Int J Gynecol Cancer. 2011;

48. Ledermann JA, Oza AM, Lorusso D, Aghajanian C, Oaknin A, Dean A, et al. Rucaparib for patients with platinum-sensitive, recurrent ovarian carcinoma (ARIEL3): post-progression outcomes and updated safety results from a randomised, placebo-controlled, phase 3 trial. Lancet Oncol [Internet]. 2020 May 1;21(5):710–22. Available from: https://doi.org/10.1016/S1470-2045(20)30061-9

49. Rosenberg JE, Hoffman-Censits J, Powles T, Van Der Heijden MS, Balar A V., Necchi A, et al. Atezolizumab in patients with locally advanced and metastatic urothelial carcinoma who have progressed following treatment with platinum-based chemotherapy: A single-arm, multicentre, phase 2 trial. Lancet. 2016;

50. Van Rooij N, Van Buuren MM, Philips D, Velds A, Toebes M, Heemskerk B, et al. Tumor exome analysis reveals neoantigen-specific T-cell reactivity in an ipilimumab-responsive melanoma. J Clin Oncol. 2013;

51. Rizvi NA, Hellmann MD, Snyder A, Kvistborg P, Makarov V, Havel JJ, et al. Mutational landscape determines sensitivity to PD-1 blockade in non-small cell lung cancer. Science (80-). 2015;

52. Snyder A, Makarov V, Merghoub T, Yuan J, Zaretsky JM, Desrichard A, et al. Genetic Basis for Clinical Response to CTLA-4 Blockade in Melanoma. N Engl J Med. 2014;

53. Strickland KC, Howitt BE, Shukla SA, Rodig S, Ritterhouse LL, Liu JF, et al. Association and prognostic significance of BRCA1/2-mutation status with neoantigen load, number of tumor-infiltrating lymphocytes and expression of PD-1/PD-L1 in high grade serous ovarian cancer. Oncotarget. 2016;

54. Bonadio R, Fogace R, Miranda V, Diz M. Homologous recombination deficiency in ovarian cancer: a review of its epidemiology and management. Clinics. 2018;

55. Bolton KL, Chenevix-Trench G, Goh C, Sadetzki S, Ramus SJ, Karlan BY, et al. Association between BRCA1 and BRCA2 Mutations and Survival in Women with Invasive Epithelial Ovarian Cancer. JAMA - J Am Med Assoc. 2012;

56. Burger RA, Brady MF, Bookman MA, Fleming GF, Monk BJ, Huang H, et al. Incorporation of bevacizumab in the primary treatment of ovarian cancer. N Engl J Med. 2011;

57. Perren TJ, Swart AM, Pfisterer J, Ledermann JA, Pujade-Lauraine E, Kristensen G, et al. A phase 3 trial of bevacizumab in ovarian cancer. N Engl J Med. 2011;

58. González Martín A, Oza AM, Embleton AC, Pfisterer J, Ledermann JA, Pujade-Lauraine E, et al. Exploratory outcome analyses according to stage and/or residual disease in the ICON7 trial of carboplatin and paclitaxel with or without bevacizumab for newly diagnosed ovarian cancer. Gynecol Oncol. 2019;

59. Giornelli GH, Mandó P. A Theoretical View of Ovarian Cancer Relapse. Emerg Med J. 2017;

60. Zhang L, Conejo-Garcia JR, Katsaros D, Gimotty PA, Massobrio M, Regnani G, et al. Intratumoral T cells, recurrence, and survival in epithelial ovarian cancer. N Engl J Med. 2003;

61. Sato E, Odunsi K, Kepner J, Odunsi T, Chen Y-T, Olson SH, et al. Intraepithelial CD8+ tumor-infiltrating lymphocytes and a high CD8+/regulatory T cell ratio are associated with favorable prognosis in ovarian cancer. Proc Natl Acad Sci. 2005;

62. Hwang W-T, Adams SF, Tahirovic E, Hagemann IS, Coukos G. Prognostic significance of tumor-infiltrating T cells in ovarian cancer: a meta-analysis. Gynecol Oncol. 2012;

63. Seung LP, Rowley DA, Dubey P, Schreiber H. Synergy between T-cell immunity and inhibition of paracrine stimulation causes tumor rejection. Proc Natl Acad Sci. 2006;92(14):6254–8.

64. Pekarek LA, Starr B a, Toledano AY, Schreiber H, Pekarek BL a, Starr B a, et al. Inhibition o f Tumor Growth by Elimination o f Granulocytes By Lisa A. Pekarek,* Barbara A. Starr,* Alicia Y. Toledano,~ and Hans Schreiber*. J Exp Med. 1995;

65. Hamilton M, Krystal G, Antignano F, Ruschmann J, Ho V, Sly L. Re: The Terminology Issue for Myeloid-Derived Suppressor Cells. Cancer Res. 2007;67(8):3986–3986.

66. Bronte V, Mandruzzato S, Murray PJ, Frey AB, Rodriguez PC, Chen S-H, et al. Recommendations for myeloid-derived suppressor cell nomenclature and characterization standards. Nat Commun [Internet]. 2016;7(1):1–10. Available from: http://dx.doi.org/10.1038/ncomms12150

67. Ostrand-Rosenberg S, Clements VK, Albelda SM, Bunt SK, Sinha P. Cross-Talk between Myeloid-Derived Suppressor Cells and Macrophages Subverts Tumor Immunity toward a Type 2 Response. J Immunol. 2014;179(2):977–83.

68. Kusmartsev S, Nefedova Y, Yoder D, Gabrilovich DI. Antigen-Specific Inhibition of CD8+ T Cell Response by Immature Myeloid Cells in Cancer Is Mediated by Reactive Oxygen Species. J Immunol. 2004;172(2):989–99.

69. Veglia F, Perego M, Gabrilovich D. Myeloid-derived suppressor cells coming of age review-article. Nat Immunol [Internet]. 2018;19(2):108–19. Available from: http://dx.doi.org/10.1038/s41590-017-0022-x

70. Condamine T, Gabrilovich DI, Dominguez GA, Youn J-I, Kossenkov A V., Mony S, et al. Lectin-type oxidized LDL receptor-1 distinguishes population of human polymorphonuclear myeloid-derived suppressor cells in cancer patients [Internet]. Vol. 1, Science immunology. 2016. 1–32 p. Available from: https://www.ncbi.nlm.nih.gov/pmc/articles/PMC5391495/pdf/nihms849112.pdf

71. Talmadge JE, Gabrilovich DI. History of myeloid derived suppressor cells (MDSCs) in the macro- and micro-environment of tumour-bearing hosts. Nat Rev Cancer. 2013;

72. Millrud CR, Bergenfelz C, Leandersson K. On the origin of myeloid-derived suppressor cells. Oncotarget. 2016;8(2):3649–65.

73. Zhang S, Ma X, Zhu C, Liu L, Wang G, Yuan X. The role of myeloid-derived suppressor cells in patients with solid tumors: A meta-analysis. PLoS One. 2016;11(10):1–11.

74. Newton K, Dixit VM. Signaling in innate immunity and inflammation. Cold Spring Harb Perspect Biol. 2012;

75. Guizani I, Boubaker S, Fehri E, Bel Haj Rhouma R, Guizani-Tabbane L, Ennaifer E. The role of Toll-like receptor 9 in gynecologic cancer. Curr Res Transl Med [Internet]. 2016;64(3):155–9. Available from: http://dx.doi.org/10.1016/j.retram.2016.01.010

76. Ai L, Mu S, Wang Y, Wang H, Cai L, Li W, et al. Prognostic role of myeloid-derived suppressor cells in cancers : a systematic review and meta-analysis. BMC Cancer. 2018;18:1220.

77. Murdoch C, Muthana M, Coffelt SB, Lewis CE. The role of myeloid cells in the promotion of tumour angiogenesis. Nat Rev Cancer. 2008;8(8):618–31.

78. Yu H, Song Y, Wang Q, Xu S, Liu Y, Wang J, et al. MicroRNA-494 Is Required for the Accumulation and Functions of Tumor-Expanded Myeloid-Derived Suppressor Cells via Targeting of PTEN. J Immunol. 2012;188(11):5500–10.

79. Okła K, Czerwonka A, Wawruszak A, Bobiński M, Bilska M, Tarkowski R, et al. Clinical Relevance and Immunosuppressive Pattern of Circulating and Infiltrating Subsets of Myeloid-Derived Suppressor Cells (MDSCs) in Epithelial Ovarian Cancer. Front Immunol. 2019;

80. Cui TX, Kryczek I, Zhao L, Zhao E, Kuick R, Roh MH, et al. Myeloid-derived suppressor cells enhance stemness of cancer cells by inducing microRNA101 and suppressing the corepressor CTBP2. Immunity. 2013;

81. Soong R-S, Anchoori RK, Yang B, Yang A, Tseng S-H, He L, et al. RPN13/ADRM1 inhibitor reverses immunosuppression by myeloid-derived suppressor cells. Oncotarget. 2016;

82. Sucheston-Campbell LE, Cannioto R, Clay AI, Etter JL, Eng KH, Liu S, et al. No evidence that genetic variation in the myeloid-derived suppressor cell pathway influences ovarian cancer survival. Cancer Epidemiol Biomarkers Prev. 2017;

83. Taki M, Abiko K, Baba T, Hamanishi J, Yamaguchi K, Murakami R, et al. Snail promotes ovarian cancer progression by recruiting myeloid-derived suppressor cells via CXCR2 ligand upregulation. Nat Commun [Internet]. 2018;9(1):1–12. Available from: http://dx.doi.org/10.1038/s41467-018-03966-7

84. Goel HL, Mercurio AM. VEGF targets the tumour cell. Nature Reviews Cancer. 2013.

85. Muthuswamy R, Odunsi K, Kalinski P, Obermajer N, Edwards RP. PGE2-Induced CXCL12 Production and CXCR4 Expression Controls the Accumulation of Human MDSCs in Ovarian Cancer Environment. Cancer Res. 2011;

86. Ranjbar R, Nejatollahi F, Nedaei Ahmadi AS, Hafezi H, Safaie A. Expression of Vascular Endothelial Growth Factor (VEGF) and Epidermal Growth Factor Receptor (EGFR) in Patients With Serous Ovarian Carcinoma and Their Clinical Significance. Iran J Cancer Prev. 2015;

87. Hart KM, Byrne KT, Molloy MJ, Usherwood EM, Berwin B. IL-10 immunomodulation of myeloid cells regulates a murine model of ovarian cancer. Front Immunol. 2011;

88. Singel KL, Emmons TR, Khan ANH, Mayor PC, Shen S, Wong JT, et al. Mature neutrophils suppress T cell immunity in ovarian cancer microenvironment. JCI Insight. 2019;

89. Pillay J, Kamp VM, Van Hoffen E, Visser T, Tak T, Lammers JW, et al. A subset of neutrophils in human systemic inflammation inhibits T cell responses through Mac-1. J Clin Invest. 2012;

90. Aarts CEM, Kuijpers TW. Neutrophils as myeloid-derived suppressor cells. European Journal of Clinical Investigation. 2018.

91. Rahman S, Sagar D, Hanna RN, Lightfoot YL, Mistry P, Smith CK, et al. Low-density granulocytes activate T cells and demonstrate a non-suppressive role in systemic lupus erythematosus. Ann Rheum Dis. 2019;

92. Trovato R, Fiore A, Sartori S, Canè S, Giugno R, Cascione L, et al. Immunosuppression by monocytic myeloid-derived suppressor cells in patients with pancreatic ductal carcinoma is orchestrated by STAT3. J Immunother Cancer. 2019;

93. Zhou J, Nefedova Y, Lei A, Gabrilovich D. Neutrophils and PMN-MDSC: Their biological role and interaction with stromal cells. Seminars in Immunology. 2018.

94. Ayantunde AA, Parsons SL. Pattern and prognostic factors in patients with malignant ascites: A retrospective study. Ann Oncol. 2007;

95. Parsons SL, Lang MW, Steele RJC. Malignant ascites: A 2-year review from a teaching hospital. Eur J Surg Oncol. 1996;

96. Elwan N, Salem ML, Kobtan A, El-Kalla F, Mansour L, Yousef M, et al. High numbers of myeloid derived suppressor cells in peripheral blood and ascitic fluid of cirrhotic and HCC patients. Immunol Invest [Internet]. 2018;47(2):169–80. Available from: https://doi.org/10.1080/08820139.2017.1407787

97. Horikawa N, Abiko K, Matsumura N, Hamanishi J, Baba T, Yamaguchi K, et al. Expression of vascular endothelial growth factor in ovarian cancer inhibits tumor immunity through the accumulation of myeloid-derived suppressor cells. Clin Cancer Res. 2017;23(2):587–99.

98. Wu L, Deng Z, Peng Y, Han L, Liu J, Wang L, et al. Ascites-derived IL-6 and IL-10 synergistically expand $CD14^{+}HLA\text{-}DR^{-/low}$ myeloid-derived suppressor cells in ovarian cancer

patients. Oncotarget. 2017;

99. A.N.H. K, N. K, K.L. S, M.J. G, K.B. M, S. D, et al. Targeting myeloid cells in the tumor microenvironment enhances vaccine efficacy in murine epithelial ovarian cancer. Oncotarget [Internet]. 2015;6(13):11310–26. Available from: http://www.impactjournals.com/oncotarget/index.php?journal=oncotarget&page=article&op=download&path%5B%5D=3597&path%5B%5D=7303%5Cnhttp://ovidsp.ovid.com/ovidweb.cgi?T=JS&PAGE=reference&D=emed17&NEWS=N&AN=604481881

100. Kim NR, Kim YJ. Oxaliplatin regulates myeloid-derived suppressor cell-mediated immunosuppression via downregulation of nuclear factor-κB signaling. Cancer Med. 2019;

101. De Biasi AR, Villena-Vargas J, Adusumilli PS. Cisplatin-induced antitumor immunomodulation: A review of preclinical and clinical evidence. Clinical Cancer Research. 2014.

102. Tseng CW, Hung CF, Alvarez RD, CorneliaTrimble, Huh WK, Kim D, et al. Pretreatment with cisplatin enhances E7-Specific CD8+ T-cell -mediated antitumor immunity induced by DNA vaccination. Clin Cancer Res. 2008;

103. Chang CL, Hsu YT, Wu CC, Lai YZ, Wang C, Yang YC, et al. Dose-dense chemotherapy improves mechanisms of antitumor immune response. Cancer Res. 2013;

104. Dijkgraaf EM, Santegoets SJAM, Reyners AKL, Goedemans R, Nijman HW, van Poelgeest MIE, et al. A phase 1/2 study combining gemcitabine, Pegintron and p53 SLP vaccine in patients with platinum-resistant ovarian cancer. Oncotarget. 2015;6(31).

105. Plate JMD, Plate AE, Shott S, Bograd S, Harris JE. Effect of gemcitabine on immune cells in subjects with adenocarcinoma of the pancreas. Cancer Immunol Immunother. 2005;

106. Soeda A, Morita-Hoshi Y, Makiyama H, Morizane C, Ueno H, Ikeda M, et al. Regular dose of gemcitabine induces an increase in CD14+ monocytes and CD11c+ dendritic cells in patients with advanced pancreatic cancer. Jpn J Clin Oncol. 2009;

107. Odunsi K. Immunotherapy in Ovarian Cancer. Ann Oncol 28. 2017;supplement:viii7–viii7.

108. Zhu X, Lang J. Programmed death-1 pathway blockade produces a synergistic antitumor effect: Combined application in ovarian cancer. J Gynecol Oncol. 2017;28(5):1–19.

109. Webb JR, Milne K, Kroeger DR, Nelson BH. PD-L1 expression is associated with tumor-infiltrating T cells and favorable prognosis in high-grade serous ovarian cancer. Gynecol Oncol. 2016;

110. Hamanishi J, Mandai M, Iwasaki M, Okazaki T, Tanaka Y, Yamaguchi K, et al. Programmed cell death 1 ligand 1 and tumor-infiltrating CD8+ T lymphocytes are prognostic factors of human ovarian cancer. Proc Natl Acad Sci. 2007;

111. Abiko K, Mandai M, Hamanishi J, Yoshioka Y, Matsumura N, Baba T, et al. PD-L1 on tumor cells is induced in ascites and promotes peritoneal dissemination of ovarian cancer through CTL dysfunction. Clin Cancer Res. 2013;

112. Zhang L, Conejo-Garcia JR, Katsaros D, Gimotty PA, Massobrio M, Regnani G, et al. Intratumoral T Cells, Recurrence, and Survival in Epithelial Ovarian Cancer. N Engl J Med. 2003;

113. Hamanishi J, Mandai M, Ikeda T, Minami M, Kawaguchi A, Murayama T, et al. Safety and antitumor activity of Anti-PD-1 antibody, nivolumab, in patients with platinum-resistant ovarian cancer. J Clin Oncol. 2015;

114. Zhang P, Su DM, Liang M, Fu J. Chemopreventive agents induce programmed death-1-ligand 1 (PD-L1) surface expression in breast cancer cells and promote PD-L1-mediated T cell

apoptosis. Mol Immunol. 2008;

115. Qin X, Liu C, Zhou Y, Wang G. Cisplatin induces programmed death-1-ligand 1(PD-L1) over-expression in hepatoma H22 cells via Erk/Mapk signaling pathway. Cell Mol Biol. 2010;

116. Peng J, Hamanishi J, Matsumura N, Abiko K, Murat K, Baba T, et al. Chemotherapy induces programmed cell death-ligand 1 overexpression via the nuclear factor-κBto foster an immunosuppressive tumor microenvironment in Ovarian Cancer. Cancer Res. 2015;

117. Zheng GXY, Terry JM, Belgrader P, Ryvkin P, Bent ZW, Wilson R, et al. Massively parallel digital transcriptional profiling of single cells. Nat Commun [Internet]. 2017;8(1):14049. Available from: https://doi.org/10.1038/ncomms14049

118. Team RC. R: A language and environment for statistical computing. 2013;

119. Stuart T, Butler A, Hoffman P, Hafemeister C, Papalexi E, Mauck WM 3rd, et al. Comprehensive Integration of Single-Cell Data. Cell. 2019 Jun;177(7):1888-1902.e21.

120. McGinnis CS, Murrow LM, Gartner ZJ. DoubletFinder: Doublet Detection in Single-Cell RNA Sequencing Data Using Artificial Nearest Neighbors. Cell Syst. 2019 Apr;8(4):329-337.e4.

121. Aran D, Looney AP, Liu L, Wu E, Fong V, Hsu A, et al. Reference-based analysis of lung single-cell sequencing reveals a transitional profibrotic macrophage. Nat Immunol. 2019 Feb;20(2):163–72.

122. Wang G, Pan X, Ding Z, Shi Y, Li L, Chang Q, et al. Targeting YAP-Dependent MDSC Infiltration Impairs Tumor Progression. Cancer Discov. 2016; 6:80–95. [PubMed: 26701088]. Cancer Discov. 2016;6(1):80–95.

123. Martinelli S, Urosevic M, Daryadel A, Oberholzer P, Baumann C, Fey M, et al. Induction of Genes Mediating Interferon-dependent Extracellular Trap Formation during Neutrophil Differentiation. J Biol Chem. 2004;279:44123–32.

124. Zhang M, Wang X, Chen X, Zhang Q, Hong J. Novel Immune-Related Gene Signature for Risk Stratification and Prognosis of Survival in Lower-Grade Glioma [Internet]. Vol. 11, Frontiers in Genetics . 2020. Available from: https://www.frontiersin.org/article/10.3389/fgene.2020.00363

125. Searle G, Pounds R, Phillips A, Kehoe S, Balega J, Singh K, et al. Prolonged interruption of chemotherapy in patients undergoing delayed debulking surgery for advanced high grade serous ovarian cancer is associated with a worse prognosis. Gynecol Oncol. 2020;

126. Cohen PA, Powell A, Böhm S, Gilks CB, Stewart CJR, Meniawy TM, et al. Pathological chemotherapy response score is prognostic in tubo-ovarian high-grade serous carcinoma: A systematic review and meta-analysis of individual patient data. Gynecologic Oncology. 2019.

127. Pomel C, Jeyarajah A, Oram D, Shepherd J, Milliken D, Dauplat J, et al. Cytoreductive surgery in ovarian cancer. Cancer Imaging. 2007;

128. Lee JY, Chung YS, Na K, Kim HM, Park CK, Nam EJ, et al. External validation of chemotherapy response score system for histopathological assessment of tumor regression after neoadjuvant chemotherapy in tubo-ovarian high-grade serous carcinoma. J Gynecol Oncol. 2017;

129. Michaan N, Chong WY, Han NY, Lim MC, Park SY. Prognostic Value of Pathologic Chemotherapy Response Score in Patients With Ovarian Cancer After Neoadjuvant Chemotherapy. Int J Gynecol Cancer [Internet]. 2018;28(9):1676–82. Available from: https://ijgc.bmj.com/content/28/9/1676

130. Youn JI, Gabrilovich DI. The biology of myeloid-derived suppressor cells: The blessing and

the curse of morphological and functional heterogeneity. European Journal of Immunology. 2010.

131. Pergamo M, Miller G. Myeloid-derived suppressor cells and their role in pancreatic cancer. Cancer Gene Therapy. 2017.

132. Moss EL, Hollingworth J, Reynolds TM. The role of CA125 in clinical practice. J Clin Pathol. 2005;

133. Lin YH, Chen YH, Chang HY, Au HK, Tzeng CR, Huang YH. Chronic niche inflammation in endometriosis-associated infertility: Current understanding and future therapeutic strategies. International Journal of Molecular Sciences. 2018.

134. Stanciu PI, Ind TEJ, Barton DPJ, Butler JB, Vroobel KM, Attygalle AD, et al. Development of Peritoneal Carcinoma in women diagnosed with Serous Tubal Intraepithelial Carcinoma (STIC) following Risk-Reducing Salpingo-Oophorectomy (RRSO). J Ovarian Res. 2019;

135. Ma P, Beatty PL, McKolanis J, Brand R, Schoen RE, Finn OJ. Circulating myeloid derived suppressor cells (MDSC) that accumulate in premalignancy share phenotypic and functional characteristics with MDSC in cancer. Front Immunol. 2019;

136. Marvel D, Gabrilovich DI. Myeloid-derived suppressor cells in the tumor microenvironment: Expect the unexpected. Journal of Clinical Investigation. 2015.

137. Okła K, Wertel I, Polak G, Surówka J, Wawruszak A, Kotarski J. Tumor-Associated Macrophages and Myeloid-Derived Suppressor Cells as Immunosuppressive Mechanism in Ovarian Cancer Patients: Progress and Challenges. Int Rev Immunol. 2016;35(5):372–85.

138. Gadducci A, Sartori E, Landoni F, Zola P, Maggino T, Maggioni A, et al. Relationship between time interval from primary surgery to the start of taxane- plus platinum-based chemotherapy and clinical outcome of patients with advanced epithelial ovarian cancer: Results of a multicenter retrospective Italian study. J Clin Oncol. 2005;

139. Bristow RE, Puri I, Chi DS. Cytoreductive surgery for recurrent ovarian cancer: A meta-analysis. Gynecologic Oncology. 2009.

140. Truong AS, Zhou M, Krishnan B, Utsumi T, Manocha U, Stewart KG, et al. Entinostat induces antitumor immune responses through immune editing of tumor neoantigens. J Clin Invest [Internet]. 2021;131(16). Available from: https://doi.org/10.1172/JCI138560

141. Smith HJ, McCaw TR, Londono AI, Katre AA, Meza-Perez S, Yang ES, et al. The antitumor effects of entinostat in ovarian cancer require adaptive immunity. Cancer. 2018;

142. Cadoo KA, Meyers ML, Burger RA, Armstrong DK, Penson RT, Gordon MS, et al. A phase II randomized study of avelumab plus entinostat versus avelumab plus placebo in patients (pts) with advanced epithelial ovarian cancer (EOC). J Clin Oncol. 2019;

143. Platell C, Cooper D, Papadimitriou JM, Hall JC. The omentum. World Journal of Gastroenterology. 2000.

144. Trellakis S, Bruderek K, Hütte J, Elian M, Hoffmann TK, Lang S, et al. Granulocytic myeloid-derived suppressor cells are cryosensitive and their frequency does not correlate with serum concentrations of colony-stimulating factors in head and neck cancer. Innate Immun. 2013;

145. Negorev D, Beier UH, Zhang T, Quatromoni JG, Bhojnagarwala P, Albelda SM, et al. Human neutrophils can mimic myeloid-derived suppressor cells (PMN-MDSC) and suppress microbead or lectin-induced T cell proliferation through artefactual mechanisms. Sci Rep. 2018;

146. Coosemans A, Baert T, Ceusters J, Busschaert P, Landolfo C, Verschuere T, et al. Myeloid-derived suppressor cells at diagnosis may discriminate between benign and malignant ovarian

tumors. Int J Gynecol Cancer. 2019;

147. Kim SI, Lee M, Kim HS, Chung HH, Kim JW, Park NH, et al. Effect of BRCA mutational status on survival outcome in advanced-stage high-grade serous ovarian cancer. J Ovarian Res. 2019;

148. Lechner MG, Liebertz DJ, Epstein AL. Characterization of Cytokine-Induced Myeloid-Derived Suppressor Cells from Normal Human Peripheral Blood Mononuclear Cells. J Immunol. 2010;

149. Li L, Wang L, Li J, Fan Z, Yang L, Zhang Z, et al. Metformin-induced reduction of CD39 and CD73 blocks myeloid-derived suppressor cell activity in patients with ovarian cancer. Cancer Res. 2018;78(7):1779–91.

150. Heuvers ME, Muskens F, Bezemer K, Lambers M, Dingemans AMC, Groen HJM, et al. Arginase-1 mRNA expression correlates with myeloid-derived suppressor cell levels in peripheral blood of NSCLC patients. Lung Cancer. 2013;

151. Soong RS, Anchoori RK, Yang B, Yang A, Tseng SH, He L, et al. RPN13/ADRM1 inhibitor reverses immunosuppression by myeloid-derived suppressor cells. Oncotarget. 2016;7(42):68489–502.

152. Rodríguez-Ubreva J, Català-Moll F, Obermajer N, Álvarez-Errico D, Ramirez RN, Company C, et al. Prostaglandin E2 Leads to the Acquisition of DNMT3A-Dependent Tolerogenic Functions in Human Myeloid-Derived Suppressor Cells. Cell Rep. 2017;

153. Obermajer N, Muthuswamy R, Lesnock J, Edwards RP, Kalinski P. Positive feedback between PGE2 and COX2 redirects the differentiation of human dendritic cells toward stable myeloid-derived suppressor cells. Blood. 2011;

154. Serafini P, Meckel K, Kelso M, Noonan K, Califano J, Koch W, et al. Phosphodiesterase-5 inhibition augments endogenous antitumor immunity by reducing myeloid-derived suppressor cell function. J Exp Med. 2006;

155. Santilli G, Piotrowska I, Cantilena S, Chayka O, D'Alicarnasso M, Morgenstern DA, et al. Polyphenol e enhances the antitumor immune response in neuroblastoma by inactivating myeloid suppressor cells. Clin Cancer Res. 2013;

156. Jain MD, Zhao H, Atkins R, Menges MA, Pope CR, Faramand R, et al. Tumor Inflammation and Myeloid Derived Suppressor Cells Reduce the Efficacy of CD19 CAR T Cell Therapy in Lymphoma. Blood. 2019;

157. Eckard SC, Chen Y, Piovesan D, Narasappa N, Park TW, Kalisiak J, et al. AB474, a potent orally bioavailable inhibitor of arginase, for the treatment of cancer. Exp Mol Ther. 2019;79(13):Abstract number: 3862.

158. Trickett A, Kwan YL. T cell stimulation and expansion using anti-CD3/CD28 beads. J Immunol Methods. 2003;275(1–2):251–5.

159. Lechner MG, Liebertz DJ, Epstein AL. Correction: Characterization of Cytokine-Induced Myeloid-Derived Suppressor Cells from Normal Human Peripheral Blood Mononuclear Cells. J Immunol. 2010;

160. Quach A, Ferrante A. The Application of Dextran Sedimentation as an Initial Step in Neutrophil Purification Promotes Their Stimulation, due to the Presence of Monocytes. J Immunol Res. 2017;

161. Zahler S, Kowalski C, Brosig A, Kupatt C, Becker BF, Gerlach E. The function of neutrophils isolated by a magnetic antibody cell separation technique is not altered in comparison to a density gradient centrifugation method. J Immunol Methods. 1997;

162. Khanna S, Graef S, Mussai F, Thomas A, Wali N, Yenidunya BG, et al. Tumor-derived GM-CSF promotes granulocyte immunosuppression in mesothelioma patients. Clin Cancer Res. 2018;

163. Kusmartsev S, Nagaraj S, Gabrilovich DI. Tumor-Associated CD8 + T Cell Tolerance Induced by Bone Marrow-Derived Immature Myeloid Cells . J Immunol. 2005;

164. Hoechst B, Ormandy LA, Ballmaier M, Lehner F, Krüger C, Manns MP, et al. A New Population of Myeloid-Derived Suppressor Cells in Hepatocellular Carcinoma Patients Induces CD4+CD25+Foxp3+ T Cells. Gastroenterology. 2008;

165. Li L, Wang L, Li J, Fan Z, Yang L, Zhang Z, et al. Metformin-induced reduction of CD39 and CD73 blocks myeloid-derived suppressor cell activity in patients with ovarian cancer. Cancer Res. 2018;

166. Dorward DA, Lucas CD, Alessandri AL, Marwick JA, Rossi F, Dransfield I, et al. Technical Advance: Autofluorescence-based sorting: rapid and nonperturbing isolation of ultrapure neutrophils to determine cytokine production. J Leukoc Biol. 2013;

167. Llufrio EM, Wang L, Naser FJ, Patti GJ. Sorting cells alters their redox state and cellular metabolome. Redox Biol. 2018;

168. Godoy HE, Khan ANH, Vethanayagam RR, Grimm MJ, Singel KL, Kolomeyevskaya N, et al. Myeloid-Derived Suppressor Cells Modulate Immune Responses Independently of NADPH Oxidase in the Ovarian Tumor Microenvironment in Mice. PLoS One. 2013;8(7).

169. Makino K, Yamamoto N, Higuchi K, Harada N, Ohshima H, Terada H. Phagocytic uptake of polystyrene microspheres by alveolar macrophages: Effects of the size and surface properties of the microspheres. Colloids Surfaces B Biointerfaces. 2003;

170. Linge IA, Kondratieva E V., Kondratieva TK, Makarov VA, Polshakov VI, Savelyev OY, et al. “Suppressor factor” of neutrophils: A short story of a long-term misconception. Biochem. 2016;

171. Chomarat P, Banchereau J, Davoust J, Palucka AK. IL-6 switches the differentiation of monocytes from dendritic cells to macrophages. Nat Immunol. 2000;

172. Si Y, Merz SF, Jansen P, Wang B, Bruderek K, Altenhoff P, et al. Multidimensional imaging provides evidence for down-regulation of T cell effector function by MDSC in human cancer tissue. Sci Immunol. 2019;

173. Mattick JS, Gagen MJ. The Evolution of Controlled Multitasked Gene Networks: The Role of Introns and Other Noncoding RNAs in the Development of Complex Organisms. Mol Biol Evol [Internet]. 2001 Sep 1;18(9):1611–30. Available from: https://doi.org/10.1093/oxfordjournals.molbev.a003951

174. Rao MS, Van Vleet TR, Ciurlionis R, Buck WR, Mittelstadt SW, Blomme EAG, et al. Comparison of RNA-Seq and Microarray Gene Expression Platforms for the Toxicogenomic Evaluation of Liver From Short-Term Rat Toxicity Studies [Internet]. Vol. 9, Frontiers in Genetics . 2019. Available from: https://www.frontiersin.org/article/10.3389/fgene.2018.00636

175. Wang Z, Gerstein M, Snyder M. RNA-Seq: A revolutionary tool for transcriptomics. Nature Reviews Genetics. 2009.

176. Ozsolak F, Milos PM. RNA sequencing: Advances, challenges and opportunities. Nature Reviews Genetics. 2011.

177. Han Y, Gao S, Muegge K, Zhang W, Zhou B. Advanced applications of RNA sequencing and challenges. Bioinform Biol Insights. 2015;

178. Chen G, Ning B, Shi T. Single-Cell RNA-Seq Technologies and Related Computational Data Analysis [Internet]. Vol. 10, Frontiers in Genetics . 2019. Available from: https://www.frontiersin.org/article/10.3389/fgene.2019.00317

179. Chu Y, Corey DR. RNA sequencing: platform selection, experimental design, and data interpretation. Nucleic Acid Ther [Internet]. 2012/07/25. 2012 Aug;22(4):271–4. Available from: https://pubmed.ncbi.nlm.nih.gov/22830413

180. https://emea.illumina.com/science/technology/next-generation-sequencing/paired-end-vs-single-read-sequencing.html [Internet]. [cited 2020 Mar 26]. Available from: https://emea.illumina.com/science/technology/next-generation-sequencing/paired-end-vs-single-read-sequencing.html

181. Civita P, Franceschi S, Aretini P, Ortenzi V, Menicagli M, Lessi F, et al. Laser Capture Microdissection and RNA-Seq Analysis: High Sensitivity Approaches to Explain Histopathological Heterogeneity in Human Glioblastoma FFPE Archived Tissues [Internet]. Vol. 9, Frontiers in Oncology . 2019. Available from: https://www.frontiersin.org/article/10.3389/fonc.2019.00482

182. Ortseifen V, Viefhues M, Wobbe L, Grünberger A. Microfluidics for Biotechnology: Bridging Gaps to Foster Microfluidic Applications [Internet]. Vol. 8, Frontiers in Bioengineering and Biotechnology . 2020. Available from: https://www.frontiersin.org/article/10.3389/fbioe.2020.589074

183. Azizi E, Carr AJ, Plitas G, Cornish AE, Konopacki C, Prabhakaran S, et al. Single-Cell Map of Diverse Immune Phenotypes in the Breast Tumor Microenvironment. Cell. 2018;

184. Tirosh I, Izar B, Prakadan SM, Wadsworth MH, Treacy D, Trombetta JJ, et al. Dissecting the multicellular ecosystem of metastatic melanoma by single-cell RNA-seq. Science (80-). 2016;

185. Zheng C, Zheng L, Yoo JK, Guo H, Zhang Y, Guo X, et al. Landscape of Infiltrating T Cells in Liver Cancer Revealed by Single-Cell Sequencing. Cell. 2017;

186. Kim K-T, Lee HW, Lee H-O, Song HJ, Jeong DE, Shin S, et al. Application of single-cell RNA sequencing in optimizing a combinatorial therapeutic strategy in metastatic renal cell carcinoma. Genome Biol [Internet]. 2016;17(1):80. Available from: https://doi.org/10.1186/s13059-016-0945-9

187. Lee M-CW, Lopez-Diaz FJ, Khan SY, Tariq MA, Dayn Y, Vaske CJ, et al. Single-cell analyses of transcriptional heterogeneity during drug tolerance transition in cancer cells by RNA sequencing. Proc Natl Acad Sci U S A [Internet]. 2014 Nov;111(44):E4726—35. Available from: https://europepmc.org/articles/PMC4226127

188. Zhang Q, He Y, Luo N, Patel SJ, Han Y, Gao R, et al. Landscape and Dynamics of Single Immune Cells in Hepatocellular Carcinoma. Cell. 2019 Oct;179(4):829-845.e20.

189. Lavin Y, Kobayashi S, Leader A, Amir E-AD, Elefant N, Bigenwald C, et al. Innate Immune Landscape in Early Lung Adenocarcinoma by Paired Single-Cell Analyses. Cell. 2017 May;169(4):750-765.e17.

190. Integrated genomic analyses of ovarian carcinoma. Nature. 2011 Jun;474(7353):609–15.

191. Verhaak RGW, Tamayo P, Yang J-Y, Hubbard D, Zhang H, Creighton CJ, et al. Prognostically relevant gene signatures of high-grade serous ovarian carcinoma. J Clin Invest. 2012;123(1).

192. Talukdar S, Chang Z, Winterhoff B, Starr TK. Single-Cell RNA Sequencing of Ovarian Cancer: Promises and Challenges. Adv Exp Med Biol. 2021;1330:113–23.

193. Konecny GE, Wang C, Hamidi H, Winterhoff B, Kalli KR, Dering J, et al. Prognostic and

therapeutic relevance of molecular subtypes in high-grade serous ovarian cancer. J Natl Cancer Inst. 2014 Oct;106(10).

194. Winterhoff BJ, Maile M, Mitra AK, Sebe A, Bazzaro M, Geller MA, et al. Single cell sequencing reveals heterogeneity within ovarian cancer epithelium and cancer associated stromal cells. Gynecol Oncol. 2017 Mar;144(3):598–606.

195. Izar B, Tirosh I, Stover EH, Wakiro I, Cuoco MS, Alter I, et al. A single-cell landscape of high-grade serous ovarian cancer. Nat Med. 2020 Aug;26(8):1271–9.

196. Hao Q, Li J, Zhang Q, Xu F, Xie B, Lu H, et al. Single-cell transcriptomes reveal heterogeneity of high-grade serous ovarian carcinoma. Clin Transl Med. 2021 Aug;11(8):e500.

197. Shilpi A, Kandpal M, Ji Y, Seagle BL, Shahabi S, Davuluri R V. Platform-Independent Classification System to Predict Molecular Subtypes of High-Grade Serous Ovarian Carcinoma. JCO Clin cancer informatics. 2019 Apr;3:1–9.

198. Hu Y, Taylor-Harding B, Raz Y, Haro M, Recouvreux MS, Taylan E, et al. Are Epithelial Ovarian Cancers of the Mesenchymal Subtype Actually Intraperitoneal Metastases to the Ovary? Front cell Dev Biol. 2020;8:647.

199. Zhao H, Li Z, Gao Y, Li J, Zhao X, Yue W. Single-Cell RNA-Sequencing Portraying Functional Diversity and Clinical Implications of IFI6 in Ovarian Cancer [Internet]. Vol. 9, Frontiers in Cell and Developmental Biology . 2021. Available from: https://www.frontiersin.org/article/10.3389/fcell.2021.677697

200. Nagasawa S, Ikeda K, Horie-Inoue K, Sato S, Takeda S, Hasegawa K, et al. Identification of novel mutations of ovarian cancer-related genes from RNA-sequencing data for Japanese epithelial ovarian cancer patients. Endocr J. 2020 Feb;67(2):219–29.

201. Shih AJ, Menzin A, Whyte J, Lovecchio J, Liew A, Khalili H, et al. Identification of grade and origin specific cell populations in serous epithelial ovarian cancer by single cell RNA-seq. PLoS One. 2018;13(11):e0206785.

202. Cheng S, Li Z, Gao R, Xing B, Gao Y, Yang Y, et al. A pan-cancer single-cell transcriptional atlas of tumor infiltrating myeloid cells. Cell [Internet]. 2021 Feb 4;184(3):792-809.e23. Available from: https://doi.org/10.1016/j.cell.2021.01.010

203. Yang Q, Zhang H, Wei T, Lin A, Sun Y, Luo P, et al. Single-Cell RNA Sequencing Reveals the Heterogeneity of Tumor-Associated Macrophage in Non-Small Cell Lung Cancer and Differences Between Sexes [Internet]. Vol. 12, Frontiers in Immunology . 2021. Available from: https://www.frontiersin.org/article/10.3389/fimmu.2021.756722

204. Zhang L, Li Z, Skrzypczynska KM, Fang Q, Zhang W, O'Brien SA, et al. Single-Cell Analyses Inform Mechanisms of Myeloid-Targeted Therapies in Colon Cancer. Cell [Internet]. 2020 Apr 16;181(2):442-459.e29. Available from: https://doi.org/10.1016/j.cell.2020.03.048

205. Gu M, He T, Yuan Y, Duan S, Li X, Shen C. Single-Cell RNA Sequencing Reveals Multiple Pathways and the Tumor Microenvironment Could Lead to Chemotherapy Resistance in Cervical Cancer. Front Oncol. 2021;11:753386.

206. Jiménez-Sánchez A, Memon D, Pourpe S, Veeraraghavan H, Li Y, Vargas HA, et al. Heterogeneous Tumor-Immune Microenvironments among Differentially Growing Metastases in an Ovarian Cancer Patient. Cell. 2017;

207. Engblom C, Pfirschke C, Pittet MJ. The role of myeloid cells in cancer therapies. Nature Reviews Cancer. 2016.

208. Méndez-Enríquez E, Hallgren J. Mast Cells and Their Progenitors in Allergic Asthma

[Internet]. Vol. 10, Frontiers in Immunology . 2019. Available from: https://www.frontiersin.org/article/10.3389/fimmu.2019.00821

209. Uxa S, Castillo-Binder P, Kohler R, Stangner K, Müller GA, Engeland K. Ki-67 gene expression. Cell Death Differ [Internet]. 2021;28(12):3357–70. Available from: https://doi.org/10.1038/s41418-021-00823-x

210. Villani AC, Satija R, Reynolds G, Sarkizova S, Shekhar K, Fletcher J, et al. Single-cell RNA-seq reveals new types of human blood dendritic cells, monocytes, and progenitors. Science (80-). 2017;

211. Bobryshev Y V, Lord RSA, Watanabe T, Ikezawa T. The cell adhesion molecule E-cadherin is widely expressed in human atherosclerotic lesions. Cardiovasc Res [Internet]. 1998 Oct 1;40(1):191–205. Available from: https://doi.org/10.1016/S0008-6363(98)00141-2

212. Privratsky JR, Newman PJ. PECAM-1: regulator of endothelial junctional integrity. Cell Tissue Res. 2014 Mar;355(3):607–19.

213. Wang G, Lu X, Dey P, Deng P, Wu CC, Jiang S, et al. Targeting YAP-Dependent MDSC Infiltration Impairs Tumor Progression. Cancer Discov. 2016 Jan;6(1):80–95.

214. Jiménez-Sánchez A, Cybulska P, Mager KLV, Koplev S, Cast O, Couturier DL, et al. Unraveling tumor–immune heterogeneity in advanced ovarian cancer uncovers immunogenic effect of chemotherapy. Nat Genet [Internet]. 2020;52(6):582–93. Available from: http://dx.doi.org/10.1038/s41588-020-0630-5

215. Truong NTH, Gargett T, Brown MP, Ebert LM. Effects of Chemotherapy Agents on Circulating Leukocyte Populations: Potential Implications for the Success of CAR-T Cell Therapies. Cancers (Basel). 2021 May;13(9).

216. Hamy A-S, Pierga J-Y, Sabaila A, Laas E, Bonsang-Kitzis H, Laurent C, et al. Stromal lymphocyte infiltration after neoadjuvant chemotherapy is associated with aggressive residual disease and lower disease-free survival in HER2-positive breast cancer. Ann Oncol Off J Eur Soc Med Oncol. 2017 Sep;28(9):2233–40.

217. Pelekanou V, Carvajal-Hausdorf DE, Altan M, Wasserman B, Carvajal-Hausdorf C, Wimberly H, et al. Effect of neoadjuvant chemotherapy on tumor-infiltrating lymphocytes and PD-L1 expression in breast cancer and its clinical significance. Breast Cancer Res. 2017 Aug;19(1):91.

218. Kwong TT, Wong CH, Zhou JY, Cheng ASL, Sung JJY, Chan AWH, et al. Chemotherapy-induced recruitment of myeloid-derived suppressor cells abrogates efficacy of immune checkpoint blockade. JHEP Reports [Internet]. 2021;3(2):100224. Available from: https://www.sciencedirect.com/science/article/pii/S2589555920301580

219. Park YH, Lal S, Lee JE, Choi Y-L, Wen J, Ram S, et al. Chemotherapy induces dynamic immune responses in breast cancers that impact treatment outcome. Nat Commun [Internet]. 2020;11(1):6175. Available from: https://doi.org/10.1038/s41467-020-19933-0

220. Tie Y, Zheng H, He Z, Yang J, Shao B, Liu L, et al. Targeting folate receptor β positive tumor-associated macrophages in lung cancer with a folate-modified liposomal complex. Signal Transduct Target Ther [Internet]. 2020;5(1):6. Available from: https://doi.org/10.1038/s41392-020-0115-0

221. Leung F, Dimitromanolakis A, Kobayashi H, Diamandis EP, Kulasingam V. Folate-receptor 1 (FOLR1) protein is elevated in the serum of ovarian cancer patients. Clin Biochem. 2013 Oct;46(15):1462–8.

222. O'Shannessy DJ, Somers EB, Palmer LM, Thiel RP, Oberoi P, Heath R, et al. Serum folate receptor alpha, mesothelin and megakaryocyte potentiating factor in ovarian cancer:

association to disease stage and grade and comparison to CA125 and HE4. J Ovarian Res. 2013 Apr;6(1):29.

223. Kurosaki A, Hasegawa K, Kato T, Abe K, Hanaoka T, Miyara A, et al. Serum folate receptor alpha as a biomarker for ovarian cancer: Implications for diagnosis, prognosis and predicting its local tumor expression. Int J cancer. 2016 Apr;138(8):1994–2002.

224. Li L, Wang R, He S, Shen X, Kong F, Li S, et al. The identification of induction chemo-sensitivity genes of laryngeal squamous cell carcinoma and their clinical utilization. Eur Arch Oto-Rhino-Laryngology [Internet]. 2018;275(11):2773–81. Available from: http://dx.doi.org/10.1007/s00405-018-5134-x

225. Fang M, Yuan J, Peng C, Li Y. Collagen as a double-edged sword in tumor progression. Tumour Biol J Int Soc Oncodevelopmental Biol Med. 2014 Apr;35(4):2871–82.

226. Wu Y-H, Chang T-H, Huang Y-F, Huang H-D, Chou C-Y. COL11A1 promotes tumor progression and predicts poor clinical outcome in ovarian cancer. Oncogene [Internet]. 2014;33(26):3432–40. Available from: https://doi.org/10.1038/onc.2013.307

227. Cheon D-J, Tong Y, Sim M-S, Dering J, Berel D, Cui X, et al. A collagen-remodeling gene signature regulated by TGF-β signaling is associated with metastasis and poor survival in serous ovarian cancer. Clin cancer Res an Off J Am Assoc Cancer Res. 2014 Feb;20(3):711–23.

228. Henke E, Nandigama R, Ergün S. Extracellular Matrix in the Tumor Microenvironment and Its Impact on Cancer Therapy. Front Mol Biosci [Internet]. 2020;6:160. Available from: https://www.frontiersin.org/article/10.3389/fmolb.2019.00160

229. Peng DH, Rodriguez BL, Diao L, Chen L, Wang J, Byers LA, et al. Collagen promotes anti-PD-1/PD-L1 resistance in cancer through LAIR1-dependent CD8+ T cell exhaustion. Nat Commun [Internet]. 2020;11(1):4520. Available from: https://doi.org/10.1038/s41467-020-18298-8

230. Ramos MIP, Tian L, de Ruiter EJ, Song C, Paucarmayta A, Singh A, et al. Cancer immunotherapy by nc410, a lair-2 fc protein blocking human lair-collagen interaction. Elife. 2021;10:1–29.

231. Chen K, Wang Q, Li M, Guo H, Liu W, Wang F, et al. Single-cell RNA-seq reveals dynamic change in tumor microenvironment during pancreatic ductal adenocarcinoma malignant progression. EBioMedicine. 2021;66.

232. Metovic J, Vignale C, Annaratone L, Osella-Abate S, Maletta F, Rapa I, et al. The oncocytic variant of poorly differentiated thyroid carcinoma shows a specific immune- related gene expression profile. J Clin Endocrinol Metab. 2020;105(12):4577–92.

233. Fehlker M, Huska MR, Jöns T, Andrade-Navarro MA, Kemmner W. Concerted down-regulation of immune-system related genes predicts metastasis in colorectal carcinoma. BMC Cancer [Internet]. 2014;14(1):1–12. Available from: BMC Cancer

234. Ramaswamy S, Ross KN, Lander ES, Golub TR. A molecular signature of metastasis in primary solid tumors. Nat Genet. 2003;33(1):49–54.

235. Løvig T, Andersen SN, Thorstensen L, Diep CB, Meling GI, Lothe RA, et al. Strong HLA-DR expression in microsatellite stable carcinomas of the large bowel is associated with good prognosis. Br J Cancer. 2002;87(7):756–62.

236. Zhao Z, Zou S, Guan X, Wang M, Jiang Z, Liu Z, et al. Apolipoprotein E Overexpression Is Associated With Tumor Progression and Poor Survival in Colorectal Cancer. Front Genet. 2018;9(December):1–10.

237. Kemp SB, Carpenter ES, Steele NG, Donahue KL, Nwosu ZC, Pacheco A, et al. Apolipoprotein E promotes immune suppression in pancreatic cancer through NF-κB-Mediated production of CXCL1. Vol. 81, Cancer Research. 2021. 4305–4318 p.

238. Su WP, Chen YT, Lai WW, Lin CC, Yan JJ, Su WC. Apolipoprotein E expression promotes lung adenocarcinoma proliferation and migration and as a potential survival marker in lung cancer. Lung Cancer [Internet]. 2011;71(1):28–33. Available from: http://dx.doi.org/10.1016/j.lungcan.2010.04.009

239. Pisani G, Baron B. NEAT1 and Paraspeckles in Cancer Development and Chemoresistance. 2020;1–13.

240. Mackey JBG, Coffelt SB, Carlin LM. Neutrophil maturity in cancer. Front Immunol. 2019;10(AUG):1–11.

241. Tulotta C, Stefanescu C, Chen Q, Torraca V, Meijer AH, Snaar-Jagalska BE. CXCR4 signaling regulates metastatic onset by controlling neutrophil motility and response to malignant cells. Sci Rep [Internet]. 2019;9(1):1–16. Available from: http://dx.doi.org/10.1038/s41598-019-38643-2

242. Shim B, Jin MS, Moon JH, Park IA, Ryu HS. High cytoplasmic CXCR4 expression predicts prolonged survival in triple-negative breast cancer patients treated with adjuvant chemotherapy. J Pathol Transl Med. 2018;52(6):369–77.

243. Holm J, Hansen SI. Characterization of soluble folate receptors (folate binding proteins) in humans. Biological roles and clinical potentials in infection and malignancy. Biochim Biophys Acta - Proteins Proteomics [Internet]. 2020;1868(10):140466. Available from: https://www.sciencedirect.com/science/article/pii/S1570963920301138

244. Leary A, Genestie C, Blanc-Durand F, Gouy S, Dunant A, Maulard A, et al. Neoadjuvant chemotherapy alters the balance of effector to suppressor immune cells in advanced ovarian cancer. Cancer Immunol Immunother [Internet]. 2021;70(2):519–31. Available from: https://doi.org/10.1007/s00262-020-02670-0

245. Prat M, Le Naour A, Coulson K, Lemée F, Leray H, Jacquemin G, et al. Circulating CD14 high CD16 low intermediate blood monocytes as a biomarker of ascites immune status and ovarian cancer progression. J Immunother Cancer. 2020;8(1):1–9.

246. Feng AL, Zhu JK, Sun JT, Yang MX, Neckenig MR, Wang XW, et al. CD16+ monocytes in breast cancer patients: Expanded by monocyte chemoattractant protein-1 and may be useful for early diagnosis. Clin Exp Immunol. 2011;164(1):57–65.

247. Subimerb C, Pinlaor S, Lulitanond V, Khuntikeo N, Okada S, McGrath MS, et al. Circulating CD14+CD16+ monocyte levels predict tissue invasive character of cholangiocarcinoma. Clin Exp Immunol. 2010;161(3):471–9.

248. Krieg C, Nowicka M, Guglietta S, Schindler S, Hartmann FJ, Weber LM, et al. High-dimensional single-cell analysis predicts response to anti-PD-1 immunotherapy. Nat Med. 2018;24(2):144–53.

249. Dijkgraaf EM, Heusinkveld M, Tummers B, Vogelpoel LTC, Goedemans R, Jha V, et al. Chemotherapy alters monocyte differentiation to favor generation of cancer-supporting m2 macrophages in the tumor microenvironment. Cancer Res. 2013;73(8):2480–92.

250. Meireson A, Devos M, Brochez L. IDO Expression in Cancer: Different Compartment, Different Functionality? Front Immunol. 2020;11(September):1–17.

251. Zhao Q, Kuang D-M, Wu Y, Xiao X, Li X-F, Li T-J, et al. Activated CD69 + T Cells Foster Immune Privilege by Regulating IDO Expression in Tumor-Associated Macrophages . J Immunol. 2012;188(3):1117–24.

252. Cheng P, Corzo CA, Luetteke N, Yu B, Nagaraj S, Bui MM, et al. Inhibition of dendritic cell differentiation and accumulation of myeloid-derived suppressor cells in cancer is regulated by S100A9 protein. J Exp Med. 2008 Sep;205(10):2235–49.

253. Sinha P, Okoro C, Foell D, Freeze HH, Ostrand-Rosenberg S, Srikrishna G. Proinflammatory S100 proteins regulate the accumulation of myeloid-derived suppressor cells. J Immunol. 2008 Oct;181(7):4666–75.

254. Srikrishna G. S100A8 and S100A9: new insights into their roles in malignancy. J Innate Immun. 2012;4(1):31–40.

255. Vetsika E, Gioulmpasani M, Skalidaki E, Katsarou A, Koinis F, Aggouraki D, et al. Effect of chemotherapy on the myeloid-derived suppressor cells percentages in the peripheral blood of advanced non-small cell lung cancer patients (TUM6P.965). J Immunol [Internet]. 2015 May 1;194(1 Supplement):141.13 LP-141.13. Available from: http://www.jimmunol.org/content/194/1_Supplement/141.13.abstract

256. Ding Z-C, Lu X, Yu M, Lemos H, Huang L, Chandler P, et al. Immunosuppressive Myeloid Cells Induced by Chemotherapy Attenuate Antitumor CD4⁺ T-Cell Responses through the PD-1–PD-L1 Axis. Cancer Res [Internet]. 2014 Jul 1;74(13):3441 LP – 3453. Available from: http://cancerres.aacrjournals.org/content/74/13/3441.abstract

257. Ding Z-C, Munn DH, Zhou G. Chemotherapy-induced myeloid suppressor cells and antitumor immunity: The Janus face of chemotherapy in immunomodulation. Oncoimmunology. 2014;3(8):e954471.

258. Murdocca M, Mango R, Pucci S, Biocca S, Testa B, Capuano R, et al. The lectin-like oxidized LDL receptor-1: a new potential molecular target in colorectal cancer. Oncotarget. 2016 Mar;7(12):14765–80.

259. Zhang J, Zhang L, Li C, Yang C, Li L, Song S, et al. LOX-1 is a poor prognostic indicator and induces epithelial-mesenchymal transition and metastasis in pancreatic cancer patients. Cell Oncol (Dordr). 2018 Feb;41(1):73–84.

260. Pucci S, Polidoro C, Greggi C, Amati F, Morini E, Murdocca M, et al. Pro-oncogenic action of LOX-1 and its splice variant LOX-1Δ4 in breast cancer phenotypes. Cell Death Dis. 2019 Jan;10(2):53.

261. Jiang L, Jiang S, Lin Y, Yang H, Zhao Z, Xie Z, et al. Combination of body mass index and oxidized low density lipoprotein receptor 1 in prognosis prediction of patients with squamous non-small cell lung cancer. Oncotarget. 2015 Sep;6(26):22072–80.

262. Jiang L, Jiang S, Zhou W, Huang J, Lin Y, Long H, et al. Oxidized low density lipoprotein receptor 1 promotes lung metastases of osteosarcomas through regulating the epithelial-mesenchymal transition. J Transl Med. 2019 Nov;17(1):369.

263. Murdocca M, De Masi C, Pucci S, Mango R, Novelli G, Di Natale C, et al. LOX-1 and cancer: an indissoluble liaison. Cancer Gene Ther [Internet]. 2021;28(10):1088–98. Available from: https://doi.org/10.1038/s41417-020-00279-0

264. Sampath P, Moideen K, Ranganathan UD, Bethunaickan R. Monocyte Subsets: Phenotypes and Function in Tuberculosis Infection [Internet]. Vol. 9, Frontiers in Immunology . 2018. Available from: https://www.frontiersin.org/article/10.3389/fimmu.2018.01726

265. Shi Y, Du L, Lv D, Li H, Shang J, Lu J, et al. Exosomal Interferon-Induced Transmembrane Protein 2 Transmitted to Dendritic Cells Inhibits Interferon Alpha Pathway Activation and Blocks Anti-Hepatitis B Virus Efficacy of Exogenous Interferon Alpha. Hepatology. 2019 Jun;69(6):2396–413.

266. Ferrantini M, Capone I, Belardelli F. Interferon-α and cancer: Mechanisms of action and new

perspectives of clinical use. Biochimie [Internet]. 2007;89(6):884–93. Available from: https://www.sciencedirect.com/science/article/pii/S0300908407001010

267. Zhao C, Lu E, Hu X, Cheng H, Zhang J-A, Zhu X. S100A9 regulates cisplatin chemosensitivity of squamous cervical cancer cells and related mechanism. Cancer Manag Res. 2018;10:3753–64.

268. Gormley JA, Hegarty SM, O'Grady A, Stevenson MR, Burden RE, Barrett HL, et al. The role of Cathepsin S as a marker of prognosis and predictor of chemotherapy benefit in adjuvant CRC: a pilot study. Br J Cancer [Internet]. 2011;105(10):1487–94. Available from: https://doi.org/10.1038/bjc.2011.408

269. Hsieh M-H, Tsai J-P, Yang S-F, Chiou H-L, Lin C-L, Hsieh Y-H, et al. Fisetin Suppresses the Proliferation and Metastasis of Renal Cell Carcinoma through Upregulation of MEK/ERK-Targeting CTSS and ADAM9. Cells [Internet]. 2019;8(9). Available from: https://www.mdpi.com/2073-4409/8/9/948

270. Chen Q, Yu D, Zhao Y, Qiu J, Xie Y, Tao M. Screening and identification of hub genes in pancreatic cancer by integrated bioinformatics analysis. J Cell Biochem. 2019;120(12):19496–508.

271. Lu Y, Zhao Q, Liao JY, Song E, Xia Q, Pan J, et al. Complement Signals Determine Opposite Effects of B Cells in Chemotherapy-Induced Immunity. Cell [Internet]. 2020;180(6):1081-1097.e24. Available from: http://dx.doi.org/10.1016/j.cell.2020.02.015

272. Saygin C, Wiechert A, Rao VS, Alluri R, Connor E, Thiagarajan PS, et al. CD55 regulates self-renewal and cisplatin resistance in endometrioid tumors. J Exp Med. 2017 Sep;214(9):2715–32.

273. Vences-Catalán F, Duault C, Kuo C-C, Rajapaksa R, Levy R, Levy S. CD81 as a tumor target. Biochem Soc Trans. 2017 Apr;45(2):531–5.

274. Quagliano A, Gopalakrishnapillai A, Kolb EA, Barwe SP. CD81 knockout promotes chemosensitivity and disrupts in vivo homing and engraftment in acute lymphoblastic leukemia. Blood Adv. 2020 Sep;4(18):4393–405.

275. Vences-Catalán F, Rajapaksa R, Srivastava MK, Marabelle A, Kuo C-C, Levy R, et al. Tetraspanin CD81 promotes tumor growth and metastasis by modulating the functions of T regulatory and myeloid-derived suppressor cells. Cancer Res. 2015 Nov;75(21):4517–26.

276. Chen P, Li X, Zhang R, Liu S, Xiang Y, Zhang M, et al. Combinative treatment of β-elemene and cetuximab is sensitive to KRAS mutant colorectal cancer cells by inducing ferroptosis and inhibiting epithelial-mesenchymal transformation. Theranostics. 2020;10(11):5107–19.

277. Bertoli S, Paubelle E, Bérard E, Saland E, Thomas X, Tavitian S, et al. Ferritin heavy/light chain (FTH1/FTL) expression, serum ferritin levels, and their functional as well as prognostic roles in acute myeloid leukemia. Eur J Haematol. 2019 Feb;102(2):131–42.

278. Lu W, Wu Y, Huang S, Zhang D. A Ferroptosis-Related Gene Signature for Predicting the Prognosis and Drug Sensitivity of Head and Neck Squamous Cell Carcinoma. Front Genet. 2021;12:755486.

279. Shih AJ, Menzin A, Whyte J, Lovecchio J, Liew A, Khalili H, et al. Identification of grade and origin specific cell populations in serous epithelial ovarian cancer by single cell RNA-seq (PLoS ONE (2018) 13: 11 (e0206785) DOI: 10.1371/journal.pone.0206785). PLoS One. 2018;13(12):1–17.

280. HERCULES. HERCULES Project: Comprehensive characterization and effective combinatorial targeting of high-grade serous ovarian cancer via single-cell analysisNo Title [Internet]. [cited 2021 Nov 29]. Available from: https://www.project-hercules.eu/#

281. Woo YL, Kyrgiou M, Bryant A, Everett T, Dickinson HO. Centralisation of services for gynaecological cancer. Cochrane database Syst Rev. 2012 Mar;2012(3):CD007945.

282. Bingle L, Brown NJ, Lewis CE. The role of tumour-associated macrophages in tumour progression: implications for new anticancer therapies. J Pathol. 2002 Mar;196(3):254–65.